Agonist stimulus trafficking by human prostanoid $CRTH_2$ (DP_2) receptors.

by Richard J. McArthur Wilson

Thesis submitted to the University of Nottingham for the degree of Doctor of Philosophy, January 2007.

For my wife, Sally, of whom I'm so proud.

It's a monsoon!

Moss Wood, Rhosygilwen.

August, 2006.

My uncle, Dr. Douglas Swallow, F.R.S.C., has a lot to answer for: his influence at an impressionable age made all the difference.

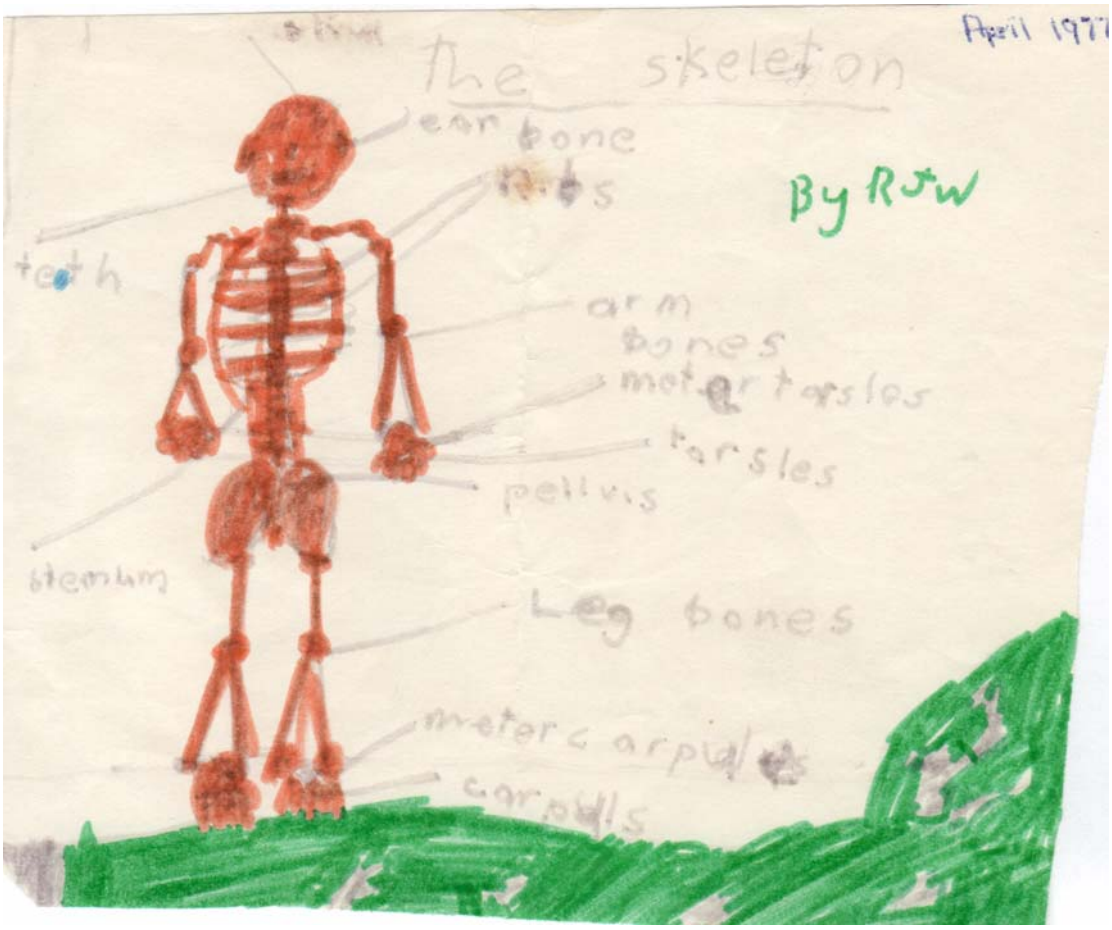

And finally, I also dedicate this work to the memory of those not here to see it:

Donald McArthur Wilson (8th April, 1928 – 18th May, 1981)

Bernice Catherine Wilson (20th Feb., 1933 – 6th Jan., 1993)

Robert McArthur Wilson (3rd Oct., 1956 – 5th Dec., 2003)

Table of Contents:

Total pages: 304
Total word count: 71,014
References: 235
Figures: 78

Abstract

Agonists of hormone receptors possess affinity (the ability to bind) & efficacy (the ability to stimulate effect). In this thesis, alternative expressions of efficacy by recombinant prostanoid Chemoattractant Receptor Homologous molecule of TH_2 cell ($hCRTH_2$) receptors have been studied using a variety of assays and pharmacological techniques.

When expressed in CHO cells, either with or without co-expression of chimeric $G\alpha_{16z49}$ G-proteins, $CRTH_2$ receptor-mediated calcium mobilisation pharmacology was found to be as published. Coupling of receptor activation to calcium elevation involved $G\beta\gamma_{i/o}$ mediated PLCβ-dependent mobilisation of both intra- & extra- calcium. In chimera-expressing cells, an additional coupling mechanism was observed which was presumably $G\alpha_{16z49}$-mediated. The relative expression of receptor and G-protein molecules in both cell types was investigated but because of deficiencies in the methods employed the relative expression is essentially unknown. Because $G\alpha_{16z49}$ & $G\beta\gamma_{i/o}$ represent different classes of PLCβ-activating G-proteins, simultaneous activation of them may have produced a synergistic response in chimera-expressing cells which may have affected the observed receptor pharmacology.

When the $G_{\alpha16z49}$ component was isolated in PTX-treated chimera-expressing CHO $G\alpha_{16z49}$ cells, reversals of potency order were observed with respect to responses in untreated cells. These were most striking for 17 phenyl PGD_2, 15 R 15 methyl $PGF_{2\alpha}$, 15 deoxy $\Delta^{12,14}$ PGJ_2 and 15 R 15methyl $PGF_{2\alpha}$. Alterations of potency order were also observed in non-chimeric cells ($G\beta\gamma_{i/o}$ coupling) compared with PTX treated chimera-expressing cells. These were most striking for indomethacin, 16,16 dimethyl PGD_2, Δ^{12} PGJ_2 and 9,10 dihydro 15 deoxy $\Delta^{12,14}$ PGJ_2.

In [^{35}S]-GTPγS accumulation assays using membranes prepared from non-chimeric cells and presumably reporting $G\alpha_{i/o}$ coupling, agonist pharmacology was similar to $G\alpha_{16z49}$ mediated calcium mobilisation data. However, the data were markedly different from $G\beta\gamma_{i/o}$-mediated calcium mobilisation data generated in non-chimeric cells. These differences were most apparent for 13,14 dihydro 15 keto PGD_2, 15 deoxy $\Delta^{12,14}$ PGJ_2 and indomethacin.

Desensitisation of agonist-stimulated calcium mobilisation was also studied. PGD_2 produced rapid & long-lasting desensitisation of $hCRTH_2$ receptors in a biphasic

manner suggesting that two desensitisation mechanisms may operate. At low concentrations of PGD_2 desensitisation was PTX-insensitive suggesting that a non-$G_{i/o}$-protein mediated mechanism may be responsible. Other $CRTH_2$ receptor agonists inhibited responses to subsequent PGD_2 EC_{80} exposure in calcium mobilisation assays. Interestingly, a group of molecules devoid of agonism in the calcium assay also inhibited PGD_2 responses. This group of molecules included 19 hydroxy prostaglandins A_2, E_2 & $F_{2\alpha}$, and PGE_2 and appeared to mediate their effects through a mechanism that did not involve a competitive interaction with PGD_2.

The data generated here show that $CRTH_2$ receptor agonist pharmacology is critically dependent on G-protein coupling partner and assay methodology, and are strongly indicative of agonist-directed stimulus trafficking. The data are consistent with the notion that $G\beta\gamma$ subunit activation is not a passive 'on-off' event but is rather an active event triggered by agonist- and GTP-dependent conformation changes in both receptor and $G\alpha$ subunit molecules.

Abbreviations:

AKT	Related to A and C kinase-α serine/threonine-protein kinase (also known as EC 2.7.11.1; RAC-PK-α; Protein kinase B; PKB; c-Akt; Akt refers to the virus from which the oncogene was first isolated).
ATP	Adenosine 5′ trisphosphate
BCA	Bicinchoninic acid
BRET	Bioluminescence resonance energy transfer
BW245C	((4S)-(3-[(3R,S)-3-cyclohexyl-3-hydropropyl]-2,5-dioxo)-4-imidazolidine- heptanoic acid)
BWA868C	(3-benzyl-5-(6-carboxyhexyl)-1-(2-cyclohexyl-2-hydroxyethylamino)-hydantoin)
$[Ca^{2+}]_i$	Concentration of intracellular calcium
cAMP	3'-5'-cyclic adenosine monophosphate
CET	Conformation Ensemble Theory
CHOK1	Chinese Hamster Ovary K1 cells (wild type)
COX	Cyclo-oxygenase
CPM	Counts per minute
CCPM	Corrected counts per minute
$CRTH_2$	Chemottractant receptor homologous molecule of Th2 cells
DAG	Diacylglycerol
DKPGD2	13,14-dihydro-15-keto-prostaglandin D_2
DMSO	Dimethyl sulphoxide
DMEM-F12	Dulbecco's modified Eagle's medium – Ham F12 mix
DP_2	Prostanoid DP_2 receptor (aka. $CRTH_2$)
DTT	Dithiothreitol
E/[A]	Concentration-effect curve
EC	Extracellular loop
ECx	Concentration of agonist required to elicit x% of a maximal effect
EDTA	Ethylenediaminetetra-acetic acid
ER	Endoplasmic reticulum
ERK	Extracellular signal-regulated kinase
FCS	Fœtal calf serum
FLIPR	Fluorescence Imaging Plate Reader

GAP	GTPase activating protein
GDP	Guanosine 5'-diphosphate
GFP	Green fluorescent protein
GPCR	G-protein coupled receptor
GRK	G-protein coupled receptor kinase
GTPase	Guanosine-5' trisphosphate hydrolase
GTPγS	[^{35}S]-guanosine-5'-O-(3-thio) trisphosphate
HEK293	Human embryonic kidney 293 cells
HEPES	N-[2-hydroxyethyl]piperazine-N'-[2-ethanesulphonic acid]
HMTB	HEPES modified Tyrode's buffer
HRP	Horseradish peroxidase
IκB	Inhibitor of nuclear factor kappa-B
IP_3	Inositol 1,4,5 trisphosphate
IP_3R	Inositol 1,4,5 trisphosphate receptor
JNK	c-Jun amino terminal kinase
L-888,607	({9-[(4-chlorophenyl)thio]-6-fluoro-2,3-dihydro-1H-pyrrolo[1,2-a]indol-1-yl}acetic acid
MAPK	Mitogen activated protein kinase
NFIU	Normalised FLIPR intensity units
NSAID	Non-steroidal anti-inflammatory drug
NSCC	Non specific cation channel
NSE	No significant effect
NS	Non significant (statistically)
NSB	Non-specific binding
OT	Occupancy Theory
PAB	Probenecid assay buffer
PBS	Phosphate buffered saline
PDL	Poly-D-lysine coated
PG	Prostaglandin
PGD_2	Prostaglandin D_2
PIP_2	Phosphatidyl inositol 4,5 diphosphate
PKA/B/C	Protein kinase A, B or C
PLCβ/γ	Phospholipase C β or γ

PMCA	Plasma membrane Ca-ATPase
PMSF	Phenylmethylsulphonylfluoride
PTX	Pertussis toxin
QSAR	Quantitative structure-activity relationship
RA	Relative activity (cf. PGD_2 = 1.0)
R:G	Receptor : G-protein
RGS	Regulator of G-protein signalling
RP	Relative potency (cf. PGD_2 = 1.0)
SAB	Sulphinpyrazone assay buffer
SAR	Structure-activity relationship
SERCA	Sarcoplasmic / endoplasmic reticulum Ca^{2+}-ATPase
SPA	Scintillation Proximity Assay
SR	Sarcoplasmic reticulum
7TMR	Seven trans-membrane sequence receptor
TC	Tissue culture
TM	Trans-membrane sequence
Tris-HCl	2-amino-2-(hydroxymethyl)-1,3-propanediol, hydrochloride
TRP1	Transient receptor potential channel 1 of *Drosophila*
Tx	Thromboxane
USP	United States Pharmacopœia
UTP	Uridine 5′ trisphosphate
WGA	Wheatgerm agglutinin

Chapter 1: Introduction

Efficacy and agonist-directed stimulus trafficking.

Drug efficacy is the key difference between enzyme and receptor pharmacology: the ability of certain molecules (agonists) to communicate chemical information resulting in activation of receptors and the transduction of that information to intracellular effectors. This thesis examines the relationship between alternative expressions of efficacy using recombinant human prostanoid Chemoattractant Receptor Homologous molecule of TH_2 cell ($hCRTH_2$) receptors expressed in Chinese Hamster Ovary (CHO) cells as a case study. In the following paragraphs of the introduction I describe our current understanding of the concept of efficacy in relation to agonist stimulus trafficking – the ability of certain agonists to preferentially activate selected response pathways.

1.1 Efficacy

The origin of the concept of efficacy can be traced back to Langley (1905) who described agonism in terms of a "receptive substance" (later referred to as a "receptor" by Ehrlich (1913)) which transferred stimuli to effector organs. Thus began the evolution of Occupancy Theory (OT) which has now become generally, if not universally, accepted as describing accurately ligand-receptor behaviour. However, the classical occupancy theory-based treatment of efficacy suffers from one major flaw which Kenakin (2002b) has termed the 'ligand paradox' and which has been vigorously propounded by Colquhoun (1987, and subsequent publications: 1993, 1998, 2006a): in theoretical terms, the thermodynamic molecular forces that control affinity are also the same as those that control efficacy (ie., affinity and efficacy are intrinsically linked) but in practical terms it has been demonstrated in numerous medicinal chemistry campaigns that affinity can be enhanced while efficacy is diminished and *vice versa*. In order to explain this and several other phenomena, the Conformation Ensemble Theory (CET) of receptor behaviour has been developed (Onaran *et al*., 2000; Kenakin, 1996; 2002b; 2004e & b; 2005) in which the paradox is resolved by considering efficacy in terms of receptor microstates characterised by individual receptor conformations, each with its own ability to activate the myriad intracellular components with which the receptor interacts.

The evolution of receptor theory through the last century is essentially the story of the development of the concept of efficacy. Occupancy theory has risen to be king but other models such as Rate Theory (Paton, 1961), Macromolecular Perturbation Theory (Belleau, 1964), and the Dynamic Receptor Hypothesis (Jacobs & Cautrecases, 1976),

which explain receptor behaviour under particular circumstances, are now enjoying something of a renaissance as they reflect certain aspects of CET.

The contributions of the early pioneers of receptor theory have been excellently reviewed in several recent papers (Colquhoun, 2006a, 2006b; Hill, 2006; Kenakin 2004d). The first quantitative treatment of OT was developed by Hill (1909) who independently derived the equations describing the Langmuir adsorption isotherm nine years before Langmuir himself did (Langmuir, 1918) as a result of analyzing the interaction between nicotine and curare in frog *rectus abdominus* muscle. Hill put forward the Hill equation (now the Hill-Langmuir equation), describing drug-receptor binding in terms of a hyperbolic function, much as we do today. Clark (1926), apparently in ignorance of this, regarded drug-receptor interaction as analogous to the combination of gases with metal surfaces described by Langmuir and to follow similar monophasic chemical interaction processes. Clark assumed that the magnitude of agonist effect was proportional to the number of receptors occupied; maximum effect (E_m) occurred when 100% occupancy was achieved. In his 1937 paper, Clark further developed his concept to resolve two properties of drugs: 1. fixation (binding); and 2. the ability to produce an effect after fixation. Clark did not treat the latter property quantitatively, the first attempt to do so was made by Ariëns (1954) who noted that not all members of a homologous series of *p*-aminobenzoic acids were active even though all apparently retained affinity. Ariëns proposed that drugs possessed two independent parameters: 1. affinity (binding described by the Law of Mass Action); and 2. intrinsic activity, *a*. Agonists possess both properties while antagonists possess only affinity. By incorporating *a* into the Michaelis-Menten (1913) equation which described the combination of enzymes and substrates, Ariëns produced a mathematical framework in which the concept of efficacy could be further developed: EC_{50} was considered to represent agonist affinity, K_a while E_m gave a measure of *a*. Since the two properties were independent, compounds of high affinity / low efficacy and *vice versa* could be accommodated. Intrinsic activity ranged on a scale from zero for antagonists to 1.0 for full agonists, with partial agonists (a term coined by Stephenson, 1956) taking values in between. In common with Clark, though, Ariëns assumed that for a full agonist, response was proportional to occupancy, that E_m occurred at 100% occupancy, and that $EC_{50} = K_a$ (ie., when 50% of the receptors were occupied). Incidentally, parallel to these developments in the concept of efficacy, Clark and Gaddum made advances in the

treatment of competitive antagonism and drew on work published by Michaelis & Menten (1913), Haldane (1930), and others. These latter authors developed concepts describing the competition of substrate and product for an enzyme's active site as early as 1913, but were not recognized by pharmacologists until Gaddum's 1937 paper.

The next significant step forward is widely credited to Stephenson (1956) but should perhaps be more correctly attributed also to Furchgott (1955) and Nickerson (1956). Noting that receptor inactivation with irreversible antagonists was capable of producing parallel dextral shift of concentration-effect (E/[A]) curves before depression of maximal agonist effects, Nickerson proposed that a receptor reserve existed in some tissues such that E_m could be achieved when only a small proportion of receptors was occupied. In other words, tissues possessed spare receptors, full occupancy was not required for a maximal agonist effect, and therefore response was not linearly proportional to occupancy. Stephenson described it thus: 1. response was some unknown positive function of occupancy, f; 2. E_m could be produced when agonist occupied only a small proportion of receptors; 3. Different drugs needed to occupy different proportions of the receptor pool to produce E_m, and therefore possessed different efficacies, e. It therefore followed that EC_{50} (the concentration of agonist required to produce a half-maximal effect) was not equal to the K_a (the concentration of agonist required to occupy 50% of receptors). It is important to note that efficacy is not synonymous with intrinsic activity: in theory it is possible for two agonists with equal intrinsic activities to occupy different proportions of the receptor pool at E_m and therefore to have different efficacies. In a further development, Furchgott (1966) resolved Stephenson's efficacy, e, into the product of intrinsic efficacy, ε, and the concentration of active receptors, $[R_T]$, thus demonstrating that efficacy is a product of drug-related (ε) and tissue-related ($[R_T]$) properties. The *mathematical* evolution of efficacy reached its current status with the proposal by Black & Leff (1983) of the Operational Model of Agonism. Black & Leff took the Stephenson / Furchgott concept of efficacy and brought greater definition to the unknown function, f, and therefore to efficacy, e. By recognizing that the relationship between receptor occupancy and ultimate effect was saturable, f was logically deduced to be a saturable hyperbolic function of occupancy. Having defined f thus, it was then possible to formulate an equation which derived a value representing efficacy, τ, from experimental data, rather than the previously used device of assuming an appropriate value. The transducer ratio,

τ, is defined as $[R_O] / K_E$ which can be re-written $[R_O] \times (1 / K_E)$ where $[R_O]$ is the concentration of receptors in the tissue and K_E is the concentration of drug-receptor complex required to produce a half-maximal stimulation of the system. By comparison with Furchgott's definition it can be seen that intrinsic efficacy, ε, is mathematically analogous to $1/K_E$ but conceptually different: ε is wholly drug dependent, whereas $1/K_E$ contains both drug- and tissue- dependent elements. The true benefit of the operational model is that within a system, the tissue-dependent factors associated with the responses evolved by two agonists cancel out and the transducer ratio becomes the ratio of agonist intrinsic efficacies. However, because Stephenson created a conceptual framework in which affinity and efficacy were distinct and separate, more latterly considered as thermodynamically impossible (Colquhoun, 1987; 1998), his treatment and models based on it (Ariëns, Furchgott, Black & Leff) have been described as "simply wrong" though "valuable…at an empirical level".

With the advent of radioligand binding techniques in the 1970's and the molecular biological revolution in the late 80's and 90's came the ability to probe the molecular / biochemical events surrounding receptor-ligand interactions and with it a revolution of the *conceptual* (molecular?) understanding of efficacy, reviewed by Hill (2006), Colquhoun (2006a & b) and Milligan and Kostenis (2006). However, as with many developments in the eclectic world of pharmacology, the first step in this part of the story owes its discovery to another branch of science: physiology. Studying the binding of oxygen and carbon monoxide to haemoglobin (Hb), Wyman (1951) proposed that the observed co-operativity of oxygen binding could be explained if the two already identified conformations of Hb had different affinities for oxygen and that the effect of oxygen binding was to shift the conformational equilibrium towards the high affinity form. The concept of induced conformation changes and differential affinity states for ligand was to prove influential and far-reaching and led directly to the concepts put forward by del Castillo and Katz (1957) and termed the 'two-state model' of ion channel activation, which was later applied to receptors. Efficacy in the two-state model, E, was defined as (ion channel opening rate constant / ion channel closing rate constant) and was shown mathematically to be inseparably linked to affinity. Nonetheless, these ideas were combined with those of Wyman to evolve the reversible two-state model in which ion channels could spontaneously open without receptor activation (Monod, *et al.*, 1965) paving the way for development of the concept of

constitutive receptor activation. An agonist was conceptually defined as a molecule that could enrich the population of activated receptors, in other words, a molecule with preferential affinity for active receptors: the greater that affinity, the more activated receptors were present. Efficacy was therefore defined as the ratio of agonist affinities for the active and inactive receptor states: $E = K_A / K_A^*$ where E is efficacy, and K_A & K_A^* represent the affinity of the agonist for the inactive and active receptor states, respectively. The ability of an agonist to have differential affinity for two states has been termed 'species bias' (Kenakin, 2004c). Colquhoun has advocated the use of this model for interpreting the behaviour of ion channels and in later treatments has invoked the presence of multiple states linking receptor binding, through various stages of conformation change to channel opening (Colquhoun, 2006b), efficacy being an unspecified function of the rate constants describing these processes.

Application of the two-state model to 7TM receptors necessitated further refinement with the demonstration in the late 1970's and early 1980's of the existence of G-proteins and the delineation of their roles as key messenger proteins linking receptors with intracellular effectors (Gilman, 1995; Rodbell, 1995). Thus G-protein coupled receptors (GPCRs) became an entity and the ternary complex model of receptor behaviour was born in order to account for biphasic *agonist* binding but only monophasic *antagonist* binding in the same system (de Lean, *et al*., 1980): in parallel with the Wyman treatment of haemoglobin binding, agonists bound to receptors, recruiting G-proteins and inducing the formation of high agonist affinity, G-protein coupled ternary complexes. Molecular manipulation of receptors and expression in recombinant systems allowed the study of GPCRs under conditions not previously attainable by the use of tissues and primary cells. Costa & Herz (1989) noted the ability of highly expressed recombinant receptors to be spontaneously (or constitutively) active and of certain antagonist molecules to inhibit this basal activation. Thus efficacy took on a vectorial quality (reviewed in Kenakin, 2004b) determined by the relative stoichiometry of receptors and G-proteins, the affinity of activated receptors for G-proteins and the natural tendency of the receptor to form an activated state. In order to take these observations into account Samama, *et al*., (1993) proposed the extended ternary complex model (ETC) – the natural consequence of combining the ternary complex model with the reversible two-state model described above. Under the ETC, receptors ($[R_i]$) can spontaneously isomerise into an active state ($[R_a]$) in a manner determined by an allosteric constant, L ($L = [R_a] / [R_i]$). The activated receptor can

couple to G-protein with or without the presence of bound agonist. The agonist ligand has a higher affinity for the activated receptor than for the inactive receptor, the ratio of affinities being given by α, while G-protein has a higher affinity for the ligand-bound receptor, the ratio of these affinities being given by γ. Thus, in the ETC, and the thermodynamically complete Cubic Ternary Complex (CTC; Weiss, *et al*., 1996a, b, c) efficacy is determined by α and γ, and may be positive or negative. Compounds with negative efficacy are termed inverse agonists.

1.2 Receptor-response pleiotropy

The models described above essentially view receptors in terms of two macroscopic states: active and inactive (Colquhoun, 1987), though as Kenakin (2004c) has pointed out, by virtue of the infinitely numerically variable nature of the parameters describing efficacy, the two-state models can be considered to be 'infinite' state models. Furthermore, in all treatments the receptor is considered to be the pharmacology-defining unit with all intracellular sequelae of agonism related to it in a linear fashion, in other words, pharmacology is genotypically determined (Kenakin, 2002d). Recent findings have questioned this assumption: we now know that receptors exhibit a broad range of activities including G-protein coupled transduction, non-G-protein coupled transduction, desensitisation, internalisation, homo- and hetero- dimerisation, and that observed pharmacology is determined by phenomena such as constitutive activation, stimulus trafficking, protean agonism and phantom gene behaviour (reviewed in Hall, *et al*., 1999; Kenakin, 2002a; Pierce, *et al.*, 2002). Receptors are thus capable of weaving a rich tapestry of intracellular events, the integrated sum of which determines the overall physiological response. Pharmacology is what we observe, and what we observe a receptor doing in response to drug challenge we can appreciate to be dominated by the environment in which the receptor resides when we study it. As such, pharmacology can be phenotypically determined (Kenakin, 2002d). In contrast to the simplistic definition of efficacy given by Colquhoun (1998), the combination of phenotypic determination and simultaneous effects on multiple pathways (activation or inhibition depending on the system set-point) gives efficacy a pleiotropic aspect which complicates both its definition and quantification.

Pleiotropy in receptor coupling was first conceived of in terms of promiscuous receptor coupling to G-proteins (reviewed in Kenakin, 1996) with the observed pharmacology

being the resultant effect of two (or, presumably, more) G-protein transduced pathways. Considerations such as these led to Scaramellini & Leff (1998) proposing the three-state model of receptor behaviour in which the receptor had specific activated states relating to each of two different G-proteins. However, while their model could account for stimulus trafficking at the empirical level (the phenomenon by which certain agonists appear to specifically direct receptor signalling traffic toward specific intracellular effector pathways) it shed no light on molecular events associated with it, nor did it provide a framework for either the complexity of trafficking we now observe, or for protean agonism. (The latter phenomenon is a behaviour exhibited by certain molecules in which the agonist activity of the molecule may appear positive, negative or neutral relative to the basal activity of the system in which it is being studied; protean agonism is believed to be an expression of the ability of receptor ligands to stabilise a discrete subset of receptor conformations which may or may not intersect with the subset found under basal system activation conditions (Kenakin, 1997)). The body of evidence in support of stimulus trafficking is now huge, and applies to the myriad of activation sequelae mentioned above (reviewed in Kenakin, 2003). Conformation Ensemble Theory provides a *heuristic* framework by which these concepts, including inverse agonism, protean agonism and pathway-selective antagonism, can be explained (Onaran, 2000; Kenakin, 2002c). Unfortunately, the Probabilistic Model of receptor behaviour that arises from it has too many parameters to be useful for quantitative purposes but is nonetheless useful as a concept and will be described below.

1.3 Conformation Ensemble Theory

The concept of protein molecules such as enzymes unfolding and refolding to adopt a multitude of tertiary structure conformations is not new (James & Tawfik, 2003) and was used as the basis for the work of Burgen (1966) who advanced the complementary ideas of conformation induction and conformation selection to explain how the interaction between a ligand and a receptor might affect the structure of the latter. Direct evidence in support of the fluid nature of protein structure has now been obtained from a variety of molecular approaches such as nuclear magnetic resonance (e.g. Woodward, *et al*., 1982; Choy & Forman-Kay, 2001), fluorescence lifetime spectroscopy (e.g. Ghanouni, *et al*., 2001), fluorescence correlation spectroscopy (Vukojević, *et al*., 2005, for review) & fluorescence-resonance energy transfer (e.g.

Buskiewicz, *et al*., 2005) studies. We can now view a receptor as a protein undergoing constant spontaneous structural re-organisation and therefore adopting a spectrum of conformations or 'states' quite independently of the presence of ligand (Peleg, *et al*, 2001). The presence of a ligand can be envisaged to stabilise a certain subset of these conformations and thus enrich the population of these states at the expense of conformations not stabilised by the ligand. Although direct evidence for this seems to be lacking, analogous data for the stabilisation of oestrogen receptor conformations by the p160 coactivator have been generated (Tamrazi, *et al.*, 2005). Some of these conformations are predicted to be compatible with the structural requirements for G-protein activation, others with the requirements for desensitisation, and yet others to have no resultant effect. So by stabilising a subset of conformations, agonists are predicted to enrich a specific subset of activation states resulting in activation of a specific spectrum of linked intracellular effector processes. In this view of receptor behaviour inverse agonists are predicted to have the opposite effect: enriching states that do not signal through the pathway under study resulting in depletion of activating conformations and producing an observed reduction in response. Neutral antagonists stabilise all conformations equally and are thus predicted to be a truly rare species (in a study of 380 antagonist-receptor pairings at 73 different GPCRs, 85% of 'antagonists' were shown to be inverse agonists [Kenakin, 2004e]). Several behaviours can be expected to naturally arise from this treatment of receptors:

1. Ligands stabilise their own set of conformations which may overlap with those stabilised by other ligands but will not be identical. This has been described by Kenakin (2002) in terms of the 'conformational cafeteria' in which certain receptor states are 'taken' by the ligand binding to it but these states are replenished to allow further selections to take place. However, the analogy can be extended to describe the ligand dependent selection of conformations to create a 'meal' of observable effects. These ideas represent a convergence between thinking applied to receptors and ion channels (the multiple activation state model for ion channels described above; Kenakin, 1995). Therefore, it follows that stimulus trafficking can be expected to be the norm, not the exception, even amongst agonists from the same series. Taken to its ultimate conclusion, this means that structure-activity relationships are highly dependent on the assay-readout selected (Kenakin, 2005) and that for a given receptor separate SAR may exist for all readouts studied.

2. Stimulus trafficking conceived of in these terms predicts two previously unrecognized drug behaviours: collateral efficacy (simultaneous and differential activation of multiple intracellular pathways by a single agonist-receptor pair) and permissive antagonism (differential inhibition of multiple activation pathways by an antagonist; Kenakin, 2005). Provided that assay systems suitable for exploitation of these behaviours can be configured for high throughput, these behaviours may provide the conceptual basis for creating therapeutic agents with greater selectivity.

3. The conformations on offer in the 'cafeteria' for a given receptor must be by definition always the same (i.e. infinitely variable between limits determined by the receptor structure). However, the subset of these that result in activation of an observable process are predicted to be limited and determined by the environment in which the receptor finds itself (phenotypic determination; Kenakin, 2002d). The principle of reciprocity may be applied here: that which induces a change is itself changed in the process. In other words, although all receptor conformations are available, they are not all *equally* available because some are selectively stabilised by the presence of other molecules in the cellular micro-environment with which the activated receptor interacts. To pursue the analogy, although the cafeteria kitchen has all the ingredients, and the cook (nature) can make all the dishes, the menu on offer changes to fit with the availability of the cook's utensils. Therefore, when a ligand enters the conformational cafeteria, it must select from what is available to create its own meal.

4. Under this model, efficacy may be defined in terms of the ability of a ligand to stabilise or enrich certain conformations at the expense of others (Onaran, *et al*., 2000). Low efficacy agonists are those capable of producing a partial enrichment (relative to full agonists) of particular conformations needed to produce a response, or may enrich conformations leading to partial activation of cellular effectors. The same response pathway in a different cell may not have the same stochastic requirements for transduction resulting in either greater or lower relative activity but the *probability of finding activating receptor conformations* remains constant.

The latter consideration forms the basis of the Probabilistic Model first developed by Onaran, *et al*. (2000) and re-presented by Kenakin (2002b). In this model, the

probability, *p*, of an activating conformation is related to ratios of receptor microstate energies, **b*, and the energy transitions between states, *j*. Different ligands (hormones or receptors) have different **b* values and alter the distribution of states differently. If two species simultaneously interact then the resulting conformations are given by the **b* values of both. Affinity and efficacy are therefore defined in terms of state redistributions governed by *p*, *b*, and *j* and, as before, are linked thermodynamically and mathematically.

1.4 Some predictions of CET

The formulation of the model does not allow for fitting of expectations to experimental data since concentration and effect terms are lacking. However, some predictions of agonist behaviour can be made if we make some assumptions about system properties. Firstly, I propose to assume that a receptor system is defined by a resting state in which the receptor can adopt any of a series of conformations with equal probability. Secondly, that an agonist will enrich a defined subset of conformations, i.e. that the agonist has a dynamic range of conformations that it *can* stabilise which is a subset of all possible conformations. This subset comprises activating and non-activating species. Thirdly, that response generation requires the *number* of activating conformations to exceed a limiting value (i.e., a threshold must be crossed). As predicted by CET, increasing concentrations of agonist will enrich both the activating conformation states and agonist-stabilised non-activating states at the expense of the other conformations available to the receptor. Under these conditions we can predict the following:

1. The probability and therefore the maximum number of receptor molecules in an activating conformation will depend on: a) agonist concentration; b) the dynamic range of the agonist since a wider range will necessitate a lower probability of any individual conformation occurring; c) the propensity of the receptor to remain in its resting state ie., the thermodynamic energy barrier to be crossed in the process of activation; d) the propensity of the receptor to spontaneously adopt non-activating conformations.
2. The response observed will depend on: a) the probability and therefore the number of active conformations required to cross the threshold; b) the dynamic range of the agonist with respect to enrichment of activating and non-activating

conformations; c) the dynamic range of the agonist with respect to activation of multiple pathways.

Item 2b deserves further consideration since this is the unique feature of this treatment. If the dynamic range is wide then even where the agonist response progresses along linear uni-molecular lines, shallow curve slopes could result as the effect of increasing agonist is diluted out by non-activating conformations. Furthermore, as agonist concentration rises, the probability of less favoured agonist-stabilised conformations appearing in appreciable numbers increases. Since the system can be predicted to possess a system maximum probability (P_{Smax}) for the most favoured states which cannot be exceeded, the effect of enriching the less-favoured states will be to *deplete* the most favoured. Depending on the relationship between these various conformations and the activating conformations relevant to the effect being measured, a bell-shaped response curve might be observed. More interestingly, this treatment predicts that a given receptor-agonist pairing could recruit one response pathway which then declines as a second (or more) pathway is recruited. Each pathway may therefore possess its own stabilisation / destabilization properties. This is a significant departure from classical treatments of receptor behaviour in which stabilisation of a pathway-activating receptor conformation may be considered to be uni-directional. Finally, partial enrichment of activating species (partial agonism) could arise from either a wide dynamic range or a dynamic range 'shifted' along the conformation axis relative to a full agonist. Therefore, study of what we term 'partial agonists' as a group may be a rich hunting ground for the detection of further examples of stimulus trafficking. We should bear in mind, though, that terms such as 'full' and 'partial' really describe environment-specific behaviours of agonists: for example, the apparently 'full' endogenous hormone ligand 5-HT can be observed to behave as an agonist in a $G\alpha_{i3}$ antibody capture [^{35}S]-GTPγS binding assay in CHO cell membranes expressing $h5HT_{1B}$ receptors in assay medium containing 100mM NaCl but as an inverse agonist in the same assay at 10mM NaCl: in other words as a protean agonist (Newman-Tancredi, *et al.*, 2003b).

1.5 Agonist-directed stimulus trafficking

Theoretical models are useful conceptual frameworks for stimulating thought and guiding the design of new experimental strategies but are only as good as the data that

support or refute them. In a debate recorded by Newman-Tancredi (2003a) in the International Congress Series, Brann and others have re-asserted the usefulness of the concept of receptor-reserve in explaining many findings initially attributed to stimulus trafficking, particularly where restricted sets of compounds have been used. However, potency order reversals, or of greater significance, efficacy (relative activity) order reversals, where adequate control of potential confounding factors exists, cannot be explained on a 'strength of signal' basis (Kenakin, 1995b; Clarke & Bond, 1997; Kenakin, 2003). Kenakin (2003) has summarised some of the original papers describing trafficked agonist responses. In Table 1 I have reviewed key findings of the literature published since 2000 which have been generated at serotonergic 5-$HT1_{A/B/D}$, adrenergic α_{2A}, dopaminergic $D_{2\ short}$, neurotensin NTS1, cannabinoid CB2, oxytocin OT and virally-encoded U51 chemokine receptors. Clarke, speaking in the same debate (Newman-Tancredi, 2003), has suggested that one might expect the degree of pharmacological divergence (and therefore the probability of observing stimulus trafficking) would increase with increasing molecular distinction between coupling pathways. Thus, comparisons of two Gα coupled pathways might be expected to yield 'strength of stimulus' based differences, while comparison of G-protein and non-G-protein coupled responses at the same receptor (such as regulation of guaninie nucleotide exchange factors [GEFs] for small G-proteins like Ras [Pak, *et al.*, 2002], regulation of Na^+/H^+ exchangers [Hall, *et al.*, 1998], and β-arrestin mediated recruitment of a wide range molecules including Src family non-receptor tyrosine kinases [Luttrell, *et al.*, 1999], ERK1/2 MAP kinases [DeFea, *et al.*, 2000] and phosphodiesterase 4 isoforms [Perry, *et al.*, 2002]; Maudsley, *et al.*, 2005, for review) might yield clearly trafficked responses. However, the data presented in Table 1 clearly shows that stimulus trafficking can be observed between responses mediated by endogenous, recombinant and mutant G-proteins, when comparing Gα with Gα, Gα with Gβγ, and G-protein coupled with non-G-protein coupled responses. Trafficking may almost be considered to be the norm but care must be exercised in the interpretation of data before stimulus trafficking can be assumed. In addition to the 'strength of stimulus' consideration other possible confounding factors include:

1. Multiple ligand binding / interaction pockets including allosteric modulation. Allosteric compounds may enhance or reduce the effect of ligands interacting at the primary (or orthosteric) ligand binding site by interacting with a distinct (or allosteric)

binding site. The allosteric enhancers increase primary ligand affinity or efficacy while allosteric antagonists produce the opposite effect (see Neubig, *et al*., 2003 for further detail). Competitive antagonists have been used to demonstrate the common receptor binding site origin of trafficked responses but the existence of pathway-dependent permissive antagonism (see above, Kenakin, 2005) invalidates this approach since it is possible for a given receptor-ligand pair to inhibit one response pathway while having no effect on an other (eg. Akin, *et al*., 2002; Pauwels, *et al*., 2003b; Shoemaker, *et al*., 2005).

2. Methodological considerations including steady state vs. kinetic (especially FLIPR-based $[Ca^{2+}]_i$) readouts (eg. Shoemaker, *et al*., 2005), sodium or GDP concentration related pre-coupling in $[^{35}S]$-GTPγS binding assays (Pauwels, *et al.*, 1997; Newman-Tancredi, *et al*., 2003), time- or agonist concentration-related readout destabilisation (chemical and biochemical; Newman-Tancredi, *et al*., 2002), and altered expression of receptor or G-protein.

3. Recruitment of multiple activation pathways in systems believed to be stimulus biased to single molecular species (eg. Newman-Tancredi, 2003).

4. Host cell to host cell differences. For example, studies comparing data generated in C6-glial cells and African Green Monkey COS-7 (SV40 transformed kidney epithelial CV1) cells (Wurch, *et al*., 1999; Pauwels, *et al*., 2003b).

1.6 Concluding remarks

A large body of evidence exists to support the existence of stimulus trafficking. Indeed some features of data already in the literature may indicate that the phenomena I have predicted in theoretical terms above, exist in reality. For example, the selective but transient recruitment of $G\alpha_{i2}$ at low concentrations of 5-HT by the 5-HT_{1A} receptor followed by the stable recruitment of $G\alpha_{i3}$ at high concentrations (Newman-Tancredi, *et al*., 2002): thus, the $G\alpha_{i2}$ activation curve appears bell-shaped. These intriguing 3-dimensional locks we refer to as 7-transmembrane receptors are sure to present us with further complexities the more we study them. The challenge is for us to make sense of them and generate quantitative frameworks within which we can exploit their properties through drug discovery. In the following chapters of this thesis, I describe investigations into agonist stimulus trafficking at recombinant prostanoid $hCRTH_2$ receptors expressed in CHO cells. The findings are novel and may point the way to the

discovery of the first molecules to selectively trigger the desensitisation of a prostanoid receptor without classical second messenger activation.

Table 1. Summary of key stimulus trafficking literature since 2000. (Selected earlier references have been included where appropriate).

Receptor	Assay 1	Assay 2	Assay 3	Findings	Reference
$5HT_{1A}$	Xenopus laevis oocytes; I_{smoth}; non G-protein mediated?	Xenopus laevis oocytes; $I_{Cl(Ca)}$; Ca^{2+}-dependent marker of GPCR activation	Xenopus laevis oocytes; GIRK; $G_{\beta\gamma}$ mediated.	Same recombinant receptor in each assay; I_{smooth} has unique profile; F13714 is agonist in assays 2 & 3 but is antagonist in assay 1.	Heusler, *et al*., (2003)
$5HT_{1A}$	CHO cells; FLIPR-based Ca^{2+} assay; $G\beta\gamma_i$ mediated.	CHO cells; [^{35}S]-GTPγS; $G\alpha_{i2}$ measured.	-	Full agonists were agonists in both assays. GTPγS assay partial agonists were inactive in FLIPR assay. Small relative activity changes in the GTPγS assay became large changes in FLIPR assay. Agonist rank order changes.	Pauwels & Colpaert, 2003.
$5HT_{1A}$	CHO cells; FLIPR-based Ca^{2+} assay; wild type receptor: $G\alpha_{15}$ fusion protein.	CHO cells; FLIPR-based Ca^{2+} assay; mutant Thr^{149}Ala receptor: $G\alpha_{15}$ fusion protein.	-	Mutation of conserved Thr in IC2 of receptor inhibits calcium responses but not cAMP inhibition responses, ie. differential pathway coupling.	Wurch, *et al*., 2003
$5HT_{1A}$	CHO cells; [^{35}S]-GTPγS; $G\alpha_{i3}$ antibody capture assay.	CHO cells; [^{35}S]-GTPγS; $G\alpha_{i3}$ antibody capture assay; unlabelled GTPγS included.	-	Low [5HT] selectively activates $G\alpha_{i3}$. High [5HT] induces switch to other G-protein and destabilisation or suppression of $G\alpha_{i3}$. Trafficking at G-protein sub unit level revealed.	Newman-Tancredi, 2002
$5HT_{1B}$	CHO cells; [^{35}S]-GTPγS; $G\alpha_{i3}$ antibody capture assay. Same assay & conditions as Newman-Tancredi, 2002.	CHO cells; [^{35}S]-GTPγS; $G\alpha_{i3}$ antibody capture assay; unlabelled GTPγS included.	-	$G\alpha_{i3}$ accumulation signal stable ipo high [5HT]. Loss of signal is specific to $5HT_{1A}$ receptor. Protean behaviour of 5HT revealed by manipulation of [Na^+] (alteration of pre-coupling).	Newman-Tancredi, 2003

$5HT_{1B}$	Rabbit common carotid artery contraction; $G\beta\gamma_{i/o}$ mediated L-type Ca^{2+} channel assay.	Inhibition of forskolin stimulated cAMP in rabbit common carotid artery; $G\alpha_{i/o}$ assay.	-	All agonists tested active in assay 2; only some active in assay 1.	Akin, *et al*., 2002
$5HT_{2C}$	Standard [^{35}S]-GTPγS accumulation assay.	[^{35}S]-GTPγS $G\alpha_{i3}$ & $G\alpha_{q/11}$ antibody capture assay.	-	Receptor highly coupled to $G\alpha_{q/11}$, less so to $G\alpha_{i3}$. Agonists are NOT trafficked between the two readouts. Strength of stimulus changes observed. Differences in coupling could underpin apparently trafficked responses at the effector level.	Cussac, *et al*., 2002
α_{2A}	COS7 cells; WT receptor; ± co-exprsn $G\alpha_{15}$; IP_3 accumulation	COS7 cells; mutant α_{2A} $Thr^{373}Lys$ receptor; ± co-exprsn $G\alpha_{15}$; IP_3 accumulation	C6 glial cells; endogenous WT receptor; $G\alpha_{i/o}$ coupled.	Mutant & WT receptor agonist profiles equivalent in COS7. Co-exprsn. $G\alpha_{15}$ reveals agonism in antagonist molecules, ie. RG pair dependent. COS7 $G\alpha_{15}$ & C6 glial WT receptor agonist profiles different: trafficking?	Wurch, *et al*., 1999
α_{2A}	CHO cells; WT receptor; co-exprsn. $G\alpha_{15}$; FLIPR assay	CHO cells; $Asp^{79}Asn$ receptor; co-exprsn $G\alpha_{15}$; FLIPR assay	CHO cells; $Thr^{373}Lys$ receptor; co-exprsn $G\alpha_{15}$; FLIPR assay	Host, G-protein, assay same, agonist rank orders different: trafficking? Assay 1 here produces agonist profile not equivalent to profile of assay 1 in Wurch, *et al*., 1999.	Pauwels & Colpaert, 2000

α_{2A}	CHO cells; WT receptor; co-exprsn. $G\alpha_{15}$ or $G\alpha_{15}$ fusion protein; FLIPR assay	CHO cells; $Ser^{200}Ala$ receptor; co-exprsn. $G\alpha_{15}$ or $G\alpha_{15}$ fusion protein; FLIPR assay	CHO cells; $Ser^{204}Ala$ receptor; co-exprsn. $G\alpha_{15}$ or $G\alpha_{15}$ fusion protein; FLIPR assay	Extends observations in 2000a paper. Mutations alter binding affinity and agonist rank order of potency. Relate to R conformations. Differences observed even for closely related molecules. Suggests agonism or antagonism not a property of molecule; rather, is a property of R, G, L, E combination, ie. of the assay system environment.	Pauwels & Colpaert, 2000b
α_{2A}	COS7 cell membranes; WT receptor; ± mutant $G\alpha_o$; $[^{35}S]$-GTPγS accumulation assay.	COS7 cell membranes; WT receptor; ± mutant $G\alpha_o$; receptor binding assay.	-	Mutant G-proteins altered agonist rank orders of potency & max. effects, and changes in R binding affinity. Therefore, reciprocal changes in R & G behaviour occur demonstrating the transmission of information in a G →R direction.	Wurch, *et al*., 2001
α_{2A}	CHO cell membranes; WT receptor; ± mutant $G\alpha_o$ or $G\alpha_{i2}$; $[^{35}S]$-GTPγS accumulation assay.	C6 glial cells; WT receptor; ± mutant $G\alpha_o$ or $G\alpha_{i2}$; inhibition of forskolin stimulated cAMP.	-	Efficacy is mutant G-protein dependent: no efficacy (+ve or –ve through $G\alpha_{i2}$; spectrum observed through $G\alpha_o$. Efficacy is assay dependent: none observed in cAMP assay. Antagonist activity suggested to be pathway dependent since lack of correlation observed. However, some 'antagonist' effects not clearly demonstrated to be so.	Pauwels, *et al*., 2003

viral u51	COS7 cells; constitutive activation; IP_3 accumulation and $G\alpha_q$-dependent CRE activation.	COS7 cells; cytokine stimulated activation; IP_3 accumulation, Ca^{2+} mobilisation, and $G\alpha_{i/o}$-dependent CRE activation assays	COS7 cells; cytokine stimulated activation; ± recombinant G-proteins; IP_3 accumulation, Ca^{2+} mobilisation, and $G\alpha_{i/o}$-dependent CRE activation assays	Cytokines tested have distinct rank orders at each readout. R coupled to all $G\alpha_i$, $G\alpha_o$, $G\alpha_q$ & $G\alpha_{11}$ proteins co-exprsd. Stimulus biased systems provided further evidence of trafficking: different G-proteins produced different effects on constitutive activity but not on cytokine rank orders.	Fitzsimmons, *et al*., 2006
CB2	CHO cells; inhibition of [^{3}H] cAMP accumulation; $G\alpha_{i/o}$ mediated.	CHO cells; pERK-MAP accumulation; $G\beta\gamma_{i/o}$ mediated.	CHO cells; calcium mobilisation; $G\beta\gamma_{i/o}$ mediated.	Assays 2 & 3 produce equivalent agonist data but potencies vary on a 'strength of stimulus basis' relative to fractional receptor occupancy. Assay 1 vs. assay 2 produces different agonist rank order of potency but not assay 1 vs. assay 3. Same coupling? Kinetics and degree of response integration with Ca^{2+} readout will confound comparisons. Also fractional receptor occupancy is based on displacement of agonist radiolabel by agonist compds.	Shoemaker, *et al*., 2005
rat NTS1	CHO cells; IP_3 accumulation; $G\alpha_{q/11}$ mediated.	CHO cell membranes; stimulation of cAMP; $G\alpha_s$ mediated.	CHO cells; arachidonic acid production; $G\alpha_{i/o}$ mediated. Assay4: CHO cell membranes; [^{35}S]-GTPγS accumulation; $G\alpha_{i/o}$ mediated.	Reversal of agonist rank order potency between assays 1 & 2. Preferential coupling of R to $G\alpha_{i/o}$ and $G\alpha_s$.	Skrzydelski, *et al*., 2003

D_{2S}	CHO cells; WT & $Thr^{343}Arg$ mutant receptors; ± $G\alpha_o$, $G\alpha_{qo}$ & $G\alpha_{15}$ G-proteins; FLIPR Ca^{2+} assay.	CHO cell membranes; WT & $Thr^{343}Arg$ mutant receptors; ± $G\alpha_o$, $G\alpha_{qo}$ & $G\alpha_{15}$ G-proteins; [^{35}S]-GTPγS accumulation.	-	Pharmacology G-protein dependent. Paper refers to multiple activation binding sites but data fit better with stimulus trafficking. Distinct binding site hypothesis requires antagonists to be simple binding blockers, ie. with no efficacy.	Pauwels *et al*., 2001
OTR	Human prostate carcinoma DU145 cell membranes; endogenous receptor; [^{35}S]-GTPγS accumulation; $G\alpha_{i/o}$ mediated.	Recombinant expressing HEK293 & Madin-Darby canine kidney cell & endogenous expressing DU145 cell proliferation; $G\alpha_{i/o}$ mediated	DU145 cells; pERK1/2 detection; $G\alpha_{i/o}$ mediated. Assay 4: HEK293 cells; recombinant receptor; IP_3 accumulation; $G\alpha_q$ mediated.	Atosiban is antagonist at $G\alpha_q$ coupled OTR and agonist via $G\alpha_{i/o}$ coupled OTR. Investigation in range of $G\alpha_q$ based systems at varying R:G expression levels needed.	Reversi, *et al*., 2005

Chapter 2: Methods.

Procedures conducted by named individuals are indicated by the bar in the margin. Unmarked text indicates procedures conducted by author.

Although the assay methods described below have been developed such that they may be used for high throughput screening (HTS), none of the data described in this thesis was obtained as part of an HTS campaign. Indeed, with the exception of GW853481X, the molecules assayed for activity at $hCRTH_2$ receptors here were specifically excluded from high- and low- throughput screening campaigns because their structures were considered unsuitable for medicinal chemistry efforts.

2.1 Cell preparation and cell culture

2.1.1 Preparation of CHO $G\alpha_{16z49}$ cell line

(BIOCAT 80890; Prepared by Tanja Alnadaf & Bob Ames, GSK; used with permission)

A construct for the $G\alpha_{16}$ G-protein in which the last 49 amino acid residues were substituted for the last 49 residues of the $G\alpha_z$ G-protein was made by the method of Mody, *et al*. (2000) and cloned into the pCIH vector. CHO cells transfected with the plasmid were dilution cloned in the presence of 400 $\mu g\ ml^{-1}$ hygromycin B.

2.1.2 Preparation of CHO $hCRTH_2$ cell lines

(BIOCATs 94875 (CHO K1 $hCRTH_2$) and 80870 (CHO $G\alpha_{16z49}$ $hCRTH_2$; prepared by Ashley Barnes & Emma Koppe, GSK; used with permission)

The coding region of the $hCRTH_2$ gene (GenBank AB008535) was cloned into pcDNA3 (Invitrogen) at the *BamH*I-*Not*I site. The clone was cut out at the XbaI and EcoRI sites, and a Klenow sequence filled in. The clone was then ligated into pCIN3 at the EcoRI & EcoRV sites. The EcoRV site was destroyed in the process but the XbaI site is present at the 3'end of the $hCRTH_2$ gene. The resulting construct was linearised with SspI before transfection.

Transfection of CHOK1 Wild Type or CHO $G\alpha_{16z49}$ cells was achieved as follows: 10 μg of linearised DNA was mixed with 0.8 ml Lipofectamine® reagent and allowed to

stand for 20 min at room temp. The DNA mixture was combined with 9 ml of Optimem® and introduced to a culture flask containing cells from which medium had been aspirated. Flasks were returned to the incubator for 6 hr at the end of which spent transfection reagent was discarded, cells rinsed with PBS, and 50 ml tissue culture medium A added (DMEM-F12, 10% FCS, 2 mM L-glutamine, 400 μg ml^{-1} hygromycin B, 100 μM flurbiprofen). After 24 hr the medium was replaced by medium additionally containing 1mg ml^{-1} neomycin (culture medium B).

Routinely, cells were cultured in the presence of the non-selective COX1/2 inhibitor flurbiprofen to prevent autocrine stimulation and down-regulation of prostanoid $hCRTH_2$ receptors by endogenously synthesised prostaglandins. It was found necessary to adjust the concentrations of the antibiotics used in order to achieve suitable growth rates. In all subsequent studies cell culture medium of the following composition was used: DMEM-F12, 10% FCS, 2mM L-glutamine, 62.5 μg ml^{-1} hygromycin B, 0.25 mg ml^{-1} neomycin, 100 μM flurbiprofen (culture medium C).

Cells were separated using flow cytometry in order to isolate individual clones in the wells of 96-well tissue culture plates. Each clone was expanded and pharmacologically characterised. Single clones displaying the largest responses to PGD_2 were selected for further study.

2.1.3 Transient transfection of CHO $hCRTH_2$ cell lines with β-ARK 495-689

A construct encoding the C-terminal (residues 495-689) of β-adrenergic receptor kinase (β-ARK) was cloned into pcDNA3 (Invitrogen) at the *BamH*I-*Not*I site (Dickenson & Hill, 1998; kindly prepared by Ms. Nicola Hawley). CHO $G\alpha_{16z49}$ host cells, CHO $G\alpha_{16z49}$ $hCRTH_2$ cells or CHO K1 $hCRTH_2$ cells were grown to 80 % confluence, medium aspirated, and then washed with PBS. Cloned pcDNA was transfected into cells using Lipofectamine® according to manufacturer's instructions. For a single 75 cm^2 tissue culture flask 0.25 ml of diluted Lipofectamine® and 40 μg of diluted pcDNA were mixed and allowed to stand for 30 min at room temperature. The DNA mixture was combined with 9 ml of Optimem® and introduced to the flask which was incubated for 6 hr (CHO K1 $CRTH_2$ cells) or 3 hr (CHO $G\alpha_{16z49}$ $CRTH_2$ cells). At the end of this period the transfection mixture was removed and 50 ml of normal culture medium re-introduced. Cells were allowed to grow for a further 24 hr (CHO $G\alpha_{16z49}$ $CRTH_2$ cells) or 48 hr (CHO K1 $CRTH_2$ cells) before being plated out for assay.

2.1.4 Cell culture regime

CHO cells expressing $hCRTH_2$ receptors had a doubling time of approximately 18 hrs (determined by subjective assessment of confluency and split ratios) and were used for assays when 80 % confluent (judged microscopically). Split ratios at passage of 1:3-1:40 in culture medium C were used in order to bring flasks to the required level of confluency on the intended days. The impact of different split ratios on receptor expression was not assessed. Typically, a 1:3 split was used for 80 % confluency on the next day from an 80-90 % confluent flask. For maintenance culture, cells were passaged twice weekly at split ratios of 1:30 or 1:40. Cells were used at passages 6-28 and were plated at 2×10^4 cells $well^{-1}$ in 384 well plates.

2.1.5 Passage technique

Quantities specified are for one 175 cm^2 tissue culture flask. Cell culture medium was removed and the cell layer washed with 10 ml sterile phosphate buffered saline (PBS). After removal of the PBS, 5 ml Versene® was added and the flask incubated at 37 °C for 2-4 min until the cells detached from the plastic. Cells were dislodged from the plastic with a sharp knock and the resulting cell suspension titurated twice to ensure clumps of cells were disaggregated. Following centrifugation (100 x g, 5 mins) Versene® was removed and the cell pellet dispersed by manual shaking of the tube. Fresh culture medium C was added (10 ml) to provide a suspension for introduction to further tissue culture flasks containing 50ml medium C. The volume of suspension added was adjusted to achieve the intended split ratio.

2.2 Calcium mobilisation assay

2.2.1 Plating of cells for assay

Cell suspensions in fresh culture medium C were prepared as described above. For use in assays, the concentration of cells present in each suspension and the distribution of cell sizes, where relevant, was determined by automated cell counting using a Sysmex® cell counter according to the manufacturer's instructions. The volume of culture medium C added to cells was adjusted to give 4×10^5 cells ml^{-1} and 50 µl of the final suspension added to each well of a sterile, black-walled, clear bottomed poly-D-lysine coated 384 well plate [Greiner, Cat No 781946] using a Multidrop® microlitre

dispenser (384 well setting, 50 µl, 24 col). Plates were incubated for 18-24 hrs at 37 °C, 5 % CO_2 in air, 95 % humidity. For assays investigating the role of $G\alpha_i$-class G-proteins, cells were plated out in media additionally containing 50 ng ml^{-1} of pertussis toxin (PTX). Deviations from this method during assay development are noted in the text.

2.2.2 Assay procedure

Immediately prior to assay, culture medium was replaced with 30 µl $well^{-1}$ of assay buffer (sodium chloride 145 mM, potassium chloride 5 mM, calcium chloride 0.8 mM, magnesium chloride 0.1 mM, glucose 10 mM, HEPES 20 mM, 3 mM probenecid, and brilliant black 1 mM, pH 7.4) containing Fluo-3 AM (4 µM) & Pluronic F127 (0.044 %) using a Multidrop® (384 well setting, 30 µl, 24 col). Following incubation (37 °C, 90 min, air, ambient humidity) plates were transferred to a Fluorescence Imaging Plate Reader (FLIPR®; Molecular Devices) to monitor changes in Fluo-3 fluorescence after addition of compounds. Compounds eliciting an increase in fluorescence were taken to be agonists. In order to assess antagonist and/or inhibitory activity, the same plates were placed back into incubation (37 °C, 11 min, air, ambient humidity) before being returned to the FLIPR instrument for addition to all wells of an EC_{80} concentration of PGD_2. Compounds resulting in inhibition of PGD_2 EC_{80} responses were taken to be receptor antagonists, signal transduction inhibitors or assay specific inhibitors (e.g. fluorescent dye quenchers). The following FLIPR protocol settings were used: pipettor speed 5 µl sec^{-1}, tip height 30 µl, 2 x 10 µl mixes at 5 µl sec^{-1}, add sample after 5 s. Data were generated in triplicate from three separate experiments often performed on the same day using separately prepared compound dilutions and cell preparations; reagents were shared.

Compound dilutions were prepared in clear polypropylene 384 well plates keeping DMSO constant at 1 %, final assay concentration. This was achieved by making compound dilution series in 100 % DMSO (highest starting concentration typically 1 mM; ten 1 / 3 v v^{-1} dilution steps; Biomek 2000®), plating out 1 µl of each concentration per well (Biomek FX®), followed by the addition of 25 µl per well of assay buffer (Multidrop®) to generate dilutions in 4 % DMSO. Addition of buffer was carried out immediately prior to use of the compound plate. The final dilution to 1 % was achieved when compounds were added to the cell plate on the FLIPR instrument

(10 μl compound dilution + 30 μl assay buffer; highest final assay concentration of compound typically 10 or 1 μM). The final dilution factor for PGD_2 EC_{80} added in antagonist mode assays was 1 in 5; PGD_2 EC_{80} was determined experimentally on each day prior to assay. FLIPR tips were re-used where the same compounds were handled. In assays where multiple additions of compounds were made to the same wells of the assay plate concentrations and volumes were adjusted such that 1% DMSO final assay concentration was not exceeded. Deviations from this method during assay development are noted in the text.

2.2.3 Calcium assay-based investigations into desensitisation of $hCRTH_2$ receptors.

Desensitisation & synergism assays involved the addition of an agonist to $hCRTH_2$ expressing cells followed by subsequent application of the same or a different agonist after a suitable incubation period. The first application of agonist is referred to as 1st treatment; the second as 2nd treatment; the style of 1st and 2nd treatments varied according to the type of data being generated. In some experiments these assays were performed following application of protein kinase inhibitors and activators; this is referred to as 'pre-treatment'. In initial time course studies transient Ca^{2+} fluxes recovered to baseline by 10 min post-challenge; PGD_2-induced desensitisation was also essentially complete by 10 min post-challenge. Therefore the incubation periods between pre-treatment & 1st treatment, and between 1st & 2nd treatments was routinely set at 11 min.

The following protocols were used:

1. <u>Time course & effect of different PGD_2 concentrations on subsequent PGD_2 E/[A] curve generation.</u> In these assays, 1st treatment involved the application of PGD_2 dilution series (as eleven 1 / 3 v v^{-1} dilution steps) in a column-wise arrangement to the first 11 columns of a 384 well plate. Following incubation for times ranging from 1 min to 120 min, 2nd application of agonist took place. For 2nd treatment, PGD_2 dilution series were added again as eleven 1 in 3 steps in a row-wise arrangement to wells already exposed to agonist on first treatment. In this way 2nd treatment agonist curves (positive-going resulting in calcium elevation) were constructed in wells all treated with the same 1st treatment PGD_2 concentration, referred to as an EC_x (concentration of agonist producing an effect equal to x % of the maximum effect produced by that agonist).

2. Generation of PGD_2 and 15 keto $PGF_{2\alpha}$ pIC_{50} data. Compound IC_{50}'s were generated against PGD_2 EC_{70}. First treatment comprised addition of a compound dilution series; 2nd treatment comprised addition of PGD_2 EC_{70} to all wells exposed to 1st treatment.

3. Effect of protein kinase inhibitors on receptor desensitisation. These studies can be considered the mirror-image of those described at 1., above. Pre-treatment involved the application of the PKA inhibitor H89, the PKA activator dibutyryl cAMP, the PKC inhibitor GF109203X, vehicle (0.25 % DMSO), or combinations of either H89 or dibutyryl cAMP with GF109203X; 1st treatment comprised application of PGD_2 E/A] curves in a row-wise fashion; 2nd treatment was application of PGD_2 dilution series in a column-wise fashion such that an inhibition curve was produced at each PGD_2 EC_x (negative-going resulting in inhibition of calcium mobilisation).

4. Effect of agonist E/[A] curve generation on subsequent E/[A] curve generation. Both desensitisation and synergism were studied with this protocol. First treatment comprised addition of agonist (PGD_2 or UTP) dilution series row-wise to the wells of a 384 well plate. For desensitisation assays 2nd treatment comprised re-application of a dilution series of the same agonist (PGD_2/PGD_2 or UTP/UTP) to the same wells of the plate such that a given concentration of agonist was added twice to each well. For synergism assays, the approach was similar but 2nd treatment involved application of the other agonist (PGD_2/UTP or UTP/PGD_2).

2.3 [^{35}S]-guanosine-5'-O-(3-thio) triphosphate binding assays

2.3.1 Adaptation of cell line to suspension culture & cell culture regime; performed by Emma Koppe & Olutu Oganah; used with permission.

To facilitate large scale cell culture and membrane preparation, adherent CHO K1 $hCRTH_2$ clones were adapted to suspension culture. Adaptation was carried out once the clone had been expanded to yield a confluent 75 cm^2 TC flask and was achieved by culture of cells in serum-free medium in 2 l plastic Erlenmeyer flasks (Fisher Scientific, Loughborough, UK) with plug caps in an Innova shaking incubator (37 °C, 145 rpm, normal air [i.e., no CO_2]; New Brunswick Scientific, Edison, N. J.). Cells were grown to approximately 1 x 10^9 cells $flask^{-1}$ in 500 ml medium (approximately 2 x 10^6 cells ml^{-1} determined by light absorbance; pre-calibrated by haemocytometer counting). Culture medium (medium D) was of the following composition: DMEM-F12, pluronic F-68 0.1

% v v^{-1}, flurbiprofen 50 μM, neomycin 0.5 mg ml^{-1}. For storage cells were frozen down in Complete® medium containing 10 % DMSO at passage 12. On resuscitation, cells were centrifuged at 100 x g and resuspended in 10 ml medium D for culture in a 75 cm^2 flask. After 24 hr culture, cells were split 1:2 and resuspended in 2 x 15 ml medium D. After a further 24 hr culture the cells were suspended in 50 ml medium and introduced to 175 cm^2 flasks. Finally, after 3 days culture the contents of each 175 cm^2 flask were introduced into Ehrlenmeyer flasks, as described above. Maintenance culture was performed by splitting cells every 5 days with a 1 in 3 split at each passage.

2.3.2 Membrane preparation; performed by Bob Middleton & Jim Coote; used with permission.

For membrane preparation, cells were harvested by centrifugation of culture medium containing cells at 500 x g for 10mins. Pellets from multiple flasks were combined to produce a single cell pellet which was resuspended in 50 ml ice-cold HE buffer (50 mM HEPES, 1 mM EDTA, 100 μM leupeptin, 25 mg ml^{-1} bacitracin, pH 7.4 with potassium hydroxide). From 5 x 2 l flasks, approx. 8 ml of cell pellet were obtained, resulting in approx. 500 mg of membrane pellet. All subsequent steps were performed at 4 °C. Cells were homogenised for three 5 s periods using an Ultra-Turrax blender on blue-black setting (c.20,000 rpm) with 1 min between each period. The resulting homogenate was plunged into ice for 30 min to allow foam to settle following which it was passed through a 25 gauge syringe needle five times. To remove large fragments of debris the homogenate was centrifuged at 450 x g for 10 min, following which the supernatant was taken and centrifuged for a further 30 min at 22,000 x g. The final supernatant was discarded and the resulting pellet resuspended in ice-cold HE buffer (2 ml per three 175 cm^2 tissue culture flasks). Aliquots (100 μl) were stored frozen at -80 °C.

2.3.3 Protein determination

Membrane preparation protein concentration was determined using the bicinchoninic acid (BCA) method using a proprietary kit and according to the manufacturer's instructions (Sigma, Poole, UK). Proteins reduce alkaline Cu(II) to Cu(I) in a concentration-dependent manner. BCA is a highly specific chromogenic reagent for Cu(I) forming a purple complex with an Abs_{max} at λ = 562 nM. Absorbance is directly

proportional to protein concentration and was measured at λ = 550 nM on a ThermoMax microplate reader (Molecular Devices, Sunnyvale, CA). Linear regression and interpolation was performed using SoftMaxPro software. Samples did not contain more than the permitted amount of interfering substances. The kit reagents did not contain detergent.

2.3.4 Assay procedure

[^{35}S]-guanosine-5'-O-(3-thio) triphosphate (GTPγS) binding assays were performed using a 384-well plate-based LEADseeker® scintillation proximity assay (SPA; Amersham Biosciences, Amersham, U.K.). The assay utilises the agonist-stimulated replacement of GDP by GTP at activated Gα G-proteins (described by McKenzie, 1992). Under resting conditions GDP occupies the nucleotide binding site of Gα G-protein subunits which associate with G$\beta\gamma$ subunits to form a complete G-protein heterotrimer. The molecule binds to receptors via the C-terminal tail of the Gα subunit. Agonist binding produces a conformation change in the intracellular C-terminal of the receptor which facilitates G-protein interaction with the receptor and which conveys the activation signal to the G-protein. A conformation change results in the nucleotide binding site having preferential affinity for GTP which now replaces GDP triggering Gα-GTP dissociation from G$\beta\gamma$ subunits which go on to activate their respective effectors. The activation is terminated by the inherent Gα subunit GTP hydrolase activity which converts the bound GTP to GDP followed by re-association of the G-protein subunits into the non-activated heterotrimer. Agonist activation of receptors induces Gα-GTP formation in a concentration-related manner. When GTP is replaced by non-hydrolysable [^{35}S]-GTPγS, Gα-[^{35}S]-GTPγS cannot be inactivated by the hydrolase activity and thus accumulates in a manner dependent upon the degree of receptor activation. SPA is a method by which the radiolabelled G-proteins may be quantified. The technique utilises scintillant-containing polymer beads (often poly-vinyl toluene) coated with wheatgerm agglutinin (WGA) to immobilise membrane fragments expressing the receptor and G-proteins of interest by binding to N-acetylglucosamine present in many membrane-associated glycoproteins. By so doing, receptor and scintillant are brought into close proximity. Binding of [^{35}S] radioligand to the receptor results in the production of β-particles close enough to the beads to produce scintillation. Particles produced by non-bound radioligand are absorbed by the assay

medium (aqueous buffer) and do not produce a signal. Scintillation is detected using a suitable scintillation counter. LEADseeker is a development of the technology designed for 384 well-plate format assays in which scintillation can be detected using a Perkin Elmer Viewlux imaging plate reader; beads used in these studies were WGA coated polystyrene.

Membranes were rapidly thawed, titurated three times with a Gilson pipette and diluted to 1 mg ml^{-1} in assay buffer (HEPES 20 mM; magnesium chloride 10 mM; sodium chloride 100 mM; pH 7.4 with 1 M potassium hydroxide (aq)) also containing saponin to facilitate passage of compounds and radioligand into membrane vesicles (150 μg ml^{-1} diluted from a 10 mg ml^{-1} saponin solution in assay buffer at room temperature) and stored on ice. LEADseeker beads were suspended at 25 mg ml^{-1} in assay buffer supplemented with saponin 150 μg ml^{-1} immediately prior to mixing with membranes. Thirty minutes prior to assay, bead and membrane solutions were mixed 1 : 2 v v^{-1} in order to immobilise membrane fragments onto the beads, guanosine 5′-diphosphate added in order to reduce pre-coupling and hence basal radioligand accumulation (GDP, 30 μM diluted from a 10 mM solution in assay buffer kept on ice), and the suspension kept on ice with occasional agitation. [^{35}S]-GTPγS solution was diluted to 1.2 nM in assay buffer; immediately prior to adding radiolabel to the assay plate, GDP was added to yield 30 μM, final assay concentration.

Assays were performed in solid white non-sterile polystyrene 384-well micro titre plates (Nalge Nunc, Nerijse, Belgium) and proceeded for 1 hr at room temperature in a total assay volume of 42 μl comprising: 1 μl antagonist or vehicle, 1 μl agonist or vehicle, 25 μl radioligand and 15 μl bead / membrane mixture (added last to start the reaction). Scintillation counting was performed using a Viewlux® imaging plate reader (Perkin Elmer, Wellesley, MA) with a 5 min β-particle counting protocol. Binding signal (generated as described above from the accumulation of Gα-[^{35}S]-GTPγS on receptor-activated G-proteins with subsequent disintegration of the radionuclide to produce β-particles in close proximity to scintillant containing polystyrene beads) was stable between 60 and 120 min. Agonists and antagonists were prepared as 40 x concentrates in DMSO in clear polystyrene V-bottom 96-well micro titre plates (Nalge Nunc). Dilution series were prepared as eleven 1 / 3 v v^{-1} steps and transferred to assay plates using a Biomek FX® liquid handling robot. For antagonist mode assays 1 μl of 40 x PGD_2 EC_{80} in DMSO was added to all wells (0.8 μM to achieve 20 nM final assay

concentration). In order to eliminate carry-over of test compounds, reactants were added in the following order: radioligand, agonist (added column-wise), compounds (added row-wise working from lowest to highest [PGD_2]), bead/membrane mixture (added row-wise working from lowest to highest [PGD_2] with tip changes to prevent carry-over).

2.3.5 Pertussis toxin treatment of membranes

CHO K1 $hCRTH_2$ cell membranes were treated with pertussis toxin (PTX) as follows (quantities given are sufficient for approximately 100 wells of a 384-well plate): 250 µl of 100 mM dithiothreitol (DTT) in GTPγS assay buffer was mixed with an equal volume of 50 µg ml^{-1} PTX solution (as described in *Reagents and Compounds;* 250 µl PBS for sham-treated samples) and left to incubate at room temperature for 1 hr (i.e. final concentrations of 50 mM DTT + 25 µg ml^{-1} PTX in a 500 µl volume). Membrane suspension (200 µl, 5.9 µg ml^{-1}) was centrifuged (10,000 x g, 10 min, room temperature), the supernatant discarded, the pellet resuspended in 240 µl PTX assay buffer (HEPES 15 mM; magnesium chloride 10 mM; EDTA 2 mM; DTT 2 mM; thymidine 20 mM; nicotinamide adenine dinucleotide 10 µM; pH 8.0 with 1 M sodium hydroxide (aq)) and mixed with 260 µl DTT / PTX mixture (i.e. final concentrations of 26 mM DTT and 13 µg ml^{-1} PTX in a 500 µl volume). The resulting mixture was incubated for 30 min at room temperature prior to centrifugation (conditions as above) and resuspension of the pellet in 500 µl GTPγS assay buffer.

2.4 Radioligand binding assay

2.4.1 Membrane preparation

For membrane preparation, cells were harvested as described under '*Passage technique*' to produce a single cell pellet which was resuspended in 50 ml ice-cold HE buffer (50 mM HEPES, 1 mM EDTA, 100 µM leupeptin, 25 µg ml^{-1} bacitracin, 1 mM PMSF, 2 µM pepstatin A, pH 7.4 with potassium hydroxide). All subsequent steps were performed at 4 °C. Cells were homogenised for three 5 s periods using an Ultra-Turrax blender on blue-black setting (approx. 20,000 rpm) with 1 min between each period. The resulting homogenate was plunged into ice for 40 min to allow foam to settle

following which it was passed through a 25 gauge syringe needle five times. To remove large fragments of debris the homogenate was centrifuged at 450 x g for 10 min, following which the supernatant was taken and centrifuged for a further 30 min at 48,000 x g. The final supernatant was discarded and the resulting pellet resuspended 10 x volume in ice-cold HE buffer without PMSF and pepstatin A (2 ml per three 175 cm^2 tissue culture flasks). Aliquots (100 µl) were stored frozen at -80 °C.

2.4.2 Protein determination

Membrane protein concentration was determined as described in section 2.3.3.

2.4.3 [^{3}H]-PGD$_2$ competition binding, and assay development

Reactions were performed in a buffer of composition: 20 mM HEPES, 10 mM magnesium chloride, 1 mM potassium EDTA, adjusted to pH 8.0 with 1 M potassium hydroxide (aq). Cold PGD$_2$ (10 µM) was used for determination of non-specific binding (nsb). U-bottom deep-well 96-well blocks (Costar) were prepared containing 25 µl [^{3}H]-PGD$_2$ with 25 µl PGD$_2$ (nsb), 25 µl buffer (total binding) or 25 µl test compound or vehicle. The reaction was initiated by the addition of 50 µl of membranes and proceeded for 60 min at room temperature, or 30 min for competition binding assays. For protein linearity assays, membrane protein was diluted in the range 0.4 – 102 µg well^{-1} for CHO K1 hCRTH$_2$, and 0.08 – 19 µg well^{-1} for CHO Gα_{16z49} hCRTH$_2$. For all other assays, 6.4 µg well^{-1} CHO K1 hCRTH$_2$ and 12.8 µg well^{-1} CHO Gα_{16z49} hCRTH$_2$ membranes were used. The reaction was terminated by rapid filtration through a 96-well GF/A glass fibre filtermat pre-soaked in assay buffer, which was subsequently dried and treated with Meltilex solid scintillant (Wallac, Turku, Finland). Results were obtained by scintillation counting (1450 Microbeta Trilux liquid scintillation counter, Wallac) using a suitable 1 min [^{3}H] counting protocol. Microbeta counter efficiency is generally around 20 % (i.e. 80 % of radionuclide disintegrations are not detected) resulting in data expressed as counts per minute, rather than disintegrations per minute. Count per minute (cpm) data were corrected by the counter software for quench and inter-detector variability. Data used were therefore corrected counts per minute (ccpm). Assays were performed in triplicate in three separate experiments.

2.4.4 [^{3}H]-PGD$_2$ saturation binding

Conditions used in this experiment were as follows: buffer composition as described above; [^{3}H]-PGD$_2$ dilution series – 1 / 2 v v^{-1}, 0.03 nM – 13 nM; membrane concentrations - CHO K1 hCRTH$_2$ 12.8 μg well^{-1}; CHO Gα_{16z49} hCRTH$_2$ 6 μg well^{-1}; CHO Gα_{16z49} host 5.8 μg well^{-1}; cold [PGD$_2$], plate preparation and other conditions as described above. The binding reaction proceeded for 60 min at room temperature and was terminated by filtration, as before. For saturation analysis, ccpm data were further corrected for counter efficiency by reference to standard samples diluted in Optiphase Gold liquid scintillant and counted on a Wallac 140905A liquid scintillation counter using a 1 min tritium counting protocol. Assays were performed in triplicate in three separate experiments.

2.5 Western blot analysis

Sodium dodecyl sulphate – polyacrylamide gel electrophoresis (SDS - PAGE) was performed using the NuPAGE ® electrophoresis system (Invitrogen, Paisley, UK) according to the manufacturer's instructions. Briefly, samples were prepared in a total volume of 100 μl comprising 50 μl sample, 25 μl LDS sample buffer and 10 μl NuPAGE sample reducing agent (dithiothreitol) in order to load 5 μg protein 10 μl^{-1} well^{-1}. The resulting mixture was incubated at 65-70 °C for 10 min, and 10 μl loaded into the wells of a 10 % Bis-tris gel with 4 μl Multi Mark molecular weight markers in lanes 1 & 12. The gel was electrophoresed for 60 min at 200 V constant in NuPAGE MOPS running buffer until the blue dye track reached the gel base. For Coomassie Blue staining and visualization the gel was immersed in Simply Blue Safestain for 24 hrs with shaking following which it was removed and rinsed with water. Stained and rinsed gels were dried overnight between two cellophane sheets previously soaked in Gel-Dry drying solution.

Western Blot was performed on electrophoresed but not stained gels using the NuPAGE XCell Mini-Cell and Blot Module according to the manufacturer's instructions. Gels were placed on a nitrocellulose membrane previously soaked in Transfer Buffer, and two 0.45 μM filter papers, also pre-soaked, before being arranged in a Western blot tank with the gel nearest the cathode. The blot was run for 60 min at 30 V, constant, in Transfer Buffer. Equivalence of protein loading was demonstrated by immersing blots in a staining solution of 0.2 % w v^{-1} Ponceau S in 3 % w v^{-1} trichloroacetic acid (aq) for

5-10 min, followed by a water rinse. Following photographic recording, dye was completely removed by washing in water for 1 hr.

Western blot antibody treatment - Nitrocellulose membranes containing proteins were blocked by soaking in Block Buffer (BB; 5 % w v^{-1} Marvel ®, 20 mM Tris-HCL, 30 mM sodium chloride, 0.1 % w v^{-1} T20) for 1hr at room temperature, with shaking. BB was then replaced by 10 ml of a 1/500 v v^{-1} dilution of primary antibody (except for $\alpha G\alpha_q$: 1/1500 v v^{-1}) in BB and incubated for 18 hrs at 4 °C, with rocking. Membranes were immersed for 10 mins in fresh wash buffer (WB; 20 mM Tris-HCL, 30 mM sodium chloride, 0.1 % w v^{-1} T20) three times before being incubated for 1 hr at room temperature in 10 ml of a 1/1000 v v^{-1} dilution of horseradish peroxidase (HRP) conjugated secondary antibody in BB. Finally, membranes were again washed by immersion for 10 mins in three changes of fresh WB.

Detection – HRP was detected using the Super Signal West Pico (SSWP) Chemiluminescent Substrate kit (Pierce, Rockford, IL). Briefly, 5 ml SSWP stable peroxide solution was added to 5 ml SSWP luminal / enhancer solution. The resulting solution was added to the antibody-treated Western blot and incubated for 5 min at room temperature, with shaking. Following this the solution was discarded and the blot wrapped in cling film before placing in a film cassette containing a Hyperfilm ECL sheet (Amersham Ltd., Amersham, UK). After exposure at room temperature (1-20 s) the film was developed.

2.6 Data Analysis

2.6.1 Data normalisation:

Data was not normalised with respect to a reference response (for example, ionomycin). Instead, data from each well in calcium mobilisation assays were normalised with respect to the basal fluorescence in that well according to the equation:

$$Normalised\ FIU = 100 \times \frac{(\max - \min)}{basal} \qquad \text{Eqtn. 1}$$

Where 'basal' is the average of five fluorescence readings taken at 1s intervals prior to addition of compounds or vehicle, 'max-min' is the result of maximum fluorescence reading minus minimum fluorescence reading in the 55 s following compound addition, and 'normalised FIU' are normalised FLIPR Intensity Units. By so doing, and

controlling the number of cells seeded into each well, variations in data due to differential cell multiplication or confluency, and differential dye loading were removed. Addition of any liquid, even buffer, to wells resulted in a transient decrease in fluorescence followed by partial recovery to a new lower steady state, therefore basal fluorescence is not synonymous with minimum fluorescence.

2.6.2 Curve fitting:

A four-parameter logistic equation of the form:

$$E = \frac{E_m [A]^{nH}}{EC_{50}{}^{nH} + [A]^{nH}} \qquad \text{Eqtn. 2}$$

was fitted to data. Thus, estimates of maximum effect (E_m), curve mid-point (EC_{50}), and Hill slope (n_H) were obtained; other terms in the equation are effect (E) and concentration ([A]).

2.6.3 Calculation of affinity estimates – antagonism. Constancy of agonist E/[A] curve shape in the presence of increasing antagonist concentrations was assessed by computerised curve-fitting followed by students t-test on asymptotes and slopes. At concentrations of antagonist producing small amounts of curve shift, agonist curve shape was often unaffected. These data were used to determine empirical estimates of apparent antagonist affinity based on the method of pA_2 determination (apparent pA_2) as follows:

Computed EC_{50} values were used to calculate affinity estimates (pA_2) according to the equation:

$$pA_2 = -\log[B] + \log(CR - 1) \qquad \text{Eqtn. 3}$$

Where [B] is the antagonist concentration and CR is the ratio of agonist E/[A] curve EC_{50} values in the presence and absence of antagonist calculated as:

$$CR = EC_{50\,TREATED} / EC_{50\,CONTROL} \qquad \text{Eqtn. 4}$$

Where constancy of agonist E/[A] curve shape in the presence of increasing antagonist concentrations was shown (assessed by computerised curve-fitting followed by students t-test on asymptotes and slopes) computed EC_{50} values were fitted to a modification of the Schild equation (Arunlakshana & Schild, 1959) suitable for non-linear regression (Lew & Angus, 1995).

$$-\log EC_{50} = -\log([B] + 10^{-pKb}) - \log c \qquad \text{Eqtn. 5}$$

Where the constant –logc is the difference between the agonist control curve EC_{50} and the antagonist affinity (pK_b). The curve fitting process also provides estimates of Schild slope and a value representing the linearity of the plot. Where these values were consistent with unit slope and linearity, the data was taken to be commensurate with the expectations of simple competitive interaction and a pK_b value was quoted.

Individual estimates of curve parameters and affinity values were obtained at each antagonist concentration in each experiment and then averaged to provide mean data. Quoted values are therefore the mean ± standard error (sem) of n separate experiments, each derived from a separate set of compound dilutions and cell preparations.

2.6.4 Calculation of affinity estimates – Saturation binding: The amount of specific radioligand binding to each receptor type was calculated as the difference between total and non-specific binding at each concentration. Three equations were fitted to data:

1. A hyperbolic plus linear equation fitted to total binding data.

$$ccpm = \frac{B\max.[B]^{nH}}{K_d^{nH} + [B]^{nH}} + m[B] \qquad \text{Eqtn. 6}$$

Where ccpm are corrected counts per minute as defined above, B_{max} is the maximum amount of radioligand binding under saturating conditions, [B] is the concentration of radioligand, K_d is the radioligand binding dissociation constant, n_H is the Hill slope, and m is the slope of the linear nsb relationship.

2. A linear equation fitted to non-specific binding data and using the value of m to constrain fitting to equation 1.

$$nsb = m[B] + c \qquad \text{Eqtn. 7}$$

Where nsb is non-specific binding, m is the slope of the relationship, [B] is the concentration of radioligand and c is the intercept of the line on the ccpm axis which should equal background radiation.

3. A hyperbolic equation fitted to specific binding data.

$$ccpm = \frac{B\max.[B]^{nH}}{K_d^{nH} + [B]^{nH}} \qquad \text{Eqtn. 8}$$

Where terms are as previously defined.

For each data set, the fitting method giving rise to parameter estimates with the smallest fitting errors was used. Where parameter estimates did not bear a close relationship to observed data, the estimates were not used regardless of the fitting error size.

2.6.5 Calculation of Z':

Z' is a statistical parameter that expresses in a single numerical value the relationship between signal window and statistical variation in the maximum and minimum response values for an assay (Zhang, *et al*., 1999). The parameter may adopt values from 1.0 (for a perfect assay with no statistical variation around the maximum and minimum values) to -∞ (for an assay with no signal window relative to the variability). In practice, values between 0 and 0.8 are obtained; values above 0.2 are acceptable for assays determining compound activity from complete concentration-effect curves. Z' is calculated as follows:

$$Z' = 1 - \frac{(3SD_{\max}) + (3SD_{\min})}{\bar{x}_{\max} - \bar{x}_{\min}} \qquad \text{Eqtn. 9}$$

Where SD is standard deviation, $\bar{x}$ is arithmetic mean, and max / min denote maximum and minimum responses.

2.6.6 Statistical analysis

For all assays, individual estimates of curve parameters and affinity values were obtained in each experiment and then averaged to provide mean data. Quoted values are therefore the mean ± standard error of the mean (s.e.m.) of n separate experiments, each derived from a separate set of compound dilutions and cell preparations. Unless otherwise stated n = 3 throughout.

Where quoted relative potency (RP) = EC_{50} (test agonist) / EC_{50} (reference agonist) and relative activity (RA) = E_{max} (test agonist) / E_{max} (reference agonist).

Statistical analysis was performed using an unpaired, two-sided Student's t-test in GenStat 8.1 (Lawes Agricultural Trust, through VSN International) software. $P < 0.05$ was taken to indicate statistical significance.

Comparison of agonist fingerprint data was performed using ANOVA in SAS System v.9.0 software (SAS, Marlow, U.K.); each compound was then compared to PGD_2 data using a Dunnett's *post hoc* comparison. Slope data were analysed as $\log_{10}$ of the slope values.

2.7 Reagents and compounds

Heat-inactivated foetal calf serum (Cat. No. 01000-147), Versene, L-Glutamine, neomycin (Geneticin; G418), & phosphate buffered saline were obtained from Gibco-BRL, Ltd., Paisley, U.K.. Dulbecco's Modified Eagle Medium HAM F12 mix, hygromycin B, flurbiprofen, probenecid, prostaglandin D_2 (PGD_2), N 6,2′-O-dibutyryladenosine 3′,5′-cyclic monophosphate sodium salt (dibutyryl cAMP), uridine 5′ triphosphate (UTP), pertussis toxin, non-steroidal anti-inflammatory drugs (NSAIDs), magnesium chloride hexahydrate, sodium chloride, guanosine diphosphate and saponin were obtained from Sigma Ltd., Poole, Dorset, U.K.. Thapsigargin, ryanodine, H-89, SC-51322 and U73122 were obtained from Biomol International L.P., Plymouth Meeting, Pennsylvania, USA. Pluronic F127 & fluo-3 acetoxy-methyl ester were obtained from Molecular Probes Inc. Brilliant Black BN was obtained from ICN Biomedicals Inc., Irvine, California, USA.. GW671021X (L-798106; 5 - Bromo - 2 - methoxy - N - [3 - (2 - naphthalene - 2 - yl - methylphenyl) - acryloyl] - benzene sulphonamide), GF109203X (2-[1-(3-dimethylaminopropyl)-1H-indol-3-yl]-3-(1H-indol-3-yl)maleimide), GW627368X ((N-{2-[4-(4,9-diethoxy-1-oxo-1,3-dihydro-2H-benzo[f]isoindol-2-yl)phenyl]acetyl} benzene sulphonamide), GW853481X (compound 10c in European Patent Application EP1170594 A2; (1-benzothiazol-2-ylmethyl-5-fluoro-2-methyl-1h-indol-3-yl)-acetic acid), AH23848B (([1α(z), 2β5α]-(±)-7-[5[[(1,1'-biphenyl)-4-yl]methoxy]-2-(4-morpholinyl)-3-oxocyclopentyl] -5-heptenoic acid), BWA868C90 (3-benzyl-5-(6-carboxyhexyl)-1-(2-cyclohexyl-2-hydroxyethylamino)-hydantoin) and BW245C ((4S)-(3-[(3R,S)-3-cyclohexyl-3-hydropropyl]-2,5-dioxo)-4-imidazolidineheptanoic acid) were obtained from GlaxoSmithKline Pharmaceuticals Ltd, Stevenage, Herts., UK. Prostanoid agonists, SC-19220 and other antagonists were obtained from Cayman Chemical Company, Ann Arbor, Michigan, U.S.A.. Rabbit polyclonal ($\alpha G\alpha_i$ [SC-262], $\alpha G\alpha_s$ [SC-823], $\alpha G\alpha_z$ [SC-388], $\alpha G\alpha_q$ [SC-393], $\alpha G\alpha_{11}$ [SC-394], $\alpha G\alpha_{q/11}$ [SC-392]) & goat polyclonal ($\alpha G\alpha_{16}$ [SC-7416]) primary antibodies, and horseradish peroxidase-conjugated bovine anti-rabbit [SC-2379] and donkey anti-goat [SC-2033] secondary antibodies were obtained from Santa Cruz Biotechnology Inc., Santa Cruz, CA).

Pertussis toxin, supplied as 200 μg ml^{-1} in 50 % glycerol, was diluted to 50 μg ml^{-1} in PBS and stored at 4 °C.

Flurbiprofen (10 mM) was made up as follows: approximately 15 mg flurbiprofen was dissolved in DMSO to produce a 100 mM solution and 12 μl of 2 M sodium hydroxide (aq) added. The resulting solution was diluted 1:10 with PBS and sterile filtered through a 0.22 μM Acrodisc® syringe filter unit or similar into a sterile container. If the solution failed to go clear following addition of the PBS then more sodium hydroxide was titrated in prior to filtration.

Fluo-3 AM was dissolved in DMSO to give a 2.27 mg ml^{-1} (2 mM) solution and was stored at 4 °C. Prior to addition to assay buffer, the Fluo-3 solution was mixed with the appropriate volume of pre-warmed pluronic F127 solution. Brilliant black was prepared as a 100 mM concentrate in MilliQ water and sterile filtered before storage at 4 °C.

PGD_2 and other prostanoid agonists were dissolved at 1 or 10 mM in absolute ethanol and stored at -20 °C. Where compounds were supplied in methyl acetate, the solvent was evaporated to dryness with gentle heating, and the prostanoid re-dissolved in ethanol.

$[^3H]$-PGD_2 (approximately 640 nM solution in 3:2:1 v v^{-1} mixture of methanol : water : acetonitrile; specific activity 5.77 TBq $mmol^{-1}$ / 3.7 MBq ml^{-1}; stored at -20 °C), $[^{35}S]$-GTPγS (900 nM, 37 MBq ml^{-1}; Amersham, U.K.) and LEADseeker® scintillation proximity assay beads were obtained from Amersham Biosciences, Amersham, UK.

pcDNA containing a sequence encoding β-ARK 495-689 was the kind gift of Ms. Nicola Hawley, Institute of Cell Signalling, Queen's Medical Centre, Nottingham, UK.

Chapter 3:

Structure-activity relationship of prostanoid receptor ligands at human prostanoid $CRTH_2$ (DP_2) receptors: critical dependence upon G-protein coupling partner.

3.1 Summary:

The cloned human prostanoid $CRTH_2$ receptor was expressed in CHO cells with the chimeric $G\alpha_{16z49}$ G-protein. Prostaglandin D_2 (PGD_2; 0.5 nM – 10 μM) produced concentration-related elevation of intracellular calcium (pEC_{50} 7.8 ± 0.2; n_H 1.1 ± 0.08) in a fluorescence-based calcium mobilisation assay. Culture of cells in the presence of the COX1/2 inhibitor flurbiprofen (100 μM) was essential for high agonist potency suggesting that endogenous prostanoid synthesis by the host cells reduces $CRTH_2$ agonist potency.

The observed rank order of agonist potency was as described in the literature for this receptor: 15 R 15 methyl PGD_2 > PGD_2 > PGJ_2 > 15 deoxy $\Delta^{12,14}$ PGJ_2 > 15 S 15 methyl PGD_2 > 13,14 dihydro 15 keto PGD_2 >> $PGF_{2\alpha}$. BW245C, PGE_2, PGI_2 & U46619 were without significant effect. The antagonists BWA868C (DP_1), SC19220 (EP_1), GW627368X (EP_4), and SQ29548 (TP) were without effect demonstrating that these receptors were not mediators of responses to PGD_2. Extracellular calcium was not required for the production of calcium transients in these experiments. However, PGD_2 responses were markedly inhibited by pertussis toxin (PTX) indicating transduction through $G\alpha_{i/o}$ class G-proteins.

When the $G_{\alpha16z49}$ component was isolated in PTX-treated chimera-expressing cells, reversals of potency order were observed compared to responses in untreated cells. These were most striking for (relative potency CHO $G\alpha_{16z49}$, CHO $G\alpha_{16z49}$ + PTX; PGD_2 = 1.0) 17 phenyl PGD_2 (85, c. 30), 15 R 15 methyl $PGF_{2\alpha}$ (11, NSE) & 15 deoxy $\Delta^{12,14}$ PGJ_2 (31, 2). The rank order of agonist potency following PTX treatment was: 15 (R) 15 methyl PGD_2 > PGD_2 > PGJ_2 = 15 deoxy $\Delta^{12,14}$ PGJ_2 > 13,14 dihydro 15 keto PGD_2 > 15 (S) 15 methyl PGD_2. $PGF_{2\alpha}$ & BW245C were without effect. The potencies of J series prostanoids were largely unaltered, while F & D series prostanoid potency decreased after PTX treatment.

15 R 15methyl $PGF_{2\alpha}$ was active in non PTX-treated cells (pEC_{50} 6.4 ± 0.08; relative activity cf. PGD_2 0.6) but inactive in PTX treated cells. In contrast, 13,14 dihydro 15 keto $PGF_{2\alpha}$ was inactive here but has been reported as a low potency agonist in a cAMP lowering assay reported elsewhere and a high potency binding ligand (pKi 8.5). These molecules may therefore represent receptor-G-protein-effector selective agonists or antagonists. Two molecules produced dextral shifts of PGD_2 E/[A] curves and were

identified as $CRTH_2$ receptor antagonists: AH23848B (pA_2 5.3 ± 0.1) and GW853481X pA_2 (6.5 ± 0.07).

These data have been used to produce an agonist pharmacophore at human prostanoid $CRTH_2$ receptors (see below) and demonstrate the critical importance of the receptor-G-protein-effector grouping as the SAR-determining unit in biochemical assays.

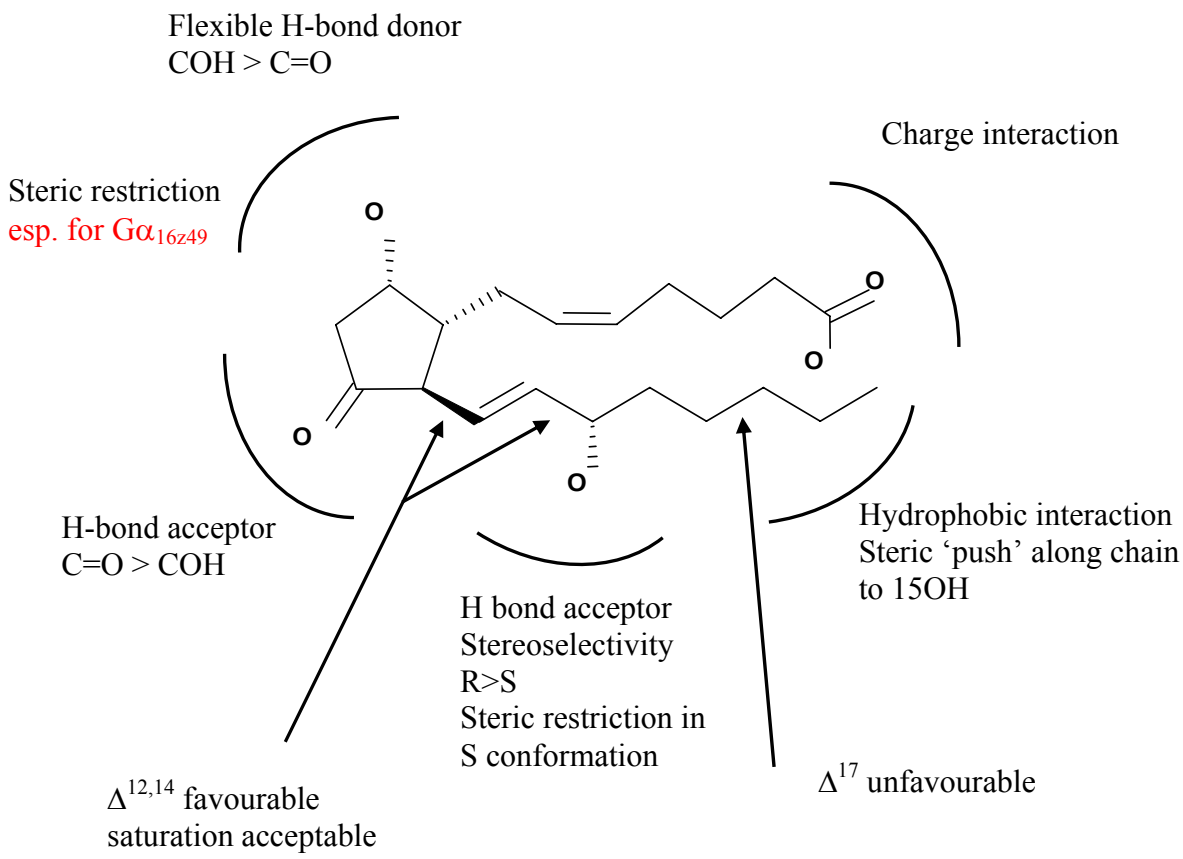

3.2 Introduction:

Heterotrimeric ($\alpha\beta\gamma$) G-proteins are a family of membrane-associated proteins. They are central to the expression of cellular responses to a range of extracellular stimuli which elicit their effects through cell-surface receptors (Downes & Gautum, 1999; Kostenis, *et al*., 2005, for reviews). There are 16 α-subunit, 5 β-subunit and 14 γ-subunit genes, each encoding a separate protein product, with splice variants existing for at least two α-subunit genes. Whilst it is clear that not all possible combinations of gene products are allowed, definitive information mapping the existence of heterotrimer combinations in all settings is limited but growing. However, it *is* possible to state that a restricted set of non-dissociating $\beta\gamma$ complexes exist but their relationship to the α-subunits is not clearly understood. Thus, there exists the potential for a large number of distinct protein complexes.

G-protein α-subunits are classified according to their sequence homology and the intracellular effectors with which they interact (Milligan & Kostenis, 2006): $G\alpha_s$ to stimulation of adenylate cyclase, $G\alpha_{i/o}$ to the opposite effect – inhibition of adenylate cyclase (though this ability is not shared by $G\alpha_t$ and $G\alpha_{gust}$; $G\alpha_{i/o}$ may also be coupled to regulation of certain Ca^{2+} and K^+ ion channels), $G\alpha_{q/11}$ to stimulation of phospholipase Cβ and elevation of intracellular calcium, and $G\alpha_{12/13}$ to stimulation of the low molecular mass G-protein Rho. This list is of effectors is by no means comprehensive and the reader is directed to the review by Milligan & Kostenis (2006) for a more thorough description. G-protein coupled receptors (GPCRs) are often classified according to the G-protein with which they classically couple but this relationship is by no means definitive: a given receptor can couple with multiple G-proteins (for example, splice variants of the prostanoid EP_3 receptor exist which can couple to $G\alpha_s$, $G\alpha_i$, & $G\alpha_q$ G-proteins; Namba, *et al*., 1993) and G-proteins exist with the property of coupling to receptors of multiple transduction classes. This latter group of G-proteins, know as 'promiscuous' or 'universal' coupling G-proteins, are members of the $G\alpha_{q/11}$ family, and comprise $G\alpha_{14}$, $G\alpha_{16}$ and its murine equivalent, $G\alpha_{15}$ (Ho, *et al*., 2001; Offermanns & Simon, 1995). 'Universal' coupling is a misnomer since many examples of GPCRs that do not couple through them are known but none-the-less they have found wide application in the arenas of orphan receptor ligand fishing (Wise, *et al*., 2004) and drug discovery assay development where the creation of cell lines

containing widely-coupling G-proteins gives the greatest probability of establishing useful screening systems for any given GPCR (Kostenis, *et al*., 2005).

In a search to identify a truly universal G-protein, much attention has focused on establishing the structural determinants of G-protein / receptor coupling specificity in order to create modified G-proteins with greater promiscuity: the so-called chimeric G-proteins. Chimeric G-proteins consist of a G-protein backbone suitable for the effector readout one wishes to exploit, with key amino residues substituted to provide coupling specificity for a desired receptor class. Building on earlier work establishing the key role of the C-terminal penta-peptide of $G\alpha_i$ and $G\alpha_s$ as a GPCR interaction site, Conklin, *et al*. (1993) demonstrated that an effective chimera could be produced allowing coupling of the normally $G\alpha_i$-coupled adenosine A_1 and dopamine D_2 receptors to inositol phosphate production by substitution of only three C-terminal amino acid residues of $G\alpha_q$ for those of $G\alpha_{i2}$ (G_q-G_{i2}3; $G_{q\text{-}i}$3). Maximally effective chimeras substituted between four and nine residues; this and other groups have established Gq-Gs, Gi-Gq, Gi-Gs, Gs-Gi and Gs-Gq chimeras displaying varying degrees of coupling promiscuity (Milligan & Rees, 1999, for review). This work has been greatly expanded and refined such that we now understand that there are at least four other regions of the G-protein molecule important to determination of receptor coupling specificity: the extreme N- and C- termini, the αN-β1 loop, the α4-β6 region and the α5 helix (Kostenis, *et al*., 2005, for review).

The promiscuous G-protein, $G\alpha_{16}$, is unable to couple to several receptors normally associated with $G\alpha_i$ class G-proteins (Mody, *et al*., 2000; Kostenis, *et al*., 2005). In order to circumvent this limitation, chimeras built on a $G\alpha_{16}$ backbone with coupling determination sequences taken from $G\alpha_{i/o}$ G-proteins have been created (Mody, *et al*., 2000). This group chose to use sequences taken from the pertussis insensitive $G\alpha_z$ G-protein because of its ability to couple a wide range of G_i coupled GPCRs to inhibition of adenylate cyclase. Two of the resulting chimeras, G_{16}-G_z25 (substitution of the α5 helix) and G_{16}-G_z44 (substitution of approximately half of the α4-β6 region and the α5 helix) were found to substantially increase the coupling promiscuity of $G\alpha_{16}$ toward G_i coupled receptors. Because of this, and the observation that $G\alpha_{16}$ is a suitable coupling partner for other chemoattractant receptors (Yang, *et al*., 2001), we decided to use a G_{16}-G_z49 chimeric G-protein to generate a calcium coupled cell line for the chemoattractant receptor, $CRTH_2$ (chemoattractant receptor homologous molecule of

Th2 cells; Nagata, *et al*., 1999) which is activated by the prostanoid prostaglandin D_2 (PGD_2).

Prostanoids are a group of lipid hormone mediators that are derived from C-20 fatty acids (Smith, 1992) by the action of cyclo-oxygenases (COX) 1, 2 (Smith, 2000, for review) and 3 (Chandrasekharan, *et al.*, 2002; Chandrasekharan & Simmons, 2004). They consist of the prostaglandins (PG) and the thromboxanes (Tx) and they elicit a wide variety of biological responses through activation of G-protein coupled receptors (Coleman, *et al*., 1994; Narumiya, *et al*., 1999; Breyer, *et al*., 2001). The prostanoid receptor family consists of eight distinct rhodopsin-like receptor proteins each being the product of an individual gene. These have been termed the DP, EP_1, EP_2, EP_3, EP_4, FP, IP and TP receptors. In most cases, the myriad biological functions stimulated by prostaglandins are transduced by activation of G-proteins (Bos, *et al*., 2004; Hata & Breyer, 2004). Thus prostanoid DP, EP_2, EP_4 and IP receptors are classically associated with elevation of intracellular cyclic adenosine monophosphate (cAMP) levels through activation of G_s G-proteins; EP_1, FP and TP receptors with elevation of intracellular calcium through G_q (though not clearly established for EP_1; Bos, *et al*., 2004); and EP_3 with reduction of intracellular cAMP levels through G_i. However, these classical associations aren't always applicable depending upon the test system under scrutiny and in the cases of EP_1, EP_3 and TP, upon the splice variant being studied (Pierce & Regan, 1998).

Recently, the ninth prostanoid receptor named $CRTH_2$ or DP_2, was identified through differential gene expression studies using human T-helper lymphocytes (Nagata, *et al.*, 1999). Prostaglandin D_2 (PGD_2; Figure 1) was later shown to be the natural ligand for this receptor (Hirai, *et al*., 2001). $CRTH_2$ is a 7-trans-membrane sequence receptor (7TMR) belonging to G-protein coupled receptor (GPCR) family A and is most closely related structurally to other leukocyte chemoattractant receptors (Abe, *et al*., 1999; Nagata & Hirai, 2003). $CRTH_2$ is coupled via pertussis-toxin sensitive $G\alpha_{i/o}$ to reduction in intracellular cAMP (Sawyer, *et al.*, 2002) and calcium mobilisation (Hirai, et al., 2001; Powell, 2003) presumably via G-βγ subunits, and through a pertussis toxin (PTX) insensitive mechanism to β-arrestin translocation (detected by a GFP-tagged β-arrestin / luciferase-tagged receptor BRET interaction and interpreted by the authors to indicate non-G-protein dependence; Mathiesen, *et al*., 2005). Evidence indicating possible $G\alpha_q$ coupling of the receptor to eosinophil shape change (species undefined;

Stubbs, *et al*., 2002; Böhm, *et al.*, 2003) relies on a lack of PTX sensitivity but has not excluded the possibility of coupling via $G\alpha_z$ nor of β-arrestin mediated activation of intracellular effectors (Hall, *et al*., 1999; Lefkowitz, *et al*., 2006). The receptor gene is located on human chromosome 11q and on murine chromosome 19 but does not share linkage with other chemoattractant molecules. $CRTH_2$ is expressed on basophils, eosinophils and Th_2 cells but not on neutrophils or Th_1 cells. Nagata and colleagues (1999) also showed that $CRTH_2$ is expressed on activated Th_2 cells including allergen-responsive cells which suggests a role for this receptor in ongoing Th_2-mediated immune reactions. Receptor activation results in Ca^{2+} mobilisation in Th_2 cells and chemotaxis in eosinophils, basophils and Th_2 cells. Parallel responses occur in eosinophils involving chemotaxis, CD11b expression and L-selectin shedding (Monneret, *et al*., 2001), and also shape change and degranulation (Gervais, *et al*., 2001).

There are some interesting structural features of the $CRTH_2$ receptor molecule. It shares only 10 % sequence homology with the most similar prostanoid receptor (the prostanoid FP receptor) and rather more homology (35 %) with chemoattractant receptors such as fMLP-1, C3a, C5a and GPCR1 (DEZ; Methner, *et al*., 1997). Unlike other prostanoid receptors, the charged arginine residue in the seventh transmembrane sequence (TM7), believed to be essential for high affinity prostanoid agonist binding (Narumiya, *et al*., 1999, for review), is absent (Nagata & Hirai, 2003). Predictably, with such low sequence homology, there are corresponding dissimilarities in other regions of the molecule important to binding of ligands to prostanoid receptors. These include sequences in extracellular loop 2 (EC2), TM2 and TM4, the significances of which are poorly understood.

Despite the structural differences, $CRTH_2$ appears to demonstrate pharmacology commensurate with a member of the classically-defined prostanoid receptor family (for example Nagata & Hirai, 2003; Powell, 2003; Sawyer, *et al.*, 2002). Its pharmacology is, however, unique and distinct from that of the prostanoid DP receptor: PGD_2, 13,14-dihydro-15-keto-PGD_2 (DK-PGD_2), prostaglandin J_2 (PGJ_2) and indomethacin are agonists but the selective DP agonist BW245C is without effect (Hirai, *et al*., 2002). A recently discovered synthetic $CRTH_2$ agonist, L-888,607 has sub-nanomolar affinity for $CRTH_2$ but only micromolar affinity for DP (Gervais, *et al.*, 2005). Furthermore, the selective DP antagonist BWA868C appears to have low affinity for (Hirai, *et al.*, 2003)

and be devoid of antagonist activity at (Monneret, *et al.*, 2001) $CRTH_2$ receptors. In a poster communication, I have confirmed and extended our knowledge of agonist activity at recombinant $hCRTH_2$ receptors transiently expressed in HEK293 cells (Wilson & Volppe, 2002) while Sawyer, *et al*. (2002) have published a competition binding 'fingerprint' for prostanoid receptor ligands and COX-inhibitors at the receptor. The aims of the present study were two-fold: firstly, to validate the commonly used approach of coupling G-protein coupled receptors (GPCRs) to a more convenient assay readout by means of a chimeric G-protein (in this case a normally $G\alpha_i$-coupled receptor to calcium influx through $G\alpha_{16z49}$); and secondly, to more fully characterise the agonist pharmacology of human prostanoid $CRTH_2$ receptors in order to generate a functional structure-activity relationship (SAR) and pharmacophore hypothesis which may assist future efforts to find selective ligands for this receptor. A number of compounds important to these studies are illustrated in Figure 1.

3.3 Results:

Results obtained by other individuals are indicated by a bar in the margin. Unmarked text indicates results obtained by the author.

3.3.1 Selection of CHO $G\alpha_{16z49}$ $hCRTH_2$ clone.

Two clones of CHO $G\alpha_{16z49}$ $hCRTH_2$ cells were selected for further study based on PGD_2 EC_{50} on initial test at passage 6.

Analysis of cell size distribution revealed that clone 8 cell populations contained a higher proportion of large volume forms than populations of clone 17. Cell plating conditions were therefore adjusted to achieve generation of confluent monolayers of cells in assay plates.

Prostaglandin D_2 (0.5 nM – 10 μM) produced concentration-related increases in $[Ca^{2+}]_i$ in cells of both clones (Figure 2; cells plated out at 5000 and 10,000 cells $well^{-1}$, clones 8 and 17, respectively). The potency (pEC_{50}) of PGD_2 was similar in both cell lines (clone 8: 7.0 ± 0.03; clone 17: 6.9 ± 0.05) but marked differences in maximum response (clone 8: 143 ± 2; clone 17: 70 ± 2; $P < 0.05$) and Z' (clone 8: 0.38 ± 0.02; clone 17: -0.47 ± 0.2; $P < 0.05$) were observed (data are mean of >120 individual E/[A] curves, or in the case of Z', of 6 determinations, produced on three separate assay occasions, at the same passage number). All subsequent data were generated in clone 8 cells.

3.3.2 Effect of indomethacin.

Blockade of endogenous prostaglandin synthesis by inclusion of the non-selective COX inhibitor indomethacin (3 μM) in the cell culture medium at passage 10 was found to increase the proportion of large 'swollen' cells in both clones at P11 in a manner which could not be quantified by the Sysmex counter I used. Clone 8 cells cultured with and without 3 μM indomethacin produced identical PGD_2 E/[A] curve parameters (Figure 3A); the only significant change produced by indomethacin was to improve assay reproducibility. When tested for agonism, indomethacin (10 μM – 0.5 nM) produced concentration related $[Ca^{2+}]_i$ elevations (Figure 3B & Table 1; cells at 1 x 10^4 cells $well^{-1}$) but was approximately 8-fold less potent than PGD_2 with a relative activity of 0.63 cf. PGD_2 (= 1.0; $P = 0.02$). When the same cells exposed to the indomethacin dilution series were challenged 11 mins later with a fixed concentration of PGD_2 (1 μM)

in the continued presence of indomethacin, an inhibitory E/[A] curve was produced (see Chapter 6 for investigation of mechanism). The inhibitory pIC_{50} of indomethacin was identical to its calcium mobilization pEC_{50} (Table 1); relative activity cf. PGD_2 = 1.0.

3.3.3 Effect of other NSAIDs: selection of flurbiprofen as cell culture medium supplement.

The NSAIDs acetyl salicylic acid (aspirin), 4-acetamidophenol (acetaminophen), diclofenac, sulindac, diflunisal, acemetacin, indole-3-acetic acid (heteroauxin), [+]-naproxen, ibuprofen, S-flurbiprofen and piroxicam did not display any agonism or desensitisation effects at concentrations up to 10 μM (Table 1). In the same experiment PGD_2 pEC_{50} was 6.3 ± 0.2 and pIC_{50} (desensitisation or inhibition vs. PGD_2 EC_{80}) was 6.6 ± 0.2 ($P > 0.05$).

Because of its high *in vitro* potency vs. COX1 and 2, flurbiprofen was selected for further study. Culture of cells in the presence of 10 μM flurbiprofen resulted in an increase in PGD_2 potency (pEC_{50}) from 6.9 ± 0.1 to 7.4 ± 0.1 and in Z' from 0.25 ± 0.1 to 0.5 ± 0.09 ($P < 0.05$). Investigation of the literature suggested that flurbiprofen is 99.95 % plasma protein bound in humans (Knadler *et al.*, 1989; Szpunar *et al.*, 1989) and that increasing the concentration used in the culture medium to 100 μM might yield a more effective free drug concentration. Culture of cells in the presence of 100 μM flurbiprofen resulted in a further increase of PGD_2 potency to 7.8 ± 0.06 and of Z' to 0.64 ± 0.02 ($P < 0.01$). Changes in E/[A] curve asymptote were not observed.

3.3.4 Development of assay protocol and requirement for extracellular calcium..

Using cells cultured in the presence of 10 μM flurbiprofen, a range of assay conditions were investigated (Table 2). The optimum set of conditions were found to be: FLIPR experiments performed at room temperature, pipettor speed 5 μl s^{-1}, pipettor height 30 μl, 2 x 10 μl mixes at 5 μl s^{-1}, camera exposure time 0.4 s, plate type Greiner poly-D-lysine coated, cell seeding density 20,000 cells $well^{-1}$, anion exchange inhibited with probenecid, dye quench with brilliant black required, pluronic acid included, flurbiprofen omitted from the assay buffer, and 0.8 mM Ca^{2+} included in the assay buffer. Replacement of cell culture medium with serum-free medium 24 hours prior to assay worsened responses to PGD_2. Where there was little to distinguish between conditions the option most similar to other assays running in our labs was chosen. All

subsequent data were generated in cells cultured in the presence of 100 μM flurbiprofen. The impact of alternative methods of data analysis on agonist (PGD_2 & UTP) curve parameters was investigated under optimal assay conditions. Analyses based on calculations as described in *Methods* (((max-min)/basal)x100) yielded pEC_{50} and slope data that were not different from analyses based on the area under the fluorescence / time curve (AUC; Table 3). PGD_2 maximum effect values expressed as a percentage of the UTP maximum effect were 40 % smaller using AUC-based analysis. Analyses based on maximum rate of fluorescence change during the increasing phase of calcium responses gave markedly lower agonist potencies and flatter PGD_2 curve slopes. All analyses were therefore performed as described in *Methods*.

3.3.5 Assessment of host cell response to prostaglandins.

CHO $G\alpha_{16z49}$ cells without the prostanoid $hCRTH_2$ receptor were grown and plated for assay as described in Methods. A non-statistically significant trend towards small decreases in basal fluorescence was produced by PGD_2 (0.17 nM-10 μM) which was insensitive to challenge with the prostanoid DP receptor antagonist BWA868C (1 μM), the putative prostanoid $hCRTH_2$ receptor antagonist GW853481X (10 μM; compound 1c in Bauer, *et al*., 2002), and the prostanoid EP_4/TP receptor antagonist AH23848B (30 μM; Figure 4). PGE_2 produced small concentration-related elevations of $[Ca^{2+}]_i$ over the same concentration range which were significant at 0.33 μM (P = 0.05) but were non-significant at 10 μM (Figure 4, panel B). The data was not of sufficient quality to obtain a robust curve fit however the following parameters were estimated: pEC_{50} 7.6 ± 0.3, E_{max} 16 ± 2. Although the mean data plot is suggestive of a biphasic E/[A] curve, examination of individual curves were clearly monophasic. PGE_2 responses were also insensitive to challenge with antagonists including the potent and selective prostanoid EP_4 receptor antagonist GW627368X. Exposure of cells to antagonists at the concentrations used did not result in basal fluorescence changes.

3.3.6 Effect of standard prostanoid receptor agonists and antagonists.

In contrast to findings in host cells, in CHO $G\alpha_{16z49}$ $hCRTH_2$ cells prostaglandins E_2 (PGE_2), I_2 (PGI_2, prostacyclin), and U-46619 were devoid of agonist effects up to 10 μM; prostaglandin $PGF_{2\alpha}$ produced small elevations of $[Ca^{2+}]_i$ at 10 μM resulting in a maximum response of 14 ± 2 % cf. PGD_2 controls (Figure 5).

BWA868C, SC19220 (prostanoid EP_1 receptor antagonist), SQ29548 (prostanoid TP receptor antagonist) and GW627368X (prostanoid EP_4 receptor antagonist) were devoid of antagonist activity up to 10 μM vs. 0.3 μM PGD_2. GW853481X antagonised PGD_2 responses to give a pIC_{50} of 6.1 ± 0.2 ($P < 0.05$ cf. control) and a slope of 2.5 ± 0.3 ($P > 0.05$; Figure 6, Panel A). Complete blockade of PGD_2 responses was not achieved, maximum inhibition being 72 ± 5 %. Further assay demonstrated that GW853481X (10 μM) produced rightward displacement of PGD_2 E/[A] curves with simultaneous upper asymptote depression (1 μM antagonist E_{max} = 81 ± 6 % of control; P = 0.05) to yield an apparent pA_2 estimate of 6.5 ± 0.06 (Figure 6, Panel B). However, higher concentrations of antagonist did not elicit any further depression of E_{max}. GW853481X did not antagonise responses to UTP (1 μM) in the same cell line. (In later experiments (Chapter 7), this molecule produced agonist-like effects in these cells at high concentrations (pEC_{50} 4.5 ± 0.1, E_{max} 5 ± 3 %)). AH23848B also antagonised PGD_2 responses but with lower potency: the maximum inhibition achieved being 24 ± 9 % at 10 μM vs. 0.3 μM PGD_2. However, AH23848B produced parallel rightward displacement of PGD_2 E/[A] curves resulting in an apparent pA_2 estimate of 5.3 ± 0.1 (Figure 7) and was devoid of agonist effects.

3.3.7 Effect of pertussis toxin treatment.

Pertussis toxin (PTX; 50 ng ml^{-1}) produced marked inhibition of responses to PGD_2 in CHO $G\alpha_{16z49}$ $hCRTH_2$ cells (Figure 8, Panel A). In the absence of PTX, PGD_2 pEC_{50} was 7.5 ± 0.06, slope 1.1 ± 0.03; in the presence of PTX PGD_2 pEC_{50} was 6.4 ± 0.06 (P=0.01), slope 1.9 ± 0.2 ($P < 0.05$), and curve maximum 15 ± 1 % cf. PGD_2 no PTX control ($P < 0.01$). The effect was reproducible over 6 rounds of passage spanning four weeks of cell culture (Figure 8, Panel B). A small passage-related change in PGD_2 pEC_{50} was observed through the course of this study (for example, PGD_2 pEC_{50} at P10 7.5 ± 0.05; at P16 6.9 ± 0.02; $P < 0.01$) which was statistically significant at all time points tested (P12, 14 & 16) in both PTX treated and untreated groups.

3.3.8 Agonist 'fingerprinting' of $hCRTH_2$ receptor in CHO $G\alpha_{16z49}$ cells ± PTX treatment.

A panel of 76 prostanoid molecules was screened for agonist activity in CHO $G\alpha_{16z49}$

$hCRTH_2$ cells with and without PTX pre-treatment at concentrations up to 10 μM (Table 4). Without PTX treatment, 65 % of the compounds tested were found to be without agonist effect. Curve slopes for active compounds were generally in the range 1.2-2.0; slopes greater than this were observed for some partial agonist compounds. The following rank order of agonist potency was obtained for the most active compounds (relative potency [RP cf. PGD_2 = 1.0], relative activity [RA cf. PGD_2 = 1.0]; full agonists shown in bold type, partial agonists in normal type): **15 (R) 15 methyl PGD_2 (0.5, 0.9)** > **PGD_2** > 15 (R) 15 methyl $PGF_{2\alpha}$ (11, 0.6) > **15 deoxy PGD_2 (20, 0.9) > PGJ_2 (27, 0.9) = 15 deoxy Δ12,14 PGJ_2 (31, 0.9)** > **15 (S) 15 methyl PGD_2 (38, 0.8)** > **13,14 dihydro 15 keto PGD_2 (39, 1.0)** > **Δ12 PGJ_2 (47, 0.9)** > **9,10 dihydro 15 deoxy Δ12,14 PGJ_2 (54, 0.9)** > **17 phenyl PGD_2 (85, 1.2)** > **PGD_3 (100, 0.8)** > 15 keto $PGF_{2\alpha}$ (131, 0.7) > **PGD_1 (224, 0.9)** > 15 (R) $PGF_{2\alpha}$ (379, 0.6) > **16,16 dimethyl PGD_2 (402, 0.8)** > 15 keto $PGF_{1\alpha}$ (408, 0.3) > $PGF_{2\alpha}$ (>400, 0.2) > butaprost methyl ester (497, 0.7) > latanoprost (794, 0.3) > cloprostenol (1585, 0.3). BW245C was without significant effect.

Following PTX treatment, the profile of agonist activity was markedly altered. Under these conditions, PGD_2 produced a maximum effect equal to 37 ± 0.9 % of the maximum response produced in non-PTX treated cells during the same experiment ($P < 0.05$; PGD_2 pEC_{50} in non-PTX treated cells 7.9 ± 0.09). A similar proportion (62 %) of compounds were without agonist effect. A group of 5 compounds (7 %) consistently produced very low level agonism, statistically not distinguishable from baseline noise, but with high potency (RP 0.23 – 0.02). For the group of compounds described above, the rank order of agonist potency was: **15 (R) 15 methyl PGD_2 (0.7, 0.9)** > **PGD_2 = 15 deoxy PGD_2 (1.0, 1.1)** > **PGJ_2 (2, 1.0) = 15 deoxy Δ12,14 PGJ_2 (2, 1.0)** > **Δ12 PGJ_2 (3, 1.0)** = 13,14 dihydro 15 keto PGD_2 (3, 0.7) > **9,10 dihydro 15 deoxy Δ12,14 PGJ_2 (4, 0.8)** > 15 (S) 15 methyl PGD_2 (6, 0.6) > 16,16 dimethyl PGD_2 (11, 0.4) >> 17 phenyl PGD_2 (max effect 0.6) = PGD_3 (max effect 0.4) = 15 keto $PGF_{2\alpha}$ (max effect 0.2) = PGD_1 (max effect 0.2). Cloprostenol, $PGF_{2\alpha}$, 15 keto $PGF_{1\alpha}$, butaprost methyl ester, 15 (R) 15 methyl $PGF_{2\alpha}$, latanoprost & BW245C were without significant effect.

3.3.9 Data Tables.

Follow on next page.

Table 1. Effects of several non-steroidal anti-inflammatory drugs (NSAIDs) in CHO $G\alpha_{16z49}$ $hCRTH_2$ cells. Cells were cultured in the presence of 3 μM indomethacin prior to assay; other conditions as defined in Methods. RP is relative potency cf. PGD_2 (= 1.0); RA is relative activity cf. PGD_2 (= 1.0). Min & max values are expressed in normalised FLIPR intensity units as described in Methods. Data are mean ± sem; n = 9.

	Agonism						**Inhibitory or antagonist effects (vs. 0.3 μM PGD_2)**					
	min	**max**	**pEC_{50}**	**slope**	**RP**	**RA**	**min**	**max**	**pIC_{50}**	**slope**	**RP**	**RA**
4-acetamidophenol	55 ± 3	47 ± 4				0	114 ± 4	115 ± 3				0
Acetyl salicylic acid	50 ± 4	47 ± 6				0	114 ± 6	117 ± 8				0
Diclofenac	63 ± 7	45 ± 3				0	122 ± 4	128 ± 4				0
Naproxen	58 ± 2	52 ± 9				0	122 ± 3	126 ± 2				0
Sulindac	60 ± 6	50 ± 5				0	119 ± 4	123 ± 9				0
Diflunisal	55 ± 8	43 ± 3				0	117 ± 3	127 ± 5				0
Acemetacin	57 ± 5	50 ± 9				0	115 ± 2	126 ± 6				0
Indomethacin	56 ± 4	104 ± 24	5.6 ± 0.2	1.3 ± 0.4	7.8	0.63	23 ± 6	132 ± 4	5.6 ± 0.06	2.0 ± 0.7	2.3	1.0
Ibuprofen	56 ± 6	53 ± 9				0	118 ± 5	121 ± 6				0
Flurbiprofen	60 ± 5	54 ± 9				0	121 ± 5	129 ± 4				0
Indole 3 acetic acid	58 ± 1	53 ± 5				0	121 ± 6	125 ± 8				0
Piroxicam	57 ± 3	57 ± 6				0	120 ± 13	130 ± 3				0
PGD_2	58 ± 5	133 ± 6	6.3 ± 0.2	1.0 ± 0.2	1.0	1.0	17 ± 6	128 ± 6	6.0 ± 0.1	1.2 ± 0.3	1	1.0
Vehicle	58 ± 4	54 ± 7				0	119 ± 6	128 ± 5				0
PGD_2 (agonist time-matched control for antagonist read)							39 ± 5	142 ± 6	6.6 ± 0.2	1.0 ± 0.06		

Table 2. Determination of assay conditions & parameters. Cells cultured in the presence of 10 μM flurbiprofen. PDL: poly-D-lysine coated; SAB – assay buffer plus sulphinpyrazone (120 μM); PAB – assay buffer plus probenecid (2.5 mM); BB – assay buffer plus brilliant black (1 mM). Data are mean ± sem of 32 E/[A] curves determined on 2 assay plates in a single assay (plate type & seeding density n=3).

Condition	**Options**	**min**	**max**	**pEC_{50}**	**slope**	**Z´**
Assay temperature	Room temp.	27 ± 1	152 ± 2	7.3 ± 0.04	1.3 ± 0.05	0.6
	37 °C	28 ± 1	141 ± 2	7.4 ± 0.04	1.4 ± 0.07	0.6
Liquid dispense speed	5 μl s^{-1}	28 ± 1	141 ± 2	7.4 ± 0.04	1.4 ± 0.07	0.6
	10 μl s^{-1}	27 ± 1	132 ± 2	7.6 ± 0.04	1.4 ± 0.09	0.7
	20 μl s^{-1}	59 ± 2	145 ± 2	7.3 ± 0.04	1.4 ± 0.09	0.3
Pipettor height	30 μl	59 ± 2	145 ± 2	7.3 ± 0.04	1.4 ± 0.09	0.3
	40 μl	57 ± 1	150 ± 2	7.3 ± 0.04	1.3 ± 0.09	0.4
Camera exposure time	0.4 s	28 ± 1	141 ± 2	7.4 ± 0.04	1.4 ± 0.07	0.6
	0.5 s	36 ± 2	144 ± 9	7.4 ± 0.04	1.1 ± 0.05	0.5
Plate type	Nunc	27 ± 1	141 ± 2	7.5 ± 0.04	1.3 ± 0.07	0.4
	Greiner PDL	36 ± 2	132 ± 2	7.5 ± 0.02	1.4 ± 0.07	0.4
Cell seeding density	5,000 $well^{-1}$	28 ± 1	114 ± 1	7.5 ± 0.04	1.3 ± 0.07	0.3
	10,000 $well^{-1}$	30 ± 1	134 ± 2	7.5 ± 0.04	1.4 ± 0.09	0.4
	20,000 $well^{-1}$	24 ± 1	170 ± 2	7.6 ± 0.04	1.1 ± 0.04	0.6
	40,000 $well^{-1}$	16 ± 1	196 ± 2	7.4 ± 0.02	0.8 ± 0.02	0.7
Anion exchange inhibitor	None	-	-	-	-	9.9
	SAB	-	-	-	-	-1.7
	PAB	18 ± 1	199 ± 3	7.9 ± 0.05	1.0 ± 0.05	0.8
Quench	None	24 ± 1	118 ± 3	8.0 ± 0.05	1.3 ± 0.1	0.1
	BB	18 ± 1	199 ± 3	7.9 ± 0.05	1.0 ± 0.05	0.8
Detergent	None	10 ± 0.2	131 ± 3	6.6 ± 0.04	1.0 ± 0.02	0.8
	Pluronic acid	9 ± 0.2	139 ± 3	6.5 ± 0.02	1.0 ± 0.02	0.8
COX inhibition during assay	None	10 ± 0.2	131 ± 3	6.6 ± 0.04	1.0 ± 0.02	0.8
	Flurbiprofen	15 ± 0.4	116 ± 3	6.4 ± 0.05	0.9 ± 0.02	0.7
Extracellular calcium (EGTA not used)	None added	24 ± 0.5	145 ± 1	6.7 ± 0.04	1.3 ± 0.07	0.7
	0.2 mM	20 ± 0.4	114 ± 1	6.7 ± 0.04	1.2 ± 0.04	0.6
	0.4 mM	20 ± 0.2	118 ± 2	6.5 ± 0.04	1.1 ± 0.05	0.7
	0.8 mM	10 ± 0.2	131 ± 3	6.6 ± 0.04	1.0 ± 0.02	0.8
	1.6 mM	24 ± 0.5	108 ± 2	6.5 ± 0.04	1.0 ± 0.04	0.6

Table 3. Impact of alternative data analysis techniques on PGD_2 and UTP E/[A] curve parameters. Data were analysed either as described in *Methods* (((max-min)/basal)x100), or by analogous processes using measurements of area under the fluorescence / time curve (AUC), or of the maximum rate of fluorescence change during the increasing phase of a calcium response (Max. Rate). Data are mean ± sem of duplicate determinations from three independent experiments.

	PGD_2			**UTP**	
	pEC_{50}	**slope**	**max as % UTP max**	**pEC_{50}**	**slope**
Max-min	7.9 ± 0.09	1.8 ± 0.3	61 ± 6	7.0 ± 0.1	1.2 ± 0.3
AUC	8.0 ± 0.09	1.4 ± 0.2	37 ± 4	6.9 ± 0.1	1.2 ± 0.2
Max rate	7.1 ± 0.2	0.9 ± 0.1	28 ± 0.3	6.0 ± 0.09	1.2 ± 0.2

Table 4. Pharmacology of prostanoid molecules in CHO $G\alpha_{16z49}$ $hCRTH_2$ cells with and without pertussis toxin (PTX) treatment. RP: relative potency cf. PGD_2 (= 1.0); RA: relative activity cf. PGD_2 (= 1.0). Data are mean ± sem; without PTX n = 4 - 10; with PTX n = 3. 11 dehydro TxB_2, 15 (R) 19 (R) hydroxy $PGF_{2\alpha}$, 13,14 dihydroxy 15 keto PGA_2, 6 keto $PGF_{1\alpha}$, 6 keto PGE_1, Δ^{17} 6 keto $PGF_{1\alpha}$, PGA_2, 15 (R) PGE_2, $PGF_{1\alpha}$, PGA_1, 13,14 dihydro 15 keto $PGF_{1\alpha}$, 15 keto PGE_1, 19 (R) hydroxy $PGF_{1\alpha}$, 11 dehydro 2,3 dinor TxB_2, PGI_2, 15 (R) 19 (R) hydroxy $PGF_{1\alpha}$, 13,14 dihydro 15 keto PGE_1, TxB_2, 15 (R) 19 (R) hydroxy PGE_2, PGK_1, 15 keto PGE_2, 20 hydroxy PGE_2, 11β 13,14 dihydro 15 keto $PGF_{2\alpha}$, 19 (R) hydroxy $PGF_{2\alpha}$, PGK_2, PGI_3, PGE_2, 19 (R) hydroxy PGE_1, PGB_2, Cicaprost, Sulprostone, BW245C, Butaprost free acid, 17 phenyl PGE_2, 16,16 dimethyl PGE_2 & Iloprost were without significant effect under either set of conditions. † denotes data from single curve fit. Statistical comparison by ANOVA followed by Dunnett's comparison to PGD_2 data; * denotes $P < 0.05$.

	Without PTX					With PTX				
Compound	**pEC_{50}**	**slope**	**max**	**RP**	**RA**	**pEC_{50}**	**slope**	**max**	**RP**	**RA**
15 (R) 15 methyl PGD_2	7.7 ± 0.04	1.6 ± 0.2	89 ± 7	0.5	0.9	6.6 ± 0.04	1.1 ± 0.04	93 ± 4	0.7	0.9
PGD_2	7.8 ± 0.1	1.3 ± 0.1	100.0	1.0	1.0	6.5 ± 0.07	1.4 ± 0.1	100.0	1.0	1.0
15 (R) 15 methyl $PGF_{2\alpha}$	6.4 ± 0.04*	1.6 ± 0.2	63 ± 5*	11	0.6			NSE		
15 deoxy PGD_2	6.8 ± 0.2*	1.7 ± 0.09	90 ± 2	20	0.9	6.5 ± 0.09	1 ± 0.1	110 ± 4	1.0	1.1
PGJ_2	6.4 ± 0.07*	1.5 ± 0.1	87 ± 3	27	0.9	6.2 ± 0.03	1.2 ± 0.03	98 ± 3	1.8	1.0
15 deoxy $\Delta^{12,14}$ PGJ_2	6.6 ± 0.0*	1.4 ± 0.04	86 ± 3	31	0.9	6.2 ± 0.0	1.6 ± 0.09	99 ± 4	1.8	1.0
15 (S) 15 methyl PGD_2	6.0 ± 0.09*	1.6 ± 0.4	82 ± 4	38	0.8	5.7 ± 0.09*	1.9 ± 0.4	61 ± 4*	5.8	0.6
13,14 dihydro 15 keto PGD_2	6.5 ± 0.04*	1.2 ± 0.07	97 ± 4	39	1.0	6.0 ± 0.04	1.4 ± 0.07	73 ± 2*	2.8	0.7
Δ12 PGJ_2	6.4 ± 0.09*	1.8 ± 0.2	91 ± 3	47	0.9	6.1 ± 0.04	2.1 ± 0.5	102 ± 2	2.5	1.0
9,10 dihydro 15 deoxy $\Delta^{12,14}$ PGJ_2	6.3 ± 0.04*	1.6 ± 0.2	89 ± 4	54	0.9	5.9 ± 0.04*	1.5 ± 0.04	83 ± 4*	3.5	0.8
17 phenyl PGD_2	6.2 ± 0.09*	1.4 ± 0.1	122 ± 4	85	1.2			61 ± 2*		0.6

PGD_3	6.0 ± 0.06*	3.7 ± 0.1*	82 ± 1*	100	0.8			38 ± 2*		0.4
15 keto $PGF_{2\alpha}$	6.0 ± 0.1*	2.0 ± 0.6	73 ± 3*	131	0.7			18 ± 5*		0.2
PGD_1	5.8 ± 0.1*	1.2 ± 0.1	89 ± 3	224	0.9			17 ± 14*		0.2
15 (R) $PGF_{2\alpha}$	5.5 ± 0.2*	1.8 ± 0.3	55 ± 2*	379	0.6			15 ± 5*		0.2
16,16 dimethyl PGD_2	5.5 ± 0.2*	3.2 ± 0.5*	78 ± 6*	402	0.8	5.4†*	3.9†	41 ± 3*	10.5	0.4
15 keto $PGF_{1\alpha}$	5.6 ± 0.06*	1.6 ± 0.3	28 ± 3*	409	0.3			NSE		
$PGF_{2\alpha}$	< 5.2		17 ± 3*	> 400	0.2			NSE		
Butaprost methyl ester	4.8 ± 0.1*	3.1 ± 1.0*	58 ± 4*	497	0.7			NSE		
Latanoprost	4.7 ± 0.2*	2.6 ± 0.7	30 ± 6*	794	0.3			NSE		
Cloprostenol	4.4 ± 0.06*	1.4 ± 0.2	31 ± 1*	1585	0.3			NSE		
Misoprostol			20 ± 1*		0.2			NSE		
15 (S) 15 methyl $PGF_{2\alpha}$			16 ± 3*		0.2			NSE		
13,14 dihydro 15 keto $PGF_{2\alpha}$			12 ± 4*		0.1			NSE		
11 deoxy 11 methylene PGD_2			10 ± 3*		0.1			NSE		
$PGF_{3\alpha}$			9 ± 4*		0.1			NSE		
13,14 dihydro PGE_1			NSE					17 ± 11*		0.2
PGE_3			NSE					19 ± 19*		0.2
20 hydroxy $PGF_{2\alpha}$			NSE					23 ± 16*		0.2
13,14 dihydro $PGF_{1\alpha}$			NSE			7.8 ± 0.1*	1 ± 0.06	5 ± 1*		0.05
13,14 dihydro 15 keto PGE_2			NSE					10 ± 5*		0.1
PGE_1			NSE			8.1 ± 0.06*	1.1 ± 0.06	13 ± 4*		0.1

PGD_1 alcohol	NSE	7.1 ± 0.3	1.9 ± 0.5	4 ± 0.6*	0.04
15 (R) 15 methyl PGE_2	NSE			16 ± 12*	0.2
13,14 dihydro 15 (R) PGE_1	NSE			9 ± 7*	0.1
19 (R) hydroxy PGA_2	NSE			14 ± 12*	0.1
15 (R) PGE_1	NSE			10 ± 1*	0.1
19 (R) hydroxy PGE_2	NSE			14 ± 6*	0.1
2,3 dinor 11β $PGF_{2\alpha}$	NSE	7.7 ± 0.2*	1.9 ± 0.6	6 ± 1*	0.1
11deoxy PGE_1	NSE	8.2 ± 0.07*	1.1 ± 0.3	8 ± 4*	0.1

Table 5. Potency and activity of indomethacin reported in literature. Data are mean (nM) ± s.e.m. Terms in table are: ↓cAMP - inhibition of forskolin stimulated cAMP accumulation; Ca^{2+} - calcium mobilisation; CTX – chemotaxis; GTPγS – GTPγS binding assay. * Denotes max effect at 10 μM.

Species	Cell line	Read out	PGD_2 EC_{50}	Indomethacin EC_{50}	RP	RA	Binding K_i / IC_{50}	Reference
Human	HEK293(EBNA)	↓cAMP	1.8±0.4	14.9±4.9	8	1.0		Sawyer, *et al.*, 2005
	HEK293 $G\alpha_{15}$	Ca^{2+}	22.1±4.4	ND			25±4	Sawyer, *et al.*, 2002
Human	L1.2	↓cAMP	0.24	4.5	19	1.0	1000	Sugimoto, *et al.*, 2005
		Ca^{2+}	1.2	49	41	1.0		
		CTX	0.5	40	80	1.0		
Human	K562	Ca^{2+}	1-5	50	10-50	1.0	8100±1900	Hirai, *et al.*, 2002
	Jurkat	CTX	< 1	c.40	> 40	2.0		
	TH2	CTX	c. 4	50-250	12-60	1.0		
	Basophil	CTX	5-25	c.250	10-50	1.0		
	Eosinophil	CTX	5-25	c.250	10-50	1.0		
Human	CHO $G\alpha_{16z49}$	Ca^{2+}	500±100	2,500±400	8	0.63		Present chapter
	CHO $G\alpha_{16z49}$ + PTX + flurbi	Ca^{2+}	15.8±8	c. 10,000	c. 40	0.58*		Present chapter
	CHO K1 + flurbi	Ca^{2+}	13 ± 6	126 ± 10	10	0.85		See Chapter 4
	CHO K1 membranes	GTPγS	8 ± 2	400 ± 0	50	1.1	See Chapter 7	See Chapter 5
Human	Unspecified						3000±1000	Hata, *et al.*, 2005a
Murine	ER293	↓cAMP	0.9	7	8	1.0	1500	Hata, *et al.*, 2005a
Murine	HEK293	↓cAMP	0.7±0.3	2.0±0.7	3	1.0	1900±300	Hata, *et al.*, 2005b

3.4 Discussion:

Definition of appropriate methodology is a key step in the preparation of any assay system for data generation and must take into account technological aspects of the instrumentation, physicochemical aspects of the reagents, biological characteristics of the assay system, as well as good laboratory practice. In this chapter, I have demonstrated the definition of suitable experimental procedures for generating quantitative SAR data at human prostanoid $CRTH_2$ receptors expressed in CHO cells also expressing the $G\alpha_{16z49}$ chimeric G-protein, the use of those data to generate alternative pharmacophore hypotheses describing agonist interaction with the receptor, and the importance of viewing the receptor / G-protein pairing as being a key determinant of pharmacological selectivity.

Clone selection was primarily based on examination of prostaglandin D_2 (PGD_2) concentration-effect (E/[A]) curve data which clearly demonstrated the superior magnitude of responses generated by clone 8. However, these data were produced by a single agonist in an un-optimised assay system, without supplementation of cell culture medium with a COX inhibitor. The absence of assay optimisation data at this stage is not likely to have impacted significantly on the choice of clone since alteration of technology- and assay methodology- related parameters made little or no impact on PGD_2 pEC_{50} or maximum effect. However, of greater potential significance is the absence of COX inhibition during this part of the study. Endogenous production of prostaglandins by cells in culture has been demonstrated for many cell lines, including CHO K1 cells (Kargman, *et al*., 1996). Foetal calf serum has been shown to concentration-dependently stimulate production of up to 0.2 ng PGE_2 per 10^6 cells per 30 mins of incubation under resting conditions (Murakami, *et al*., 1996) though figures for PGD_2 are lacking. The mechanism by which this occurs is unclear but presumably relates to the presence of various growth factors, cytokines, hormones and other proteins in the serum, some of which may activate cell surface receptors on CHO cells. Over 36 hrs of cell culture in a 175 cm^2 tissue culture flask as much as 16 nmol of PGE_2 could be produced (calculation based on Murakami, *et al*., 1996, assuming c. 3 x 10^8 cells $flask^{-1}$ at confluency). Much will be spontaneously hydrolysed or metabolized, as discussed below, but it seems likely that local concentrations near to the cells will be sufficient to result in autocrine stimulation of prostanoid receptors with the potential to cause desensitisation or down-regulation. The data I present here shows a significant

increase in PGD_2 pEC_{50} when cells are cultured in the presence of an effective concentration of COX inhibitor, implying (but not proving) that inhibition of prostaglandin synthesis has resulted in response pathway up-regulation. It is unknown whether cells of clones 8 and 17 produce equal amounts of prostaglandin, whether receptor desensitisation is indeed occurring (see Chapter 6 for further investigation), if it does whether it progresses along identical pathways in both clones, and therefore whether the clones would respond identically to effective COX inhibition. It is also unknown whether CHO K1 cells express significant amounts of prostaglandin 15 dehydrogenase (PG15dH) and thus whether metabolism of PGD_2 to 15 keto PGD_2 can occur to any appreciable extent over the time course of the assay. For this reason, it would have been desirable to simultaneously assay another metabolically resistant agonist such as 15 (R) 15 methyl PGD_2. Thus, it is conceivable that the true performance of these clones was masked by poorly controlled assay conditions.

The non-selective COX 1/2 inhibitor indomethacin (3 μM; Figure 1) was without effect on PGD_2 pEC_{50} and maximum responses but increased the variability of responses to a fixed concentration of PGD_2. As described above, the inclusion of a COX inhibitor was expected to improve assay performance by preventing autocrine receptor activation and desensitisation. In addition to COX inhibition, indomethacin possesses a range of other activities including inhibition of a PGD_2 11-ketoreductase (Lovering, *et al.*, 2004) and is also an agonist at prostanoid $CRTH_2$ receptors (Hirai, *et al.*, 2001; Sawyer, *et al.*, 2002; Stubbs, *et al.*, 2002; Sugimoto, *et al.*, 2005). The data presented here shows that indomethacin, like PGD_2, produces a profound and rapid inhibition of the ability of cells to respond to subsequent PGD_2 EC_{80} challenge. The net effect of cell culture with indomethacin on PGD_2 responses will therefore be the sum of simultaneous prostaglandin synthesis inhibition (and therefore agonist response potentiation), inhibition of a PGD_2 metabolic pathway, plus direct receptor activation possibly leading to subsequent desensitisation, and occupancy of the receptor leading to a partial agonist / full agonist interaction. It seems surprising, then, that indomethacin did not produce more marked effects on PGD_2 responses: culture medium contained 3 μM indomethacin which would be expected to produce c. 30 % inhibition of PGD_2 responses. The difference may reflect possible recovery from the inhibitory effect during the 90 min dye-loading phase of the experiment since cell culture medium was replaced by

indomethacin-free assay buffer at the start of the assay. This will be investigated further in Chapter 6.

Indomethacin is reported to be a potent and full agonist at prostanoid $CRTH_2$ receptors in human native, human recombinant and animal native receptor assays with potencies relative to PGD_2 (RP) of 15-50 (Table 5). In these studies PGD_2 potency in the order of 1-20 nM was described. In my hands the relative potency (RP) of indomethacin was 8 with a relative activity (RA) of 0.63 against a PGD_2 potency (EC_{50}) of 0.2 μM. This is the first demonstration that indomethacin is a low efficacy (partial) agonist at human prostanoid $CRTH_2$ receptors and suggests that receptor-response coupling efficiency in these cells is relatively poor. (PGD_2 potency is also low compared to that reported elsewhere (Table 5)). The pharmacophore giving rise to prostanoid $CRTH_2$ receptor binding and agonism is likely to be unrelated to the COX 1/2 inhibitor pharmacophore since other NSAIDs were devoid of agonist and antagonist activity at the receptor. Indeed, in common with Hirai, *et al*., (2002), I found the structurally related plant auxin indole-3-acetic acid was without effect suggesting that the agonism shown by indomethacin has specific structural requirements. It is conceivable that indomethacin is producing an effect through activation of endogenous 5-hydroxytryptamine 1B receptors (Dickenson & Hill, 1998) but three lines of evidence argue against this: firstly, in CHO K1 $hCRTH_2$ cells, indomethacin is a partial agonist (pEC_{50} 6.9 ± 0.1) and shifts PGD_2 E/[A] curves with an apparent pA_2 of 6.1 ± 0.1 (Chapter 7); secondly, indomethacin displaces [^{3}H]-PGD_2 from CHO K1 $hCRTH_2$ cell membranes (pIC_{50} 7.5 ± 0.2; Chapter 7); thirdly, a large body of evidence has been reported (e.g. Armer, *et al*., 2005; Hata, *et al*., 2005) that indomethacin and other, but not all, indole-based molecules have high affinity for prostanoid $CRTH_2$ receptors. Sawyer, *et al.*, (2002) found that sulindac possessed some affinity for the receptor (pK_i 5.4) and so some inhibition would be expected here. However, the sulphone form of the molecule has much lower affinity (pK_i 4.7) which would be below the detection limit of this assay. Interestingly, the desensitisation potency of indomethacin was identical to its potency as an agonist but with a maximum effect equal to that of PGD_2, i.e. complete inhibition of responses to 0.3 μM PGD_2, suggesting that agonist exposure leads to an inhibition that is amplified with respect to the calcium mobilisation response. Since indomethacin is a partial agonist, the expectation is that its E/[A] curve is superimposable on its receptor occupancy curve. As described in Table 5, most affinity estimates for indomethacin at

prostanoid $CRTH_2$ receptors range between 1 and 8 μM; the EC_{50} of 2.5 μM obtained here is entirely consistent with the previous data. Prostanoid $CRTH_2$ receptors are described as being coupled to both calcium mobilisation and inhibition of adenylate cyclase through $G\alpha_{i/o}$ (Sawyer, *et al*., 2002, 2005; Sugimoto, *et al*., 2005), to β-arrestin recruitment via a non-PTX sensitive mechanism (Mathiesen, *et al*., 2005), and possibly via $G\alpha_{q/11}$ or $G\alpha_z$ to eosinophil shape change (Stubbs, *et al*., 2002; Böhm, *et al*., 2003). In studies using inhibition of forskolin-stimulated cAMP production as the assay readout, agonist potencies are consistently around 10-fold higher than in corresponding calcium mobilisation assays in the same cell line (Sawyer, *et al*., 2002, 2005; Sugimoto, *et al*., 2005). Therefore, it seems reasonable to assume that calcium mobilisation and cAMP reduction occur in parallel in the cells used here. Therefore, the observed inhibition of agonist responses subsequent to an initial exposure of cells to agonists may be occurring as a result of other, better-coupled, response pathways that have not been measured in these studies, e.g. inhibition of adenylate cyclase, activation of MAP kinases or regulation of K^+ channels.

The 2-arylpropionic acid, S-flurbiprofen (Figure 1), is a potent, non-selective, COX1/2 inhibitor which was without effect at human prostanoid $CRTH_2$ receptors. R-flurbiprofen is much less active as a COX inhibitor but the enantioselectivity associated with other actions of flurbiprofen such as γ-secretase inhibition (Gasparini, *et al*., 2005; Peretto, *et al*., 2005) inhibition of apoptosis involving p53 (Grosch, *et al*., 2005) activation of c-Jun-terminal-N-kinase (Grosch, *et al.*, 2003), inhibition of hepatic mitochondrial β-oxidation and oxidative phosphorylation (Browne, *et al*., 1999) and antimicrobial activity against certain fungal infections (Chowdhury, *et al*., 2003), varies. None of the non-COX activities are predicted to have a direct effect on prostaglandin synthesis, action, and metabolism, however, flurbiprofen is also a substrate for human cytochrome P450 2C9 (Wester, *et al*., 2004), a cytochrome with preference for lipophilic acids such as prostaglandins. Cytochrome dependent ω- or 20- hydroxylation of prostaglandins followed by β-oxidation to a carboxylic acid is a major metabolic route for prostaglandins, while cP450s of the 2B, 2C and 2J families, particularly cP450 2C9, metabolise arachidonic acid to epoxyeicosatrienoic acids (EETs; Michaelis, *et al*., 2005). Although information specifically relating to cP450 2C9 in CHO cells is not available, it is widely reported in the literature that CHO cells possess a fully functioning mitochondrial cP450 system even though endogenous expression of specific

cytochromes including 1B1 (Luch, *et al.*, 1998) and 2D6 (Ding, *et al.*, 2001) may be low or absent. Therefore, it is conceivable that in addition to suppressing the synthesis of prostaglandins in CHO cells, flurbiprofen simultaneously acts to inhibit the shunting of arachidonic acid into the EET synthetic pathway and, of greater potential significance, the metabolic inactivation of prostaglandins. This latter effect would serve to both increase autocrine receptor desensitisation and inhibit metabolism of exogenously applied prostaglandin. However, given the wide distribution of prostaglandin 15 dehydrogenase (PG15dH) in hamsters (Terada, *et al.*, 2001) and the presence of the enzyme in rat ovarian tissues (Inazu & Fujii, 1996), it seems reasonable to assume that CHO cells express PG15dH and that increased persistence of prostaglandins in the cells or the culture milieu is unlikely to occur. An effect on the metabolism of exogenously applied prostaglandins is not suspected because assays performed using non-NSAID treated cells revealed that application of flurbiprofen solely during the assay period did not alter PGD_2 E/[A] curve parameters.

Estimates of the potency of flurbiprofen as a COX inhibitor, and of the rank order of activities shown by a range of NSAIDs vary according to the methodology used. However, flurbiprofen is consistently shown to be of high potency at both COX-1 and -2. Recently, a third COX isoform has been identified, COX-3, at which ibuprofen has been shown to have higher potency than at the other COX isoforms (Chandrasekharan, *et al.*, 2002; reviewed in Chandrasekharan & Simmons, 2004). The expression of COX-3 in CHO cells is as yet undetermined but it seems likely that flurbiprofen will also be active at this enzyme.

Of great importance to the application of flurbiprofen in this setting is its high plasma protein binding. This has been estimated at over 99.9 % (Knadler, *et al.*, 1986; Evrard, *et al.*, 1996) in human plasma, and has been shown to be similarly high in the plasma of other species. Cell culture medium contains 10 % foetal calf serum which is sufficient to bind approximately 99 % of the flurbiprofen added, leaving free concentrations of 0.1 and 1 μM (30 and 300 x COX-1 K_i, respectively) at nominal concentrations of 10 and 100 μM. Thirty-fold K_i is insufficient to achieve adequate enzyme inhibition but 300-fold K_i can be considered to achieve near total inhibition of prostaglandin synthesis. This is borne out by the PGD_2 potency data which shows incremental increases as [flurbiprofen] rises from zero, to 10 μM, and finally to 100 μM. As discussed above, based on our current knowledge of flurbiprofen this is likely to be via COX inhibition

rather than some other aspect of the molecule's pharmacology. Concentrations above this were not tested because of the technical difficulties associated with the sterile preparation of high concentration flurbiprofen solutions but if these can be overcome it may be possible to achieve further increases in PGD_2 potency.

It is not my intention to discuss every detail of the assay development data since it is largely self-explanatory. Where a particular reagent or technique did not lead to an increase in assay performance, the selection of methodology was based on the cheapest, simplest or most standardised technique with respect to other assays running in the lab at that time. Certain features of the method do deserve particular mention. Since running the assay at 37 ºC made no difference to PGD_2 E/[A] curve parameters, assays were run at room temperature. The FLIPR® instrument possesses a built-in 384 tip pipettor which has settings for dispense speed, dispense height, number of reagent mixes and so on. Details such as these are rarely defined in the scientific literature but make a critical difference on the quality of the data that can be obtained. Artefacts caused by addition of liquids to assay wells generate 'responses' which arise from dye concentration changes or mechanical stimulation of the cells as added liquid flows over them. The latter effect increases as flow increases and the data presented in Table 2 shows larger basal responses with reduced Z' at relatively modest pipettor speeds. Similarly, little data is published comparing alternative organic anion transport inhibition strategies as mechanisms for ensuring Fluo 3 retention by cells. Here, sulphinpyrazone was without effect, giving rise to results identical to those obtained in the complete absence of inhibitor, and confirming the use of probenecid as a standard intervention. The development of a homogenous assay format using the sulphonamide quenching dye brilliant black BN was found to be necessary since a more conventional wash protocol led to detachment of cells from the plasticware. Brilliant black may interfere with certain agonists, typically peptide molecule agonists such as prokineticin (ligand for AXOR8) and TARC (ligand for CCR4; Coma, I. & de los Frailles, M., personal communication), and others such as angiotensin, bradykinin & neurokinin (Molecular Devices; http://www.moleculardevices.com/pdfs/MultispanPoster.pdf). This is likely to arise from a charged interaction with multiple centres of negative charge in the brilliant black molecule but in the case of prostanoids, this will result in a repulsion of the negatively charged carboxylate group. The data indicate that there is no effect of brilliant black on PGD_2 potency. Lastly, the vehicle concentration used (1 % DMSO) is at the limit of acceptability to the CHO cells used here. Addition of vehicle

was observed to produce low magnitude transient calcium fluxes which did not alter responses to subsequent addition of PGD_2. Concentrations of DMSO above this increased the variability around responses to a fixed concentration of PGD_2 (1 μM) and resulted in wells failing to respond to agonist on an apparently random basis. It is possible that during the transfection and clone expansion process, cells were selected with greater resistance to solvent exposure, allowing the use of a high solvent concentration such as this.

Calcium fluxes in response to PGD_2 in CHO $G\alpha_{16z49}$ $hCRTH_2$ cells do not require the presence of extracellular calcium thus indicating the endoplasmic reticulum (ER) as the likely source of the calcium and implicating the phospholipase C β – inositol 1,4,5 triphosphate (PLCβ – IP_3) pathway as the coupling mechanism. Furthermore, the ability of pertussis toxin (PTX) to abolish responses in CHO K1 $hCRTH_2$ cells and to reduce responses in CHO $G\alpha_{16z49}$ $hCRTH_2$ cells by 85 % suggests the involvement of $G\alpha_{i/o}$ G-proteins, presumably coupling to PLCβ through the Gβγ subunits (see Chapter 4). Because responses in CHO K1 $hCRTH_2$ cells were abolished, all $G\alpha_{i/o}$ coupling in CHO $G\alpha_{16z49}$ $hCRTH_2$ cells should also have been abolished. Therefore, the small signal remaining after PTX treatment in the chimeric cell lines is assumed to be due to coupling through the chimeric G-protein since the expression of this molecule is taken to be the only difference between the two receptor-expressing cell lines. Although incubation with higher concentrations of PTX was not attempted, incubation of double the number of cells with the same concentration of PTX produced identical results. The weakness of this signal is not typical of calcium coupling through the alpha subunits of $G\alpha_q$ class G-proteins which raises the possibility that this signal is actually mediated via Gβγ subunits. In this regard, it is interesting to note that curve slopes in non PTX-treated cells are generally lower and indicative of coupling through two response pathways. In experiments comparing PGD_2 E/[A] curves in cells ± PTX treatment conducted in parallel, PGD_2 curve slope was found to increase (data in text at section 3.3.7) however this effect was lost when mean data sets from non-parallel experiments were compared (Table 4). The increase in slope presumably reflects removal of the $G\alpha_{i/o}$ coupling pathway and is contrary to the expected result of interruption of synergising interactions (see below). Further delineation of this response pathway is clearly needed perhaps using the $G\alpha_q$ inhibitor YM254890 (Takasaki, *et al*., 2004), the phosphatidyl choline specific PLC (β) inhibitor U73122 (Walker, *et al.*, 1998), and the

non-IP_3 receptor inhibitor ryanodine. In addition, over-expression of a βγ-subunit scavenger such as the C-terminal of β adrenoreceptor kinase 1 (β ARK1 495-689; Dickinson & Hill, 1998) would provide confirmation of the molecular identity of the coupling partners in the chimeric cell line.

CHO $G\alpha_{16z49}$ host cells were essentially devoid of responses to PGD_2. The small decreases in basal fluorescence observed were most likely due to addition artefacts in this experiment. CHO cells are reported to endogenously express prostanoid EP_4 receptors (Crider, *et al*., 2000) which classically do not couple to calcium mobilisation. However, we have generated data in separate studies (not shown) that indicates PTX-sensitive coupling of EP_4 receptors in highly expressing recombinant systems, raising this as a possibility. Indeed, the bell-shaped E/[A] curve produced by PGE_2 here is indicative of a dual mechanism of action but insensitivity to challenge with the EP_4/TP receptor antagonist GW627368X (Wilson, *et al.*, 2006) effectively rules prostanoid EP_4 receptors out. Similarly, the inactivity of DP & $CRTH_2$ antagonists rules out these receptors. Taken together prostanoid EP_1 ($G\alpha_q$-like coupling) and EP_3 (splice-dependent $G\alpha_{i/o}$, α_s, & α_q coupling) receptors remain as likely candidates. Given that the maximum response to PGE_2 in the host cells was c.10 % of the PGD_2 maximum response in receptor expressing cells, and that PGE_2 was without effect in receptor expressing cells, if an endogenous EP receptor is present, its impact on the overall study will be minimal. The lack of effect of PGE_2 in receptor-expressing cells could arise from dual opposing effects on intracellular calcium. Indeed, the activity of other E series prostaglandins in PTX-treated cells (see below) support the notion that an endogenous receptor *is* present.

Agonist pharmacology in CHO $G\alpha_{16z49}$ $hCRTH_2$ cells bore the hallmark features of prostanoid $CRTH_2$ receptors: lack of activity of PGE_2, $PGF_{2\alpha}$, PGI_2 & U-46619; high potency responses to PGD_2 but not the prostanoid DP_1 receptor agonist BW245C; agonist rank order of potency 15 R 15 methyl PGD_2 > PGD_2 > PGJ_2 > 15 deoxy $\Delta^{12,14}$ PGJ_2 > 15 S 15 methyl PGD_2 > 13,14 dihydro 15 keto PGD_2; insensitivity of PGD_2 responses to the prostanoid DP_1 receptor antagonist BW868C; and sensitivity to the putative prostanoid $CRTH_2$ receptor antagonist GW853481X (Bauer, *et al*., 2002; see references cited in Table 5 for agonist pharmacology). Furthermore, PGD_2 responses were insensitive to prostanoid TP, EP_4 & EP_1 receptor antagonists, discharging the risks associated with endogenous expression of prostanoid EP_4 and EP_1 receptors, and the

established pharmacophoric overlap with prostanoid TP receptors indicated by the activity of ramatroban reported in Ishizuka, *et al*., 2004.

Interestingly, the prostanoid TP / EP_4 receptor antagonist AH23848B (Figure 1; Brittain, *et al*., 1985) was an antagonist at prostanoid $CRTH_2$ receptors. The low potency of AH23848B necessitated the use of a high concentration of the compound in order to observe displacement of PGD_2 E/[A] curves. This also prevented a clear demonstration of the compound's mechanism of action since higher antagonist concentrations could not be achieved. In the presence of 30 μM antagonist, the PGD_2 E/[A] curve was shifted to the right with no depression of the upper asymptote. There was, however, a non statistically-significant increase in curve slope. Increased curve slopes can indicate complexities in the behaviour of the antagonist or of the biological system, for example multiple PGD_2-sensitive receptors or the presence of a physicochemically protected sub-population of receptors that the antagonist cannot access. Given that the trend is non-significant and that increased curve slopes have not been observed with the use of this compound elsewhere in this thesis (chapter 4., figure 8) it seems likely that this is an isolated observation. The apparent pA_2 value of AH23848B vs. prostanoid $CRTH_2$ receptors is similar to its established affinity at prostanoid EP_4 receptors and to its previously reported binding pK_i of 5.5 at human prostanoid $CRTH_2$ receptors (Sawyer, *et al*., 2002). I therefore propose that AH23848B should be reclassified as a prostanoid $CRTH_2$ / EP_4 / TP receptor antagonist.

These data also confirm that compound 1c (GW853481X; Figure 1) in Bauer, *et al*., 2002, is indeed a prostanoid $CRTH_2$ receptor antagonist, and establish an apparent pA_2 estimate of 6.5 for the molecule. The compound did not elicit any agonist effects over the concentration range tested here but in later experiments (see Chapter 7) did produce agonist like effects at higher concentrations (pEC_{50} 4.5) which may explain the non-total inhibition of PGD_2 EC_{70} by this compound (Fig. 6, Panel A) and which may contribute to the observed depression of PGD_2 E_{max} noted below. The selectivity of the compound was confirmed by its lack of activity against UTP acting at the endogenous $P2_{Y2}$ receptor in these cells. Although agonist E_{max} was decreased by treatment with 1 μM antagonist, higher concentrations did not elicit any further decreases. This suggests that curve depression was neither a systematic effect of the compound nor an expression of hemi-equilibrium phenomena (a common observation in calcium mobilisation assays where the response takes place in a time frame (seconds) too fast for agonist and

antagonist to establish a new equilibrium at the receptor). Notwithstanding the E_{max} effect, PGD_2 curves were shifted to the right in a parallel fashion suggesting GW853481X is competitive. Indeed, the constancy of the apparent pA_2 estimate across the antagonist concentrations tested is also indicative of a reversible competitive interaction. The trend (non significant) in apparent pA_2 estimates towards lower values at higher antagonist concentrations is likely to be a reflection of the impact of upper asymptote depression on curve midpoint location. Analysis based on mid-points is only valid where no depression of agonist E_{max} occurs. If depression does occur, analysis in this way is likely to result in pA_2 under-estimation while hemi-equilibrium will distort affinity estimates in the opposite manner, leading to over-estimation. Therefore, the affinity reported here is a reasonable estimate and GW853481X may be described as a competitive prostanoid $CRTH_2$ receptor antagonist. (In Chapter 7, data will be presented showing no E_{max} depression by GW853481X and resulting in a pK_b determination by Schild analysis of 6.3 ± 0.16).

The panel of 76 prostanoid molecules produced a range of activities at human prostanoid $CRTH_2$ receptors and have established for the first time a comprehensive agonist fingerprint for the receptor. Although there is no *a priori* reason to expect binding and functional assay data to correlate, comparison of binding pK_i values taken from Sawyer, *et al*., 2002, with functional pEC_{50} values generated in non-PTX treated cells yielded a correlation coefficient (r^2) of 0.88 (Figure 9). However, this is misleading since the slope of the regression is significantly less than 1.0, and functional pEC_{50} data are $\geq$1.0 log unit lower than binding pK_i data for all molecules except PGD_2. The rank order and pEC_{50} values for agonists obtained here is consistent with data presented for calcium mobilisation elsewhere and lends further weight to the widely acknowledged principle that binding is not a good indicator of function. However, the binding data do appear to correlate with potencies determined using cAMP lowering as the functional assay readout ($r^2 = 0.90$, slope = 1.0; Figure 9; Sawyer, *et al*., 2002). The latter data indicate high efficiency receptor-effector coupling and under these circumstances the impact of efficacy on potency is reduced (affinity driven potency; Kenakin, 1999). The converse is true in poorly coupled systems where efficacy is a more important determinant of potency. In the present studies, calcium mobilisation data are indicative of poor coupling (low PGD_2 and indomethacin potencies c.f. literature values) and would be expected to demonstrate efficacy-driven agonist potencies. A number of functionally inactive compounds have been reported to possess

binding affinity; pK_i's for these compounds are close to or beyond the detection limit of the functional assay and so are not expected to be active. One notable exception is 13,14 dihydro 15 keto $PGF_{2\alpha}$ (Figure 1; pK_i 8.5) which produced small responses at 10 μM (12 % of PGD_2 max), was of low potency in the cAMP assay, and was excluded from the correlation described above. Binding pK_i was estimated by competitive displacement of [^{3}H]-PGD_2, consistent with an orthosteric competitive interaction. Thus 13,14 dihydro 15 keto $PGF_{2\alpha}$ could be an antagonist at human prostanoid $CRTH_2$ receptors with respect to calcium mobilisation, but an agonist with respect to cAMP reduction. Whether this is an example of a 'permissive antagonist' (Kenakin, 2005) will depend on the nature of the hypothesized antagonism and will be investigated in Chapter 7. In this respect it would be interesting to determine whether this molecule could activate or inhibit the PTX-insensitive β-arrestin recruitment of prostanoid $CRTH_2$ receptors reported by Mathiesen, *et al*. (2005).

Before discussing the impact of PTX treatment on agonist activity, I wish to make some observations relating to agonist SAR at human prostanoid $CRTH_2$ receptors in non PTX-treated CHO $G\alpha_{16z49}$ $hCRTH_2$ cells. Only prostaglandin D (9 hydroxy 11 keto), J ($\Delta^{9,10}$ 11 keto) and $F_{2\alpha}$ (9,11 dihydroxy) cyclopentane ring groups gave rise to molecules with agonist activity with the rank order D > J > $F_{2\alpha}$. Although hydroxyl group hydrogen atoms are weakly acidic (pK_a ~ 16) the main functionalities of these and carbonyl groups in this setting are as hydrogen bond (H-bond) donors (hydroxyl) and acceptors (hydroxyl and carbonyl). H-bond acceptor functionality at C11 is shared by all three ring systems and it would appear that that conferred by carbonyl groups is more effective at stimulating agonism, possibly by adoption of alternative resonance structures. The rigid conformation accorded by the C=O double bond may access a binding / activation motif that the more flexible and less electronegative –OH group cannot. It is therefore surprising that prostaglandin E (9 keto 11 hydroxy), I (11 keto 6,9 fused tetrahydrofuran), and K (9,11 diketo) structures are inactive. These findings can be reconciled if the binding pocket accessed by the head group is sterically restricted such that a small flexible H-bond donor is needed at C9 with specific spatial relationship to a conformationally rigid H-bond acceptor at C11. The importance of the C11 carbonyl is re-iterated by the complete lack of activity shown by 11 deoxy 11 methylene PGD_2. Alternatively, the fatty side chains of prostaglandins have a high degree of conformational freedom which is critically affected by substitutions onto the

cyclopentane ring. Thus the relationship of H-bond donors and acceptors may exert their effect through alteration of side chain conformation.

Stereoselectivity around the C15 position has been demonstrated by Monneret, *et al.* (2003), for D series prostaglandins. These data confirm the finding that 15R stereochemistry gives rise to higher potency than 15S for D series prostaglandins and extends it to include F series prostaglandins. All naturally occurring prostaglandins, have 15S hydroxy stereochemistry but 15 R $PGF_{2\alpha}$ is more potent than $PGF_{2\alpha}$. 15 R PGD_2 is not available but is predicted to have higher potency than PGD_2 but not 15 R 15 methyl PGD_2 since 15 R $PGF_{2\alpha}$ has lower potency than 15 R 15 methyl $PGF_{2\alpha}$. Interestingly, the effect of C15 methyl substitution depends on the stereochemical arrangement: 15 S 15 methyl reduces potency / activity, while 15 R 15 methyl increases potency for both D and F series prostaglandins. These data may suggest that in the R conformation, the 15 hydroxy group is exposed and interaction with the receptor is facilitated. The role of the $–CH_3$ group may be to sterically hinder 15 hydroxy group interactions in the S configuration but to enhance it in the R form. However, the obligate importance of the 15 hydroxy group is called into question by data for 15 deoxy variants of D and J series prostaglandins. Thus 15 deoxy PGD_2 is less potent than PGD_2 but 15 deoxy variants of PGJ_2 are equipotent. This may reflect the precise conformation of the β side chain which in the case of the J series molecules is affected by C=C double bond rearrangement from C13 to C12 and 14. Thus, the presence of a C15 hydroxy may be required to stabilise a conformation through H-bond interactions which is also stabilised by the presence of $\Delta^{12,14}$ double bonds. Circumstantial evidence in support of the importance of the C=C double bonds is given by the reduction in potency shown by PGD_1 and PGD_3. Other authors have suggested that PGD_3 and PGD_2 are equipotent (Monneret, *et al.*, 2003) so taken together these data may indicate the presence of a Δ^{17} reductase enzyme in the eosinophil assay used by Monneret.

The direction of the H-bond interaction is difficult to assess: 15 keto PGD_2 is less potent suggesting H-bond donation is required but 15 keto $PGF_{1\alpha}$ and 15 keto $PGF_{2\alpha}$ are more potent than their respective natural prostaglandins suggesting H-bond acceptance is required. The common functionality in these groups is H-bond acceptance; the differences may arise from the positioning of oxygenated groups on the cyclopentane ring with the rigidity of the carbonyl at C15 being required to overcome the lack of spatial restriction in the C11 hydroxy group of F series molecules. Forcing the C11

group into its binding pocket may also be demonstrated by the $PGF_{2\alpha}$ analogues cloprostenol and latanoprost which both carry bulky aromatic hydrocarbon groups at the C18 position. Indeed 17 phenyl ω 18,19,20 trinor PGD_2 also retains activity but presumably the reduction in potency relative to PGD_2 is now due to hindrance of C15 hydroxy interactions since 16,16 dimethyl PGD_2 is only weakly active.

Lastly, although substitution of an isopropyl group into the C1 carboxylic acid group in latanoprost retains activity, complete loss of the carboxylate functionality abolishes activity, as in PGD_1 alcohol. Thus a picture emerges of an agonist pharmacophore for human prostanoid $CRTH_2$ receptors in non-PTX treated cells, illustrated in Figure 10. The coupling partner in this setting is assumed to be βγ subunits of $G\alpha_{i/o}$ G-proteins but this requires greater definition since coupling through $G\alpha_{16z49}$ also occurs simultaneously.

SAR data at the same receptor in PTX-treated cells (i.e. assumed to be coupled through the $G\alpha_{16z49}$ G-protein) were more complicated. The rank order of agonist potencies, and the stereochemistry within the D and J series were preserved but relative to each other there was a marked drop in the potency of D series agonists. There was an even greater drop in the potency of F series agonists suggesting that although an H-bond acceptor is still required at C11, there is increased spatial stringency around the C9 position for activation of $G\alpha_{16z49}$. One molecule, 15 R 15 methyl $PGF_{2\alpha}$, displayed a dramatic change in activity, becoming inactive in the PTX treated cells: possibly an example of a G-protein specific agonist at human prostanoid $CRTH_2$ receptors. PGD_2 E_{max} under these conditions was insufficient for quantitative analysis of competition but did permit GW853481X pIC_{50} determination (6.4 ± 0.3), which was consistent with non PTX-treated values.

These pharmacophoric requirements are apparently contravened by an A series molecule (9 keto $\Delta^{10,11}$) and several E series (9 keto 11 hydroxy) molecules that showed very weak activity. Features of the SAR (lack of C11 H-bond functionality, opposite stereochemistry at C15) are strongly indicative of a second pharmacophore at a different protein. Indeed, C15 S > R is the typical stereoselectivity demonstrated by other prostanoid receptors. As discussed above, there is evidence from studies in CHO $G\alpha_{16z49}$ host cells that may indicate the presence of an endogenous prostanoid EP_1 or EP_3 receptor in these cells. Alternatively, if one 'flips' these molecules such that the functional group at C9 occupies the space formerly occupied by the group at C11 it is

possible to envisage a possible mechanism for E and A series prostaglandins to dock with the pharmacophore. It is also interesting to note that PGE_1 and $_3$ are both active while PGE_2 is inactive, suggesting that the fully flexible β chain in PGE_1 and the conformationally restricted chain in PGE_3 both position the C15 group favourably while this is not possible in PGE_2 itself. However, given the molecular contortions needed to bring the C15 hydroxyl group into position, this alternative binding modality seems unlikely. A further possibility is that these agonists are acting at a second agonist binding site on the receptor. If this were so then complexities in agonist and antagonist pharmacology might be expected, for example agonist-specific antagonist affinities and complex radioligand binding (see chapter 7 for further comments) but the detection of small responses in chimera-expressing host cells suggests that another receptor type may be present.

These data highlight some of the difficulties inherent to pharmacophore generation. All compound potencies, affinities and activities, irrespective of their origin in binding or functional assays, are the combined product of affinity *and* efficacy (Colquhoun, 1987, 1998; references cited in Rang, 2006). In many functional settings, this will involve activity at multiple, sometimes opposing, transduction and regulation pathways producing a composite snapshot of compound SAR specific to that pharmacological environment: bad news for receptor classification studies! These data demonstrate large changes in agonist rank order of potency generated in the same cell line under two different G-protein coupling conditions and highlight the critical importance of the coupling partner as a determinant of compound activity.

The choice of coupling partner in recombinant cell based assays is usually based on pragmatism and is often decided simply on the basis of 'the one that works first'. Greater rationality can be applied by tailoring the biological reagent to provide an assay reporting the biochemical changes relevant to the physiological process under investigation. Thus native G-proteins are always first choice but where multiple transduction pathways exist, perhaps mediated by different second messengers, then care must be taken to select the pathway of most relevance to the ultimate application. However, the concept of selecting 'the right *one*' may be considered redundant since the simple answer is that 'they are *all* right'. Assay systems that provide for greater integration of biochemical processes in whole single cells, groups of cells, and whole tissues may provide integrative SAR more predictive of eventual *in vivo* activity.

The data presented in this chapter have raised some important questions which will be addressed in subsequent chapters:

1. Definition of prostanoid SAR at human $CRTH_2$ receptors coupled through $G\alpha_{i/o}$ alone using $G\alpha$ and $G\beta\gamma$ readouts.
2. Relationship between this pharmacophore (activity based) and the receptor structure (structure based pharmacophore).
3. Screening for prostanoids with affinity but no efficacy (antagonists).
4. Greater definition of calcium mobilisation signal transduction.
5. Exploration of the significance and SAR of agonist induced desensitisation.
6. Examination of 13,14 dihydro 15 keto $PGF_{2\alpha}$ and 15 R 15methyl $PGF_{2\alpha}$ as putative R-G pair selective agonists.

and finally,

7. The antagonist properties of AH23848B at human prostanoid $CRTH_2$ receptors.

3.5 Figure caption list:

Figure 1. Structures of some molecules relevant to these studies.

Figure 2. Prostaglandin D_2 (PGD_2) concentration effect curves in CHO $G\alpha_{16z49}$ $hCRTH_2$ cells of clonal cell lines 8 and 17, plated out at 5,000 and 10,000 cells $well^{-1}$, respectively (taking into account their different growth characteristics, this represented the same degree of confluency for the two clones). Cells were grown in the absence of COX inhibition. Data are mean ± sem of twelve E/[A] curves from three separate assays. Terms are as defined in Methods.

Figure 3. Panel A: Prostaglandin D_2 (PGD_2) concentration effect curves in CHO $G\alpha_{16z49}$ $hCRTH_2$ cells of clonal cell line 8. Cells grown ± indomethacin (3 μM). Data are mean ± sem of twelve E/[A] curves from three separate assays. Panel B: PGD_2 and indomethacin E/[A] curves in clone 8 cells grown in the absence of COX inhibitors. Data are mean ± sem of sixteen E/[A] curves from three separate assays.

Figure 4. Panel A: Prostaglandin D_2 (PGD_2) and PGE_2 concentration effect curves in CHO $G\alpha_{16z49}$ (host) and CHO $G\alpha_{16z49}$ $hCRTH_2$ ($CRTH_2$) cells. Cells grown in the presence of flurbiprofen (100 μM). Data are mean ± sem of six E/[A] curves from three separate assays. Panel B: Effect of prostaglandins or vehicle on CHO $G\alpha_{16z49}$ (host) cells. * denotes P = 0.05. Panel C: Effect of vehicle, 30 μM AH23848B, 10 μM GW853481X or 1 μM BWA868C on responses to 10 μM PGD_2 or PGE_2 in CHO $G\alpha_{16z49}$ (host) cells.

Figure 5. Representative data showing the effect of the prostaglandins PGD_2, PGE_2, $PGF_{2\alpha}$, PGI_2 and the prostanoid U-46619 in CHO $G\alpha_{16z49}$ $hCRTH_2$ cells. Data are mean ± sem of four E/[A] curves generated in a single experiment. Data in text and tables for these compounds were generated over four experimental occasions.

Figure 6. Panel A: Inhibition of responses to 0.3 μM PGD_2 by GW853481X in CHO $G\alpha_{16z49}$ $hCRTH_2$ cells. Data are mean ± sem of seven E/[A] curves generated separately in the same experimental occasion. Panel B: PGD_2 E/[A] curves generated

in the presence of vehicle or increasing concentrations of GW853481X (Schild analysis) and, inset, Clarke plot of antagonist pA_2 estimated at each concentration of antagonist vs. log[antagonist concentration]. Data are mean ± sem of four E/[A] curves generated separately in the same experimental occasion.

Figure 7. Panel A: Inhibition of responses to 0.3 μM PGD_2 by AH23848B in CHO $G\alpha_{16z49}$ $hCRTH_2$ cells. Data are mean ± sem of seven E/[A] curves generated separately in the same experimental occasion. Panel B: PGD_2 E/[A] curves generated in the presence of vehicle or 30 μM AH23848B. Data are mean ± sem of six E/[A] curves generated in three separate assays.

Figure 8. Effect of pertussis toxin treatment on responses to PGD_2 in CHO $G\alpha_{16z49}$ $hCRTH_2$ cells. Panel A: PGD_2 E/[A] curves in PTX-treated or -untreated cells at passage 10 (P10). Data shown are for 2×10^4 cells $well^{-1}$; treatment of 4×10^4 cells $well^{-1}$ produced identical results. Panel B: Left chart: Maximum responses to PGD_2 in PTX-treated cells at passages 10-16 (P10-16) compared with responses in untreated control (C) cells; Right chart: PGD_2 pEC_{50} in PTX-treated and -untreated cells at P10-16. Data are mean ± sem of twelve E/[A] curves generated in three separate experiments. * denotes $P < 0.01$ cf. PGD_2 pEC_{50} in PTX-untreated or ** PTX-treated cells at P10.

Figure 9. Correlation plots of functional assay pEC_{50} data with binding assay pK_i values (Sawyer, *et al.*, 2002). Panel A: Calcium assay pEC_{50} (this study) vs. pK_i; Panel B: cAMP assay pEC_{50} (Sawyer) vs. pK_i.

Figure 10. Summary of agonist pharmacophore at human prostanoid $CRTH_2$ receptors expressed in CHO $G\alpha_{16z49}$ cells deduced from agonist potency data in non-pertussis toxin treated cells. Activity is therefore assumed to represent coupling through the βγ subunits of $G\alpha_{i/o}$.

3.6 Figures

Follow on next page

Figure 1

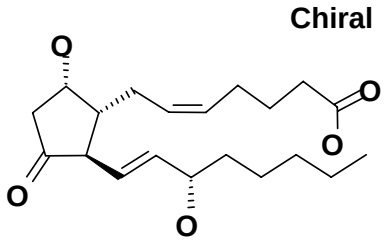

Prostaglandin D_2

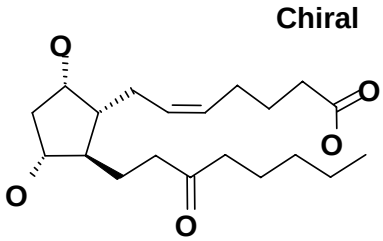

13,14 dihydro 15 keto prostaglandin $F_{2\alpha}$

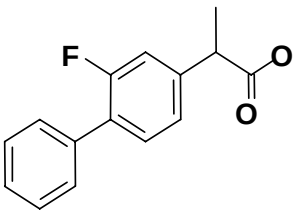

Flurbiprofen

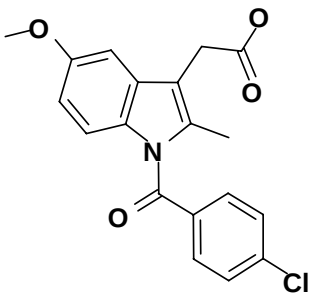

Indomethacin

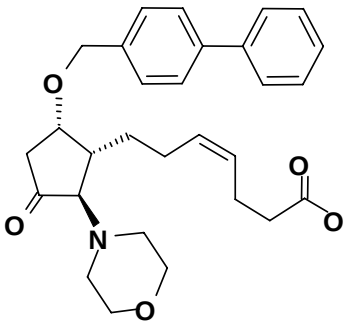

AH23848B

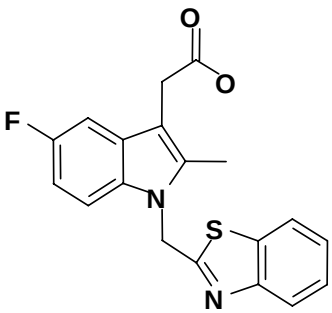

GW853481X

Figure 2

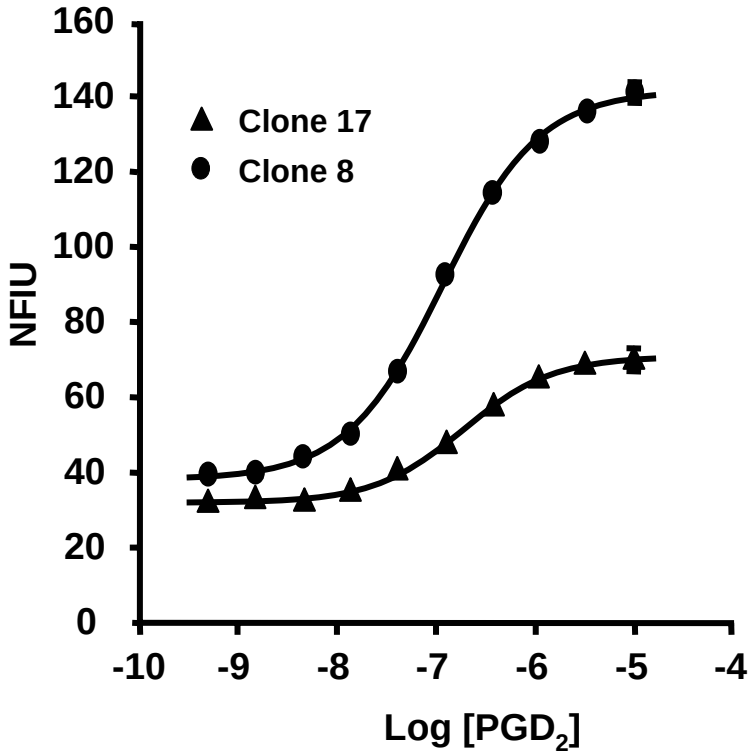
160
140
120
100
80
60
40
20
0
NFIU
Clone 17
Clone 8
-10
-9
-8
-7
-6
-5
-4
Log [PGD2]

Figure 3

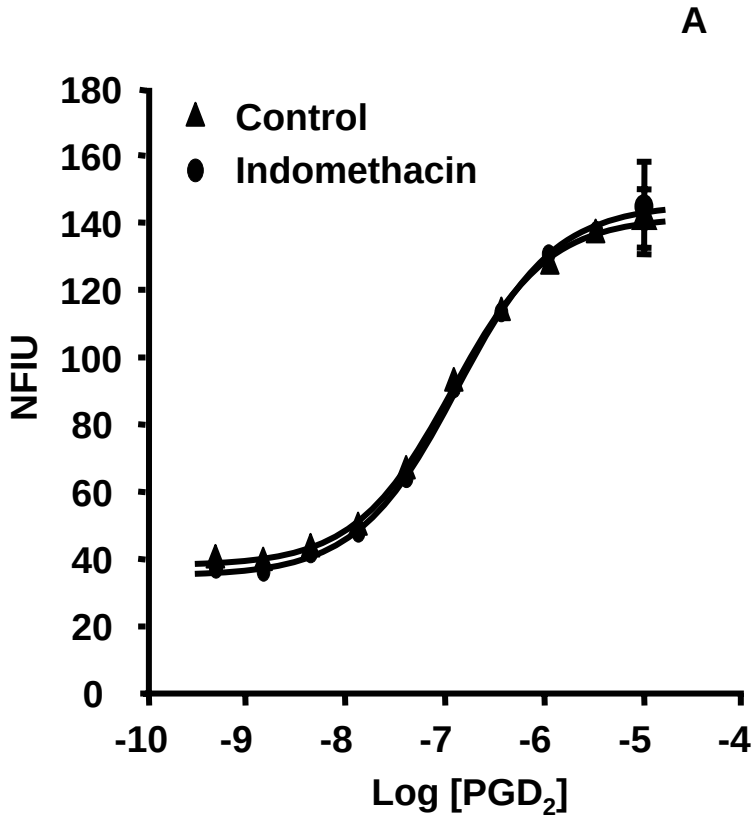
A
Control
Indomethacin
NFIU
180
160
140
120
100
80
60
40
20
0
-10
-9
-8
-7
-6
-5
-4
Log [PGD2]

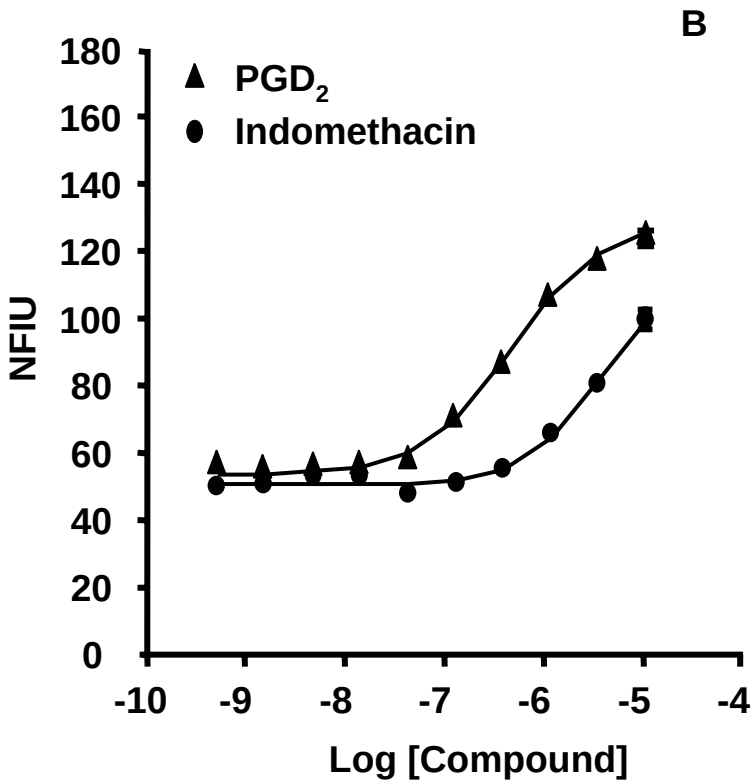
B
PGD2
Indomethacin
NFIU
180
160
140
120
100
80
60
40
20
0
-10
-9
-8
-7
-6
-5
-4
Log [Compound]

Figure 4

Panel A

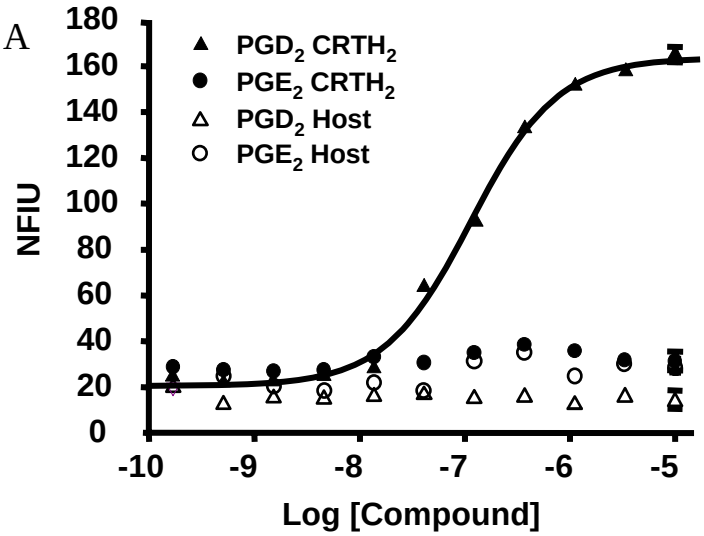

Panel B

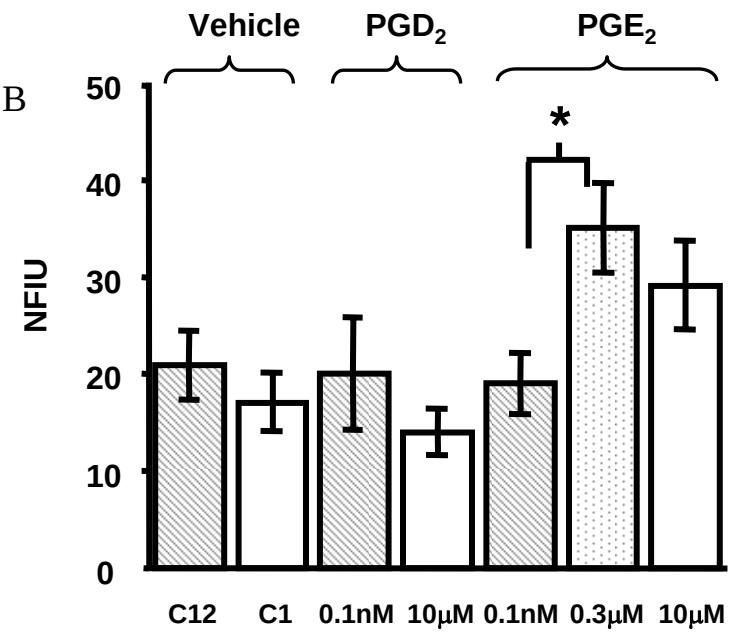

Panel C

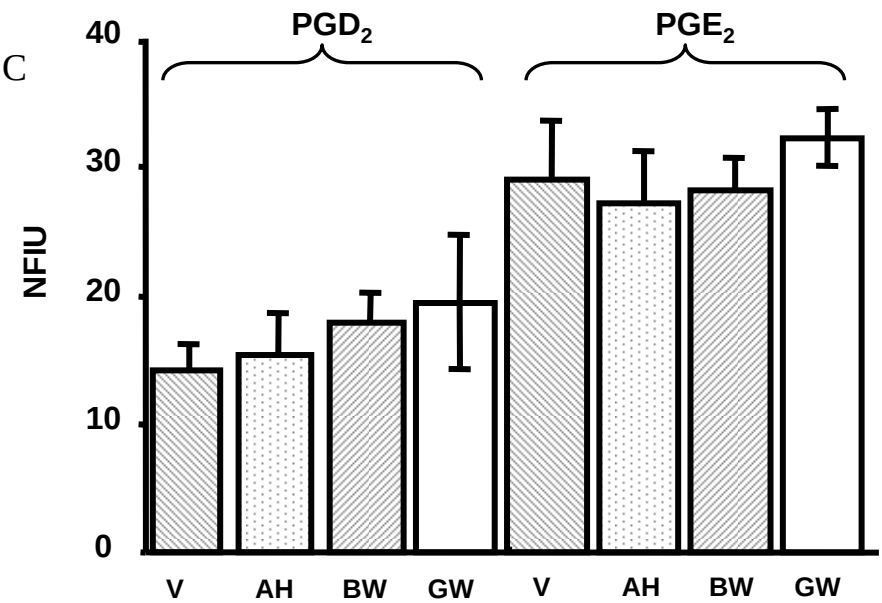

Figure 5

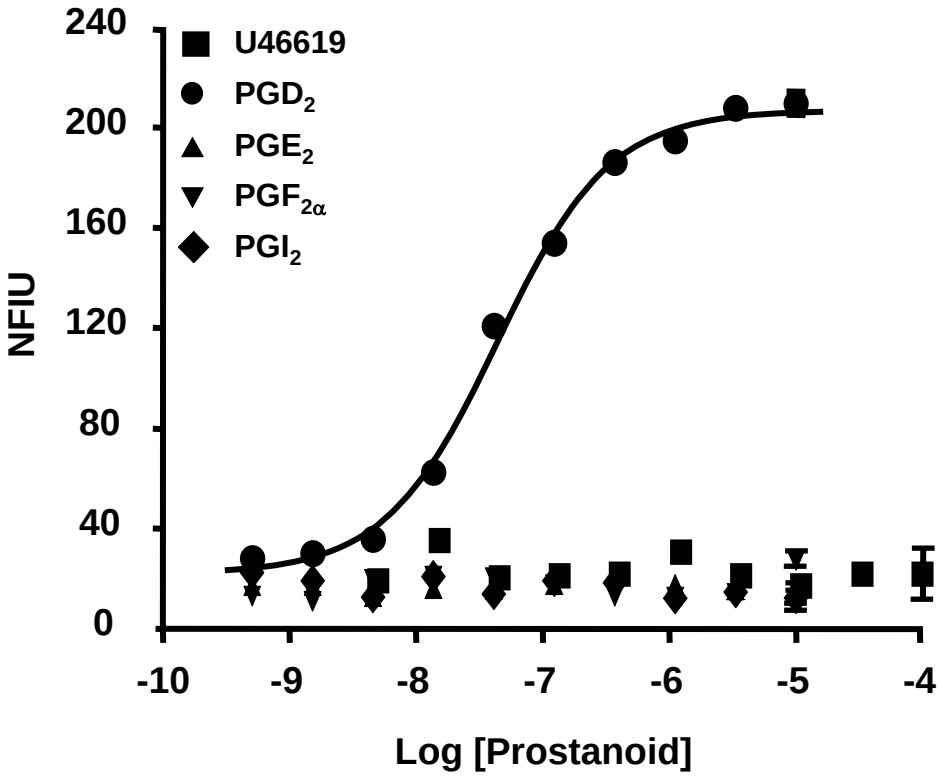
240
200
160
120
80
40
0
NFIU
U46619
PGD2
PGE2
PGF2α
PGI2
-10
-9
-8
-7
-6
-5
-4
Log [Prostanoid]

Figure 6

Panel A

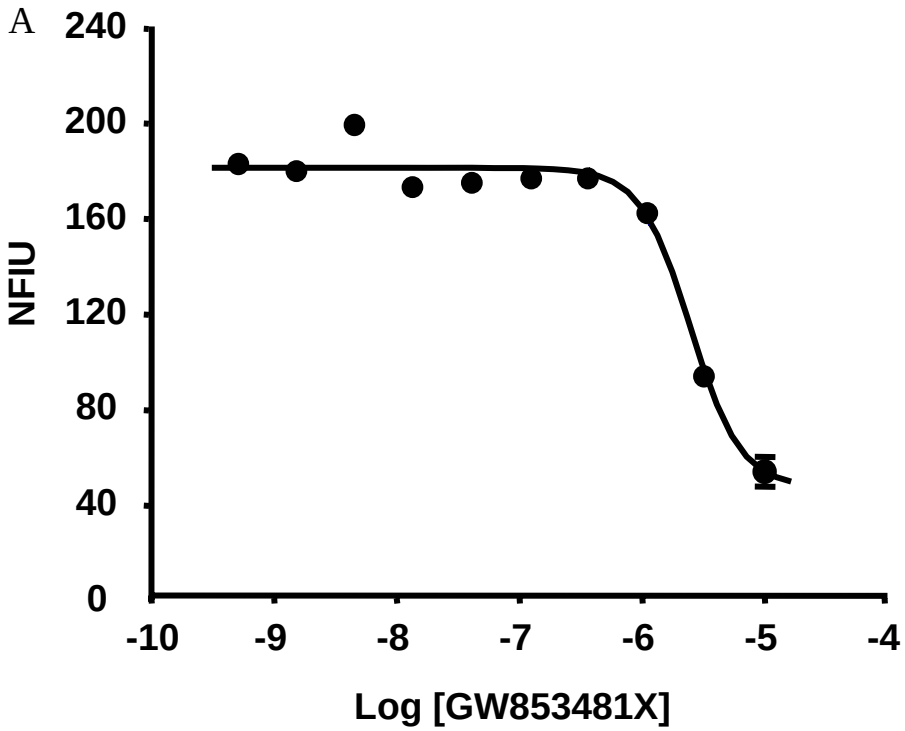

Panel B

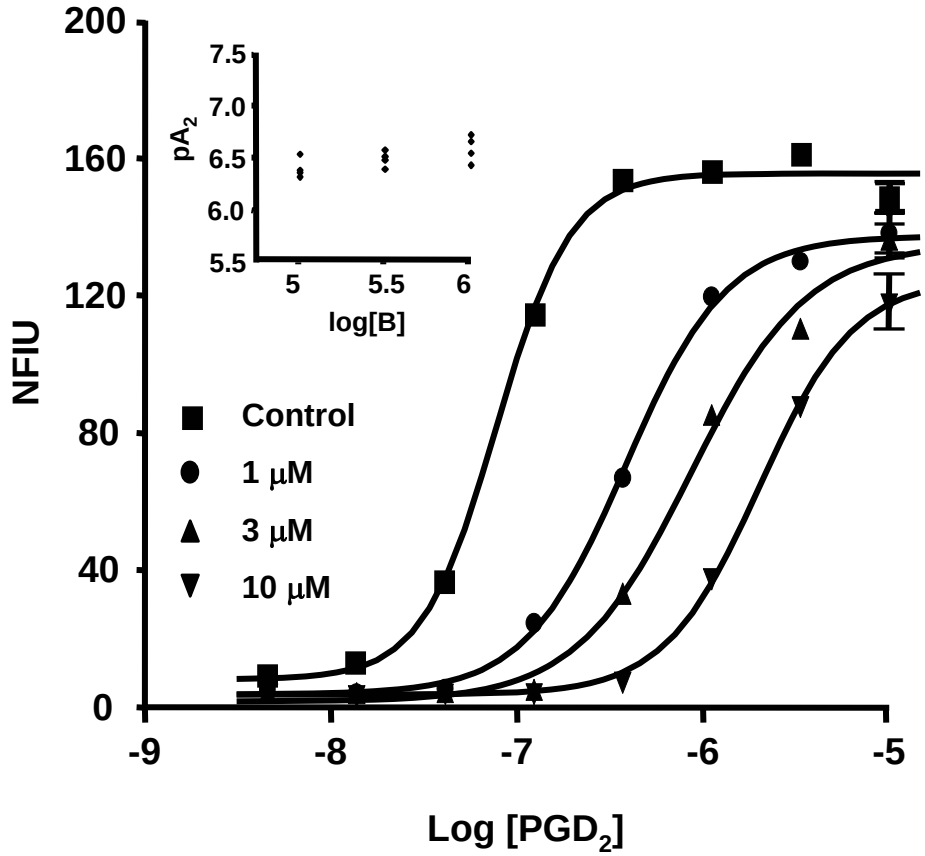

Figure 7

Panel A

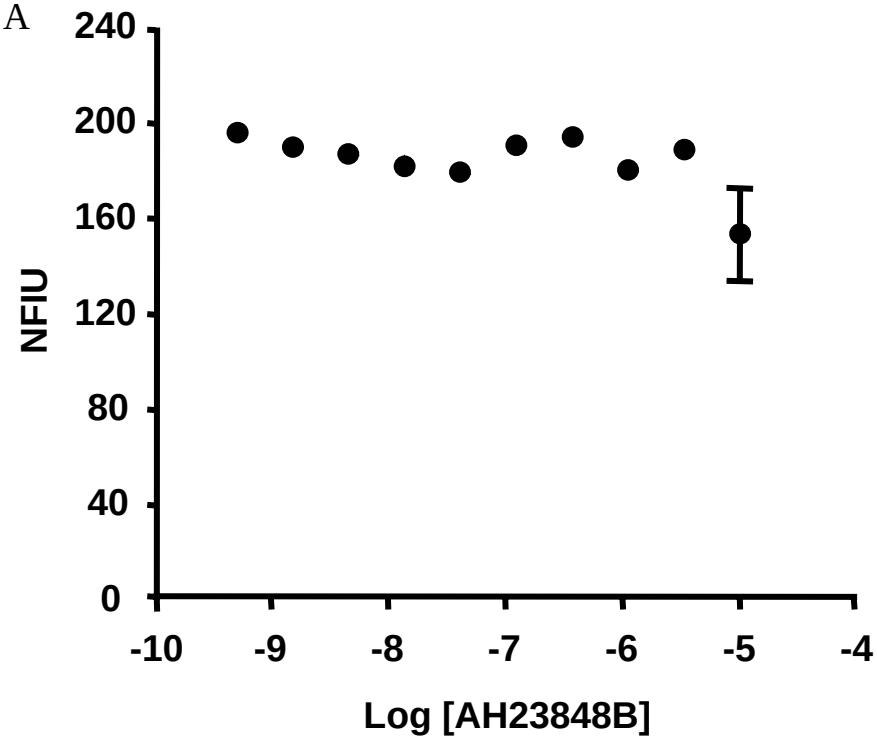

Panel B

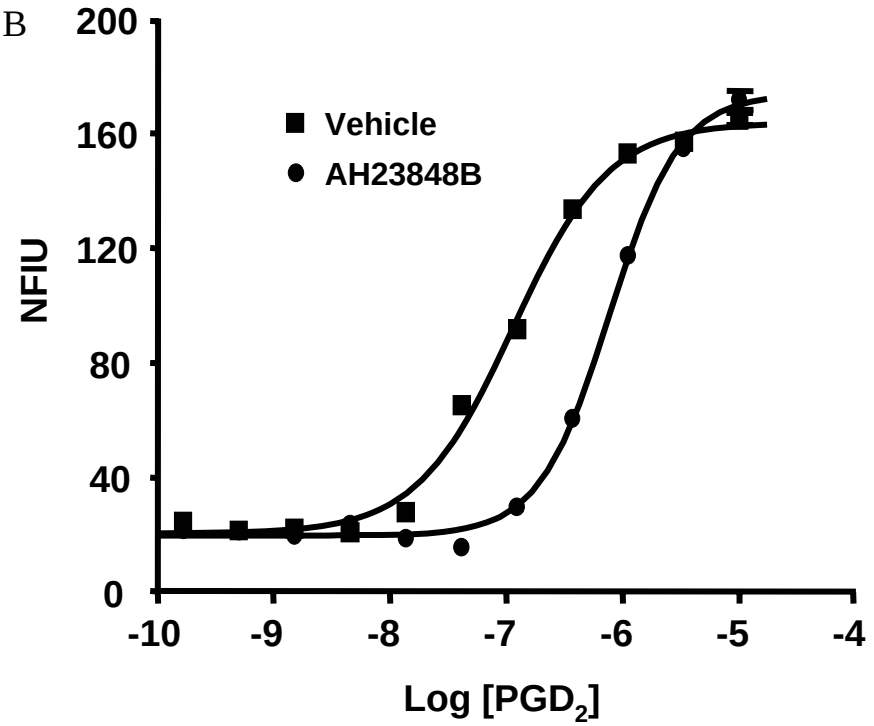

Figure 8

Panel A

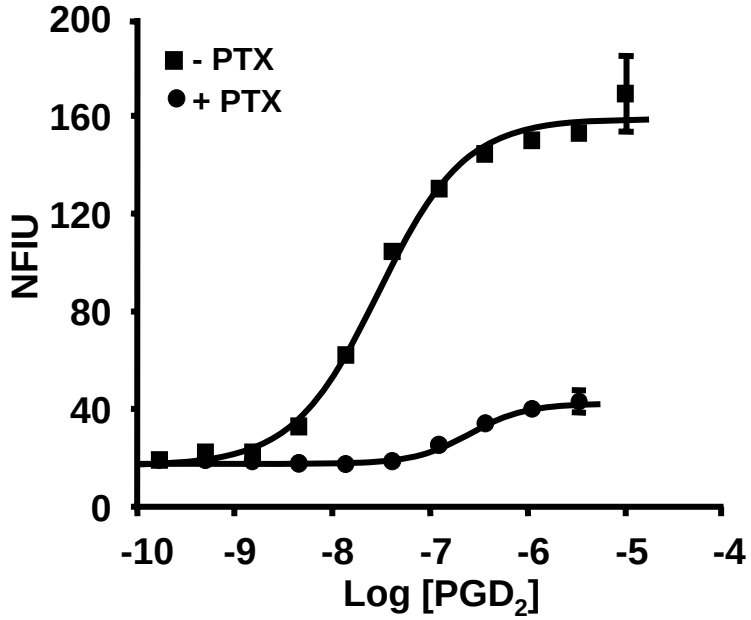

Panel B

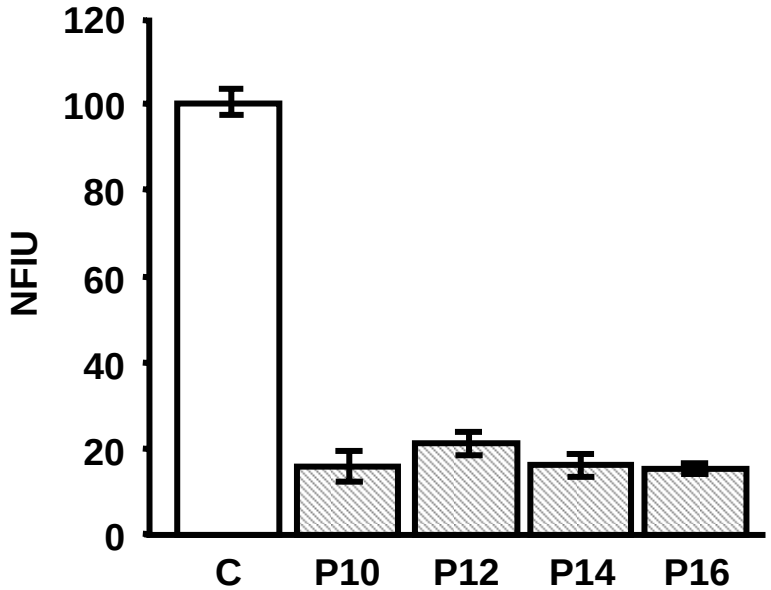

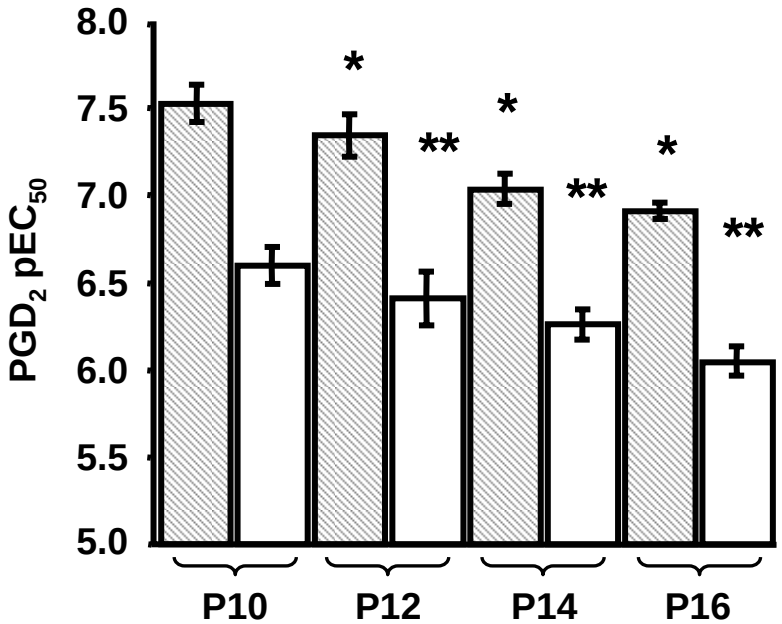

Figure 9

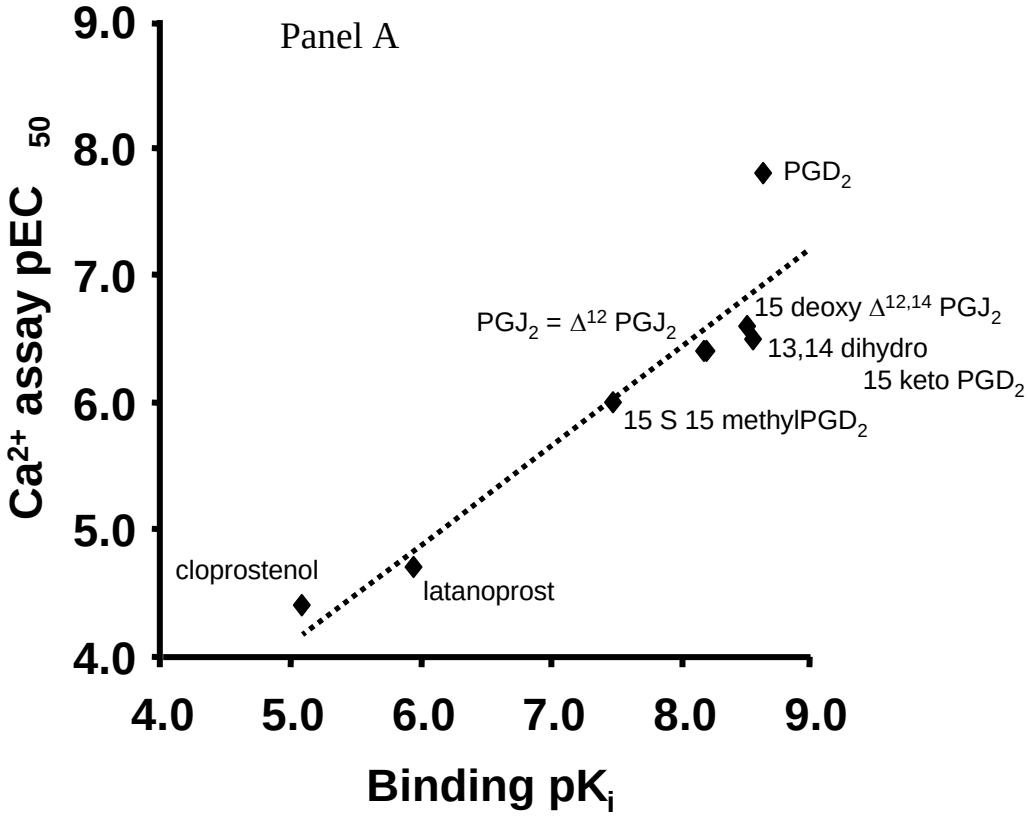
Panel A
9.0
8.0
7.0
6.0
5.0
4.0
Ca2+ assay pEC 50
PGD2
15 deoxy Δ12,14 PGJ2
PGJ2 = Δ12 PGJ2
13,14 dihydro
15 keto PGD2
15 S 15 methylPGD2
cloprostenol
latanoprost
4.0
5.0
6.0
7.0
8.0
9.0
Binding pKi

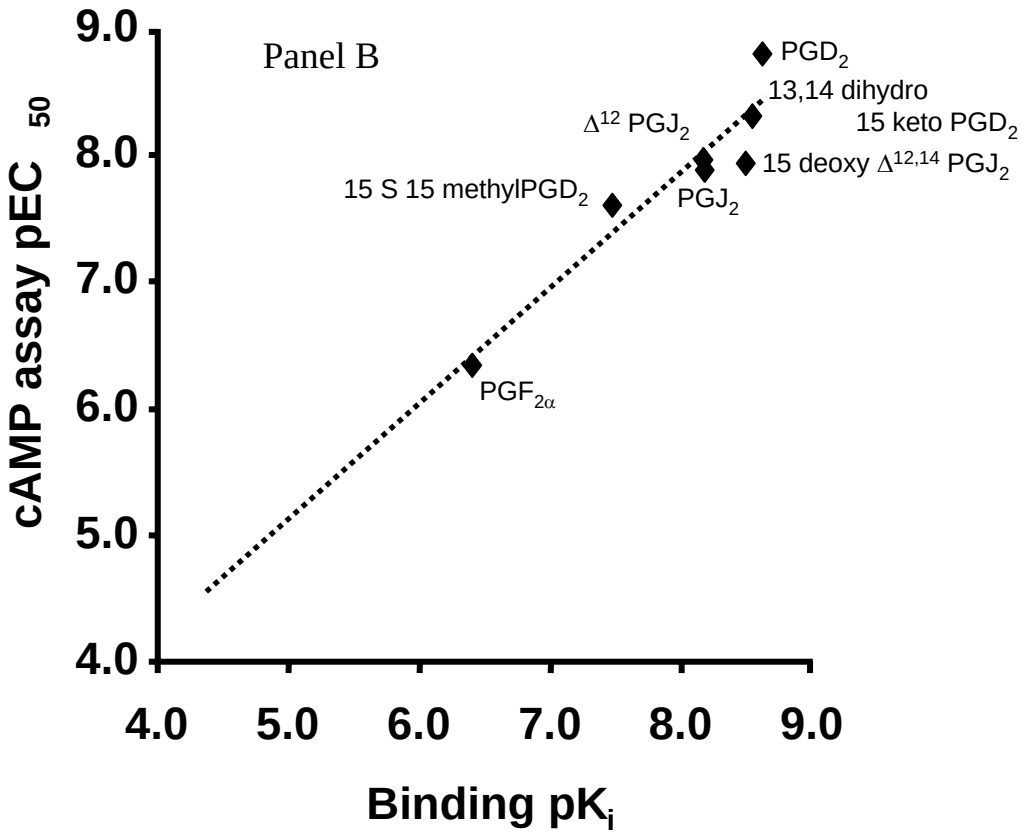
Panel B
9.0
8.0
7.0
6.0
5.0
4.0
cAMP assay pEC 50
PGD2
13,14 dihydro
Δ12 PGJ2
15 keto PGD2
15 deoxy Δ12,14 PGJ2
15 S 15 methylPGD2
PGJ2
PGF2α
4.0
5.0
6.0
7.0
8.0
9.0
Binding pKi

Figure 10

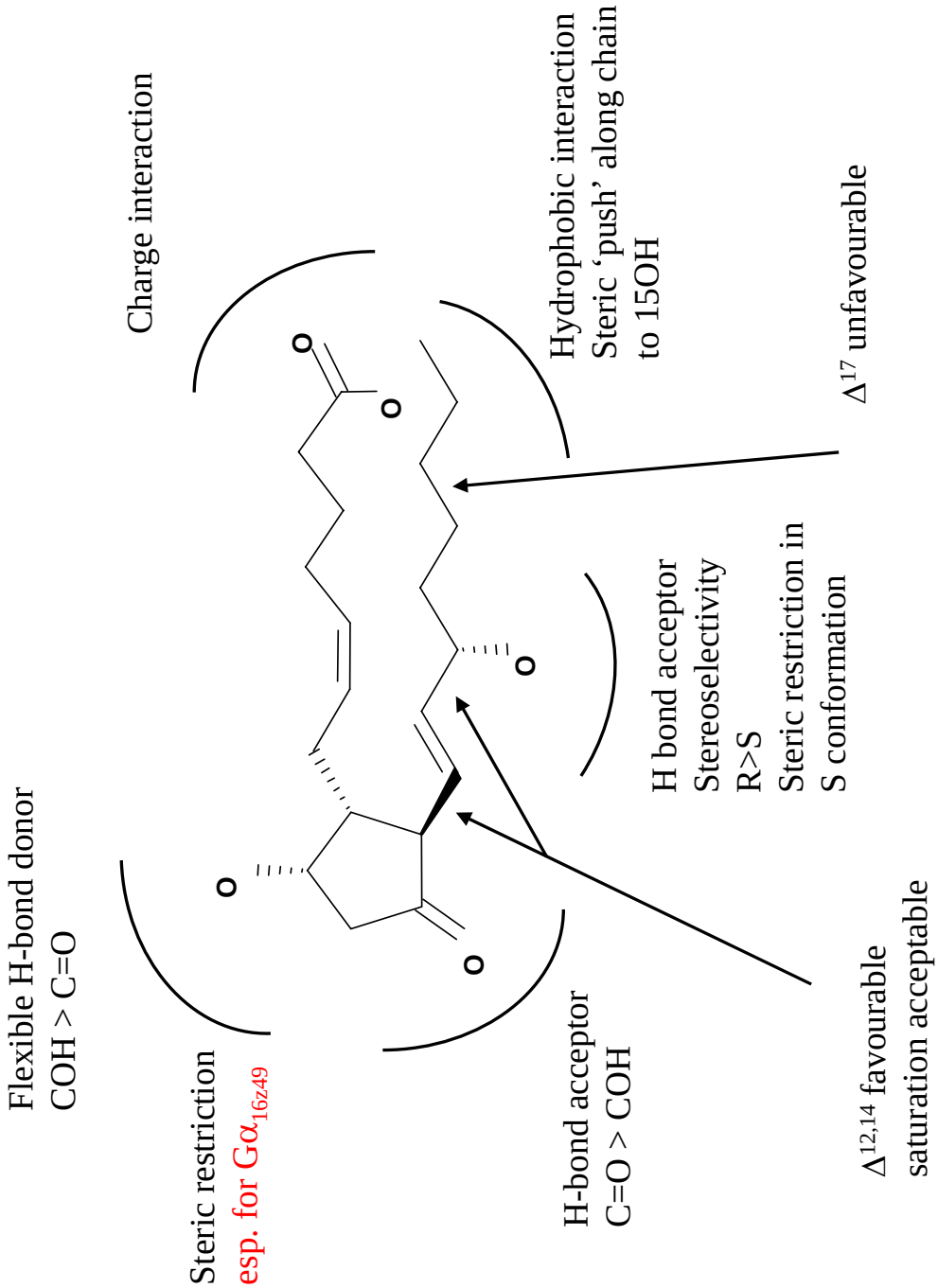
Flexible H-bond donor
COH > C=O
Charge interaction
Hydrophobic interaction
Steric 'push' along chain
to 15OH
Δ^{17} unfavourable
Steric restriction
esp. for $G\alpha_{16z49}$
H bond acceptor
Stereoselectivity
R>S
Steric restriction in
S conformation
H-bond acceptor
C=O > COH
$\Delta^{12,14}$ favourable
saturation acceptable

Chapter 4:

Agonist stimulus trafficking by human prostanoid $CRTH_2$ (DP_2) receptors coupled to calcium mobilisation through chimeric $G\alpha_{16z49}$ and endogenous $G\beta\gamma_{i/o}$ G-protein subunits.

4.1 Summary:

In chapter 3 it was shown that human prostanoid $CRTH_2$ receptors expressed in CHO cells with chimeric $G\alpha_{16z49}$ G-proteins couple to calcium mobilisation through pertussis toxin-sensitive & -insensitive mechanisms with different agonist rank orders of potency. To further investigate this phenomenon a cell line expressing the receptor without the chimeric G-protein was made and again studied using a calcium mobilisation assay. CHO K1 host cells were devoid of responses to prostaglandins while non chimera-expressing CHO K1 $hCRTH_2$ cells responded to PGD_2 with concentration-related elevation of calcium (pEC_{50} 7.9 ± 0.06; n_H 3.4 ± 0.4; n=12).

As found previously in chimera-expressing cells, prostanoid $CRTH_2$ receptor pharmacology was confirmed in non-chimeric cells by the agonist rank order of potency: 15 R 15 methyl PGD_2 > PGD_2 > PGJ_2 > 15 deoxy $\Delta^{12,14}$ PGJ_2 >>> $PGF_{2\alpha}$. BW245C, PGE_2, PGI_2 & U46619 produced no significant effect. PGD_2 responses were insensitive to the DP receptor antagonist BWA868C (1μM) but were sensitive to the putative $CRTH_2$ receptor antagonists AH23848B & GW853481X (pA_2 5.5 ± 0.06 & 6.6 ± 0.3, respectively; n=3).

Saturation radioligand binding was conducted in membranes from both chimeric and non-chimeric receptor-expressing cells using [^{3}H]-PGD_2 as radiolabel. Analysis revealed the presence of a single population of binding sites. Affinity (pK_d) and receptor expression (B_{max}) estimates were: CHO K1 $hCRTH_2$ pK_d = 8.6 ± 0.2, B_{max} = 3.6 ± 1.1 pmol mg^{-1}; CHO $G\alpha_{16z49}$ $hCRTH_2$ pK_d = 8.7 ± 0.06, B_{max} = 9.9 ± 2.9 pmol mg^{-1} (n=3). Western blot analysis revealed the presence of $G\alpha_{i-2}$, $G\alpha_{i-3}$, $G\alpha_z$, $G\alpha_s$ and $G\alpha_q$ G-proteins in both cell types. Expression appeared greatest in CHO $G\alpha_{16z49}$ $hCRTH_2$ cells suggesting that the relative expression of receptor and G-proteins in the two cell lines is equivalent. However, deficiencies in the methods employed mean the true R:G ratio is unknown.

Pertussis toxin (PTX; 50 ng ml^{-1}) abolished responses to PGD_2 in CHO K1 $hCRTH_2$ cells suggesting that calcium mobilisation is entirely mediated by $G_{i/o}$ class G-proteins in this cell line. (Partial (85 %) inhibition in chimera-expressing cells has been shown previously in Chapter 3). Transient expression of the C-terminal of β-adrenergic receptor kinase (β-ARK 495-689) resulted in a 43 ± 12 % inhibition of PGD_2 E_{max} in CHO K1 $hCRTH_2$ cells but not in CHO $G\alpha_{16z49}$ $hCRTH_2$ cells (n=3). This suggests that PTX-sensitive PLCβ stimulation in both cell types is Gβγ

subunit-dependent. Calcium mobilisation in both cell types ± PTX (where applicable) was independent of extracellular Ca^{2+} and was fully inhibited by thapsigargin (3 μM), U71322 (3 μM) and heparin (1 USP unit $well^{-1}$). These results suggest that prostanoid $hCRTH_2$ receptors couple to calcium mobilisation in both CHO cell lines via $G\beta\gamma_{i/o}$ and / or $G\alpha_{16z49}$ subunit-mediated PLCβ activation, IP_3 generation and release of ER-stored calcium via IP_3 receptor operated Ca^{2+} channels.

Using a panel of 65 prostanoid molecules, prostaglandins of the D, F & J series were found to be agonists at $CRTH_2$ receptors in non-chimera-expressing cells (n=3). D series molecules had potencies ranging from 8.0 ± 0.07 (15 R 15 methyl PGD_2) to 5.0 ± 0.03 (PGD_3); J series molecules ranging from 6.7 ± 0.03 (PGJ_2) to 6.3 ± 0.02 (9,10 dihydro 15 deoxy $\Delta^{12,14}$ PGJ_2); and F series molecules ranging from 5.5 ± 0.02 (15 R $PGF_{2\alpha}$) to 54 ± 16 % at 10μM ($PGF_{2\alpha}$). Several other F series molecules were inactive. Compared to the $G\alpha_{16z49}$-mediated responses in PTX treated chimera-expressing cells reversals of potency order were observed. These were most striking for (relative potency (RP) CHO K1, CHO $G\alpha_{16z49}$; c.f. PGD_2 = 1.0) indomethacin (10, c.40) 16,16 dimethyl PGD_2 (158, 11), Δ^{12} PGJ_2 (32, 2.5) and 9,10 dihydro 15 deoxy $\Delta^{12,14}$ PGJ_2 (40, 3.5). In terms of absolute potency J series agonists were little affected e.g. 15 deoxy $\Delta^{12,14}$ PGJ_2 (pEC_{50} CHO K1, CHO $G\alpha_{16z49}$: 6.5 ± 0.02, 6.2 ± 0.03) while F series agonists were most affected (e.g. 15 R $PGF_{2\alpha}$ 5.5 ± 0.02, 15 ± 8 % stimulation at 10 μM).

These data demonstrate marked reversals of agonist rank orders of potency in well characterised prostanoid $CRTH_2$ receptor assay systems and cannot be explained by a simple 'strength of stimulus' model of agonist behaviour. The potential effects of a synergising interaction between $G\alpha_{16z49}$ and $G\beta\gamma_{i/o}$ mediated signals has not been excluded and could affect the interpretation of the potency changes observed. The data could be consistent with the expectations of agonist stimulus trafficking and provide the first demonstration of chimeric G-protein-specific agonist pharmacology.

4.2 Introduction:

In chapter 3, I presented data confirming published agonist rank orders of potency and extended it to provide a comprehensive agonist fingerprint of human prostanoid $CRTH_2$ receptors expressed in CHO cells with the chimeric $G\alpha_{16z49}$ G-protein. Surprisingly, calcium mobilisation in these cells was found to be pertussis toxin (PTX) sensitive even though both wild-type $G\alpha_{16}$ and $G\alpha_z$ subunits from which the chimera is constructed are PTX-insensitive. Following PTX treatment, residual responses to prostanoid agonists could still be observed but the rank order of agonist potency was markedly altered. Thus, in these cells, 85 % of the calcium mobilisation response to PGD_2 was assumed to be mediated by PTX sensitive $G\beta\gamma_{i/o}$ subunits, and 15 % by PTX insensitive $G\alpha_{16z49}$ subunits. Agonist pharmacology was critically dependent upon the cell line and conditions employed: in non PTX-treated cells agonist responses arose from activation of both pathways. The present study was therefore undertaken to produce SAR in CHO cells expressing human prostanoid $CRTH_2$ receptors without the chimera in order to provide data generated solely by $G\beta\gamma_{i/o}$ subunit coupling. By comparison with data generated through $G\alpha_{16z49}$ coupling, I present evidence which strongly suggests that prostanoid $hCRTH_2$ receptors traffic agonist stimuli to their coupling G-protein partners.

4.3 Results:

4.3.1 Selection of CHO K1 hCRTH$_2$ clone

Prostaglandin D_2 (0.5 nM – 10 μM) produced concentration-related increases in $[Ca^{2+}]_i$ in cells of both clones (Figure 1). The potency (pEC_{50}) of PGD_2 was similar in both cell lines (clone 10: 8.3 ± 0.04; clone 15: 8.1 ± 0.04; $P < 0.05$) as was Z′ (clone 10: 0.54; clone 15: 0.60) but marked differences in maximum response were observed (clone 10: 77 ± 4 NFIU; clone 15: 158 ± 6 NFIU; $P < 0.01$; mean of 8 individual E/[A] curves, or in the case of Z′, of 1 determination from eight duplicate data points, produced on a single assay occasion). Similar trends were observed with the prostanoids (pEC_{50}, upper asymptote[NFIU]; clone 10; clone 15; n = 24) 13,14 dihydro 15 keto PGD_2 (7.5 ± 0.06, 71 ± 2; 7.4 ± 0.04, 149 ± 2), 15 R 15 methyl PGD_2 (8.6 ± 0.02, 69 ± 1; 8.6 ± 0.02, 138 ± 5) and $PGF_{2\alpha}$ (ND, 62 ± 2; ND, 88 ± 5). Statistical comparisons: potencies NS; max $P < 0.05$. Clone 15 cells used subsequently.

4.3.2 Determination of protein concentration

A single batch of membranes from each cell line specified below was prepared for the experiments described in this chapter. The following estimates of protein concentration in CHO cell membranes were generated: CHO $G\alpha_{16z49}$ host 0.08 ± 0.03 mg ml^{-1}; CHO K1 hCRTH$_2$ 5.9 ± 0.3 mg ml^{-1}; CHO $G\alpha_{16z49}$ hCRTH$_2$ 1.2 ± 0.06 mg ml^{-1} (n = 3).

4.3.3 Saturation radioligand binding

Data describing the development of the assay method will be presented in chapter 7. CHO $G\alpha_{16z49}$ host cells (5.8 μg $well^{-1}$ membrane protein) did not bind [^{3}H]-PGD_2 (0.05 - 16 nM). Cells transfected with human prostanoid CRTH$_2$ receptors bound [^{3}H]-PGD_2 in a concentration related manner (Figures 2 & 3). Non-linear regression of data resulted in the following estimates of affinity (K_d) and number of binding sites (B_{max}): CHO K1 hCRTH$_2$ $pK_d = 8.6 \pm 0.2$, $B_{max} = 3.6 \pm 0.8$ pmol mg^{-1}, $n_H = 1.3 \pm 0.3$; CHO $G\alpha_{16z49}$ hCRTH$_2$ $pK_d = 8.7 \pm 0.06$, $B_{max} = 9.9 \pm 2.0$ pmol mg^{-1}, $n_H = 1.5 \pm 0.5$ (all n = 3). Linear Scatchard transformation of the data indicated the presence of a single population of saturable binding sites. However, given the methodological deficiencies pointed out in Chapter 7, these B_{max} estimates could be as little as 50 % of the true B_{max}.

4.3.4 Western blot analysis

Ponceau S staining showed that protein loading was equivalent across all wells (Figure 4).

Western blot analysis revealed the presence of $G\alpha_{i-2}$, $G\alpha_{i-3}$, $G\alpha_z$, $G\alpha_s$ and $G\alpha_q$ G-proteins in all three cell types (Figure 5). The amount of staining for all proteins varied in the order: CHO $G\alpha_{16z49}$ $hCRTH_2$ > CHO $G\alpha_{16z49}$ > CHO K1 $hCRTH_2$. Blots for $G\alpha_q$ and $G\alpha_{q/11}$ revealed multiple immunoreactive bands of molecular weight 39-45 kDa in all samples. The $G\alpha_q$ antibody labelled a 45 kDa band in the $G\alpha_{16z49}$ expressing cell lines but not CHO K1 $hCRTH_2$ cells; this band was also detected in all samples by the $G\alpha_{q/11}$ antibody. In contrast, the $G\alpha_{q/11}$ antibody detected a weakly staining band at 38 kDa only in the chimeric cell lines, with no correlate detected by the $G\alpha_q$ antibody. Two bands of approximately 80 kDa were detected by the $G\alpha_z$ antibody in all samples. The $G\alpha_i$ antibody failed to label $G\alpha_{i-1}$ and $G\alpha_{i-2}$ positive controls while the $G\alpha_{16}$ antibody failed to develop. Staining with the $G\alpha_{11}$ antibody was largely unsuccessful, with clear evidence of 'negative staining', but may have detected an immunoreactive protein of 40 kDa. Bands of high (c. 100 kDa) and low (c. 25 kDa) molecular weight were also detected in all blots.

4.3.5 Assessment of CHO K1 host cell response to prostaglandins.

Uridine triphosphate (UTP; 1.7 nM – 100 μM) produced concentration-related increases in fluorescence and yielded a pEC_{50} of 7.3 ± 0.1 and E_{max} of 235 ± 35 (n = 3) normalised FLIPR intensity units (NFIU). Vehicle (1 % DMSO) produced large calcium fluxes in this cell line which were observed to increase in magnitude with increasing dye-loading time (64 ± 5 NFIU at 60 min loading time). Prostaglandins D_2, E_2, $F_{2\alpha}$ & U-46619 (0.17 nM – 10 μM), and iloprost (17 pM – 1 μM) did not produce any significant effect over that of vehicle (Figure 6). A vehicle concentration-effect relationship was not established in this cell line. The prostanoid receptor antagonists AH23848B & GW853481X (both 10 μM), and BWA868C, GW627368X, GW671021X, SC-51322 & SQ-29548 (all 1 μM) also produced no effect on basal fluorescence, or on fluorescence in the presence of PGD_2 and PGE_2 (both 0.17 nM - 10 μM; data at 10 μM presented in Figure 7; result of statistical comparison = NS).

4.3.6 Effect of standard prostanoid receptor agonists and antagonists in CHO K1 $hCRTH_2$ cells.

Prostaglandins E_2 (PGE_2), iloprost and U-46619 were devoid of agonist effects up to 10 μM; prostaglandin $PGF_{2\alpha}$ produced small elevations of $[Ca^{2+}]_i$ at 10 μM resulting in a maximum response of 54 ± 11 % cf. PGD_2 controls ($P < 0.05$). The non-selective COX 1 / 2 inhibitor indomethacin was an agonist (pEC_{50} 6.9 ± 0.07, RP = 10; max effect 84 ± 4 %, RA = 0.85).

The putative prostanoid $CRTH_2$ receptor antagonists AH23848B and GW853481X antagonised PGD_2 responses giving rise to apparent pA_2 estimates of 5.5 ± 0.07 (Figure 8, Panel A) and 6.6 ± 0.4, respectively (Panel B). AH23848B inhibited PGD_2 E_{max} in a concentration-related manner producing 22 ± 12 % inhibition at 30 μM, while GW853481X elicited 18 ± 10 % inhibition at 3 μM (both $P < 0.05$).

4.3.7 Effect of pertussis toxin treatment.

CHO K1 $hCRTH_2$ cells. In the absence of Pertussis toxin (PTX) PGD_2 pEC_{50} was 7.6 ± 0.1, slope 1.5 ± 0.1. PTX (50 ng ml^{-1}) reproducibly produced complete inhibition of responses to PGD_2 over 6 rounds of passage spanning four weeks of cell culture (Figure 9, Panels A & B). Passage-related changes in PGD_2 pEC_{50} were not observed but the potency at P16 was significantly lower than at P10, though not when compared to P14 (PGD_2 pEC_{50} at P10 7.5 ± 0.05; at P16 6.9 ± 0.02; $P < 0.05$; at P14 7.2 ± 0.05; NS).

CHO $G\alpha_{16z49}$ $hCRTH_2$ cells. Under the same conditions of PTX treatment the 85 % inhibition of PGD_2 E_{max} described in Chapter 3 was reproducible over 6 rounds of passage spanning four weeks of cell culture.

4.3.8 Experiments with inhibitors of the calcium mobilisation pathway

All data reported in this section are from n=3 independent experiments. Vehicle (0.25 % DMSO) produced small, transient changes in basal fluorescence in both CHO K1 $hCRTH_2$ (28 ± 9 NFIU) and CHO $G\alpha_{16z49}$ $hCRTH_2$ (42 ± 9 NFIU) cells but the effect was greatly diminished in CHO $G\alpha_{16z49}$ $hCRTH_2$ cells incubated with PTX (19 ± 4; Panel A of Figures 10, 11 and 12; $P < 0.05$). Addition of H-89, ryanodine and U71322 (all 3 μM) produced effects equivalent to that of vehicle addition. Thapsigargin (3 μM) produced a large increase in fluorescence (178 ± 18 NFIU) which reached a maximum after 20 s and subsequently decayed by 30 % over the next 30 s. Fluorescence returned to basal levels over the following 15 mins (equilibration period before addition of PGD_2). Heparin (1 USP unit per well; 125 μg ml^{-1}) produced variable changes in basal fluorescence in each assay ranging from no effect to 29 ± 12 NFIU (calculated across the 11 treated wells in each assay) while the lipofectamine vehicle for heparin (0.31-2.5 % v v^{-1}) produced no significant effect (Panel A, Figure 13). Transient transfection of cells with the C-terminal of β-adrenergic receptor kinase (β-ARK 495-689) resulted in 43 ± 12 % inhibition of PGD_2 E_{max} in CHO K1 $hCRTH_2$ cells ($P < 0.05$;

Figure 14) and no inhibition in CHO $G\alpha_{16z49}$ $hCRTH_2$ cells (calculated from matched PGD_2 control and treated data).

PGD_2 E/[A] curves (0.17 nM – 10 μM) were unaffected by pre-treatment with either vehicle, lipofectamine, H-89 or ryanodine (Panel B of Figures 10, 11 and 12). U71322 treatment totally abolished responses to PGD_2 in CHO $G\alpha_{16z49}$ $hCRTH_2$ cells ± PTX and reduced the E_{max} in CHO K1 $hCRTH_2$ cells by 84 % (control 152 ± 11; U71322 treated 25 ± 9 NFIU; $P < 0.01$). Thapsigargin totally abolished increases in fluorescence in response to PGD_2 in both cell lines ± PTX (where applicable). However, in the presence of thapsigargin, PGD_2 produced small but reproducible concentration-related reductions in fluorescence in both cell types which were abolished by PTX treatment (not statistically significant). Heparin treatment without the incorporation of lipofectamine vehicle reduced responses to 10 μM PGD_2 by 82 % (control 166 ± 3; heparin treated 30 ± 28 NFIU; $P < 0.01$; Panel B, Figure 13). Responses were totally abolished when lipofectamine was included.

4.3.9 Agonist 'fingerprinting' of $hCRTH_2$ receptor

4.3.9.1 CHO K1 cells without PTX treatment. A panel of 76 prostanoid molecules was screened for agonist activity in CHO K1 $hCRTH_2$ cells without PTX treatment at concentrations up to 10 μM (Table 1). A large proportion (72 %) of compounds were without agonist effect. Amongst the active compounds, curve slopes were generally steep (1.8-3.7). Slope parameters in excess of this were shown by 15 R 15 methyl $PGF_{2\alpha}$ (5.1 ± 2), 15 S 15 methyl PGD_2 (5.2 ± 1.8), 15 keto $PGF_{2\alpha}$ (8 ± 1.1) and 15 R $PGF_{2\alpha}$ (8.2 ± 1.4). The following rank order of agonist potency was obtained for the most active compounds (relative potency [RP cf. PGD_2 = 1.0], relative activity [RA cf. PGD_2 = 1.0]; full agonists shown in bold type, partial agonists in normal type): **15 R 15 methyl PGD_2 (0.8, 0.9)** > **PGD_2** = **15 deoxy PGD_2 (10, 1)** > **PGJ_2 (16, 0.9)** > **15 deoxy $\Delta^{12,14}$ PGJ_2 (25, 0.9)** = **13,14 dihydro 15 keto PGD_2 (32, 0.9)** = **Δ^{12} PGJ_2 (32, 1)** = 9,10 dihydro 15 deoxy $\Delta^{12,14}$ PGJ_2 (40, 0.7) > **PGD_1 (79, 0.8)** = **15 S 15 methyl PGD_2 (78, 0.9)** > **17 phenyl PGD_2 (100, 0.9)** > **16,16 dimethyl PGD_2 (158, 0.9)** > 15 R 15 methyl $PGF_{2\alpha}$ (251, 0.4) = **PGD_3 (254, 0.9)** = 15 R $PGF_{2\alpha}$ (251, 0.7) > 15 keto $PGF_{2\alpha}$ (316, 0.6) >> 15 keto $PGF_{1\alpha}$ (max effect 0.2) = $PGF_{2\alpha}$ (max effect 0.5) = latanoprost (max effect 0.1) = cloprostenol (max effect 0.1). Butaprost methyl ester, 15 S 15 methyl $PGF_{2\alpha}$, BW245C & 13,14 dihydro 15 keto $PGF_{2\alpha}$ were all without significant effect. These data correlated well with data previously obtained in CHO

$G\alpha_{16z49}$ $hCRTH_2$ cells without PTX treatment and presented in chapter 3 (Figure 15): maximum effect correlation coefficient (r^2) = 0.9; agonist pEC_{50} r^2 = 0.83.

4.3.9.2 CHO $G\alpha_{16z49}$ cells + PTX treatment. The same panel of prostanoid molecules was screened for agonism in CHO $G\alpha_{16z49}$ $hCRTH_2$ cells with PTX pre-treatment (reported in Chapter 3 and represented in Table 1 for comparison). These data correlated poorly with the data from CHO K1 $hCRTH_2$ cells without PTX treatment (Figure 16): maximum effect correlation coefficient (r^2) = 0.56; agonist pEC_{50} r^2 = 0.65. (For regression analysis, where compounds were inactive in the +PTX pEC_{50} data set, a value of 4.5 was assigned. Therefore, the true r^2 value is lower than 0.65).

4.3.10 Data Tables.

Follow on next page.

Table 1. Pharmacology of prostanoid molecules in CHO K1 $hCRTH_2$ cells without PTX treatment. RP: relative potency cf. PGD_2 (=1.0); RA: relative activity cf. PGD_2 (=1.0). Data are mean ± sem of four - ten separate E/[A] curves generated over two - four assay occasions. Butaprost methyl ester, Misoprostol, 15 S 15 methyl $PGF_{2\alpha}$, 13,14 dihydro 15 keto $PGF_{2\alpha}$, 11 deoxy 11 methylene PGD_2, $PGF_{3\alpha}$, 11 dehydro TxB_2, 15 R 19 R hydroxy $PGF_{2\alpha}$, 13,14 dihydro PGE_1, PGE_3, 20 hydroxy $PGF_{2\alpha}$, 13,14 dihydroxy 15 keto PGA_2, 6 keto $PGF_{1\alpha}$, 6 keto PGE_1, Δ^{17} 6 keto $PGF_{1\alpha}$, PGA_2, 15 R PGE_2, $PGF_{1\alpha}$, PGA_1, 13,14 dihydro $PGF_{1\alpha}$, 13,14 dihydro 15 keto PGE_2, 13,14 dihydro 15 keto $PGF_{1\alpha}$, PGE_1, 15 keto PGE_1, 19 R hydroxy $PGF_{1\alpha}$, PGD_1 alcohol, 15 R 15 methyl PGE_2, 15 R 19 R hydroxy $PGF_{1\alpha}$, 13,14 dihydro 15 keto PGE_1, 13,14 dihydro 15 R PGE_1, 11 dehydro 2,3 dinor TxB_2, 19 R hydroxy PGA_2, TxB_2, 15 R 19 R hydroxy PGE_2, PGK_1, 15 keto PGE_2, 20 hydroxy PGE_2, 15 R PGE_1, 11β 13,14 dihydro 15 keto $PGF_{2\alpha}$, 19 R hydroxy $PGF_{2\alpha}$, 19 R hydroxy PGE_2, 2,3 dinor 11β $PGF_{2\alpha}$, PGK_2, PGI_3, PGE_2, 19 R hydroxy PGE_1, PGB_2, 11deoxyPGE_1, Cicaprost, Sulprostone, BW245C, Butaprost free acid, 17 phenyl PGE_2, 16,16 dimethyl PGE_2 & Iloprost were without significant effect. PGI_2 was not tested. Statistical comparison by ANOVA followed by Dunnett's comparison to PGD_2 data; * denotes $P < 0.05$.

Compound	pEC_{50}	slope	max	RP	RA
15 R 15 methyl PGD_2	8.0 ± 0.07	2 ± 0.3	93 ± 2	0.8	0.9
PGD_2	7.9 ± 0.06	3.4 ± 0.4	100 ± 4	1.0	1.0
15 deoxy PGD_2	6.9 ± 0.03*	2.6 ± 0.4	95 ± 2	10	1.0
Indomethacin	6.9 ± 0.07*	5.5 ± 3.2	84 ± 4*	10	0.8
PGJ_2	6.7 ± 0.03*	2.6 ± 0.7	88 ± 1	16	0.9
15 deoxy Δ12,14 PGJ_2	6.5 ± 0.03*	2.7 ± 0.2	91 ± 4	25	0.9
13,14 dihydro 15 keto PGD_2	6.4 ± 0.1*	3.7 ± 0.9	94 ± 2	32	0.9
Δ^{12} PGJ_2	6.4 ± 0.07*	3.2 ± 1.0	103 ± 3	32	1.0

9,10 dihydro 15 deoxy $\Delta^{12,14}$ PGJ_2	6.3 ± 0.03*	3.3 ± 0.5	69 ± 22*	40	0.7
15 S 15 methyl PGD_2	6.0 ± 0.03*	5.2 ± 1.8	90 ± 1	79	0.9
PGD_1	6.0 ± 0.07*	1.8 ± 0.2	83 ± 1*	79	0.8
17 phenyl PGD_2	5.9 ± 0.03*	2.7 ± 0.7	86 ± 6*	100	0.9
16,16 dimethyl PGD_2	5.7 ± 0.07*	2.2 ± 0.6	86 ± 6*	158	0.9
15 R 15 methyl $PGF_{2\alpha}$	5.5 ± 0.03*	5.1 ± 2.1	43 ± 2*	251	0.4
PGD_3	5.5 ± 0.03*	3.5 ± 0.4	92 ± 7	251	0.9
15 keto $PGF_{2\alpha}$	5.4 ± 0.03*	8 ± 1.1	58 ± 8*	316	0.6
15 R $PGF_{2\alpha}$	5.5 ± 0.03*	8.2 ± 1.4	73 ± 9*	251	0.7
15 keto $PGF_{1\alpha}$			16 ± 3*		
$PGF_{2\alpha}$			54 ± 11*		
Latanoprost			14 ± 3*		
Cloprostenol			12 ± 3*		

Table 2. Summary of G-proteins detected in Chinese Hamster Ovary cells by Western Blot, and reported in literature.

Citation	$G\alpha_s$	$G\alpha_{i1}$	$G\alpha_{i2}$	$G\alpha_{i3}$	$G\alpha_o$	$G\alpha_z$	$G\alpha_q$	$G\alpha_{11}$	$G\alpha_{12}$	$G\alpha_{13}$
This study	✓	×	✓	✓		✓	✓	✓		
Xu, *et al*., 2005			✓	✓	✓				✓	
De Lapp, *et al*., 1999				✓			✓(or 11)			
Newman-Tancredi, *et al*., 1999	✓				✓ (or i)		✓(or 11)			
van der Westerlo, *et al*., 1995	✓						✓(or 11)			✓
Chambers, *et al*., 1994	✓	×	✓				✓(or 11)			
McKenzie & Milligan, 1990		×	✓							

Table 3. Binding affinity of prostaglandin D_2 (PGD_2) at human prostanoid $CRTH_2$ receptors reported in literature. Data are mean ± s.e.m.

Cell line	Type	Radioligand	Affinity (nM)	B_{max} (pmol mg^{-1})	Comment	Reference
L1.2	K_i	[^{3}H] ramatroban	23			Sugimoto, *et al.*, 2005
COS-7	K_d	[^{3}H]-PGD_2	12.9 ± 2.1	57.5 fmol / 30k cells		Mathiesen, *et al.*, 2005
CHO K1	K_d	[^{3}H]-PGD_2	12.1	10.2	ex-Euroscreen	
HEK293	K_i	[^{3}H]-PGD_2	1.7 ± 0.8			Gervais, *et al.*, 2005
CHO	K_i	[^{3}H]-PGD_2	12.9			Gazi, *et al.*, 2005
K562	K_i	[^{3}H]-PGD_2	61 ± 23			Nagata, *et al.*, 2003
HEK293	K_d	[^{3}H]-PGD_2	2.5 ± 1.1	7.8 ± 2.9	low affinity site K_d 109 ± 68; B_{max} 29.5 ± 9.5	Sawyer, *et al.*, 2002
	K_i	[^{3}H]-PGD_2	2.4 ± 0.2			
CHOK1	K_d	[^{3}H]-PGD_2	2.7 ± 2	3.6 ± 1.1		Present study
CHO $G\alpha_{16z49}$	K_d	[^{3}H]-PGD_2	2.3 ± 0.5	9.9 ± 2.9		

4.4 Discussion:

In Chapter 3, I presented data defining suitable assay conditions for the determination of quantitative SAR data in CHO cells expressing the human prostanoid $CRTH_2$ receptor with the chimeric $G\alpha_{16z49}$ G-protein. Data obtained following treatment of CHO $G\alpha_{16z49}$ $hCRTH_2$ cells with pertussis toxin (PTX) established an agonist fingerprint for prostanoid $CRTH_2$ receptors which differed markedly from that obtained in non PTX-treated cells. These data I took to represent coupling through $G\alpha_{16z49}$ subunits (PTX-treated) or a mixture of $G\alpha_{16z49}$ and $G\beta\gamma_{i/o}$ subunits (non PTX-treated) but coupling via $G\alpha_q$ and / or $G\alpha_z$ was not ruled out. The data were insufficient to firmly establish the impact of the chimeric G-protein on prostanoid $CRTH_2$ receptors and the chapter closed posing a number of questions. In this chapter I have delineated the molecular pathway coupling prostanoid $CRTH_2$ receptor activation to calcium mobilisation in CHO cells, demonstrated the equivalence of $CRTH_2$: $G\alpha_{i/o}$ stoichiometry in CHO $G\alpha_{16z49}$ $hCRTH_2$ and CHO K1 $hCRTH_2$ cells, and established new SAR data at prostanoid $CRTH_2$ receptors coupled through $G\beta\gamma_{i/o}$ subunits free from the influence of the chimera. The impact of the chimeric $G\alpha_{16z49}$ G-protein on $CRTH_2$ receptor pharmacology is significant and I present alternative pharmacophores deduced from these data.

Comparison of agonist E/[A] curves clearly demonstrated the suitability of CHO K1 $hCRTH_2$ clone 15 for use in these studies. Clone selection data presented in Chapter 3 was affected by two deficiencies: 1. Use of un-optimised assay methodology; 2. Failure to employ metabolically resistant prostanoid agonists. Neither of these factors have affected the data presented in this chapter. In addition to using the methodology developed in Chapter 3, a range of agonists of different chemical series, and of differing susceptibility to metabolism produced identical rank orders of potency and activity in the clones examined. The selection of clone 15 is therefore based on a more reliable data set.

A comprehensive analysis of the G-proteins expressed by CHO K1 cells is not available. However, using Western blot techniques analogous to those used here, other authors have shown the presence of $G\alpha_s$, $G\alpha_{i2}$, $G\alpha_{i3}$, $G\alpha_o$, $G\alpha_q$, $G\alpha_{11}$, $G\alpha_{12}$ & $G\alpha_{13}$ (Table 2 & references cited therein). Quantification of protein expression is not possible from the data presented here since the level of protein saturation by antibody has not been assessed, neither has a positive control been run for most of the G-proteins studied. Because of these deficiencies it has not been possible to make definitive identifications of stained protein bands. However, assuming that the antibodies have detected the proteins against which they have been raised, it

has been possible to make qualitative comparisons of expression between membrane samples since Ponceau S staining demonstrated equivalent protein loading in each lane. The anti $G\alpha_i$ primary antibody used here was raised against the conserved C-terminal amino acid sequence of rat $G\alpha_{i3}$ and was expected to be active at all three $G\alpha_i$ proteins. Certainly, the antibody is functional, so it seems surprising that it failed to detect any of the recombinant $G\alpha_i$ positive control proteins. Nonetheless, two bands of the correct approximate molecular weight (c. 40 kDa) were detected in each membrane sample which presumably correspond to $G\alpha_{i2}$ and $G\alpha_{i3}$ since an absence of $G\alpha_{i1}$ has been demonstrated previously in CHO cells (Table 2 and references cited therein). The lack of control staining may therefore reflect insufficient loading, incorrect handling, or may suggest that the control proteins are not authentic. A further band of high molecular weight (c. 100 kDa) was detected, presumably representing a G-protein dimer which may have arisen as an artefact of sample preparation. Similar high MW bands were also visible in blots for $G\alpha_s$, $G\alpha_q$ and $G\alpha_{q/11}$. Expression of $G\alpha_i$ proteins was highest in the two cell lines also expressing the $G\alpha_{16z49}$ chimera and was highest of all in CHO $G\alpha_{16z49}$ $hCRTH_2$ cells. Since the manufacturer's literature states that this antibody does not cross react with non-Gαi proteins this could arise either as a result of expression of the chimera (and subsequent to the generation of a new intracellular signal: the chimera can couple to any available receptor, not just $hCRTH_2$) or of cell culture in the presence of the selection antibiotic, hygromycin B. Hygromycin B is a bactericidal aminoglycoside produced by Streptomyces hygroscopicus which inhibits protein synthesis in many species including higher eukaryotes (references in Pfister, *et al.*, 2003). In contrast to the typical 2-deoxystreptamines, hygromycin B inhibits protein synthesis by blocking ribosomal translocation without causing significant misreading *in vivo*. Thus, the potential for hygromycin B to alter the expression of proteins is obvious. A net increase in expression probably results here because the low concentration used stimulates a compensatory up-regulation of the synthetic apparatus in cells also expressing the hygromycin resistance gene. The altered synthesis appears to apply generally to all proteins since increased expression of $G\alpha_s$ and $G\alpha_q$ G-proteins may also be observed, and saturation radioligand binding of $[^3H]$-PGD_2 to prostanoid $hCRTH_2$ receptors estimates a B_{max} in chimera-expressing cells approximately three-fold higher than that in CHO K1 cells (see below). Interestingly, the highest expression levels were observed in cells cultured in the presence of both hygromycin B *and* geneticin (G418), a semi-synthetic aminoglycoside antibiotic. Geneticin is also reported to bind to membrane phospholipids and to interact with phospholipase C subtypes

(references in Kung, *et al*., 1997). Since both cell lines expressing prostanoid $CRTH_2$ receptors are cultured in the presence of geneticin this will not impact on comparisons of pharmacology between the cell types but may invalidate CHO $G\alpha_{16z49}$ cell pharmacology since these cells were cultured only with hygromycin.

Blots for $G\alpha_q$ and $G\alpha_{q/11}$ revealed multiple immunoreactive bands of molecular weight 49-52 kDa in all samples. It is tempting to speculate that the 52 kDa band detected by the $G\alpha_q$ antibody only in $G\alpha_{16z49}$ expressing cells represents the chimera but given the high MW, and the detection of this band by the $G\alpha_{q/11}$ antibody in all three samples, doubt exists over the identity of this protein. In contrast, the faint band at 45 kDa detected by the $G\alpha_{q/11}$ antibody in the chimeric cell lines may represent $G\alpha_{11}$ up-regulated by culture in the presence of hygromycin since no correlate was detected by the $G\alpha_q$ antibody. The couplet of approximately 75 kDa detected by the $G\alpha_z$ antibody does not correspond to monomeric $G\alpha_z$ (40 kDa; Casey, *et al*., 1990) but could represent dimers of both complete and C-terminal truncated forms of the protein. If this were so, then it raises the possibility that the PTX insensitive component of signalling in CHO $G\alpha_{16z49}$ $hCRTH_2$ cells is due to $G\alpha_z$ coupling. However, no such resistant coupling is observed in CHO K1 $hCRTH_2$ cells which also stain for this G-protein making $G\alpha_z$ coupling unlikely.

Both non-linear regression and linear Scatchard transformation of radioligand saturation data indicated the presence of a single population of saturable binding sites with K_d estimates commensurate with published data (Table 3 and references cited therein). In their 2002 study, Sawyer *et al*. detected the presence of two binding sites using similar binding conditions but with final radioligand concentrations of up to 80 nM. Apart from the obvious cost disadvantage, such high radioligand concentrations also suffer from high vehicle levels (7 % ethanol in their case) and were not employed in this study. Sawyer's HEK 293 (EBNA) cells transfected with human prostanoid $CRTH_2$ receptors were cultured in the presence of high concentrations of four antibiotics (penicillin, streptomycin, G418, and hygromycin B) and as discussed above, culture with these agents has the potential to alter protein expression. Therefore, while the detection of the low affinity site must be treated with some caution, the data presented here do not rule its existence out. Indeed, data presented in Chapter 7 will suggest that a pool of receptor protein not observed in these saturations *does*, in fact, exist.

Saturation binding was undertaken in order to estimate the concentration of prostanoid $CRTH_2$ receptors expressed in the two cell lines used here. Receptor concentration is routinely expressed as pmol of receptor per mg of protein and is therefore critically dependent

on accurate [protein] determination. The bicinchoninic acid (BCA) technique employed here is widely used and regarded as sufficiently accurate for these purposes. However, accurate construction of standard protein samples and the ability of the standard to represent the properties of the test protein is paramount. Bovine serum albumin is a typical standard protein and is assumed to be suitable: the impact of other standards on the final estimate was not tested. However, the obvious difference here is that BSA is a soluble protein, while the sample under test was a preparation of membranes, most of which are likely to exist as a suspension of vesicles. The samples were not treated with detergent making detection of intravesicular protein not possible. Even though the statistical errors around the [protein] determination are relatively small (amounting to c. 5 % error) and can be taken to be reasonably reliable for comparative purposes, failure to detect the intravesicular protein will have resulted in an underestimate of protein concentration. Nonetheless, the data indicate three-fold greater expression of receptor on CHO $G\alpha_{16z49}$ $hCRTH_2$ cells relative to CHO K1 $hCRTH_2$ cells, and no binding to host cell membranes (despite the low protein concentration in the membrane preparation, similar amounts of protein per well for all three membrane samples were achieved in the binding assay). The estimates generated by non-linear regression agreed very closely with those obtained by linear transformation of the data and can therefore be considered reasonably reliable. However, according to the ternary complex model of receptor behaviour (DeLean, *et al*., 1980) agonist radioligands such as [^{3}H]-PGD_2 preferentially label the high affinity G-protein coupled state of the receptor and thus estimates of the number of binding sites obtained in this way are critically dependent on the amount of G-protein coupled to the receptor. Many factors can affect the degree of pre-coupling, such as the presence of divalent cations, sodium, GDP / GTP ratio and G-protein expression (Graeser & Neubig, 1992). The sodium concentration in the assay mixture was virtually zero: sodium was omitted from the buffer, pH adjustment was performed with KOH, and EDTA was included to chelate any remaining sodium. However, as with the protein determination, membrane vesicles may have created micro-environments with locally higher [Na^+]. As discussed above, the Western blot data indicate increased expression of G-proteins in CHO $G\alpha_{16z49}$ $hCRTH_2$ cells relative to CHO K1 $hCRTH_2$ cells and cast doubt on the estimates of receptor expression since more G-protein could increase the conversion of receptor molecules to the high affinity binding state. It is not possible to deduce whether this is the case but the Western Blot data is strongly suggestive of increased protein synthesis which is expected to apply equally to all proteins if regulation is at the level of the synthetic machinery and not at

the level of mRNA transcription. Overall, the receptor : G-protein stoichiometry relevant to calcium signal transduction appears to be similar in the two cell lines since the potency of PGD_2 is similar (CHO K1 $hCRTH_2$: 7.9 ± 0.06; CHO $G\alpha_{16z49}$ $hCRTH_2$ [no PTX]: 7.8 ± 0.1). Thus, although changes in protein expression have been detected they appear to be of insufficient magnitude to produce alteration of agonist behaviour, however it is important to realise that given the deficiencies in both binding and blot data, the R:G stoichiometry in the two cell lines tested is essentially not known. Finally, PGD_2 responses appear to be shifted to the right with respect to the binding pKd. The reason for this is unclear, even allowing for the use of an agonist radioligand, but may relate to the inhibition of PLC by geneticin.

As shown in Chapter 3, calcium fluxes in response to PGD_2 in CHO $G\alpha_{16z49}$ $hCRTH_2$ cells do not require the presence of extracellular calcium (indicating calcium release from the endoplasmic reticulum; ER) while pertussis toxin (PTX) abolishes responses in CHO K1 $hCRTH_2$ cells and reduces responses in CHO $G\alpha_{16z49}$ $hCRTH_2$ cells by 85 % (suggesting coupling through $G_{i/o}$ class G-proteins). Because calcium is mobilised from intracellular stores, the likely PTX-sensitive coupling partners are $G\beta\gamma_{i/o}$ subunits. The residual signal in the chimeric cell lines is assumed to be due to coupling through the $G\alpha_{16z49}$ G-protein but the low agonist potency and activity via this mechanism is not typical of $G\alpha$ coupling to PLCβ. The CHO cells used here have been shown to express $G\alpha_z$ and $G\alpha_{q/11}$ which could couple in a PTX-insensitive manner. However, non-chimera expressing cells also express these G-proteins but do not exhibit PTX-insensitive responses to PGD_2 making coupling via $G\alpha_z$ or $G\alpha_{q/11}$ unlikely. While the effect of PTX treatment was constant over the time course of these experiments, small but significant changes in agonist potency were seen. However, since comparative data sets were generated at the same passage using independently generated reagents, this is of little consequence.

To further delineate the mechanism of signal transduction, PGD_2 E/[A] curves in the presence of various calcium signalling pathway inhibitors were assessed. Transient transfection of cells with the C-terminal of β-adrenergic receptor kinase (β-ARK 495-689) using conditions similar to those used here has been shown to result in a 41 % inhibition of adenosine A_1 receptor mediated $[^3H]$-IP_3 responses in CHO cells via sequestration of G-protein βγ subunits (Dickenson & Hill, 1998, and references cited therein). The 43 % reduction in PGD_2 E_{max} in CHO K1 $hCRTH_2$ cells observed here is of a similar magnitude. Taken with the observed total ablation of signalling in these cells by PTX, this indicates that prostanoid $CRTH_2$ receptors in these cells couple via $G\beta\gamma_{i/o}$ subunits to calcium mobilisation. While studies have

not been conducted to demonstrate the specificity of the inhibition for PGD_2 mediated responses, because the conditions used here are so similar to those in the literature, one can reasonably assume that it is mediated by the transfected protein. The lack of inhibition observed in the CHO $G\alpha_{16z49}$ $hCRTH_2$ cells, either with or without PTX treatment suggests firstly, that the chimeric G-protein can compensate for small reductions in $G\beta\gamma_{i/o}$ functionality in these cells, and secondly, that $G\alpha_{16z49}$ (and not its cognate $G\beta\gamma$ subunits) mediates signal transduction in PTX treated chimeric cells. Larger degrees of inhibition have been demonstrated by other groups (e.g. 80 % inhibition of adrenergic $\alpha 2_A$ mediated spinophilin recruitment in HEK293 cells; Brady, *et al.*, 2005) which may indicate differences in transfection efficiency, protein expression levels or differential ability of β-ARK 495-689 to sequester different $G\beta\gamma$ subunit types.

The PLCβ/γ inhibitor U71322 totally abolished PGD_2 induced increases in $[Ca^{2+}]_i$ in both cell lines, with and without PTX treatment (where applicable) confirming that calcium mobilisation is wholly PLC-dependent and that both $G\beta\gamma_{i/o}$ and $G\alpha_{16z49}$ activate PLC isoforms. Other activities of U71322 such as inhibition of Ca^{2+}-ATPase, phosphatidyl inositol 4 phosphate kinase inhibition and non-PLC/non-PKC mediated inhibition of integrin expression on platelets (Lockhart & McNicol, 1999) are probably of little consequence in this context.

The ability of the sarco-endoplasmic reticulum Ca^{2+} ATPase (SERCA, 'calcium pump') inhibitor thapsigargin (Treiman, *et al.*, 1998), but not of ryanodine (which displays concentration-dependent agonist and antagonist properties), to produce elevation of intracellular calcium and inhibit responses to PGD_2 suggests the involvement of IP_3R-mediated calcium release from internal endoplasmic reticulum calcium stores. In the presence of thapsigargin, PGD_2 elicited reductions in basal fluorescence in both cell types but not following PTX treatment suggesting that prostanoid $CRTH_2$ receptors couple via $G_{i/o}$ G-proteins to a calcium-sequestering or -removing mechanism, perhaps involving $G\alpha_i$ mediated Ca^{2+} channel regulation. Care must be exercised in interpreting this result: thapsigargin inhibits the calcium response and any calcium-dependent transduction / desensitisation processes but does not inhibit IP_3 / DAG formation, DAG-dependent MAPK activation, adenylate cyclase inhibition and β-arrestin translocation. Therefore, thapsigargin treatment may have simply revealed the presence of a normally activated calcium homeostasis mechanism. However, although the magnitude of the fluorescence observed at very low PGD_2 concentrations is similar to that of vehicle in untreated cells, the time-course profile of

fluorescence changes and the lower basal fluorescence level are very different suggesting that the 'vehicle effect' is not the same (Figure 10, Panel C). The effect of thapsigargin is therefore to reduce the magnitude of a fluorescence change of uncertain physiological relevance under conditions of a large calcium gradient between the cytoplasm and the internal calcium stores (i.e. favouring calcium sequestration). As mentioned above, PTX blunts the vehicle effect and so the absence of the calcium sequestration effect from PTX-treated cells probably reflects the absence of the vehicle effect. Taken together, it seems unlikely that the CHO K1 $hCRTH_2$ dataset has been contaminated by the presence of an unobserved calcium sequestration mechanism absent from the PTX-treated CHO $G\alpha_{16z49}$ $hCRTH_2$ cells but further investigation is obviously warranted. Taking all these data together, it is now possible to describe the mechanism of calcium mobilisation in both CHO K1 $hCRTH_2$ and CHO $G\alpha_{16z49}$ $hCRTH_2$ cells as shown in Figure 17.

CHO K1 host cells appeared to be sensitive to 1 % DMSO vehicle in a manner related to the duration of the dye-loading period. This concentration of vehicle was considered to be desirable since many prostanoid molecules have limited solubility in water; GW853481X was particularly insoluble. DMSO (1 %) produced smaller effects in the other CHO cell lines studied in this thesis which may reflect selection of vehicle-resistant cells as a by-product of the clone selection process. Effects such as these have been traditionally interpreted as an indication of generalised solvent-induced membrane or protein disruption but it is becoming recognised that DMSO can also have some fairly specific effects at the molecular level, for example, as an agonist for the pregnane X receptor (PXR; NR1I2; Su & Waxman, 2004). DMSO vehicle effects in CHO $G\alpha_{16z49}$ $hCRTH_2$ cells appeared to be PTX-sensitive implying the activation of a receptor-G-protein mediated mechanism possibly via a specific DMSO-sensing receptor or through generalised perturbation of $G\alpha_{i/o}$ coupled receptors, or indeed of the G-proteins themselves. However, in the presence of 1 % DMSO, CHO K1 host cells were devoid of responses to prostanoid receptor agonists, while a panel of prostanoid receptor antagonists failed to produce any significant effects in the presence of PGD_2 and PGE_2 indicating that these host cells do not possess a calcium-linked prostanoid receptor. The finding of small PGE_2-induced calcium changes in CHO $G\alpha_{16z49}$ cells described in Chapter 3 reflects chimera-specific coupling to a prostanoid receptor of the $G\alpha_{i/o}$ or $G\alpha_q$-coupling classes and therefore most probably a prostanoid EP_1 or EP_3 receptor.

As with CHO $G\alpha_{16z49}$ $hCRTH_2$ cells, agonist pharmacology in CHO K1 $hCRTH_2$ cells also bore the hallmark features of prostanoid $CRTH_2$ receptors: lack of activity of PGE_2, $PGF_{2\alpha}$,

PGI_2 & U-46619; high potency responses to PGD_2 but not the prostanoid DP_1 receptor agonist BW245C; agonist rank order of potency 15 R 15 methyl PGD_2 > PGD_2 > PGJ_2 > 15 deoxy $\Delta^{12,14}$ PGJ_2 > 15 S 15 methyl PGD_2 > 13,14 dihydro 15 keto PGD_2; insensitivity of PGD_2 responses to the prostanoid DP_1 receptor antagonist BW868C; and sensitivity to the putative prostanoid $CRTH_2$ receptor antagonists AH23848B & GW853481X. It is therefore, perhaps, not surprising that a high degree of correlation was observed in agonist potency and activity data generated in the two cell lines. Figure 18 displays agonist potency data for the two cell lines in a 'Shuffle Diagram', so named because it allows one to see relative changes in SAR amongst compound series rather like shuffling cards in a pack. It is obvious from this diagram, how similar the data sets are. Indeed, the concordance extends further such that the pharmacophore model developed in Chapter 3 applies equally well to data generated using CHO K1 $hCRTH_2$ cells (Figure 19). This finding is interesting given the postulated synergising interaction between $G\alpha_{16z49}$ and $G\beta\gamma_{i/o}$ discussed in chapter 6: the pharmacophoric equivalence observed suggests that the synergising interaction is dominated by the $G_{\beta\gamma}$ signal and that the effect of the α_{16z49} signal is merely to amplify it. However, the non-equivalence of pharmacophores resulting from the sole activation of $G\alpha_{16z49}$ with those involving $G_{\beta\gamma}$ signals reveals subtleties in the amplification factor generated which are likely to be important in certain settings.

Data generated in CHO K1 $hCRTH_2$ cells with the antagonist AH23848B differed from that obtained in chimera-expressing cells. In CHO K1 cells, AH23848B produced concentration-related PGD_2 E_{max} depression which, as described in Chapter 3 for GW853481X data, could indicate the emergence of hemi-equilibrium due to the inability of the antagonist to establish a new equilibrium with the receptor in the presence of agonist during the time frame of the calcium mobilisation response. In recombinant cell-based systems, this is often driven by slow antagonist off-rate kinetics (i.e. low k_{off}) which are frequently associated with high antagonist affinity. The apparent pA_2 of AH23848B for $hCRTH_2$ receptors is 5.5, while literature reports are consistent with the molecule being a competitive antagonist of prostanoid EP_4 (most recently Davis, *et al.*, 2004) and TP (Brittain, *et al.*, 1985) receptors with no suggestion of non-receptor mediated actions. If, as noted above, the lower G-protein expression in CHO K1 $hCRTH_2$ cells results in poorer receptor-effector coupling (which may be the case since the agonist radioligand detects a smaller number of high affinity sites in these cells), then the smaller control PGD_2 E_{max} values observed in these cells relative to chimera-expressing cells may indicate that maximum effect requires near 100 % receptor

occupancy. Therefore, since hemi-equilibrium effects are occupancy-dependent (Kenakin, 2004b) these cells may be more sensitive to the phenomenon. Kenakin (2004c) also notes that unstirred liquid layers may exist close to the cell monolayer in 384 well plate-based experiments which may also give rise to hemi-equilibrium effects. However, these are not suspected in the present experiments because the FLIPR pipettor head conducts two 10 µl mixes of the well contents during the assay. DMSO is readily miscible with aqueous buffers and would tend to prevent the formation of an unstirred layer.

An interesting feature of the agonist data obtained using CHO K1 $CRTH_2$ cells are the high curve slopes achieved compared with data obtained in non-PTX treated chimera-expressing cells. The synergism between $G\alpha_{16z49}$ and $G\beta\gamma_{i/o}$ subunits postulated elsewhere in this thesis would be expected to lead to increased curve slopes in the chimeric cell line but the observed data is contrary to this. One possibility might be that the two coupling partners are recruited sequentially giving rise to a flatter slope in the chimeric cell line. Alternatively, the amplification may be limited to an effect on lower concentrations of agonist, having the effect of selectively left-shifting responses up to a threshold mid-way up the agonist E/[A] curve and thus flattening slope. The latter hypothesis may be supported by the observed biphasicity in PGD_2 E/[A] curves amplified by pre-exposing cells to UTP ($G\alpha_q$ signal; chapter 6) where the upper part of the agonist response curve appears to be largely unaltered. If this explanation were correct one might expect the slope parameters for different agonists in CHO K1 $CRTH_2$ cells to be fairly similar and those in chimera-expressing cells to be more variable due to the variability in the amplifying factors generated by the various agonists (see above). The opposite trend is apparent from the data raising the possibility that the effect of synergism here is to smooth out agonist responses over a wider concentration range. In endogenously constituted systems this may allow greater control of overall response levels and therefore fine-tuning of physiological responses. The reason why agonist responses produce generally higher and more variable slope values in non-chimeric cells is unclear and seems to imply the presence either of a threshold effect not present or suppressed in chimera-expressing cells, or the presence of a threshold-smoothing effect absent from the non-chimeric cells. The impact of this phenomenon on the relative potency values obtained is difficult to assess. A synergy-related left shift of agonist responses in chimera-expressing cells is unlikely to affect all agonists equally resulting in variable alterations of relative potency with respect to RP in non-chimeric cells. The pharmacophoric differences between the non-PTX treated chimeric cell line and the other two data sets may therefore relate to the interruption of synergy. However,

even if this is the case, the differences reflect another aspect of agonist stimulus trafficking since the resultant effect of the synergising signals differ between agonists. Finally, these considerations shed no new light on the discrepancy between PGD_2 occupancy (determined by radioligand binding) and agonist response curves since the effect of the synergy seems to be to amplify responses to low concentrations of agonist and to left-shift agonist pEC_{50} values though this is still far to the right of the binding pK_d.

Thus, it is now possible to determine the impact of the change from $G\beta\gamma_{i/o}$ mediated coupling to $G\alpha_{16z49}$ mediated coupling on prostanoid $CRTH_2$ receptor pharmacology. Viewing the data sets in their entirety, there is little or no correlation between CHO K1 $hCRTH_2$ and CHO $G\alpha_{16z49}$ $hCRTH_2$ + PTX agonist potency and relative activity data (Figures 16 & 20). The correlations appear to suggest that some full agonists in the non-chimeric system have become partial agonists in the chimeric system. However, this is an artefact of the inclusion of data for some compounds that did not elicit full E/[A] curves in the chimera-expressing system in order to get a more accurate estimate of the overall correlation. In other words, non-chimeric cell agonist E_{max} data has been correlated with agonist effect at highest concentration tested in the chimeric system. For those compounds still generating full E/[A] curves, the relative activity remained unchanged suggesting that there is no fundamental change in coupling efficiency despite the putative three-fold difference in $[^3H]$-PGD_2 binding sites (but as noted above the R:G ratio is essentially unknown). The accuracy of the B_{max} estimates generated here is questionable but the relative amounts in the two $CRTH_2$-expressing cell lines can be assessed since they are both subject to the same confounding factors. Since the amount of G-protein detected by Western blot appears to follow the number of binding sites, R:G stoichiometry seems to be constant leading to the expectation that agonist receptor-effector coupling should also be constant. However, elevated G-protein expression will of itself lead to the detection of a higher number of high affinity agonist binding sites because of the effect of G-protein pre-coupling to the receptor. Therefore, receptor expression may well be constant between the two cell lines with greater pre-coupling in the chimera-expressing cells. Thus, one would expect agonist responses to be of greater magnitude and potency in CHO $G\alpha_{16z49}$ cells but the rank order of potency and relative activity in the two cell lines to be connected by a simple 'strength of stimulus' relationship. Agonist profiling in both cell types (+ PTX treatment in chimeric cells) showed that indomethacin, D, F & J series but not E series prostaglandins were agonists at $CRTH_2$ receptors. When the $G\alpha_{16z49}$ component was isolated in PTX-treated CHO $G\alpha_{16z49}$ cells,

reversals of potency order were observed (compared to the $G\beta\gamma_{i/o}$-mediated response in CHO-K1 cells). These were most striking for (relative potency CHO K1, CHO $G\alpha_{16z49}$; potency of PGD_2 = 1.0) indomethacin (10, c.40) 16,16 dimethyl PGD_2 (158, 11), Δ^{12} PGJ_2 (32, 2.5) and 9,10 dihydro 15 deoxy $\Delta^{12,14}$ PGJ_2 (40, 3.5). In terms of absolute potency J series agonists were little affected e.g. 15 deoxy $\Delta^{12,14}$ PGJ_2 (pEC_{50} CHO K1, CHO $G\alpha_{16z49}$: 6.5 ± 0.04, 6.2 ± 0.03) while F series agonists were most affected (e.g. 15 R $PGF_{2\alpha}$ 5.5 ± 0.04, only 15 ± 8 % stimulation at 10 μM). Classically, a gross change in agonist rank order such as this, if detected in non-recombinant cells, would be taken as an early indication of a new receptor subtype but this clearly is not the case here.

Prostanoids of the F and D series possessing a 15 hydroxy group were most critically affected by the switch in coupling partner having much lower potency at the chimera-coupled receptor (Figure 20). Two alternative views of these data may be conceived:

1. **The chimera is well-coupled**. In this scenario, D series compounds indicated in Figure 20 with black arrows are largely unaffected by the switch, while the compounds indicated with red arrows now activate the receptor with much lower potency. Thus J series and many D series compounds are unaffected while agonists possessing the 15 hydroxy group are now unable to activate the receptor with high potency and F series compounds are almost inactive. Some features of the data set support this view: a) The relative activity of agonists producing complete E/[A] curves is unchanged; b) F series (partial) agonists would be predicted to elicit E/[A] curves of potency similar to that in non-chimeric cells but with reduced maximum activity but this has not been observed; c) The agonist 13,14 dihydro 15 keto PGD_2 has paradoxically increased in potency and undergone a rank order reversal with respect to PGD_3 (although the absolute changes in potency are small, the relative change is of 0.4 log units). From this view of the data, one would deduce that the 15 hydroxy group is critical to high potency agonism through native $G\beta\gamma_{i/o}$ class proteins but that the benefit of this substituent is lost when the receptor is chimera-coupled. Inspite of this alteration in the importance of C15, the R > S stereochemical relationship is preserved. The C11 carbonyl is an obligate requirement for chimera-coupled agonism being present in all active agonists; the H-bond acceptor at C9 may still confer some benefit to D series molecules but is unable to support agonism without the presence of the carbonyl. The impact of β-chain modification on J series molecules cannot be fully described since few compounds are available but seems to be of little importance. On the other hand, β-chain modified D series compounds show a range of activities though many of these modifications result in inactivity implying that the combined

effect of the C11 carbonyl and C9 hydroxyl is to push the β-chain into a conformationally (PGD_1 and PGD_3) and sterically (16,16 dimethyl PGD_2 and 17 phenyl PGD_2) restricted pocket not accessed by J series molecules. The natural conclusion is, therefore, that the requirements for agonism have become *more* stringent (Figure 21).

2. **The chimera is poorly coupled**. Under these conditions all compounds now activate the receptor with lower absolute potency but the compounds indicated with black arrows activate the receptor with higher *relative* potency to the compounds indicated by red arrows. The observations made above are still pertinent but now a much *lower* degree of β-chain stringency must be invoked. This would be consistent with the notion that less stringent R-G activation requirements underpin the promiscuity of $G\alpha_{16}$. There are no indications from the data set to support this scenario and so a high degree of coupling has been assumed. Therefore simple 'strength of signal' changes appear to be insufficient to account for these data.

Can these findings be related to the structure of the receptor? It is important to realise that the altered SAR represents differential G-protein activation by the same receptor. In other words, the ligands are binding to the same receptor, with the same binding and activation residues implicated, and the same alteration of receptor tertiary structure. Presumably, what differs is the impact of these changes on the tertiary structure of the different G-proteins. However, G-protein pre-coupling to receptors and high affinity receptor state stabilisation is widely acknowledged (described in Kenakin, 2004b). It follows from consideration of the extended ternary complex model (Samama, *et al*., 1993) that alteration of receptor affinity for ligands by G-proteins is expected. Therefore, one cannot rule out the possibility that the chimera may alter receptor – ligand binding interactions. Although it is tempting to speculate that those ligands active (and therefore with affinity) at native coupled receptors but inactive at chimera-coupled receptors might represent chimera-specific antagonists, an alternative explanation might be that the chimera has reduced their binding affinity for the receptor.

A structure-based ligand docking model of murine $CRTH_2$ has been recently presented by Hata, *et al*. (2005). Using site-directed mutagenesis and determining the binding affinity of PGD_2, 13,14 dihydro 15 keto PGD_2, indomethacin and ramatroban, these authors have suggested that PGD_2 occupies a binding pocket situated between the transmembrane helices and orientated in an opposite manner to that of other prostanoid receptors: the cyclopentane head group occupies the space between TMIII and TMVI with the C9 hydroxyl stabilised by a hydrogen bond with Glu-268 of TMVI; the α-chain carboxylate forms a charge interaction

with Lys-209 of TMV; Arg-178 in ECII is believed to impose 'geometric constraints' on the binding pocket. There are some attractive features of this model: firstly, the carbonyl at C11 could interact with His-106 in TMIII to form a hydrogen bond – this would allow J series prostanoids to bind; secondly, the importance of Arg-178 could be to form an H-bond with the C15 hydroxy group and because ECII is linked by a disulphide bridge to ECI/TM3 this might provide a mechanism by which a high agonist potency conformation might be induced; thirdly, bulky β-chain substituents might sterically interact with ECII residues to prevent H-bond formation at C15; and fourthly, it might explain why PGD_1 alcohol is inactive since it would fail to interact with Lys-209. Thus a picture emerges of ligand recognition mediated by TMIII & TMVI, with recognition of agonist both here and at ECII / TMV. Simple predictions of agonist potency based on strength of H-bond acceptance at C15 cannot be made since stereochemical orientation is so important. However, the data I present here suggests a greater importance of the His-106 (donor) / C11-carbonyl (acceptor) interaction relative to the Glu-268 (acceptor) / C9-hydroxy (donor – since C9 acceptors are inactive) interaction. This lends further support to the model and explains the observed inactivity of C9 acceptor substituted prostanoids.

An objection to this view of the ligand binding pocket is that with the exception of Glu-268, mutation of all the other residues mentioned above to alanine resulted in abolition of PGD_2 binding Hata, *et al*. (2005), whereas the data I present clearly show that abolition of certain interactions by modification of the agonist do not result in complete loss of activity. This could indicate that the mutations have resulted in greater molecular changes than the intended interruption of ligand binding, and therefore that our understanding of the binding pocket is incomplete.

To summarise, the switch from $G\beta\gamma_{i/o}$ to what is assumed to be $G\alpha_{16z49}$ coupling of prostanoid $hCRTH_2$ receptors does significantly alter agonist SAR. In other words, I have demonstrated that for agonists, chimera-specific pharmacology is more than a theoretical hazard in drug discovery, and that there is a need to validate each non-native G-protein / receptor pairing created. Chimera-specific antagonists, if they exist, would be a further extension of the potential difficulty into the realm of antagonism and would indeed be an exciting discovery.

The work I have presented in Chapter 4 goes a long way towards addressing several of the questions posed at the end of Chapter 3 including a clear demonstration of divergent pharmacology where a receptor is coupled through Gβγ and Gα subunits. Can the same be demonstrated where alternative subunits of the same G-protein couple to the same receptor?

For this a [^{35}S]-GTPγS binding assay using membranes generated from CHO K1 hCRTH$_2$ cells is needed to generate SAR data for the receptor coupled to G$\alpha_{i/o}$ activation, and this is presented in Chapter 5.

4.5 Figure caption list:

Figure 1. Prostaglandin D_2 (PGD_2) and 15 R 15 methyl PGD_2 concentration effect curves in CHO K1 $hCRTH_2$ cells of clonal cell lines 10 and 15. Data for 13,14 dihydro 15 keto PGD_2 and $PGF_{2\alpha}$ shown only for clone 15. Data are mean ± sem of twenty-four E/[A] curves from three separate assays.

Figure 2. Saturation radioligand binding of [^{3}H]-PGD_2 to CHO K1 cells expressing $hCRTH_2$ receptors alone. Panel A: Total, specific and non-specific binding. K_d and B_{max} estimated by non linear regression. Panel B: Scatchard transformation of specific binding data showing fit to single binding site.

Figure 3. Saturation radioligand binding of [^{3}H]-PGD_2 to CHO cells expressing both $G\alpha_{16z49}$ G-proteins and $hCRTH_2$ receptors. Panel A: Total, specific and non-specific binding. K_d and B_{max} estimated by non linear regression. Panel B: Scatchard transformation of specific binding data showing fit to single binding site.

Figure 4. Representative Ponceau S stain of nitrocellulose protein blot prepared as described in *Methods*. Samples and molecular weight markers as indicated (kDa). Image shows equivalent staining in all lanes indicating equivalent sample loadings.

Figure 5. Western blots developed with antibodies for G-proteins as follows: Panel A – anti $G\alpha_i$ & $G\alpha_z$; Panel B – anti $G\alpha_q$, $G\alpha_{q/11}$, $G\alpha_{11}$, $G\alpha_{16}$; Panel C – anti $G\alpha_s$. Samples in all panels are: M - molecular weight markers; 1 – CHO K1 $hCRTH_2$ membranes; 2 – CHO $G\alpha_{16z49}$ $hCRTH_2$ membranes; 3 – CHO $G\alpha_{16z49}$ host membranes. Additional samples in Panel A are: 4 – recombinant rat $G\alpha_{i3}$; 5 – recombinant rat $G\alpha_{i2}$; 6 – recombinant rat $G\alpha_{i1}$. Procedures as described in *Methods*. Films exposed for 1 s except for $G\alpha_i$, $G\alpha_z$ and $G\alpha_q$ which were exposed for 20 s. Molecular weight markers as indicated (kDa).

Figure 6. Concentration effect curves in CHO K1 host cells generated in response to uridine triphosphate (UTP), a range of prostanoid receptor agonists, 1 % DMSO vehicle and buffer, as detailed in figure legend. Data are mean ± sem of three

independent experiments conducted on the same day. Vehicle effects observed were significantly larger than effects observed in other settings.

Figure 7. Effect of prostanoid receptor antagonists, 1 % DMSO vehicle and buffer on CHO K1 host cells. Key to abbreviations:- AH: AH23848B 10 μM; BW: BW868C 1 μM; GW6: GW627368X 1 μM; L: L-798106 a.k.a. GW671021X 1 μM; SC: SC-51322 a.k.a. GW773521X 1 μM; GW8: GW853481X a.k.a. Compound 1c 10 μM; SQ: SQ-29548 1 μM; V: 1 % DMSO vehicle; B: buffer. Panel A: Effect of antagonists and vehicle on otherwise untreated CHO K1 cells; Panel B: Effect of antagonists and vehicle on responses to PGD_2 10 μM; Panel C: Effect of antagonists and vehicle on responses to PGE_2 10 μM. Data are mean ± sem of three independent experiments conducted on the same day.

Figure 8. Antagonism of PGD_2 by GW853481X and AH23848B in CHO K1 $CRTH_2$ cells. Panel A: PGD_2 E/[A] curves generated in the presence of vehicle or increasing concentrations of AH23848B (Schild analysis) and, inset, Clarke plot of antagonist pA_2 estimated at each concentration of antagonist vs. log[antagonist concentration]. Data are mean ± sem of four E/[A] curves generated separately in the same experimental occasion. Panel B: PGD_2 E/[A] curves generated in the presence of vehicle or increasing concentrations of GW853481X (Schild analysis) and, inset, Clarke plot of antagonist pA_2 estimated at each concentration of antagonist vs. log[antagonist concentration]. Data are mean ± sem of three E/[A] curves generated separately in the same experimental occasion.

Figure 9. Effect of pertussis toxin treatment on responses to PGD_2 in CHO K1 $hCRTH_2$ cells. Panel A: PGD_2 E/[A] curves in PTX-treated or -untreated cells at passage 10 (P10). Panel B: Left chart: Maximum responses to PGD_2 in PTX-treated cells at passages 10-16 (P10-16) compared with responses in untreated control (C) cells; Right chart: PGD_2 pEC_{50} in PTX-untreated cells at P10-16. Data are mean ± sem of twelve E/[A] curves generated in three separate experiments. * denotes $P < 0.05$ cf. PGD_2 pEC_{50} in PTX-untreated cells at P10.

Figure 10. Investigations using inhibitors of cell signalling molecules in CHO K1 $hCRTH_2$ cells. Panel A: Effect of inhibitors on basal fluorescence. Panel B: Effect of inhibitors on PGD_2 E/[A] curves. Panel C: Representative calcium flux time courses in response to exposure of cells to 10 μM PGD_2, 0.25 % DMSO vehicle (V), vehicle in the presence of 3 μM thapsigargin (V+T) and buffer (B). All inhibitors were added at 3 μM (final assay concentration) in 0.25 % DMSO vehicle. Data are mean ± sem of three independent experiments.

Figure 11. Investigations using inhibitors of cell signalling molecules in CHO $G\alpha_{16z49}$ $hCRTH_2$ cells. Panel A: Effect of inhibitors on basal fluorescence. Panel B: Effect of inhibitors on PGD_2 E/[A] curves. All inhibitors were added at 3 μM (final assay concentration) in 0.25 % DMSO vehicle. Data are mean ± sem of three independent experiments.

Figure 12. Investigations using inhibitors of cell signalling molecules in CHO $G\alpha_{16z49}$ $hCRTH_2$ cells treated with pertussis toxin (50 ng ml^{-1}). Panel A: Effect of inhibitors on basal fluorescence. Panel B: Effect of inhibitors on PGD_2 E/[A] curves. All inhibitors were added at 3 μM (final assay concentration) in 0.25 % DMSO vehicle. Data are mean ± sem of three independent experiments.

Figure 13. Investigations with heparin in CHO K1 $hCRTH_2$ cells. Panel A: Effect of vehicle on PGD_2 E/[A] curves. Vehicle was either buffer or buffer + lipofectamine (Lipo) 0.3, 1.25 or 2.5 % v v^{-1}. Panel B: Effect of heparin (1USP unit $well^{-1}$; 125 μg ml^{-1}) on PGD_2 E/[A] curves. Heparin was pre-mixed with lipofectamine for 30 mins prior to assay. Data are mean ± sem of three independent experiments.

Figure 14. Effect of transient transfection of cells with the C-terminal of β-adrenergic receptor kinase (β-ARK 495-689) in: Panel A - CHO K1 $hCRTH_2$ cells; Panel B - CHO $G\alpha_{16z49}$ $hCRTH_2$ cells; Panel C - CHO $G\alpha_{16z49}$ $hCRTH_2$ cells with pertussis toxin (50 ng ml^{-1}) treatment. Data are mean ± sem of three independent experiments.

Figure 15. Correlation plots of functional assay potency and activity data obtained in CHO K1 $CRTH_2$ cells with that obtained in CHO $G\alpha_{16z49}$ $hCRTH_2$ cells without PTX

treatment. Panel A: correlation of pEC_{50} data; Panel B: correlation of maximum effect data.

Figure 16. Correlation plots of functional assay potency and activity data obtained in CHO K1 $CRTH_2$ cells with that obtained in CHO $G\alpha_{16z49}$ $hCRTH_2$ cells with PTX treatment. Panel A: correlation of pEC_{50} data; Panel B: correlation of maximum effect data.

Figure 17. Schematic representation of calcium mobilisation pathways in CHO K1 $hCRTH_2$ and CHO $G\alpha_{16z49}$ $hCRTH_2$ cells based on data described in *Results*. Abbreviations: $hCRTH_2$ – human chemoattractant receptor homologous molecule of Th2 cells; $G\alpha$ & $G\beta\gamma$ – alpha subunit and beta/gamma subunit complex of GTP-binding protein; $PLC\beta/\gamma$ – phospholipase C β or γ; PIP_2 – phosphatidyl inositol diphosphate; DAG – diacyl glycerol; IP_3 – inositol triphosphate; IP_3R – inositol triphosphate receptor; ER – endoplasmic reticulum.

Figure 18. SAR Shuffle diagram displaying agonist potency SAR in CHO K1 $hCRTH_2$ and CHO $G\alpha_{16z49}$ $hCRTH_2$ cells, the latter without PTX treatment.

Figure 19. Summary of agonist pharmacophore at human prostanoid $CRTH_2$ receptors expressed in CHO K1 cells ($G\beta\gamma_{i/o}$ coupling) deduced from agonist potency data.

Figure 20. SAR Shuffle diagram displaying agonist potency SAR in CHO K1 $hCRTH_2$ and CHO $G\alpha_{16z49}$ $hCRTH_2$ cells with PTX treatment.

Figure 21. Summary of agonist pharmacophore at human prostanoid $CRTH_2$ receptors deduced from agonist potency data in pertussis toxin-treated CHO $G\alpha_{16z49}$ cells ($G\alpha_{16z49}$ coupling).

4.6 Figures

Follow on next page.

Figure 1

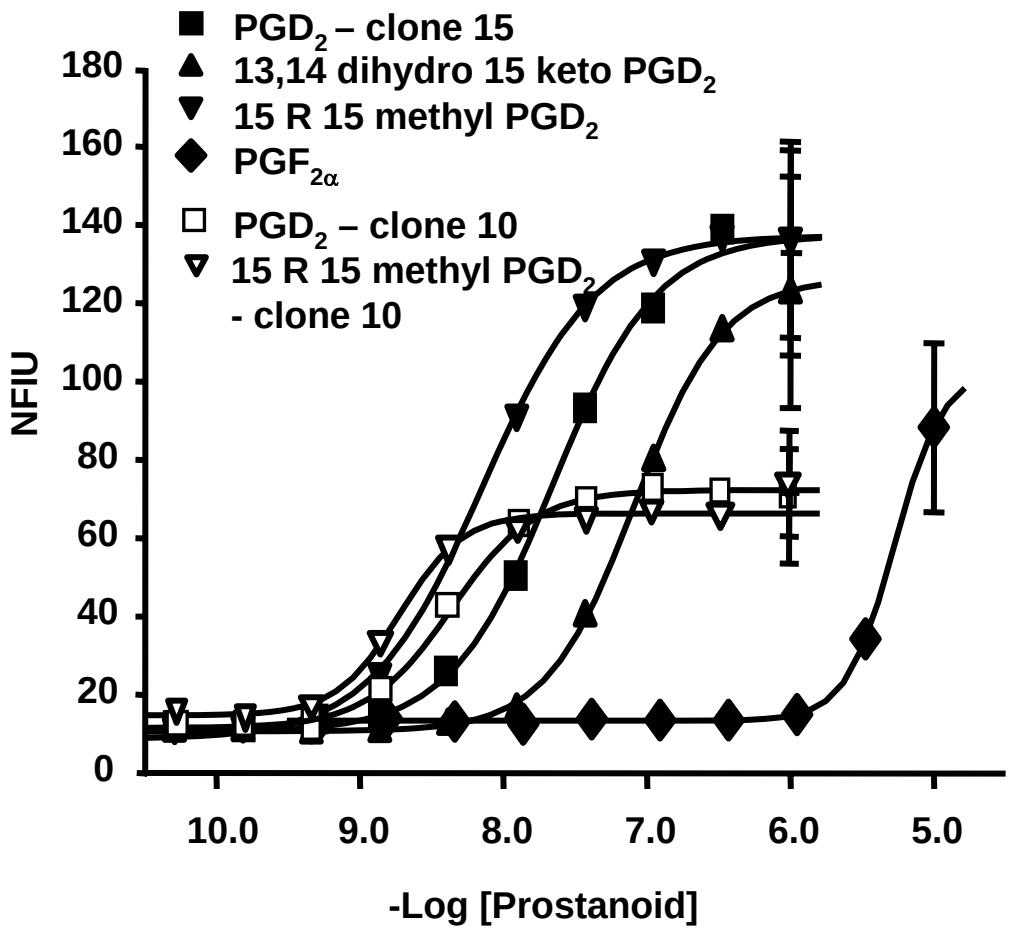
PGD2 – clone 15
13,14 dihydro 15 keto PGD2
15 R 15 methyl PGD2
PGF2α
PGD2 – clone 10
15 R 15 methyl PGD2
- clone 10
NFIU
180
160
140
120
100
80
60
40
20
0
10.0
9.0
8.0
7.0
6.0
5.0
-Log [Prostanoid]

Figure 2

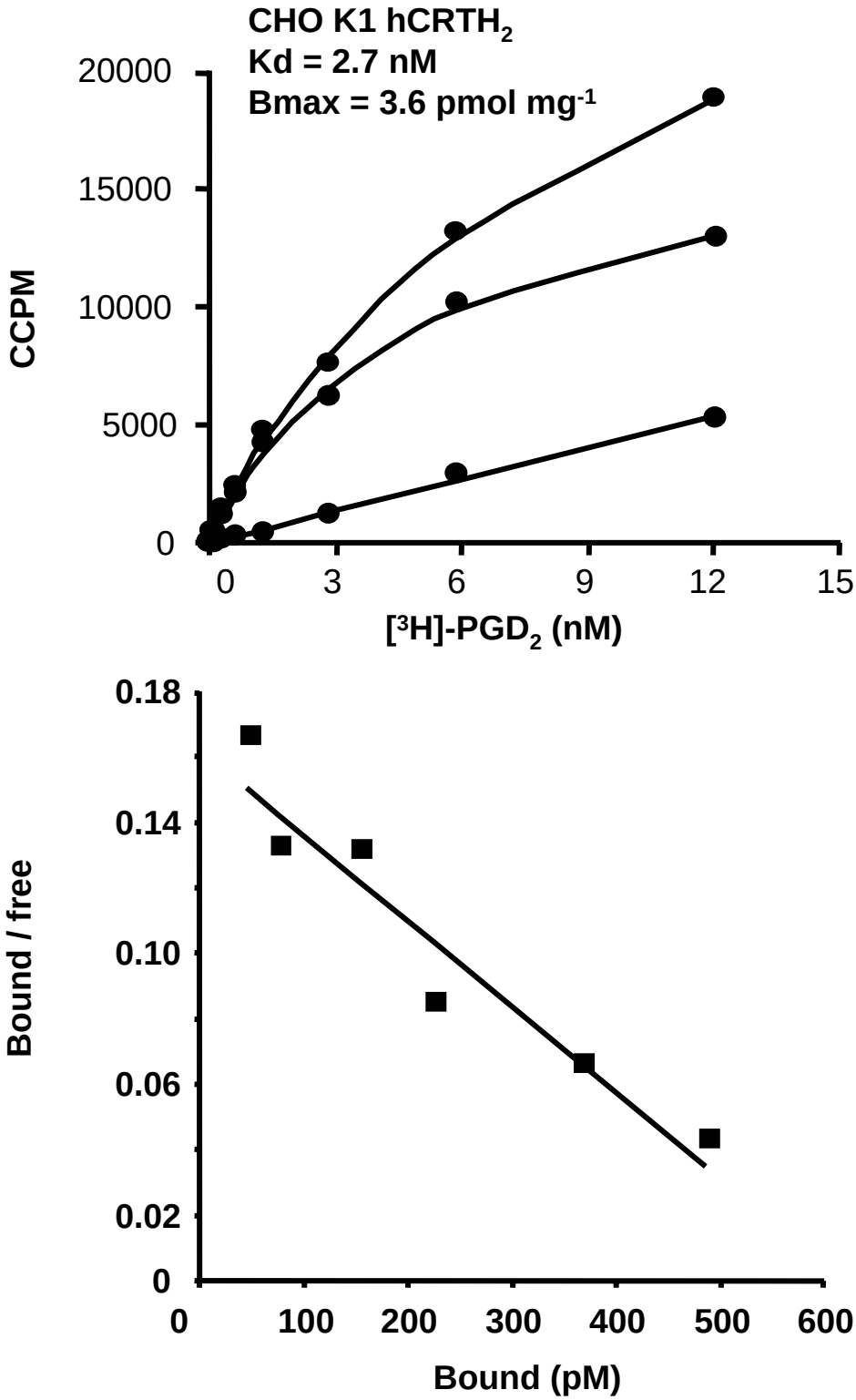
CHO K1 hCRTH2
Kd = 2.7 nM
Bmax = 3.6 pmol mg-1
CCPM
20000
15000
10000
5000
0
0
3
6
9
12
15
[3H]-PGD2 (nM)
Bound / free
0.18
0.14
0.10
0.06
0.02
0
0
100
200
300
400
500
600
Bound (pM)

Figure 3

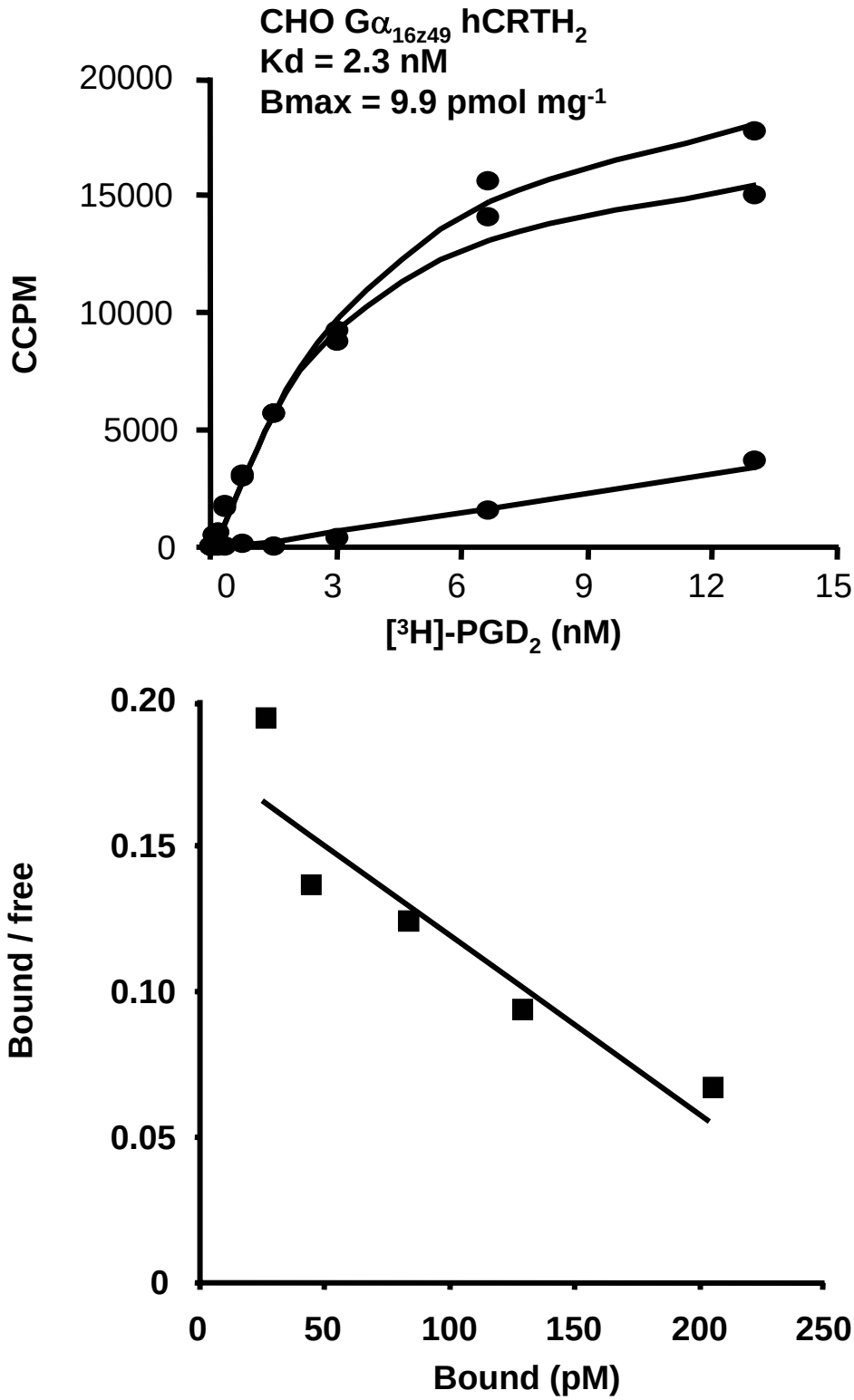
CHO Gα16z49 hCRTH2
Kd = 2.3 nM
Bmax = 9.9 pmol mg-1
CCPM
20000
15000
10000
5000
0
0
3
6
9
12
15
[3H]-PGD2 (nM)
Bound / free
0.20
0.15
0.10
0.05
0
0
50
100
150
200
250
Bound (pM)

Figure 4

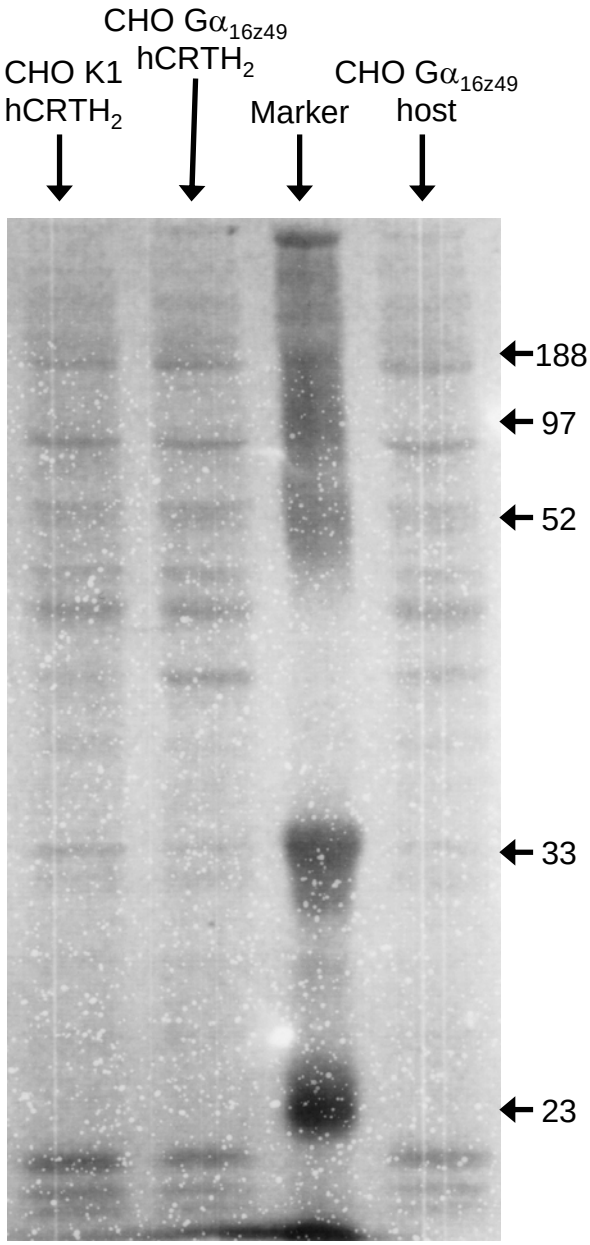
CHO Gα16z49
hCRTH2
CHO K1
hCRTH2
Marker
CHO Gα16z49
host
188
97
52
33
23

Figure 5 – Panel A

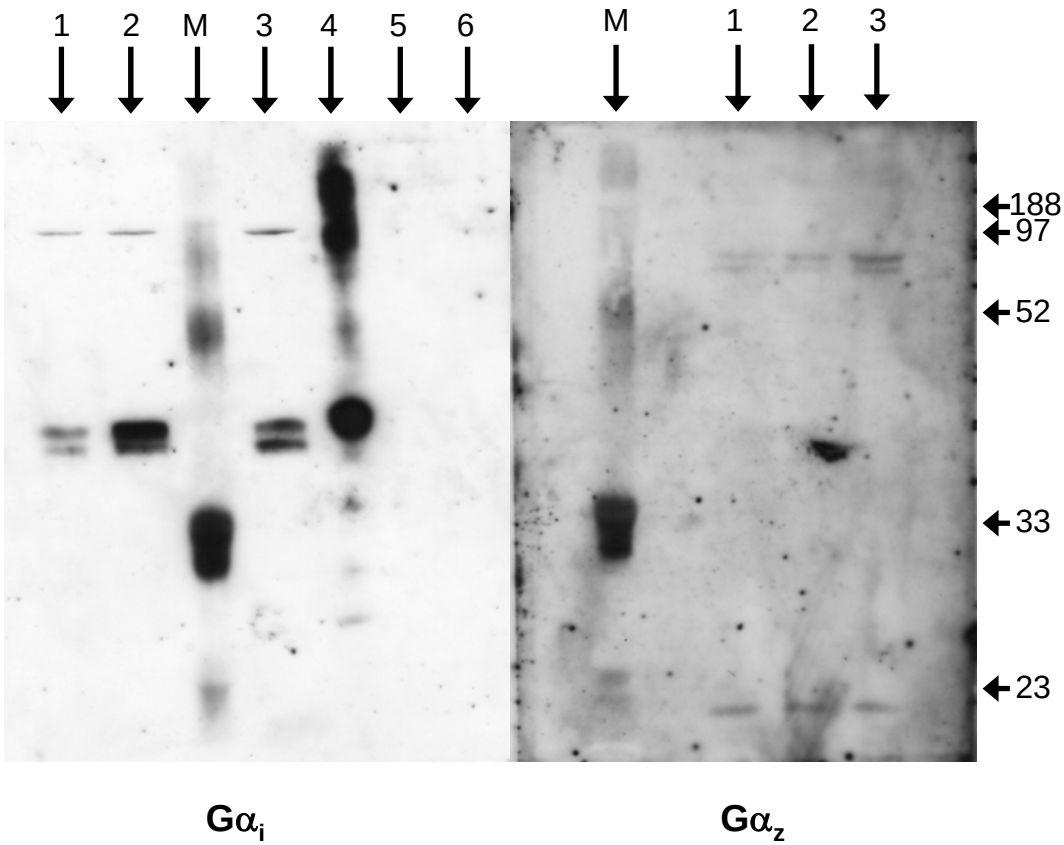

Figure 5 – Panel B

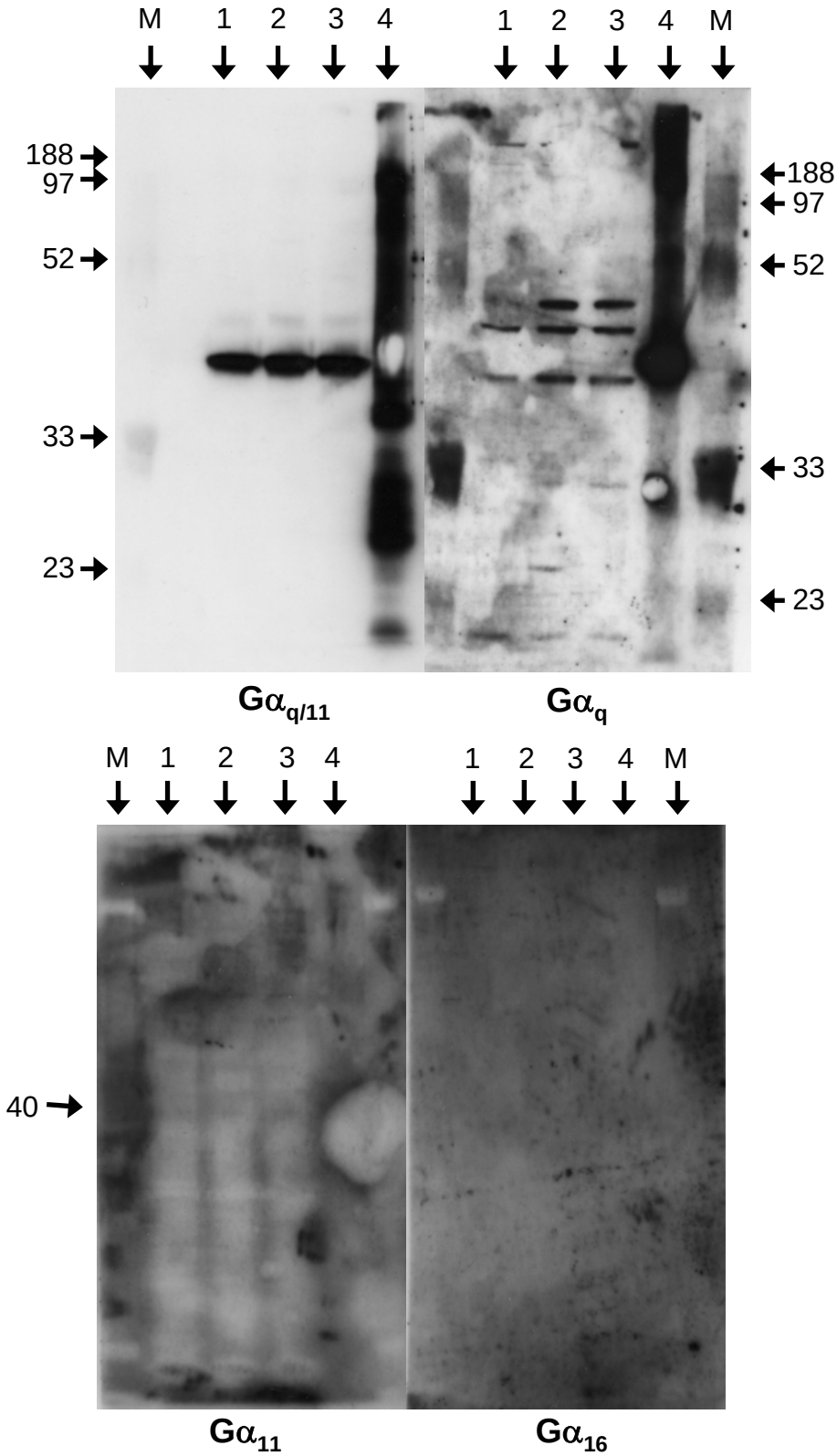

Figure 5 – Panel C

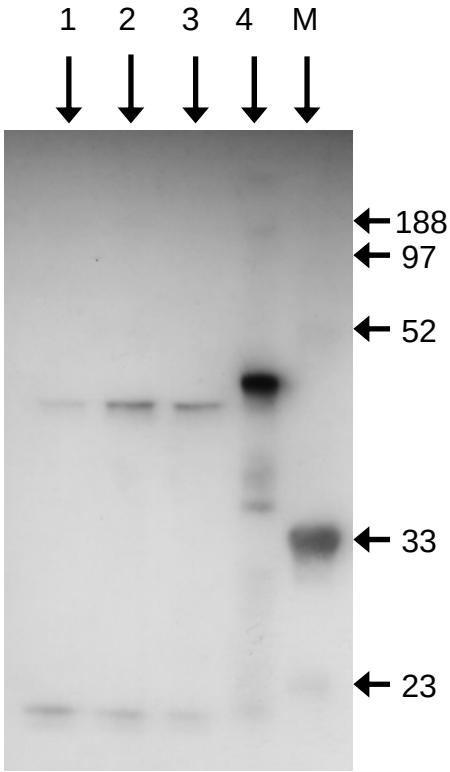

$G\alpha_S$

Figure 6

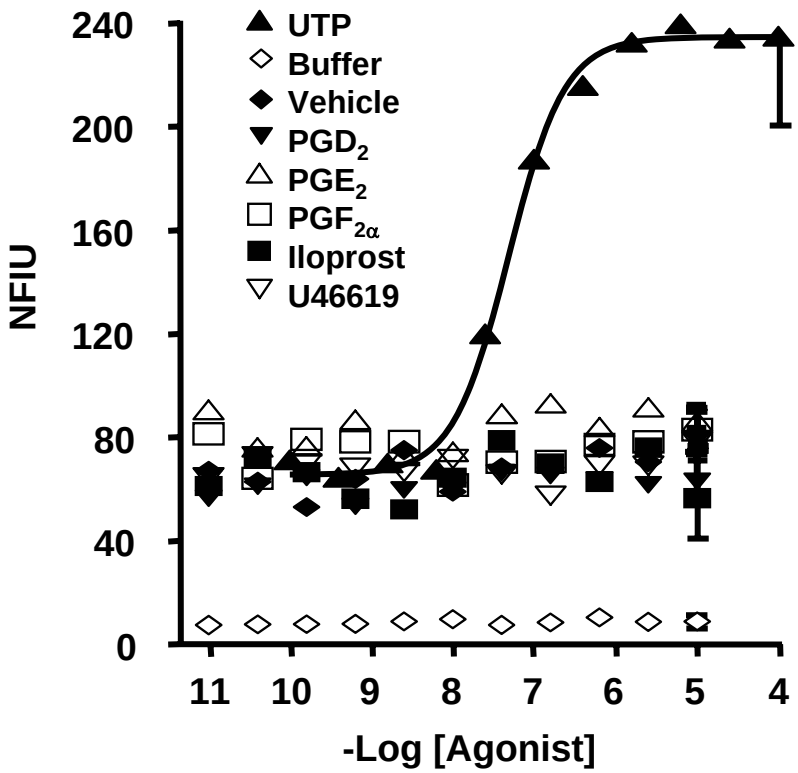
240
200
160
120
80
40
0
NFIU
UTP
Buffer
Vehicle
PGD2
PGE2
PGF2α
Iloprost
U46619
11
10
9
8
7
6
5
4
-Log [Agonist]

Figure 7

Panel A

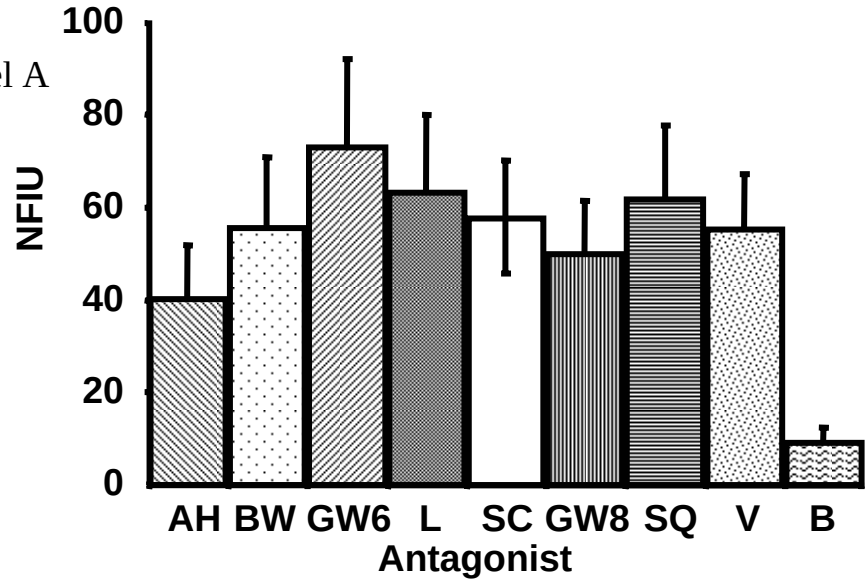

Panel B

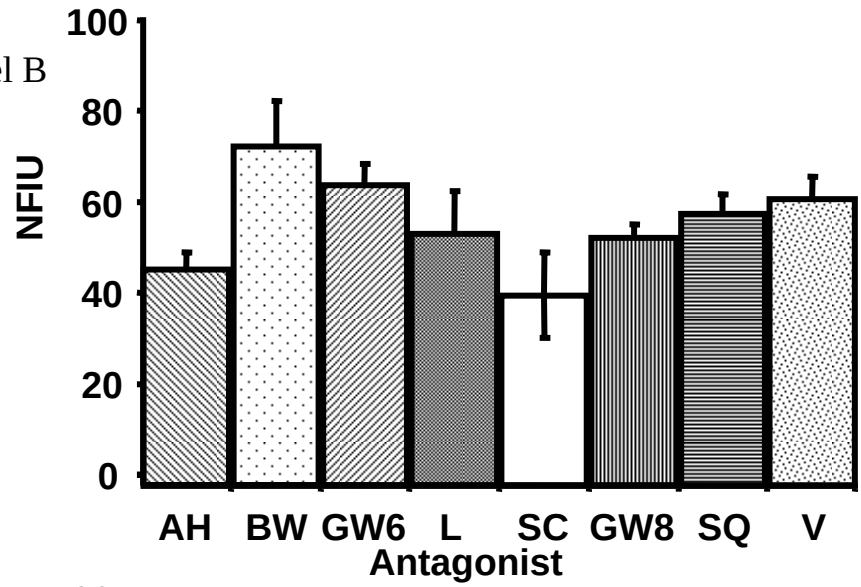

Panel C

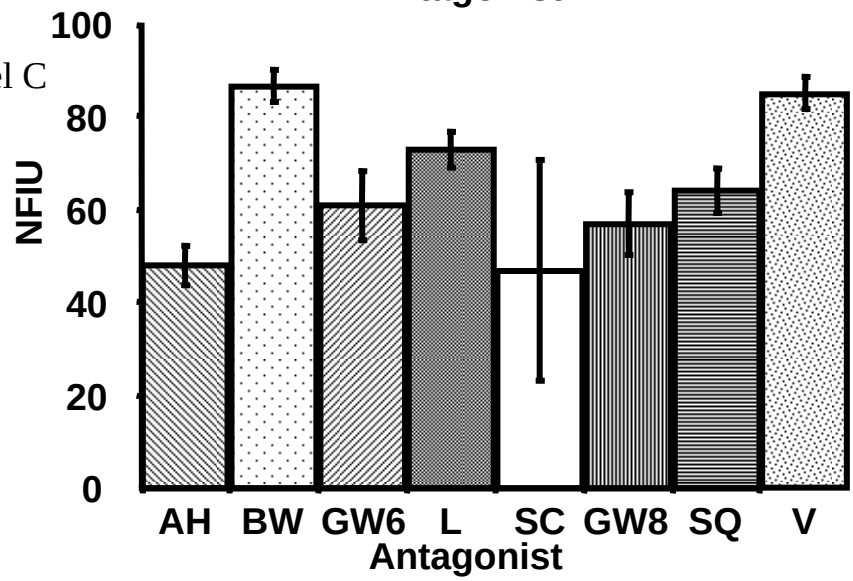

Figure 8.

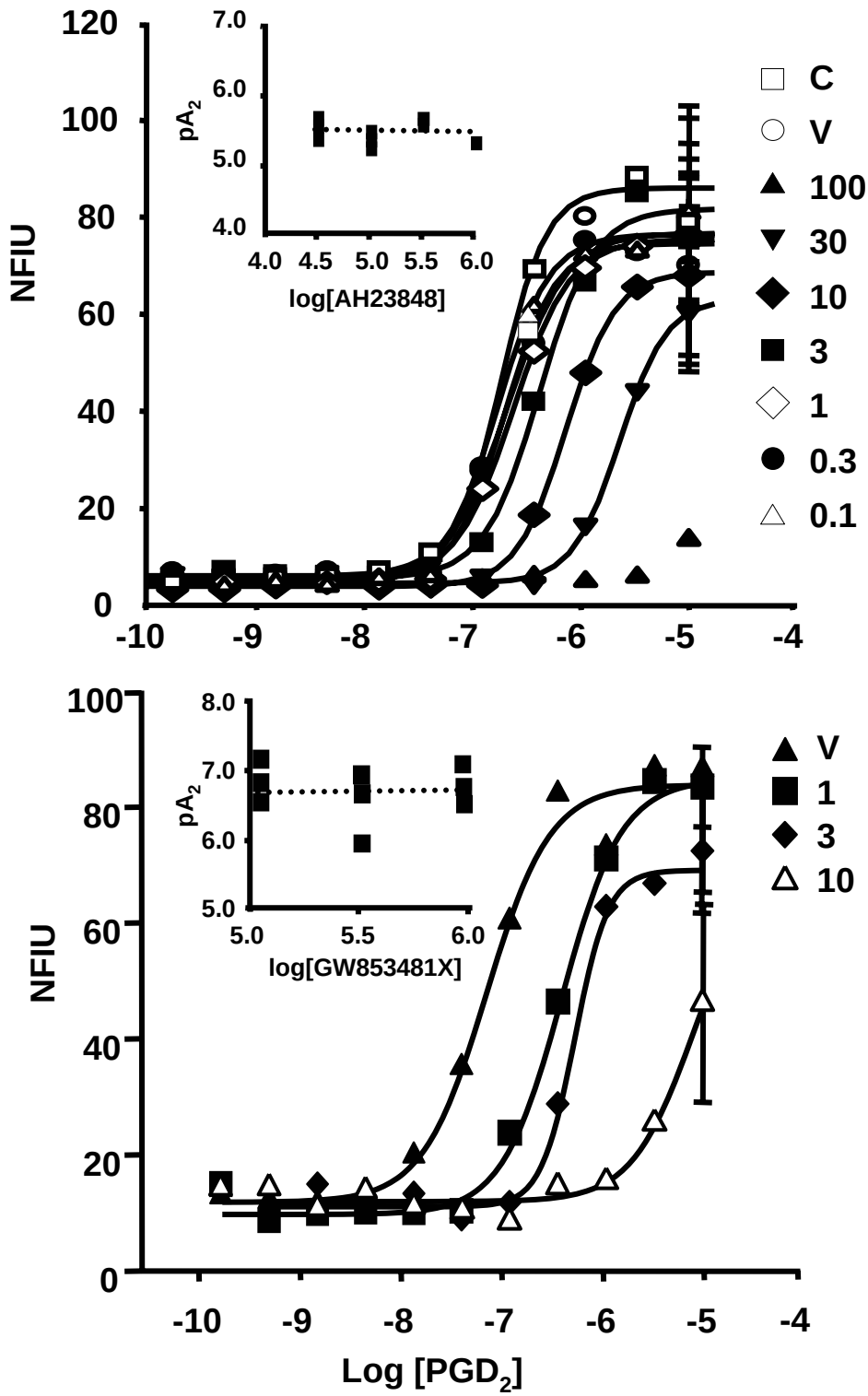
120
100
80
60
40
20
0
NFIU
-10
-9
-8
-7
-6
-5
-4
7.0
6.0
5.0
4.0
pA2
4.0 4.5 5.0 5.5 6.0
log[AH23848]
C
V
100
30
10
3
1
0.3
0.1
100
80
60
40
20
0
NFIU
8.0
7.0
6.0
5.0
pA2
5.0 5.5 6.0
log[GW853481X]
V
1
3
10
-10
-9
-8
-7
-6
-5
-4
Log [PGD2]

Figure 9

Panel A

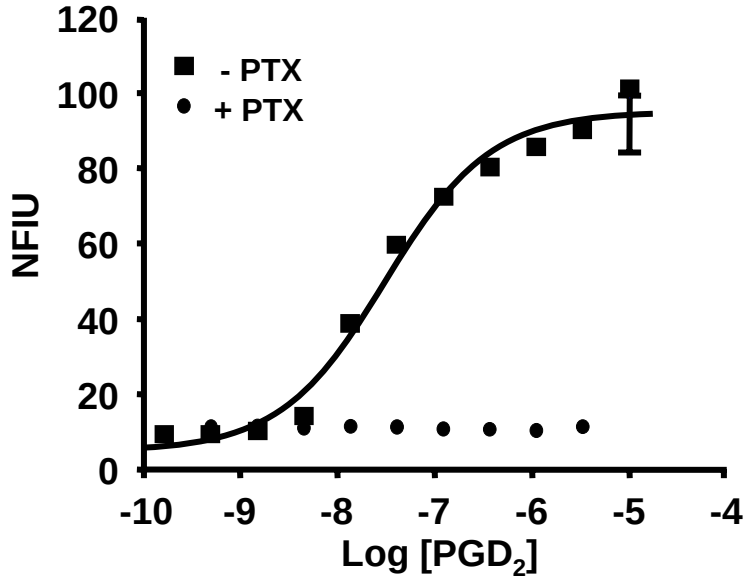

Panel B

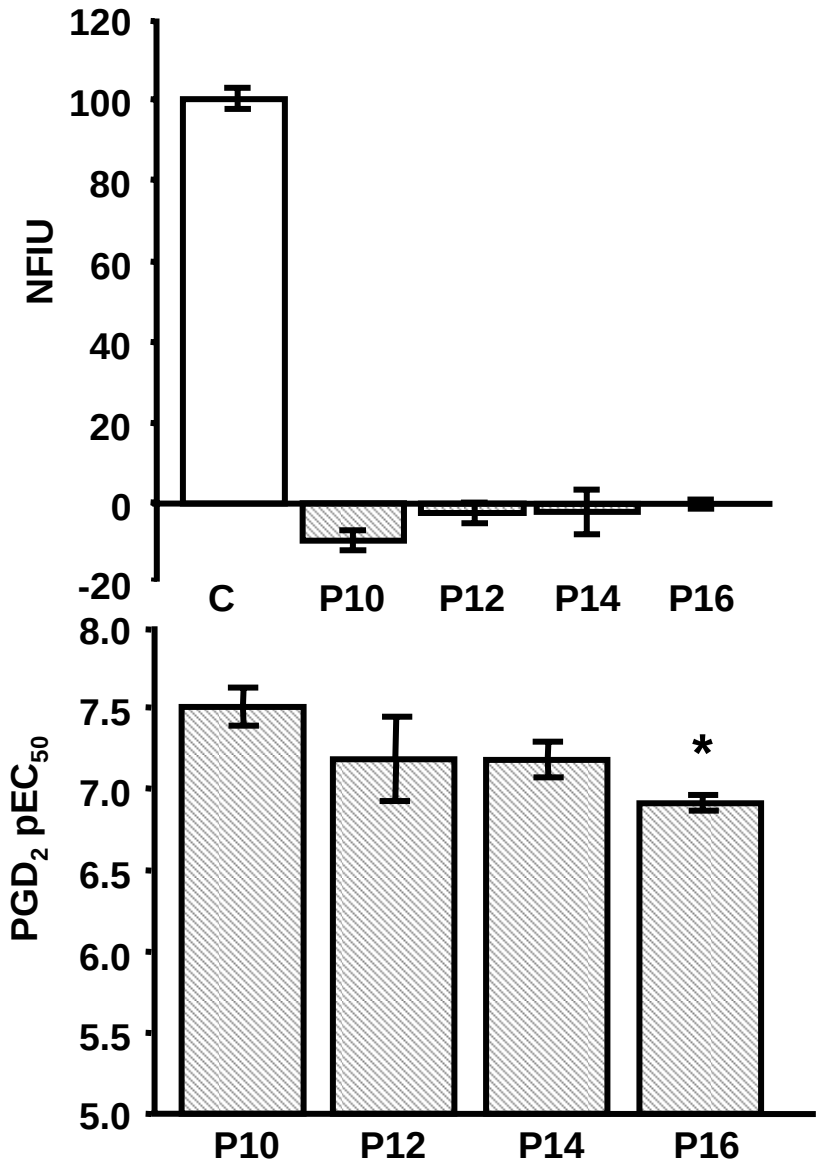

Figure 10.

Panel A

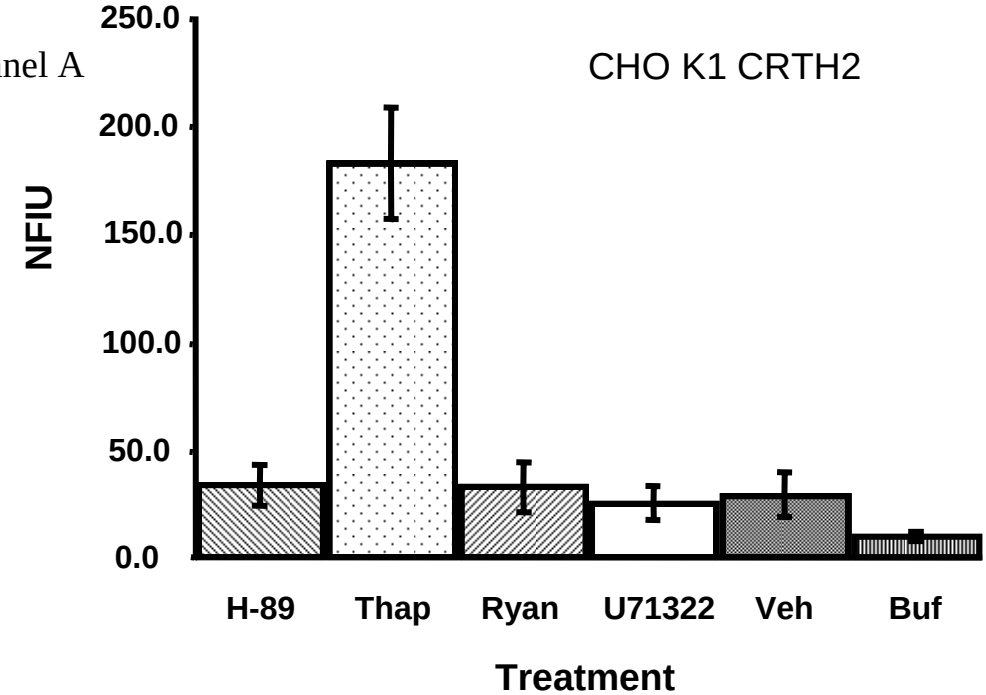

Panel B

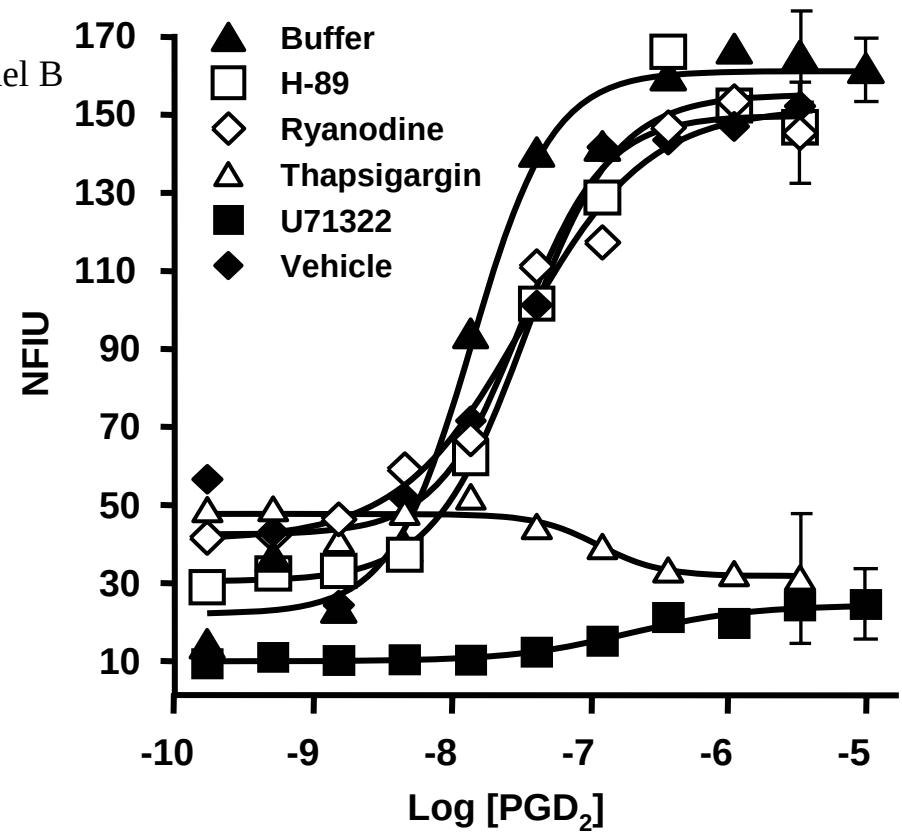

Figure 10.

Panel C

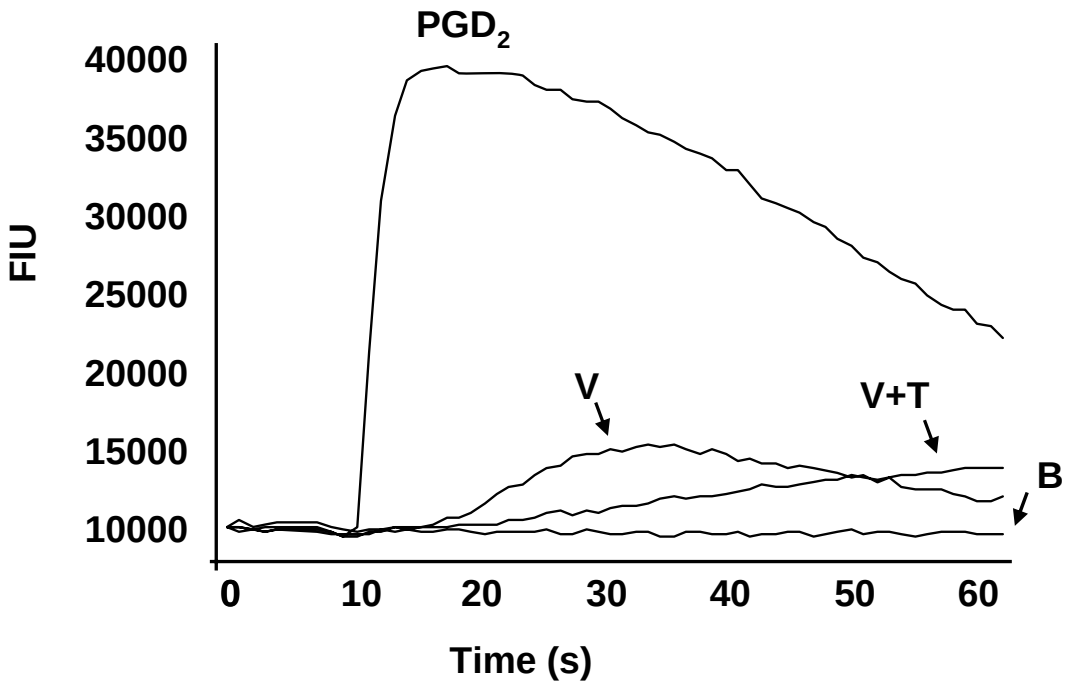

Figure 11

Panel A

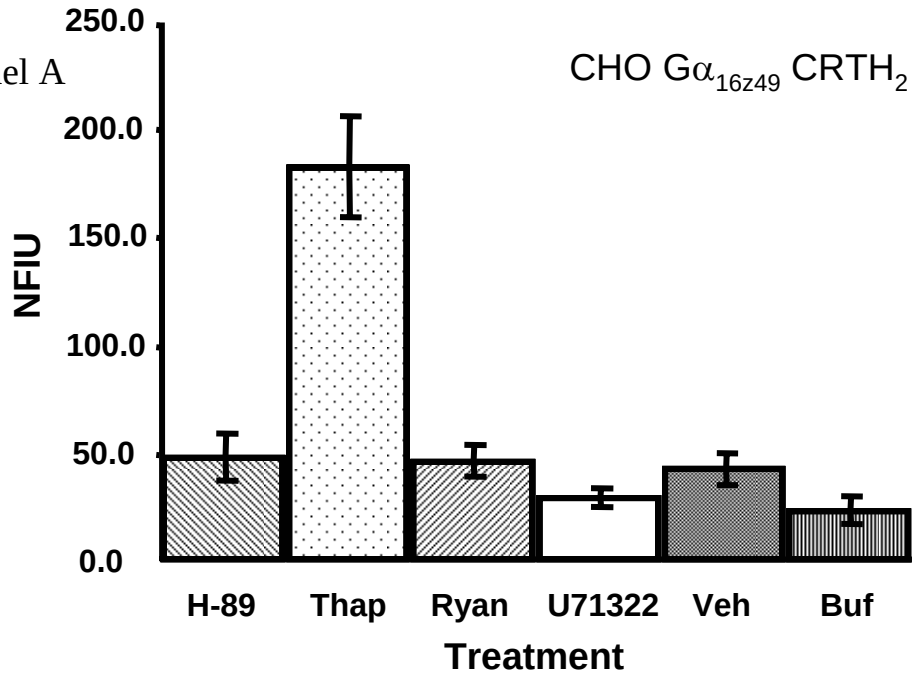

Panel B

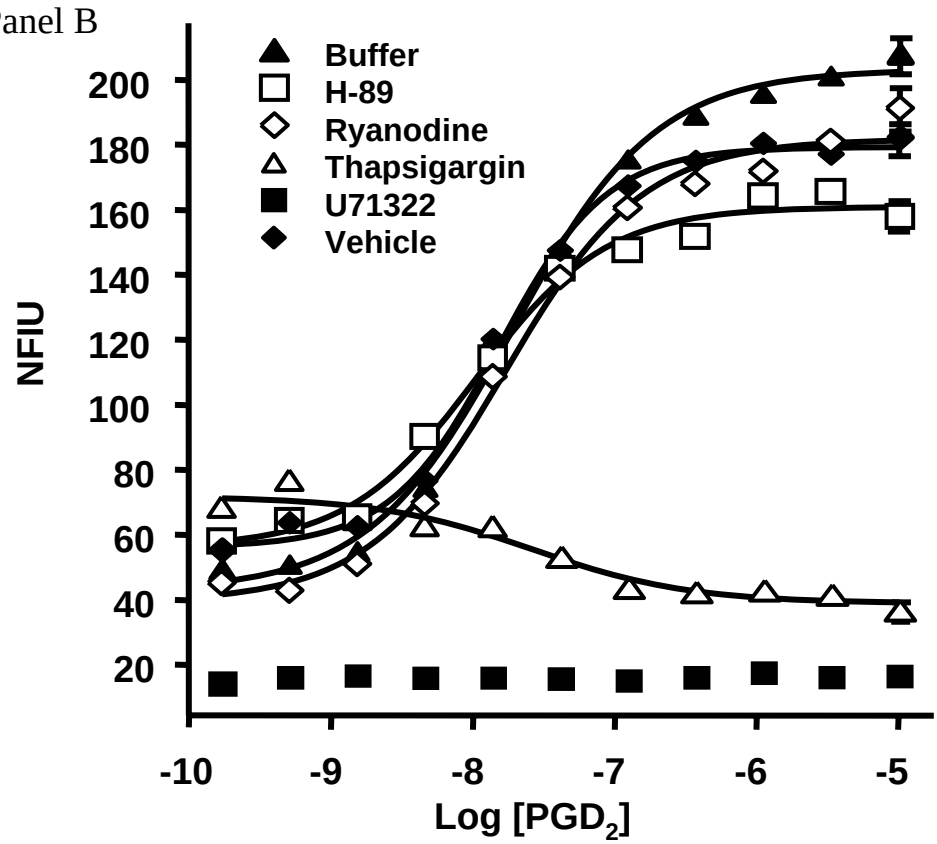

Figure 12

Panel A

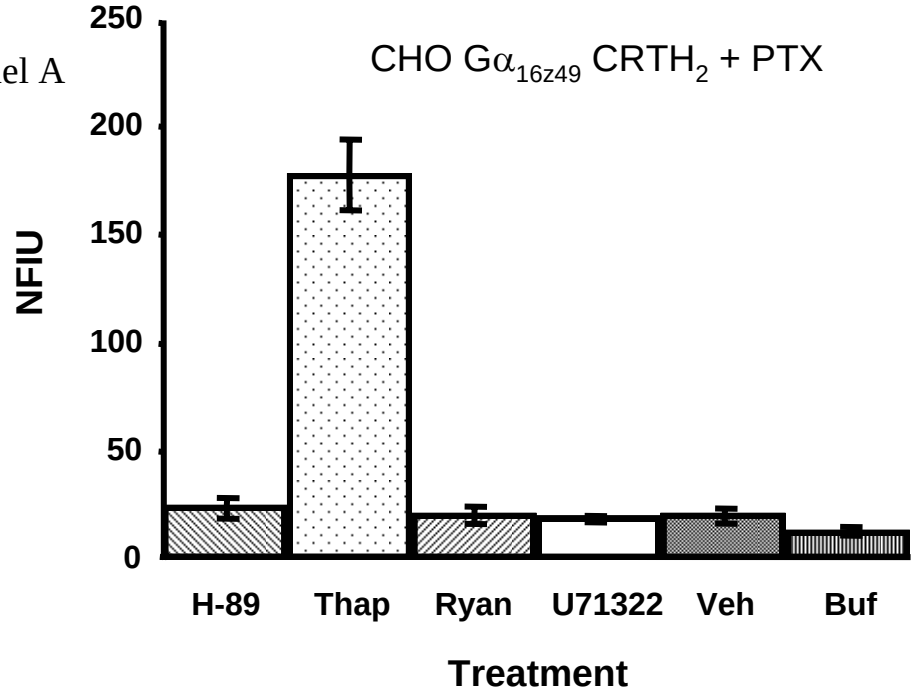

Panel B

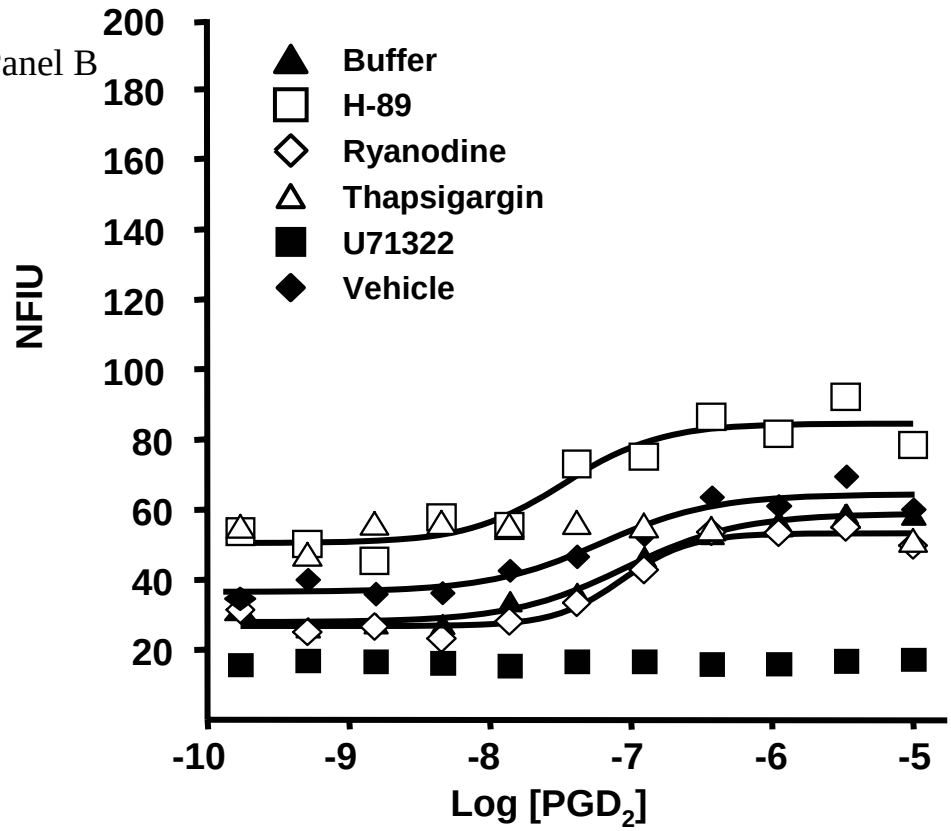

Figure 13.

Panel A

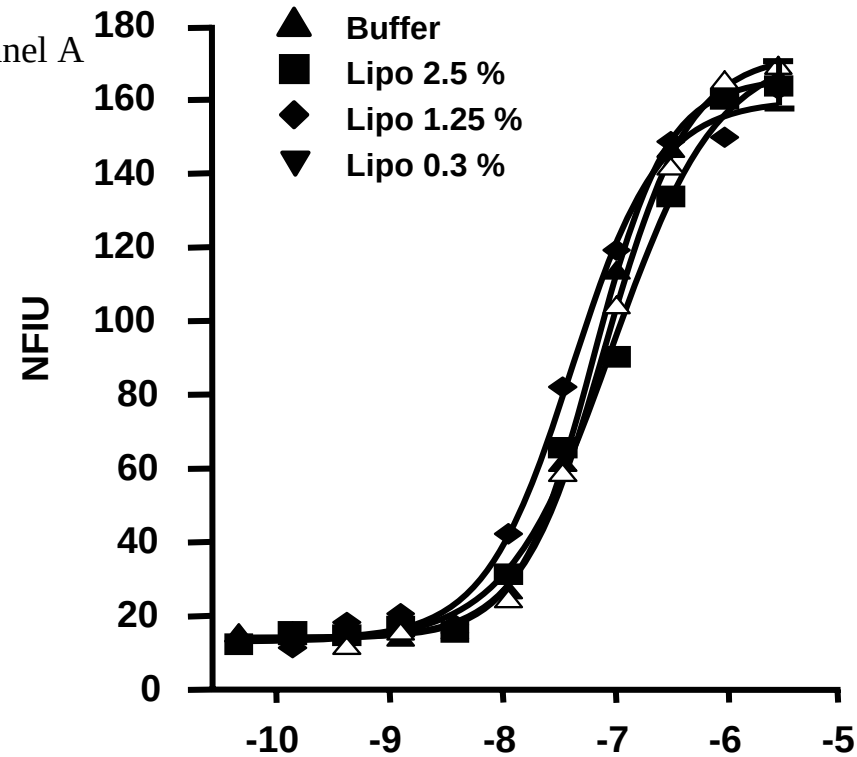

Panel B

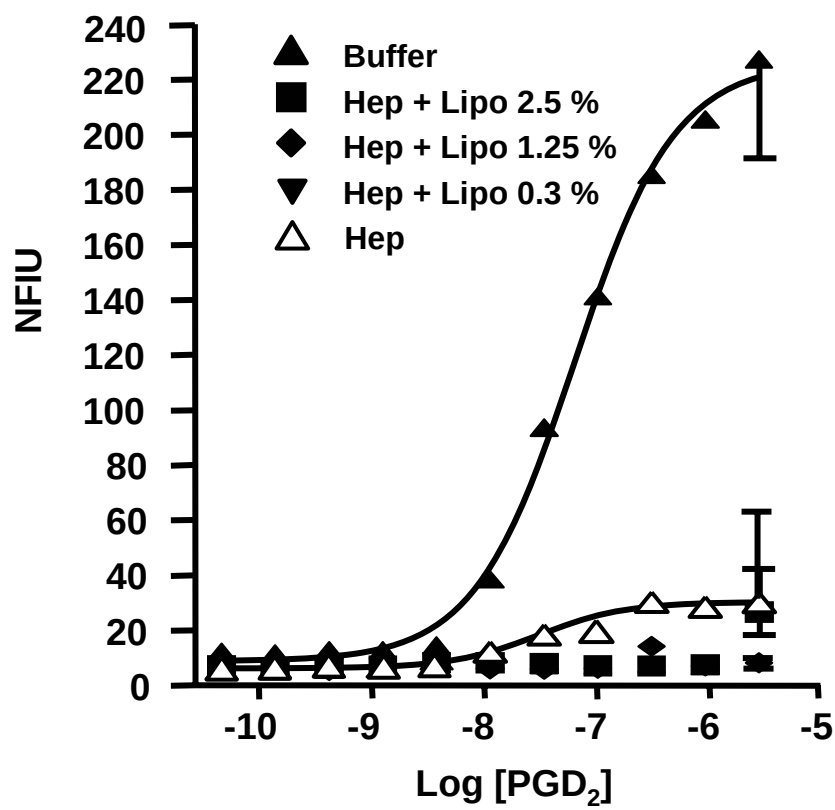

Figure 14.

Panel A

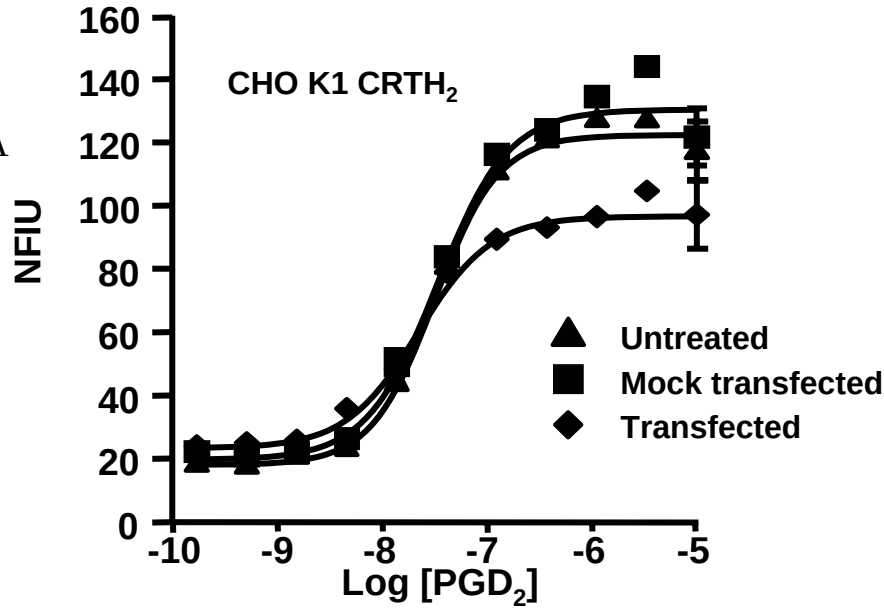

Panel B

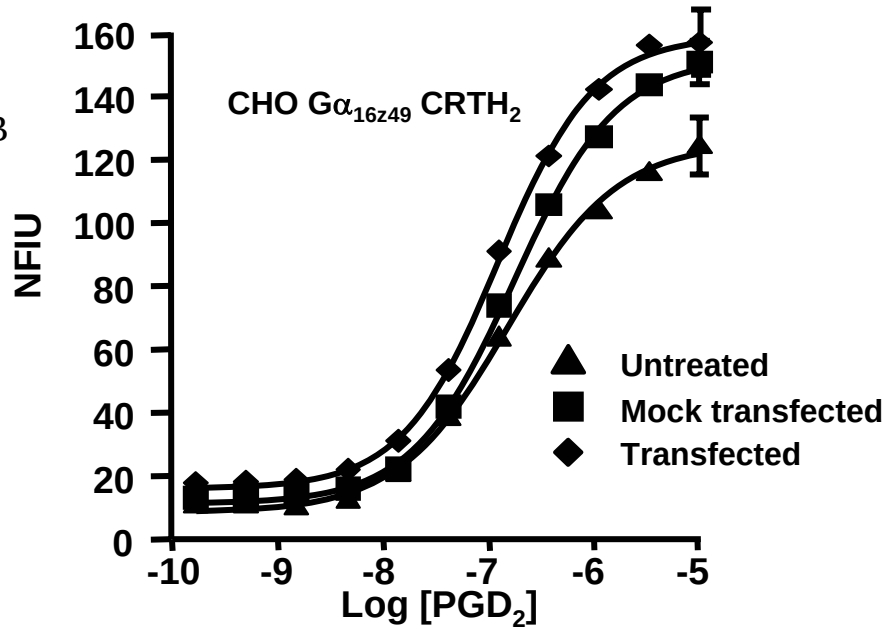

Panel C

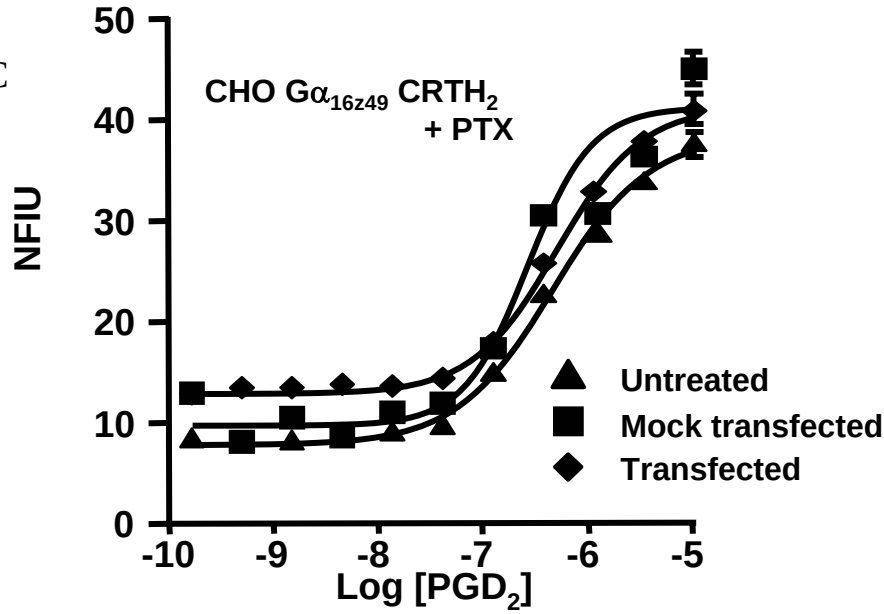

Figure 15.

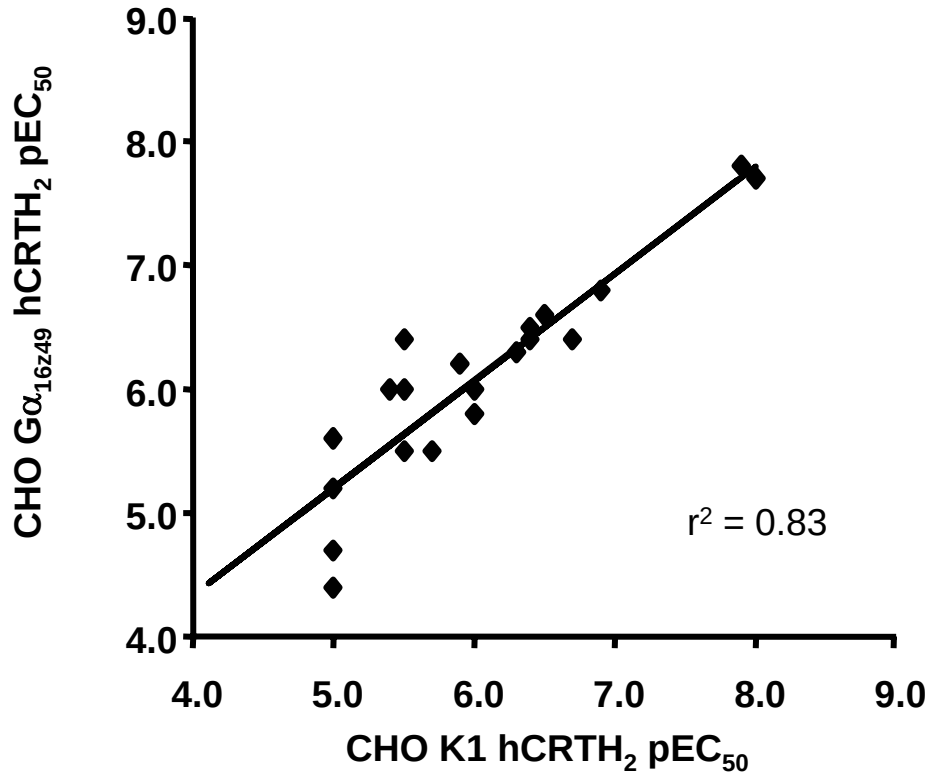
9.0
8.0
7.0
6.0
5.0
4.0
CHO Gα16z49 hCRTH2 pEC50
r2 = 0.83
4.0
5.0
6.0
7.0
8.0
9.0
CHO K1 hCRTH2 pEC50

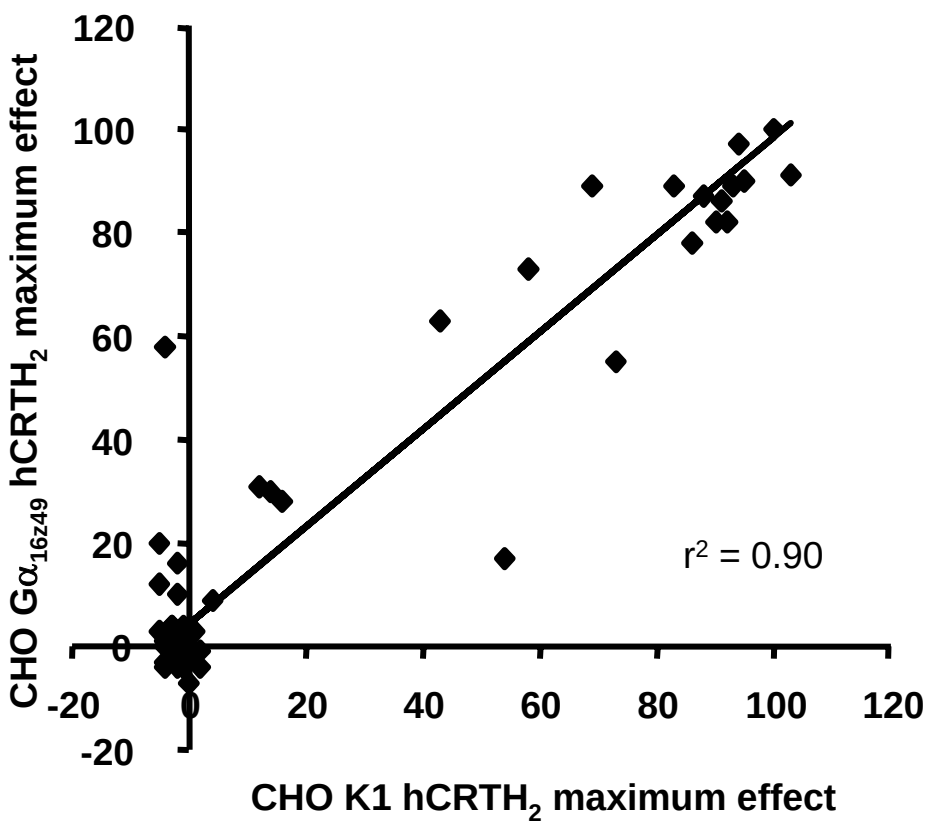
120
100
80
60
40
20
0
-20
CHO Gα16z49 hCRTH2 maximum effect
r2 = 0.90
-20
0
20
40
60
80
100
120
CHO K1 hCRTH2 maximum effect

Figure 16.

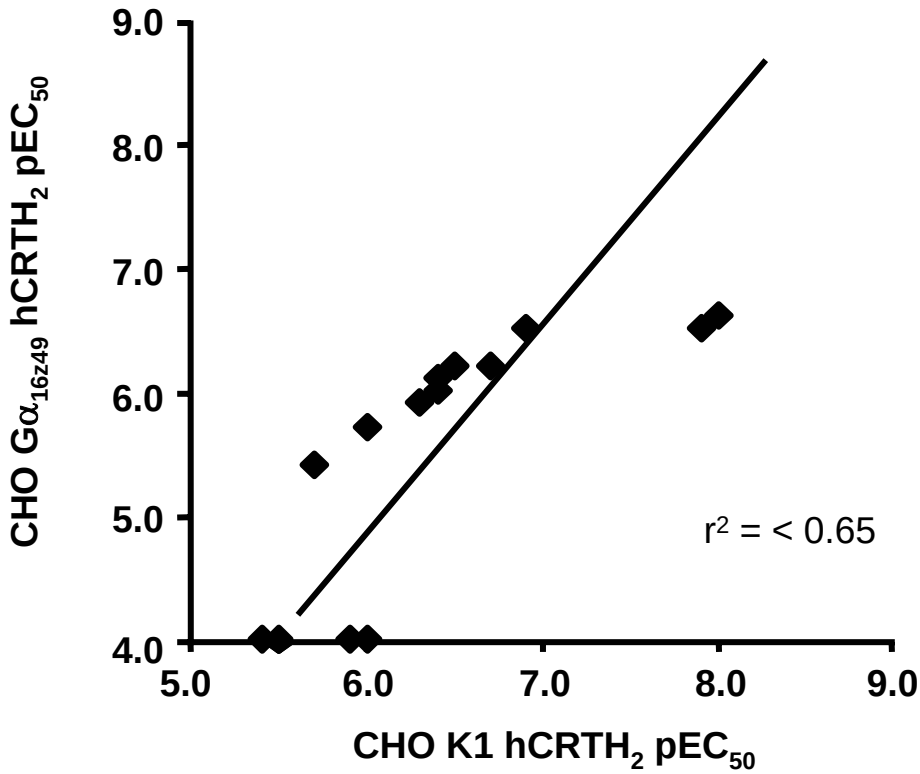
9.0
8.0
7.0
6.0
5.0
4.0
5.0
6.0
7.0
8.0
9.0
CHO Gα16z49 hCRTH2 pEC50
CHO K1 hCRTH2 pEC50
r2 = < 0.65

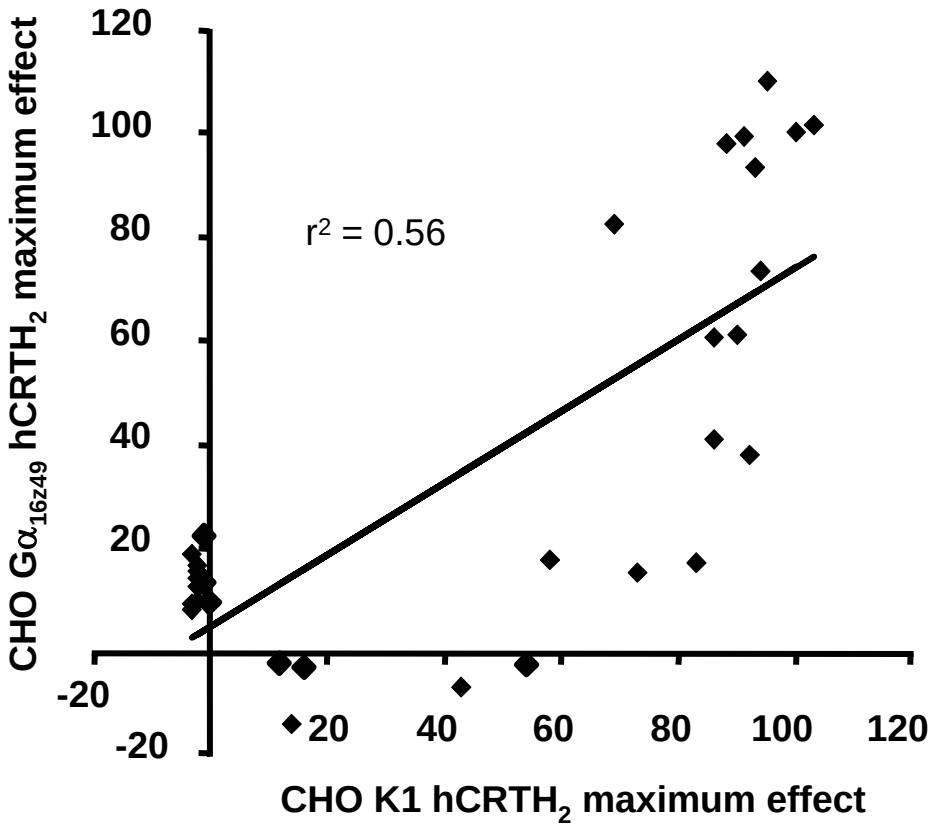
120
100
80
60
40
20
-20
-20
20
40
60
80
100
120
CHO Gα16z49 hCRTH2 maximum effect
CHO K1 hCRTH2 maximum effect
r2 = 0.56

Figure 17.

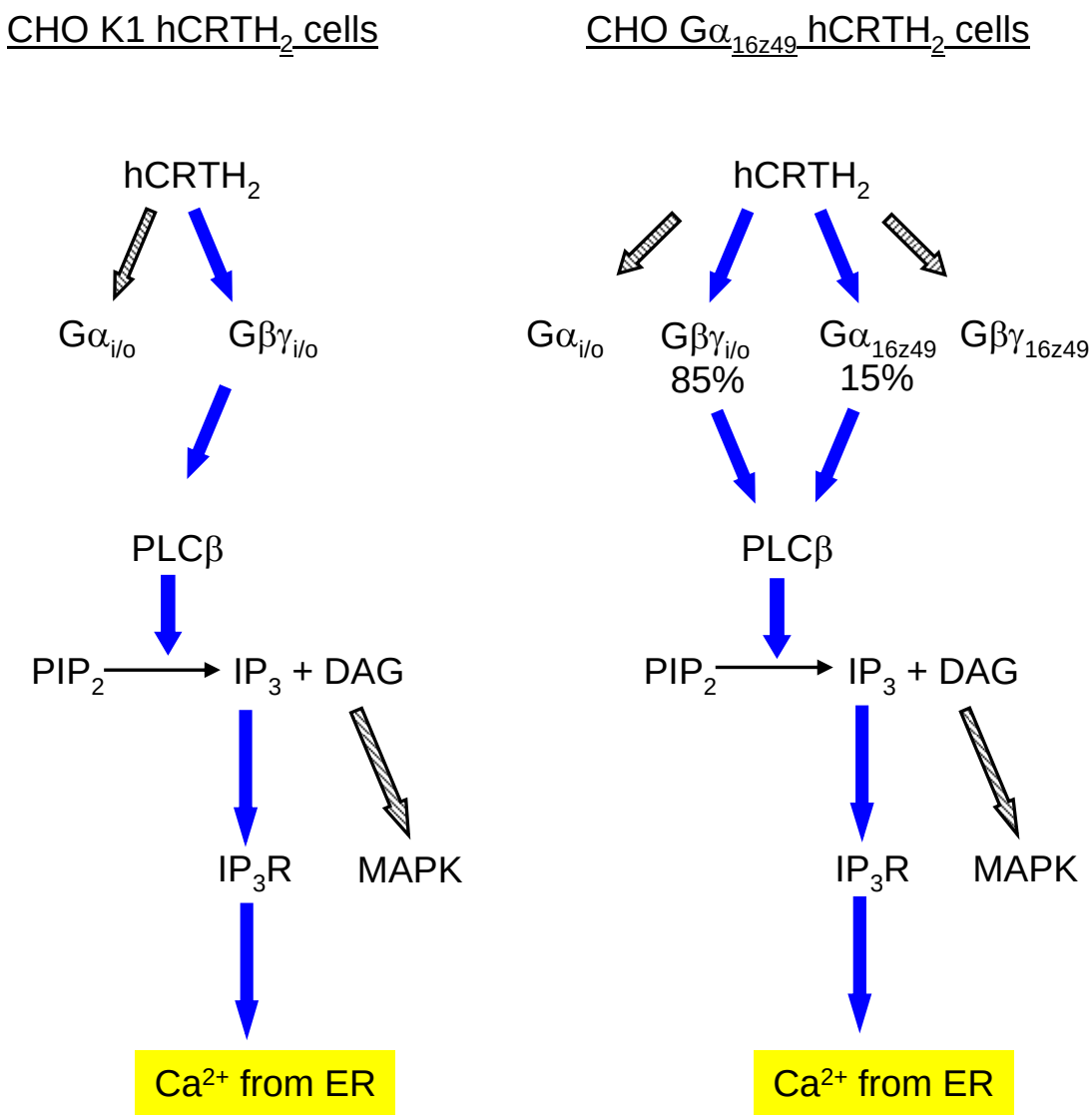
CHO K1 hCRTH2 cells
hCRTH2
Gαi/o
Gβγi/o
PLCβ
PIP2
IP3 + DAG
IP3R
MAPK
Ca2+ from ER
CHO Gα16z49 hCRTH2 cells
hCRTH2
Gαi/o
Gβγi/o
85%
Gα16z49
15%
Gβγ16z49
PLCβ
PIP2
IP3 + DAG
IP3R
MAPK
Ca2+ from ER

Figure 18.

CHO $G\alpha_{16z49}$ $hCRTH_2$ No PTX

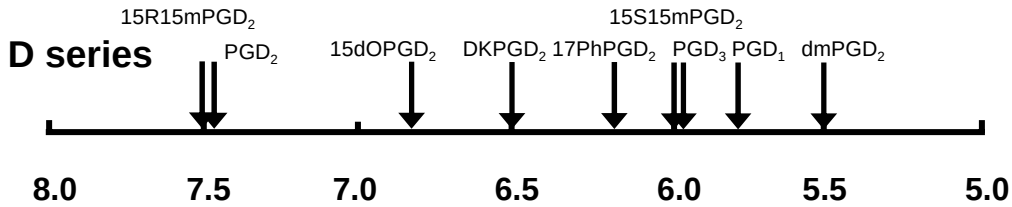

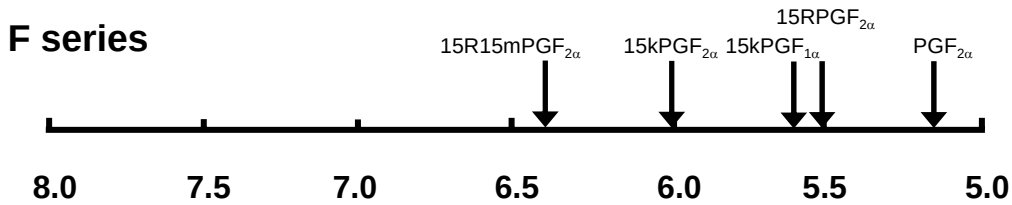

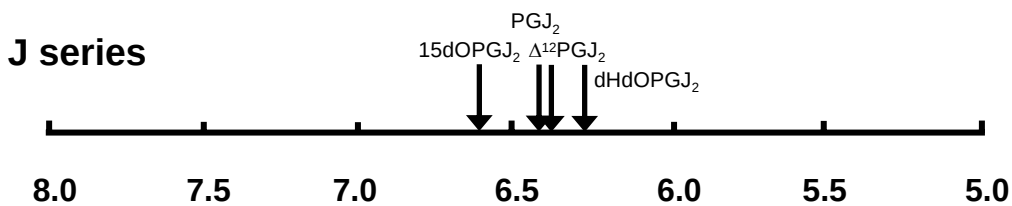

CHO K1 $hCRTH_2$

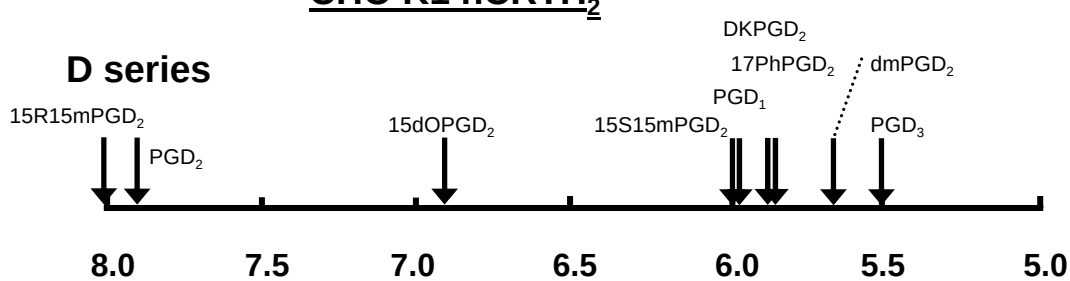

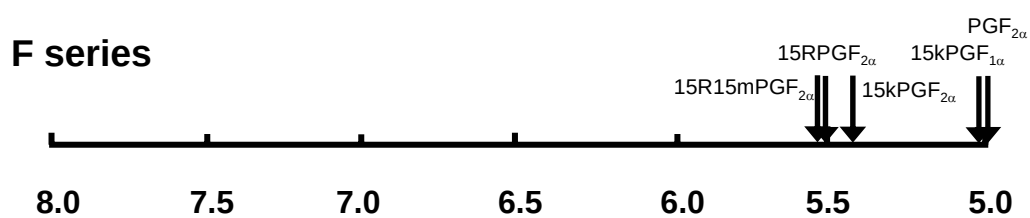

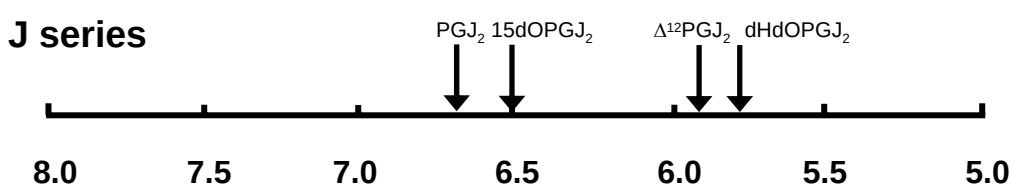

Figure 19.

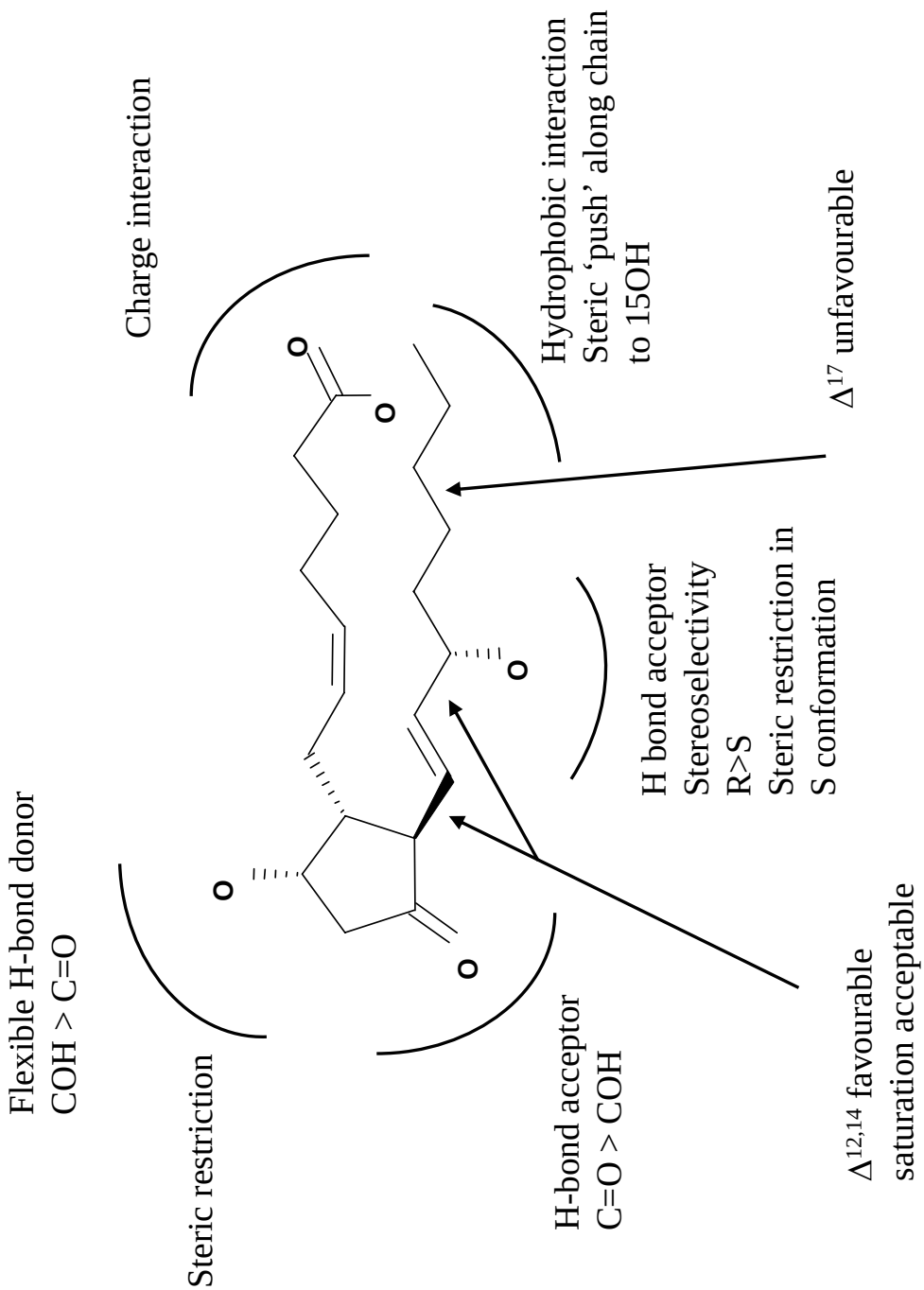
Flexible H-bond donor
COH > C=O
Charge interaction
Steric restriction
H-bond acceptor
C=O > COH
Hydrophobic interaction
Steric 'push' along chain
to 15OH
H bond acceptor
Stereoselectivity
R>S
Steric restriction in
S conformation
Δ^{17} unfavourable
$\Delta^{12,14}$ favourable
saturation acceptable

Figure 20. **CHO $G\alpha_{16z49}$ $hCRTH_2$ + PTX**

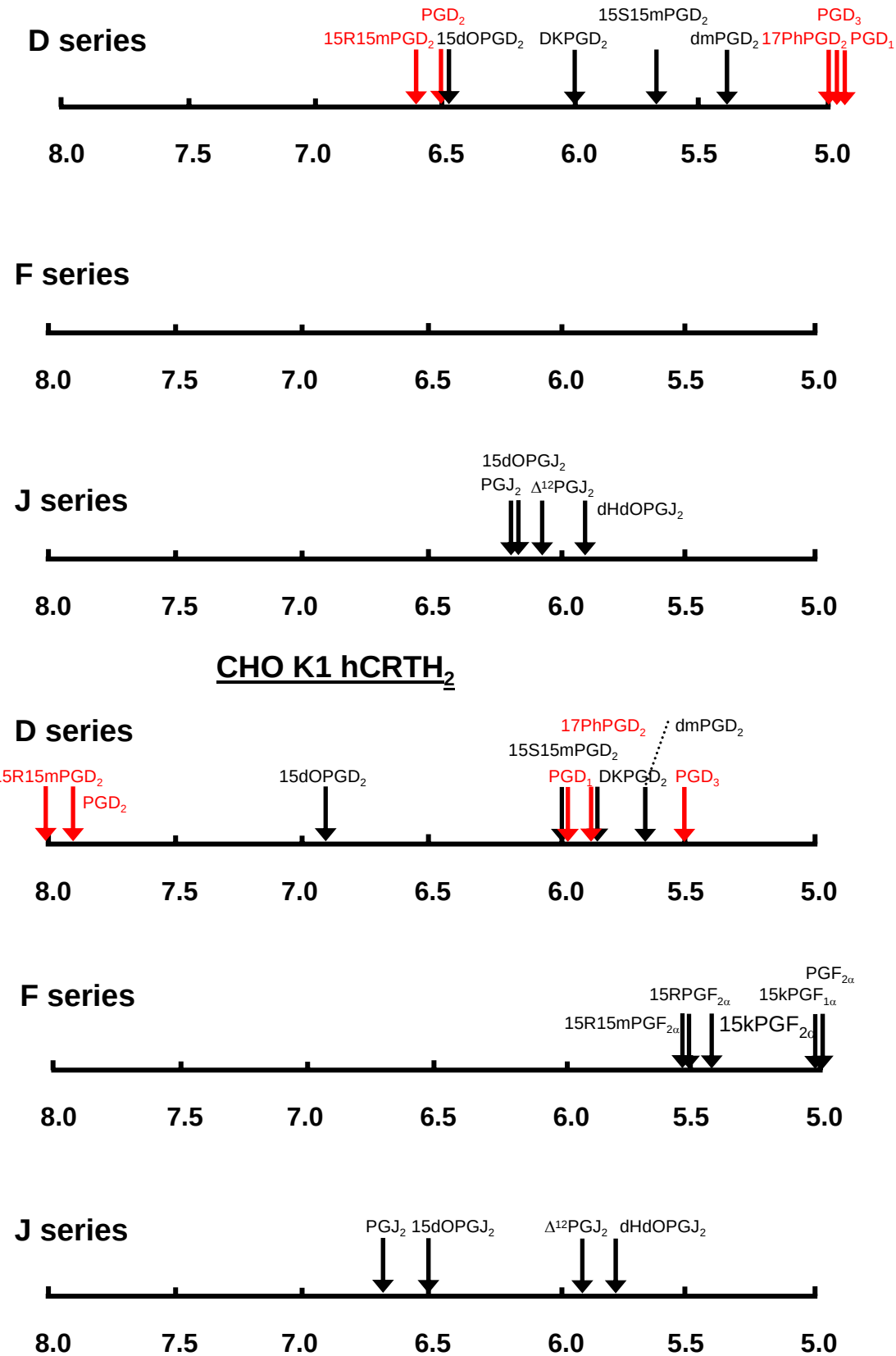

Figure 21.

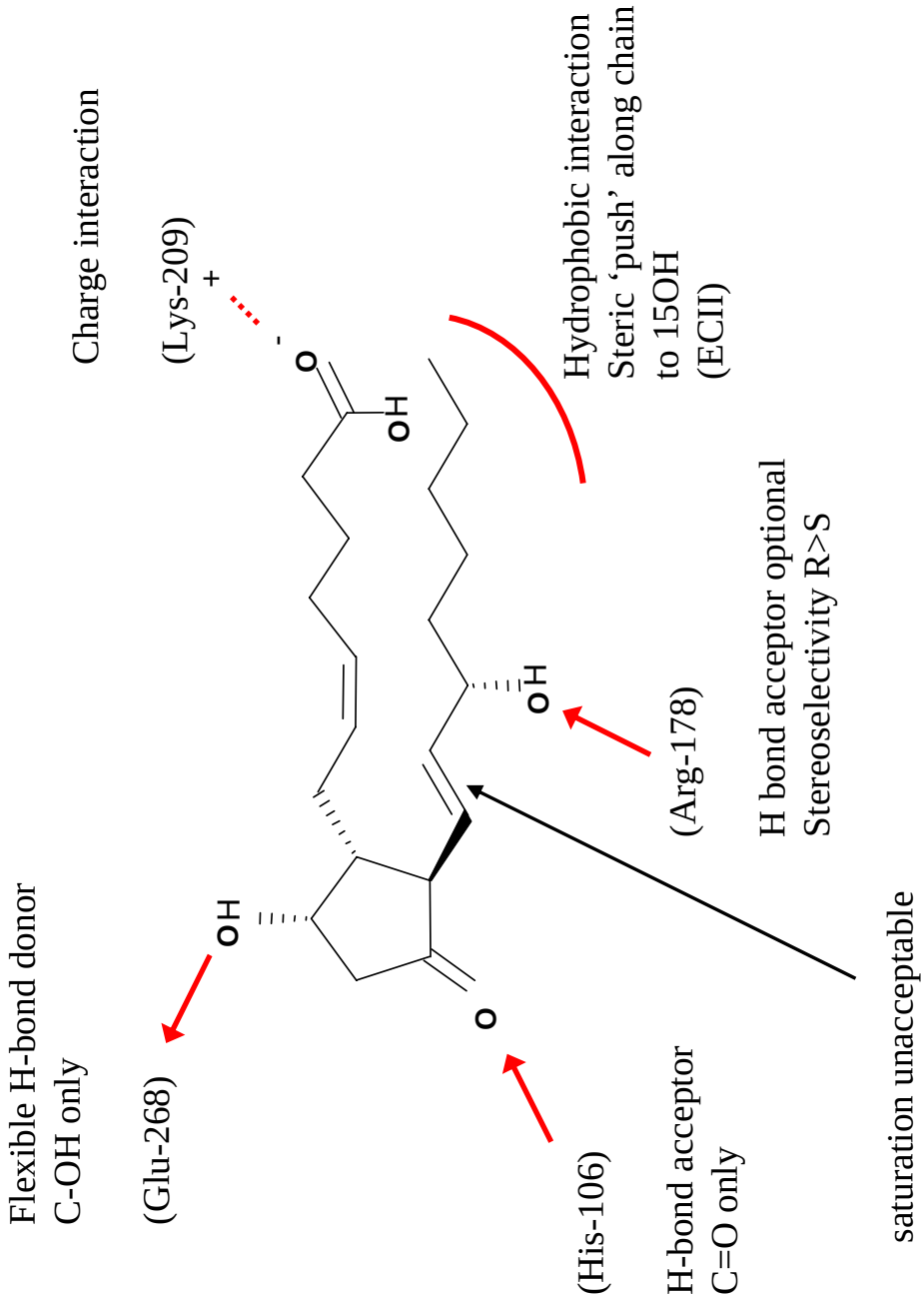
Charge interaction
(Lys-209)
+
-
O
OH
Hydrophobic interaction
Steric 'push' along chain
to 15OH
(ECII)
OH
(Arg-178)
H bond acceptor optional
Stereoselectivity R>S
Flexible H-bond donor
C-OH only
(Glu-268)
OH
O
(His-106)
H-bond acceptor
C=O only
saturation unacceptable

Chapter 5:

Agonist stimulus trafficking by human prostanoid $CRTH_2$ (DP_2) receptors coupled through $G\alpha_{i/o}$ G-protein subunits to accumulation of [^{35}S]-GTPγS and through either $G\alpha_{16z49}$ or $G\beta\gamma_{i/o}$ subunits to calcium mobilisation.

5.1 Summary:

In chapter 4, data strongly indicative of agonist stimulus trafficking by human prostanoid $CRTH_2$ receptors coupled to calcium mobilisation either through $G\beta\gamma_{i/o}$ or $G\alpha_{16z49}$ was shown. The equivalence of receptor : G-protein stoichiometry in the cell lines used was not demonstrated. Here, I extend these observations to study the agonist pharmacology of responses mediated by $G\alpha_{i/o}$ using a [^{35}S]-GTPγS accumulation assay. In this way, I aim to study responses mediated by the Gα and Gβγ subunits of the same G-protein.

Prostaglandin D_2 (PGD_2) stimulated accumulation of [^{35}S]-GTPγS in CHO K1 $hCRTH_2$ cell membranes in a monophasic, concentration-dependent and pertussis toxin-sensitive manner (pEC_{50} 8.1 ± 0.03, slope 1.3 ± 0.09; n = 12). CHO K1 host cell membranes were devoid of responses. Prostanoid $CRTH_2$ receptor pharmacology was demonstrated by sensitivity to the agonists 15 R 15 methyl PGD_2 (all n = 3; pEC_{50} 8.1 ± 0.1), PGJ_2 (7.6 ± 0.1), 13,14 dihydro 15 keto PGD_2 (7.5 ± 0.07), indomethacin (6.4 ± 0.06), & $PGF_{2\alpha}$ (5.5 ± 0.3) and to the putative $CRTH_2$ receptor antagonists AH23848B and GW853481X (pK_b 6.9 ± 0.1 & 7.5 ± 0.1, respectively).

A panel of 34 other prostanoid molecules were also tested for agonism. Comparison with calcium mobilisation data generated through $G\beta\gamma_{i/o}$ subunit coupling in the same cell line revealed several examples of potency and relative activity rank order reversals indicative of stimulus trafficking. The greatest determinant of prostanoid agonist sensitivity to coupling partner was found to be the cyclopentyl head group. Agonist sensitivity varied in the order: F series > D series > J series. Signals transduced in response to each series appeared to be trafficked relative to the other series. Three molecules were identified as being most sensitive to changes in the coupling partner ([^{35}S]-GTPγS RP, RA; calcium RP, RA): 13,14 dihydro 15 keto PGD_2 (4.0, 1.0; 32, 0.9), 15 deoxy $\Delta^{12,14}$ PGJ_2 (3.2, 1.1; 25, 0.9) & indomethacin (50, 1.1; 10, 0.8). Indomethacin showed a marked preference for coupling through Gβγ subunits (based on potency) but higher relative activity at Gα subunits.

In contrast with this, comparison of [^{35}S] accumulation data with calcium mobilisation data generated through $G\alpha_{16z49}$ subunits in PTX-treated CHO $G\alpha_{16z49}$ $hCRTH_2$ cells showed equivalence of potency and relative activity rank orders with

differences in absolute values commensurate with altered signal amplification. This suggests that chimeric $G\alpha_{16z49}$ G-proteins are an appropriate surrogate for endogenous $G\alpha$ mediated coupling of human prostanoid $CRTH_2$ receptors but not of endogenous $G\beta\gamma$ mediated coupling. Validation of chimera-based screening strategies should therefore make use of a range of physiologically relevant assay readouts for comparative studies.

5.2 Introduction:

Drug efficacy is the ability of certain molecules to communicate chemical information resulting in activation of receptors and the transduction of that information to intracellular effectors. It is the sum of multiple and diverse intracellular events triggered by receptor activation that determines the overall physiological response to an agonist. What we observe a receptor doing in response to drug challenge we now appreciate to be dominated by the environment in which the receptor resides when we study it. As such, receptor pharmacology is phenotypically determined (Kenakin, 2002d) and dependent upon the coupling partners available to a receptor in any given system.

Pleiotropy in receptor coupling was first conceived of in terms of promiscuity of receptor coupling to G-proteins (reviewed in Kenakin, 1996) with the observed pharmacology being the resultant effect of two (or, presumably, more) G-protein transduced pathways. Many receptors have now been observed that activate certain response pathways in preference to others, though both may be available for coupling. This phenomenon, known as stimulus trafficking, is supported by a huge body of evidence (reviewed in Kenakin, 2003, *Introduction*, and Urban, *et al*., 2007) and provides scope for two previously unrecognized drug behaviours: collateral efficacy (simultaneous and differential activation of multiple intracellular pathways by a single agonist-receptor pair) and permissive antagonism (differential inhibition of multiple activation pathways by an antagonist; Kenakin, 2005). The hallmarks of stimulus trafficking behaviour are potency order reversals and / or efficacy (relative activity) order reversals, where adequate control of potential confounding factors has been achieved (Kenakin, 1995b; Clarke & Bond, 1997; Kenakin, 2003). In particular, care must be taken to exclude the impact of simple changes in the strength of receptor-effector coupling which can have differential effects on affinity- and efficacy- driven agonists (exemplified in Kenakin, 1999).

In Chapters 3 and 4 I put forward evidence supporting the notion that stimulus trafficking of responses through $G\beta\gamma_{i/o}$ and $G\alpha_{16z49}$ G-proteins coupled to human prostanoid $CRTH_2$ receptors was a real phenomenon. However, the comparison made was between an endogenously coupling system ($G\beta\gamma_{i/o}$) and a highly exotic genetically engineered recombinant coupling system ($G\alpha_{16z49}$) under conditions of non-equivalent receptor : G-protein (R:G) stoichiometry. Nonetheless, ‘strength of signal’ based

changes in agonist pharmacology could be distinguished from trafficked responses. In order to extend these observations, I have sought to detect agonist stimulus trafficking mediated by $G\alpha$ and $G\beta\gamma$ subunits of the same G-protein coupled to human prostanoid $CRTH_2$ receptors in the same host cell type, thereby establishing *a priori* the equivalence of R:G stoichiometry and the cellular environment in which the biological systems under comparison were synthesised. In this chapter, I have developed a 384-well format [^{35}S]-GTPγS binding assay for the measurement of $G\alpha_{i/o}$ activation and compared agonist and antagonist SAR data with that obtained through calcium mobilisation stimulated by $G\beta\gamma_{i/o}$ and $G\alpha_{16z49}$ G-proteins.

5.3 Results:

5.3.1 Selection of CHO K1 hCRTH$_2$ suspension culture clone

Dilution clones of adherent CHO K1 cells transfected with human prostanoid CRTH$_2$ receptors were selected initially with neomycin (1 mg ml^{-1}) and flurbiprofen (10 μM). This was subsequently reduced to 0.5 mg ml^{-1} neomycin to promote cell growth upon conversion to suspension culture at passage 7 (P7). Under these conditions (and flurbiprofen 50 μM) only two clones grew sufficiently quickly to warrant further examination: clones 5 and 15. In an unoptimised 96-well plate-based [^{35}S]-guanosine-5'-O-(3-thio) triphosphate (GTPγS) binding assay using wheatgerm agglutinin coated polystyrene beads in the absence of guanosine diphosphate (GDP), 1 nM [^{35}S]-GTPγS, read after 210 mins and using a small-scale membrane batch produced specifically for this assay, both clones produced concentration-related accumulation of GTPγS in response to prostaglandin D$_2$ (PGD$_2$; Figure 1). Concentration / effect (E/[A]) curve parameters were equivalent for both clones (clone 5 / clone 15: pEC$_{50}$ 6.3 / 6.2; maximum effect 147 / 147 cpm; slope (n_H) 1.0 / 2.0; non statistically significant). Radioligand binding in membranes from un-transfected CHO K1 cells was unaffected by exposure to PGD$_2$. Clone 15 was chosen for all further work based on its superior growth characteristics.

5.3.2 Determination of protein concentration

Protein concentration of CHO K1 hCRTH$_2$ cell membranes was 5.9 ± 0.3 mg ml^{-1}.

5.3.3 Development of assay protocol.

A range of assay conditions were investigated (Table 1). The optimum set of conditions were found to be: membranes 10 μg well^{-1} (equivalent to 10 μl of suspension); LEADseeker beads 125 mg well^{-1} (equivalent to 5 μl of suspension); [^{35}S]-GTPγS 1.2 nM (delivered in 25 μl); GDP 30 μM (added to bead membrane mixture and radioligand to give 30 μM final assay concentration; Figure 2); saponin 150 μg ml^{-1} (to facilitate solubilisation of membranes and passage of compounds into membrane vesicles); incubation time 60 min; read within 120 min. [GDP] dependency was constant irrespective of radioligand concentration and incubation time. In some cases, the option allowing for the most economical use of reagents was chosen.

5.3.4 Effect of standard prostanoid receptor agonists and antagonists.

Under optimised assay conditions PGD_2 was an agonist with potency (pEC_{50}; n = 12) 8.1 ± 0.03, slope 1.3 ± 0.09, and E_{max} 385 ± 4 cpm (Figure 3). PGD_2 E/[A] curves were monophasic under all conditions studied. $PGF_{2\alpha}$ and indomethacin were also agonists (pEC_{50}, E_{max} (cf. PGD_2 = 100 %; n = 3): 5.5 ± 0.3, 48 ± 8 %; 6.4 ± 0.03, 113 ± 8 %, respectively) but PGE_2 was without significant effect. The putative prostanoid $CRTH_2$ receptor antagonists AH23848B and GW853481X produced parallel rightward displacement of PGD_2 E/[A] curves (Figure 4 Panel A & figure 5, respectively) giving rise to pK_b estimates of 6.9 ± 0.1 and 7.5 ± 0.1, respectively (n = 3). In addition, AH23848B antagonised PGD_2 EC_{80} (5nM) responses resulting in > 100 % inhibition and a pIC_{50} of 6.2 ± 0.07 (Figure 4, Panel B; n = 3).

5.3.5 Pertussis toxin treatment of CHO K1 hCRTH$_2$ membranes

PGD_2 stimulated accumulation of [^{35}S]-GTPγS in untreated membranes, pEC_{50} 7.6 ± 0.3, E_{max} 394 ± 40 cpm. The potency and E_{max} of PGD_2 in sham- and PTX- treated membranes was reduced (pEC_{50}, E_{max}; sham, PTX treated: 7.2 ± 0.4, 131 ± 40; 6.9 ± 0.2, 64 ± 28; all $P < 0.05$ cf. untreated controls; Figure 6). PTX therefore inhibited PGD_2 responses by 56 % ($P < 0.05$ cf. sham-treated). Data was not corrected for loss of either membranes themselves nor for loss of accessory proteins from membranes during treatment.

5.3.6 Agonist 'fingerprinting' of hCRTH$_2$ receptor

A panel of 34 prostanoid molecules representing a subset of the compounds examined in Chapters 3 and 4, were screened for agonist activity in membranes derived from CHO K1 $hCRTH_2$ cells (Table 2). No agonist effect was shown by 50 % of the compounds. The following rank order of agonist potency was obtained (relative potency [RP cf. PGD_2 = 1.0], relative activity [RA cf. PGD_2 = 1.0]; full agonists shown in bold type, partial agonists in normal type): **15 R 15 methyl PGD_2 (1.0, 0.9)** = **PGD_2** > **PGJ_2 (3, 0.9) = 15 deoxy $\Delta^{12,14}$ PGJ_2 (3, 1.1)** > **13,14 dihydro 15 keto PGD_2 (4, 1.0)** > **9,10 dihydro 15 deoxy $\Delta^{12,14}$ PGJ_2 (6, 1.1)** > **15 S 15 methyl PGD_2 (16, 1.0)** > **indomethacin (50, 1.1)** > 15 R $PGF_{2\alpha}$ (79, 0.4) = **17 phenyl PGD_2 (79, 1.1)** > 15 keto $PGF_{2\alpha}$ (100, 0.6) > 13,14 dihydro 15 keto $PGF_{2\alpha}$ (126, 0.4) > $PGF_{2\alpha}$ (398, 0.5) > 11

deoxy 11 methylene PGD_2 (1995, 0.7) > $PGF_{1\alpha}$ = PGI_3 (both max effect = 7 %) >> 15 keto $PGF_{1\alpha}$ = BW245C (=NSE).

5.3.7 Data Tables

Follow on next page.

Table 1. Determination of assay conditions and parameters. Data are: E/[A] curves - mean ± sem of four curves; bead / membrane matrix data - mean ± sem of nine data points; both data determined on 2 assay plates in a single experimental occasion.

Condition	Min	Max	pEC_{50}	Z´	Other conditions
[GDP] 0 μM	250 ± 1	321 ± 1	8.1 ± 0.02	0.93	Membranes 5 μg $well^{-1}$
0.1 μM	263 ± 2	329 ± 2	8.6 ± 0.02	0.71	Beads 125 μg $well^{-1}$
0.3 μM	242 ± 1	318 ± 2	8.5 ± 0.06	0.75	[[^{35}S]-GTPγS] 0.3 nM
1 μM	234 ± 3	298 ± 5	9.1 ± 0.2	0.36	incubation time 2 hrs
3 μM	222 ± 5	288 ± 0.06	8.7 ± 0.06	0.64	
10 μM	151 ± 5	261 ± 3	8.7 ± 0.06	0.6	
30 μM	141 ± 3	232 ± 2	8.4 ± 0.2	0.67	
100 μM	134 ± 1	187 ± 4	8.1 ± 0.3	0.48	
[Membrane] 2.5 μg $well^{-1}$	135 ± 2	148 ± 2		-1.5	[[^{35}S]-GTPγS] 0.3 nM
5 μg $well^{-1}$	137 ± 1	164 ± 2		-0.1	incubation time 2 hrs
10 μg $well^{-1}$	151 ± 4	195 ± 3		-0.2	Bead 62.5 μg $well^{-1}$ [GDP] 30 μM
20 μg $well^{-1}$	165 ± 2	230 ± 5		0.49	
2.5 μg $well^{-1}$	181 ± 2	192 ± 2		-2.3	
5 μg $well^{-1}$	184 ± 1	204 ± 3		-0.65	Bead 125 μg $well^{-1}$
10 μg $well^{-1}$	199 ± 3	244 ± 4		-0.4	
20 μg $well^{-1}$	209 ± 2	292 ± 12		-0.08	

2.5 μg well^{-1}	228 ± 2	239 ± 2		-2	Bead 187 μg well^{-1}
5 μg well^{-1}	235 ± 1	252 ± 4		-1.47	Bead 187 μg well^{-1}
10 μg well^{-1}	242 ± 3	297 ± 5		-0.15	
20 μg well^{-1}	258 ± 4	343 ± 6		0.05	
2.5 μg well^{-1}	267 ± 3	275 ± 2		-3.89	Bead 250 μg well^{-1}
5 μg well^{-1}	272 ± 2	292 ± 1		-0.8	
10 μg well^{-1}	282 ± 3	335 ± 3		-0.02	
20 μg well^{-1}	279 ± 3	373 ± 9		-0.12	
[[^{35}S]-GTPγS] 0.3 nM	135 ± 4	191 ± 16	8.1 ± 0.1	-0.3	Membranes 10 μg well^{-1}
0.6 nM	198 ± 12	305 ± 13	8.5 ± 0.2	-0.2	Beads 125 μg well^{-1}
1.2 nM	328 ± 9	541 ± 9	8.3 ± 0.06	0.5	[GDP] 30 μM
2.4 nM	512 ± 15	863 ± 14	8.2 ± 0.1	0.6	incubation time 2 hrs
Incubation time 1 hr	228 ± 4	525 ± 7	8.1 ± 0.06	0.8	Membranes 10 μg well^{-1}
2 hr	337 ± 7	587 ± 8	8.3 ± 0.06	0.7	Beads 125 μg well^{-1}
3 hr	335 ± 8	496 ± 16	8.3 ± 0.1	0.2	[GDP] 30 μM
4 hr	291 ± 3	392 ± 21	8.2 ± 0.4	-0.3	[[^{35}S]-GTPγS] 1.2 nM
DMSO tolerance 0 %	147 ± 8	304 ± 14	6.8 ± 0.3	0.25	Membranes 10 μg well^{-1}
0.6 %	161 ± 10	370 ± 18	7.0 ± 0.1	0.3	Beads 125 μg well^{-1}
1.25 %	175 ± 8	361 ± 10	6.8 ± 0.2	0.5	[GDP] 30 μM; incubation time 2 hr
2.5 %	169 ± 14	351 ± 50	6.8 ± 0.06	-0.8	[[^{35}S]-GTPγS] 1.2 nM

Table 2. Pharmacology of prostanoid molecules in CHO K1 $hCRTH_2$ cell membranes without PTX treatment ([^{35}S]-GTPγS accumulation through $G\alpha_{i/o}$). RP: relative potency cf. PGD_2 (=1.0); RA: relative activity cf. PGD_2 (=1.0). Data are mean ± sem of three independent E/[A] curves generated in a single assay occasion. 15 S 15 methyl $PGF_{2\alpha}$, 11 dehydro TxB_2, 13,14 dihydro PGE_1, PGE_3, PGE_3, 20 hydroxy $PGF_{2\alpha}$, 13,14 dihydro $PGF_{1\alpha}$, 13,14 dihydro 15 keto PGE_2, PGE_1, PGD_1 alcohol, 15 R 15 methyl PGE_2, 13,14 dihydro 15 R PGE_1, 19 R hydroxy PGA_2, 15 R PGE_1, 19 R hydroxy $PGF_{2\alpha}$, 19 R hydroxy PGE_2 & 2,3 dinor 11β $PGF_{2\alpha}$. were without significant effect. † denotes single curve fit. Statistical comparison by ANOVA followed by Dunnett's comparison to PGD_2 data; * denotes $P < 0.05$.

Compound	pEC_{50}	slope	max	RP	RA
15 R 15 methyl PGD_2	8.1 ± 0.1	1.8 ± 0.4	87 ± 3	1.0	0.9
PGD_2	8.1 ± 0.06	1.3 ± 0.2	100	1.0	1.0
PGJ_2	7.6 ± 0.06	1.3 ± 0.1	92 ± 1	3.2	0.9
15 deoxy $\Delta^{12,14}$ PGJ_2	7.6 ± 0.1*	1.3 ± 0.06	113 ± 2	3.2	1.1
13,14 dihydro 15 keto PGD_2	7.5 ± 0.06*	0.9 ± 0.1	95 ± 1	4.0	1.0
9,10 dihydro 15 deoxy $\Delta^{12,14}$ PGJ_2	7.3 ± 0.06*	1.1 ± 0.1	112 ± 4	6.3	1.1
15 S 15 methyl PGD_2	6.9 ± 0.06*	1.1 ± 0.1	96 ± 2	16	1.0
Indomethacin	6.4 ± 0.02*	0.9 ± 0.1	113 ± 7	50	1.1
15 R $PGF_{2\alpha}$	6.3 ± 0.06*	1.0 ± 0.1	54 ± 4*	63	0.6
15 keto $PGF_{1\alpha}$	6.2 ± 0.2*	1.1 ± 0.1	37 ± 5*	79	0.4
17 phenyl PGD_2	6.2 ± 0.1*	1.2 ± 0.3	111 ± 8	79	1.1
15 keto $PGF_{2\alpha}$	6.1 ± 0.06*	1.5 ± 0.3	62 ± 5*	100	0.6

13,14 dihydro 15 keto $PGF_{2\alpha}$	6.0 ± 0.1*	1.4 ± 0.2	39 ± 4*	126	0.4
$PGF_{2\alpha}$	5.5 ± 0.2*	0.8 ± 0.2	48 ± 6*	398	0.5
11 deoxy 11 methylene PGD_2	4.8†*	0.8†	74 ± 13	1995	0.7
$PGF_{1\alpha}$			7 ± 8		
PGI_3			7 ± 2		

5.4 Discussion:

The assay developed here is a traditional, total Gα G-protein activation assay and does not distinguish between Gα subunit types as an antibody capture assay would. Using antibody capture techniques Newman-Tancredi, *et al*. (2003) have demonstrated that human serotonergic 5-HT_{1B} receptors expressed in CHO-K1 cells couple sequentially to different Gα subunit types as 5-HT concentrations increase: low concentrations recruit $G\alpha_{i3}$ whilst higher concentrations appear to stimulate a switch to a different subunit type presumed to be $G\alpha_{i2}$ since CHO cells do not express $G\alpha_{i1}$. The initiating observation prompting investigation with antibody capture techniques was one of biphasic 5-HT E/[A] curves in a traditional [^{35}S]-GTPγS accumulation assay. In the data reported here, PGD_2 E/[A] curves are monophasic with slope (Hill coefficient) 1.3 though the four-fold agonist dilution series employed would tend to mask any fine detail in the curve shape. Interestingly, the data set includes agonists with slope as high as 1.8 (15 R 15 methyl PGD_2) and as low as 0.9 (13,14 dihydro 15 keto PGD_2). Hill coefficients of 1.0 are consistent with, but not proof of, simple uni-molecular interactions between ligand, receptor and intracellular effectors; deviations from unity suggest differences in recruitment of signalling molecules. Slopes greater than 1.0 may indicate co-operative activation of receptors and intracellular effectors resulting in signal amplification, for example recruitment of signalling molecules into signalsomes, or co-operative recruitment of multiple agonist binding sites. Values less than one may suggest restricted signal activation by, for example, activation of opposing signalling networks, agonist degradation or restricted access of the agonist to the receptor.

PGD_2 stimulated [^{35}S]-GTPγS accumulation and $[Ca^{2+}]_i$ mobilisation were both PTX-sensitive indicating the involvement of $G_{i/o}$ class G-proteins. Possible candidate subunits for the mediation of radiolabel accumulation are $G\alpha_{i2}$, α_{i3}, and α_o though data demonstrating the association of particular subtypes with prostanoid $CRTH_2$ receptors has not yet been published. PTX treatment only achieved a 56 % inhibition of radiolabel accumulation but since conditions for this experiment were not investigated the PTX sensitivity of the 44 % of signal remaining cannot be surmised. PTX is a toxin derived from the bacterium *Bordetella pertussis* which catalyses the NAD-dependent ADP-ribosylation of a cysteine residue 5 residues from the C-terminal end of $G\alpha_i$ & $G\alpha_o$ G-proteins (but not of $G\alpha_z$; Locht & Antoine, 1995; Offermans & Schulz, 1994). The toxin molecule is reduced and activated by glutathione in living cells (Kaslow &

Burns, 1992) but this must be achieved biochemically with dithiothreitol (DTT) for treatment of a membrane preparation. The DTT concentration used is a balance between the concentration required for enzyme activation and that which results in unacceptable damage to membrane proteins (Ribeiro-Neto & Rodbell, 1989; McKenzie, 1992; Ismailov, *et al*., 1994; Albrecht, *et al*., 2000; Kitts, *et al*., 2000). Furthermore, when added to cells, PTX treatment takes place over 18 - 24 hrs prior to assay whereas the membrane-based procedure takes place over 30 - 60 min. These considerations are likely to result in the observed less-than-total inhibition of $G\alpha_{i/o}$ using the membrane-based procedure and cast doubt on the basis for the signal remaining after PTX treatment: incomplete inhibition of $G\alpha_i$ / $G\alpha_o$, or non-$G\alpha_{i/o}$ coupling through e.g. $G\alpha_z$ or $G\alpha_{q/11}$? It would therefore have been preferable to treat cells before membrane preparation for these studies. However, given the total abolition of calcium signalling by PTX in CHO K1 $hCRTH_2$ cells it is possible to rule out prostanoid $CRTH_2$ receptor coupling to the PTX-insensitive $G\alpha_z$ and $G\alpha_{q/11}$ G-proteins. It therefore seems reasonable to assume that all radiolabel accumulation is due to activation of $G\alpha_{i2}$, $G\alpha_{i3}$ and / or $G\alpha_o$. In this respect it is tempting to speculate that the bell-shaped chemotactic response curves generated with Jurkat cells (Hirai, *et al*., 2002), eosinophils (Monneret, *et al*., 2003; Mimura, *et al*., 2005) and murine L1.2 pre-B cells (Sugimoto, *et al.*, 2005) are due to sequential recruitment of separate coupling partners. Other investigators have used similar reagent concentrations and incubation times to achieve similar degrees of inhibition (Ribeiro-Neto & Rodbell, 1989; McKenzie, 1992; Ismailov, *et al*., 1994; Albrecht, *et al*., 2000; Kitts, *et al*., 2000) but the amount of DTT (26 mM) in the final reaction mixture was higher than used elsewhere. Sham treated membranes demonstrated a large inhibition of PGD_2 stimulated radiolabel accumulation suggesting that conditions were too harsh, possibly as a result of the DTT concentration. The receptor does possess cysteine residues which would be reduced in the presence of DTT leading to disruption of protein folding and possible loss of function.

A further aspect of the data presented by Newman-Tancredi, *et al*. (2003) may also be reflected in the present data set. The high potency activation of $G\alpha_{i3}$ gave rise to a bell-shaped recruitment isotherm; in other words, either the activated receptor-$G\alpha_{i3}$-radiolabel complex was destabilised by higher concentrations of 5-HT, or its formation was suppressed. If the former, then candidate mechanisms might involve receptor desensitisation by membrane associated enzymes such as GRK's which may lie behind

the observed short duration of stable signal in the present assay. Other possibilities include time-dependent receptor dimerisation and loss of activating conformations, receptor digestion by proteases (note no protease inhibitors were included in the assay buffer) or simple chemical GTPγS hydrolysis though the speed of signal loss is not commensurate with this. Desensitisation mechanisms will be considered further in chapter 6.

The method developed here was biased towards the detection of low efficacy agonists through the use of a high [Na^+] (100 mM) and [GDP] (30 μM) which together served to prevent constitutive receptor activation, reduce basal [^{35}S]-GTPγS accumulation, and maximise the window for observation of agonism. The result of this is that the system was insensitive to inverse agonism and increased agonist relative activities (though PGD_2 potency was similar to that obtained in the CHO K1 $hCRTH_2$ calcium assay) creating the impression that coupling to $G\alpha_{i/o}$ was more sensitive to agonism than coupling via $G\beta\gamma_{i/o}$. Weaker coupling of receptors to Gβγ mediated pathways has been noted in a number of systems including rabbit common carotid artery (Akin, *et al.*, 2002), human serotonergic 5-HT_{1A} receptors (Pauwels & Colpaert, 2003; Wurch & Pauwels, 2003), cannabinoid CB2 receptors (Shoemaker, *et al.*, 2005) and rat neurotensin NTS1 receptors (Skrzydelski, *et al.*, 2003), all expressed in CHO cells. Of particular relevance here, it has also been suggested in studies of prostanoid $CRTH_2$ receptors using cAMP inhibition in HEK cells and calcium mobilisation in CHO cells also expressing recombinant $G\alpha_{15}$ (Sawyer, *et al.*, 2002). The results presented here are consistent with this finding but care should be exercised in drawing this conclusion: the relevance of the GTPγS-based coupling to more physiological settings such as inhibition of forskolin stimulated cAMP has not been determined here, and while data from such assays at 5-HT_{1A} receptors have been found to be in agreement (for example, Pauwels, *et al.*, 1993, 1997) stimulus trafficking has also been observed between these readouts, at least for adrenergic α_{2A} receptor antagonists (Pauwels, *et al.*, 2003).

The relationship between [^{35}S]-GTPγS - based and [Ca^{2+}]$_i$ - based agonist pharmacology is interesting. Calcium mobilisation data obtained using CHO $G\alpha_{16z49}$ $hCRTH_2$ cells ($G\alpha_{16z49}$ mediated activation of PLCβ/γ in whole CHO $G\alpha_{16z49}$ $hCRTH_2$ cells) produced a rank order of potency and relative activity that was identical to that obtained in the [^{35}S]-GTPγS accumulation assay ($G\alpha_{i/o}$ activation in membranes of CHO K1 $hCRTH_2$ cells). Absolute potency and relative activity values were lower in the calcium assay in

a manner consistent with 'strength of signal' based changes of transduction. As noted in chapter 4, the low potency of agonists acting through the chimera is unexpected given the success of several investigators to couple a diverse range of receptors through this G-protein (reviewed in Kostenis, *et al.*, 2005) including chemoattractant receptor family members such as CCR1 (Tian, *et al*., 2004) fMLP and C5a receptors (Mody, *et al*., 2000; Liu, *et al*., 2003) with which prostanoid $CRTH_2$ receptors share greatest amino acid sequence homology. Significantly, the chimera employed here incorporates the last 49 residues of $G\alpha_z$, rather than the z44 substitution specified in the literature. The z44 substitution encompasses residues in the α5 helix, β6 strand and parts of the α4/β6 loop structures which comprise the receptor-contacting interface of the G-protein. Mody, *et al*. (2000), noted that a z66 substitution resulted in a failure of the G-protein to couple to calcium mobilisation, while Ho, *et al*., (2004) have refined our knowledge of the crucial residues responsible for coupling specificity in the α5 helix. However, neither author has demonstrated whether the observed changes in coupling efficacy are due to loss or enhancement of interaction with the receptor or with PLCβ *per se*. The present results appear to suggest that a relatively small modification of an additional five residues in the α4/β6 loop may have a large negative impact on coupling of the chimeric G-protein to prostanoid $CRTH_2$ receptors though clearly, further investigation is required. The observation of high potency / low activity agonism by E-series prostaglandins at prostanoid $hCRTH_2$ receptors expressed with the chimeric G-protein and noted in chapter 3 was not replicated in the [^{35}S]-GTPγS accumulation assay. This lack of activity lends support to the notion that these molecules do not activate $G\alpha_{i/o}$ through prostanoid $CRTH_2$ receptors and that their exclusion from the pharmacophores presented in earlier chapters was appropriate. No evidence in support of the presence of prostanoid EP_1 or EP_3 receptors has been generated but their activation remains the most likely explanation for these data.

In contrast, agonist calcium mobilisation pharmacology generated using CHO K1 $hCRTH_2$ cells ($G\beta\gamma_{i/o}$ mediated PLCβ/γ activation in whole CHO K1 $hCRTH_2$ cells) showed altered rank orders of potency and relative activity compared with the GTPγS assay. Comparison of these data sets provides the strongest evidence yet of agonist-directed stimulus trafficking at prostanoid $CRTH_2$ receptors since they are free of the confounding factors listed in *Introduction*. In particular, by examining assay readouts based on the same biological system I have established *a priori* the equivalence of R:G

stoichiometry and the cellular provenance of the systems under comparison. Whilst the precise molecular definition of the G-protein coupling partner has not been made, both pathways use PTX-sensitive $G_{i/o}$ class G-proteins and are initiated by the same R:G interaction (or interactions). Similarly, while the methodologies compare kinetic FLIPR assay data with steady-state radiolabel accumulation data (though note comments above), the impact of this difference is negligible since the chimera-based FLIPR assay data yields an identical rank order to the GTPγS assay and allows a distinction to be made from simple 'strength of signal' based changes. Activation of multiple, distinct ligand binding sites on the $CRTH_2$ receptor molecule giving rise to distinct pharmacology can also be excluded by consideration of two lines of evidence: 1. Schild analysis of two structurally dissimilar prostanoid $CRTH_2$ receptor antagonists, AH23848B and GW853481X produced profiles of antagonism in both assay formats consistent with an action at a single receptor type, i.e. competitive interaction; 2. Analysis of saturation radioligand binding data by both linear (Scatchard) and non-linear regression revealed the presence of a single class of saturable receptor (chapter 4). (However, as noted in Chapter 7, other lines of evidence may suggest the presence of multiple ligand interaction sites). Therefore, the alterations of agonist potency and activity rank order can be taken to represent agonist stimulus trafficking of response and suggest that the relationship between Gβγ activation and Gα activation is not simply 'on - off' in nature. Rather, these data suggest that a graded activation of Gβγ is possible, related to the nature of agonist interaction with the receptor and in keeping with the notion that, 'the Gβγ-dimer is not merely a passive binding partner with the sole purpose of stabilising Gα but, rather, Gβγ actively participates in receptor-mediated G protein activation' (Cabrera-Vera, *et al*, 2003).

The data are strikingly similar to those presented by Pauwels & Colpaert (2003) for $[^{35}S]$-GTPγS accumulation and $[Ca^{2+}]_i$ mobilisation by 5-HT_{1A} receptors expressed in CHO K1 cells. Serotonergic receptor agonists produced pathway-specific activity and rank orders of potency, with the GTPγS assay appearing to be more sensitive to agonist activity. The key difference here is that agonists demonstrate a graded pattern of relative activities in both the calcium and GTPγS assays rather than the all-or-nothing profile exhibited by calcium-coupled 5-HT_{1A} receptors. Indeed, while most compounds had lower relative activity (cf. 5-HT) in the 5-HT_{1A} GTPγS assay, the present data show a series of relative activity changes, with some increasing while others decrease. Whilst

it is possible with the present data to make some 'broad-brush' observations concerning *classes* of agonist, the devil is in the detail and no entirely satisfactory pattern can be observed leaving stimulus trafficking the most plausible explanation that accounts for all of the data.

Taking first of all the comparison of chimera-generated calcium data ($G\alpha_{16z49}$ coupled) with the non-chimeric GTPγS data ($G\alpha_{i/o}$ coupled; Figure 7, Table 2). The data show changes strongly suggestive of 'strength of signal' based alterations of potency and activity, the GTPγS assay clearly amplified agonist responses with respect to the calcium data. Agonists of all three classes (D, F & J series) appear to have been affected equally but in particular F series agonists have been interspersed amongst agonists of the other series in the SAR Shuffle diagram, creating the false impression of trafficked agonist responses. It is clear that side chain substitutions determine the precise relationships between agonists of the same class while the greatest determinant of agonist potency is the oxygen functional chemistry of the prostanoid cyclopentyl head group. These data also demonstrate that the chimeric Gα subunit is a reasonable surrogate for endogenous Gα subunit activation and are in keeping with Clarke's prediction of less obvious or no stimulus trafficking where molecular coupling partners are similar (Clarke, speaking in Newman-Tancredi, 2003a).

The picture that emerges from comparison of the non-chimeric calcium mobilisation data ($G\beta\gamma_{i/o}$ coupled) with the non-chimeric GTPγS accumulation data ($G\alpha_{i/o}$ coupled) is rather different (Figure 8, Tables 2, Chapter 4). Although a top-level view of the data shows similar agonist-class related changes in potency to those described above, a closer examination reveals changes in agonist potency rank orders within and between classes. For example, 13,14 dihydro 15 keto PGD_2 which was a sensitive indicator of trafficking between chimeric and non-chimeric responses (chapter 4), has again displayed the greatest change in absolute and rank potency (pEC_{50}, RP calcium; pEC_{50}, RP GTPγS: 6.4, 32; 7.5, 4); 15 keto $PGF_{1\alpha}$ has also undergone potency rank order reversal with respect to 15 keto $PGF_{2\alpha}$ (pEC_{50}, RP calcium; pEC_{50}, RP GTPγS: 15 keto $PGF_{1\alpha}$ - NA, NA; 6.2, 79; 15 keto $PGF_{2\alpha}$ – 5.4, 316; 6.1, 100). Perhaps more significantly, three compounds display particular changes in activity that are not consistent with the expectations of 'strength of signal based' amplification: indomethacin which becomes less potent in the GTPγS assay but with increased relative activity (pEC_{50}, RA calcium; pEC_{50}, RA GTPγS: 6.9, 0.84; 6.4, 1.13); 15 R $PGF_{2\alpha}$

which becomes more potent but with reduced relative activity (5.5, 0.73; 6.3, 0.54); and 17 phenyl PGD_2 which undergoes an increase in potency smaller than that of other amplified agonists but with an increase in relative activity (5.9, 0.86; 6.2, 1.11). Looking between agonist series, the net result of these changes is to 'shuffle' agonists into a new rank order but care should be exercised here: some of these changes can be explained on the basis of agonist-class specific sensitivity to stimulus amplification. In contrast to the chimera / non-chimera calcium data where J series compounds were little affected (c. 0.25 log unit change) these same compounds appear to be the most affected by the non chimeric $G\alpha$ / $G\beta\gamma$ switch (c. 1 log unit change). However, agonist-class specific sensitivity to amplification could still be considered a manifestation of stimulus trafficking since the receptor / G-protein pair are responding differently to the agonists.

The present data are interesting in the light of previously published data. Sawyer, *et al*., (2002) observed that the potency order of 12 agonists at prostanoid $CRTH_2$ receptors was constant irrespective of assay readout (calcium mobilisation in $G\alpha_{15}$ expressing cells or inhibition of cAMP in HEK293(T) cells). However, comparison with the present data further confirms the sensitivity of 13,14 dihydro 15 keto PGD_2 to the coupling partner employed: pEC_{50} 13,14 dihydro 15 keto PGD_2, PGJ_2; $G\alpha_{15}$: 7.3, 6.3; $G\alpha_{i/o}$ this study: 7.5, 7.6; $G\beta\gamma_{i/o}$ this study: 6.4, 6.7. Indeed, Sugimoto, *et al.*, (2005) have also generated data that reveal a potency rank order shift of 13,14 dihydro 15 keto PGD_2 with respect to the present data: calcium mobilisation in L1.2 cells: $PGD_2 \geq$ 15 R 15 methyl PGD_2 > 13,14 dihydro 15 keto PGD_2 > indomethacin > 15 deoxy $\Delta^{12,14}$ PGJ_2; calcium mobilisation in non-chimeric CHO cells (this study): $PGD_2 \geq$ 15 R 15 methyl PGD_2 > indomethacin > 15 deoxy $\Delta^{12,14}$ PGJ_2 > 13,14 dihydro 15 keto PGD_2. The sensitivity of 13,14 dihydro 15 keto PGD_2 may also be related to the shallow slope it presents in the GTPγS assay (noted above). Clearly, further work is needed to understand this behaviour.

The data reported by Sugimoto present several other noteworthy features. As with Sawyer's data, the agonist potency rank order data for calcium mobilisation and inhibition of cAMP in L1.2 cells are identical and indicate only stimulus amplification-based changes in absolute potency. However, when viewed together all three sets of data detect readout-related changes in the behaviour of indomethacin: inhibition of cAMP in L1.2 cells (Sugimoto, *et al.*, 2005) indomethacin >> 15 deoxy $\Delta^{12,14}$ PGJ_2; inhibition of cAMP in HEK293(T) cells (Sawyer, *et al.*, 2002) indomethacin = 15

deoxy $\Delta^{12,14}$ PGJ_2; accumulation of [^{35}S]-GTPγS, (this study) 15 deoxy $\Delta^{12,14}$ PGJ_2 >> indomethacin. In keeping with my data in the GTPγS assay, Sugimoto also notes that in both the calcium mobilisation and cell migration assays (both in L1.2 cells) 15 deoxy $\Delta^{12,14}$ PGJ_2 is a more efficacious agonist than PGD_2 itself. However, my data also show that this relative activity relationship is reversed in calcium assays in CHO cells. It therefore appears that three agonists are particularly sensitive to the molecular identity of the coupling partner of human prostanoid $CRTH_2$ receptors: 13,14 dihydro 15 keto PGD_2, 15 deoxy $\Delta^{12,14}$ PGJ_2 and indomethacin.

Outside of the patent literature, a number of reports, including the present study, have described antagonists for the prostanoid $CRTH_2$ receptor. These antagonists fall into three classes: compounds believed to be simple competitive antagonists such as the indole-3-acetic acids described by Armer, *et al*. (2005), and the 4-aminotetrahydroquinolines of Mimura, *et al*. (2005); pathway *specific* antagonists such as the indoles described by Mathiesen, *et al*. (2005; though alternative explanations have not been excluded); and atypical competitive antagonists such as ramatroban (Sugimoto, *et al.*, 2005), as well as AH23848B and GW853481X reported here which appear to show agonist and / or pathway dependent affinity. By comparison with calcium assay data presented in Chapters 3 and 4, the latter two compounds show preferential affinity for the [^{35}S]-GTPγS pathway ($G\alpha_{i/o}$ coupling) over the calcium mobilisation pathway ($G\beta\gamma_{i/o}$ coupling) of 25- (AH23848B) and 8-fold (GW853481X). Whilst technical deficiencies are always a possibility in any experiment, the magnitude of these fold-increases do not lend themselves to simple errors in compound handling. Indeed, based on the calcium mobilisation data, one would have to unwittingly use a top final assay concentration of AH23848B of 3 mM (compound handling plate concentration of 0.3 M) in order mistakenly arrive at this affinity estimate! Similarly, the difference cannot be accounted for by considering the differential kinetics of the two assay systems: the faster kinetics of the calcium assay would tend to increase the affinity of the antagonists, not decrease it. Therefore, the true difference in affinity could be greater than that quantified here. It is difficult to conceive of a mechanism by which this phenomenon could occur. There is no evidence of non receptor-mediated effects in either assay and as noted above, several lines of evidence support the existence of a single orthosteric binding site for agonists and antagonists. Pathway-dependent effects have been said to require an allosteric mode of interaction (Kenakin,

2005) and, in this case, this would involve pseudo-competitive allosteric effects in both assay formats. However, it is also conceivable that differences in antagonist affinity at the same orthosteric site might arise when the receptor couples to different G-proteins if it is accepted that the effect of the activated receptor on the G-protein has a reciprocal effect on the receptor and transmits a conformation change to the latter molecule resulting in a change at the orthosteric binding site (Hill, S., personal communication). Evidence exists in support of this concept, for example the effect of G-protein coupling on agonist binding affinity (Kenakin, 2004c). Alternatively, the difference may relate to the use of whole cells in the calcium assay and membranes in the presence of saponin in the GTPγS assay: the former allows access to the receptor only from outside the cell while the latter allows access from both sides with the assistance of a solubilising agent. Thus, the affinity of these compounds in the GTPγS assay may represent a 'methodology assisted affinity' rather than a coupling pathway dependent affinity.

At a conceptual level, the molecular determinants of stimulus trafficking between $G\alpha_{i/o}$ and $G\beta\gamma_{i/o}$ are not difficult to understand. The process begins with a heterotrimeric Gαβγ-GDP complex coupled to the agonist-free $CRTH_2$ receptor (McKenzie, 1992). The coupling is understood to be via the C-terminal of the Gα subunit and not to involve residues of the Gβγ subunits. Agonist binding confers a conformation change which results in an affinity change at the nucleotide binding site of the Gα subunit and the exchange of GTP for GDP. The dissociation of the Gβγ subunits from the Gα subunit ensues and during this period of dissociation, the G-protein subunits interact with their effectors. The transduction period ends with the hydrolysis of GTP back to GDP and the re-association of the subunits. The conformation change induced by agonist binding we can now interpret as a collection of stabilised conformations of both the receptor and the Gα subunit (since it is also a protein macromolecule and subject to the same conformational considerations). This information is transmitted to the Gβγ subunits through their contact points with the Gα subunit and presumably result in stabilisation of a collection of conformations of this protein giving rise to the observed differences in response. Thus, Gβγ activation can be viewed to possess a 'volume control' and not simply as an 'on – off' event'. Furthermore, as Cabrera-Vera, *et al* (2003) point out, the potential for direct receptor-Gβγ interaction resulting in the activation of the latter has been recognised at the molecular level, lending further weight to this notion.

The pharmacophores that describe the assay readout specific interactions of agonists with prostanoid $CRTH_2$ receptors therefore describe the differential ability of certain molecules to drive transduction through the Gα subunit and on to the Gβγ subunits. Because the Gβγ subunits only undergo limited rearrangement on activation (references cited in Mirshahi, *et al*., 2006) there is limited scope for trafficking based on differential conformational changes at this point. Trafficking probably represents differential conformational changes in the Gα subunit which result in differential transmission of data to the Gβγ complex. So we can now interpret the pharmacophores developed in chapters 3 and 4 in terms of the ability of compounds to stimulate conformation changes in the Gα subunit. In terms of agonist structure the major determinants of signal transduction appear to reside in the cyclopentyl head group, C15 and C1 carbon substitutions. In terms of effector output, an additional factor may include the ability of activated Gα to 'steal' Gβγ by preferential interaction with its own effectors (adenylate cyclase).

Why are 13,14 dihydro 15 keto PGD_2, 15 deoxy $\Delta^{12,14}$ PGJ_2 and indomethacin particularly sensitive to the additional 'push' required to transmit activation data through to Gβγ? In the case of indomethacin, Hata, *et al*. (2005), have commented that it appears to possess greater intrinsic efficacy than PGD_2 itself towards inhibition of cAMP at murine receptors and calcium mobilisation at human receptors. However, this comment was based on examination of potencies vs. binding affinity and didn't take into account maximal effects. As shown in Table 5, chapter 3, most authors have found the relative activity of indomethacin to be 1.0. The data presented in chapter 3 is the first demonstration that indomethacin can behave as a partial agonist and this casts doubt on this explanation. Indomethacin clearly gives Gβγ a stimulus with greater potency relative to Gα, and Gα a stimulus resulting in greater activity: either could be considered to represent greater relative efficacy. Hata's molecular simulations have highlighted possible interactions between indomethacin and Lys209 in TMV (carboxylic acid charge stabilised H-bond interaction similar to the C1 carboxylate of prostanoid agonists) and Phe110 in TMIII (hydrophobic interaction with N-(p-chlorobenzoyl); similar to or in place of the C11 carbonyl interaction with His106). In other words, key interactions made by prostanoid agonists with Arg178 in EC2 and Glu268 in TMVI are absent and this may underpin its ability to transduce differently. Similarly, 13,14 dihydro 15 keto PGD_2 and 15 deoxy $\Delta^{12,14}$ PGJ_2 also lack the potential

for interaction with Arg178 since both lack C15 hydroxy groups and the possibility for stereochemical arrangement at this point.

These data demonstrate that stimulus trafficking by the prostanoid $CRTH_2$ receptor can occur when coupled either through $G\alpha$ or $G\beta\gamma$ subunits of the same $G_{i/o}$ class G-protein. The greatest determinant of prostanoid agonist sensitivity to coupling partner appears to be the oxygen functionality of the cyclopentyl head group. Agonist sensitivity varied in the order: F series > D series > J series. Signals transduced in response to each series appeared to be trafficked relative to the other series. Three agonist molecules have been identified as the most sensitive markers of trafficking at this receptor: 13,14 dihydro 15 keto PGD_2, 15 deoxy $\Delta^{12,14}$ PGJ_2 and indomethacin. The usefulness of the chimeric $G\alpha_{16z49}$ G-protein has been further qualified such that validation of such strategies for generating convenient assays must include a range of physiologically relevant readouts in the terms-of-reference. Lastly, receptor desensitisation may have affected assay data with its own pharmacological profile and this possibility will be explored further in the next chapter.

5.5 Figure caption list:

Figure 1. Representative data showing prostaglandin D_2 (PGD_2) stimulated binding of [^{35}S]-GTPγS binding in membranes derived from CHO K1 $hCRTH_2$ cells of clones 5 and 15, and from un-transfected CHO K1 cells. Assay methodology was unoptimised; specific conditions are described in *Results*. Data are mean of duplicate points generated in the same experiment.

Figure 2. Prostaglandin D_2 (PGD_2) stimulated binding of [^{35}S]-GTPγS binding in membranes derived from CHO K1 $hCRTH_2$ cells of clone 15, in the presence of indicated concentrations of GDP. Assay conditions: 5 μg protein well^{-1}, 125 μg beads well^{-1}, 0.3 nM [^{35}S]-GTPγS, 3 hr incubation. Data are mean of duplicate points generated in a single experiment.

Figure 3. [^{35}S]-GTPγS accumulation in membranes derived from CHO K1 $hCRTH_2$ cells in response to prostaglandin D_2 (PGD_2), PGE2, $PGF_{2\alpha}$ and indomethacin. Assay conditions were optimised as described in *Methods* & *Results*.: 10 μg protein well^{-1}, 125 μg beads well^{-1}, 1.2 nM [^{35}S]-GTPγS, 30 μM GDP, 60 min incubation. Data are mean ± sem of three independent experiments.

Figure 4. Antagonism of prostaglandin D_2 (PGD_2) stimulated [^{35}S]-GTPγS accumulation by AH23848B in membranes derived from CHO K1 $hCRTH_2$ cells. Panel A: Parallel rightward displacement of PGD_2 E/[A] curves in the presence of increasing concentrations of AH23848B resulting in pK_b estimate of 6.9 ± 0.1. Panel B: Inhibition of response to application of PGD_2 EC_{80} by increasing concentrations of AH23848B resulting in pIC_{50} estimate of 6.2 ± 0.07. Data are mean ± sem of three independent experiments.

Figure 5. Antagonism of prostaglandin D_2 (PGD_2) stimulated [^{35}S]-GTPγS accumulation by GW853481X in membranes derived from CHO K1 $hCRTH_2$ cells showing parallel rightward displacement of E/[A] curves in the presence of increasing concentrations of antagonist. pK_b estimate: 7.5 ± 0.1. Data are mean ± sem of three independent experiments.

Figure 6. Inhibition of prostaglandin D_2 (PGD_2) stimulated [^{35}S]-GTPγS accumulation by pertussis toxin in membranes derived from CHO K1 $hCRTH_2$ cells. Sham treatment reduced responses relative to untreated controls but data was not controlled for membrane or protein recovery. Data are mean ± sem of three independent experiments.

Figure 7. SAR Shuffle diagram displaying agonist potency SAR in CHO K1 $hCRTH_2$ [^{35}S]-GTPγS accumulation assay without PTX treatment and CHO $G\alpha_{16z49}$ $hCRTH_2$ cell calcium assay with PTX treatment.

Figure 8. SAR Shuffle diagram displaying agonist potency SAR in CHO K1 $hCRTH_2$ [^{35}S]-GTPγS accumulation assay and CHO K1 $hCRTH_2$ cell calcium assay (without PTX treatment).

Figure 9. Comparative E/[A] curves for PGD_2 & indomethacin in [^{35}S]-GTPγS accumulation assays (assay A), and calcium mobilisation assays at CHO K1 $hCRTH_2$ cells (assay B) and CHO $G\alpha_{16z49}$ $hCRTH_2$ cells treated with PTX (50 ng ml^{-1}; assay C). Data has been scaled such that PGD_2 E_{max} = 100 % in each assay. Data are mean ± sem; PGD_2 n = 10 - 12, indomethacin n = 3.

5.6 Figures

Follow on next page

Figure 1

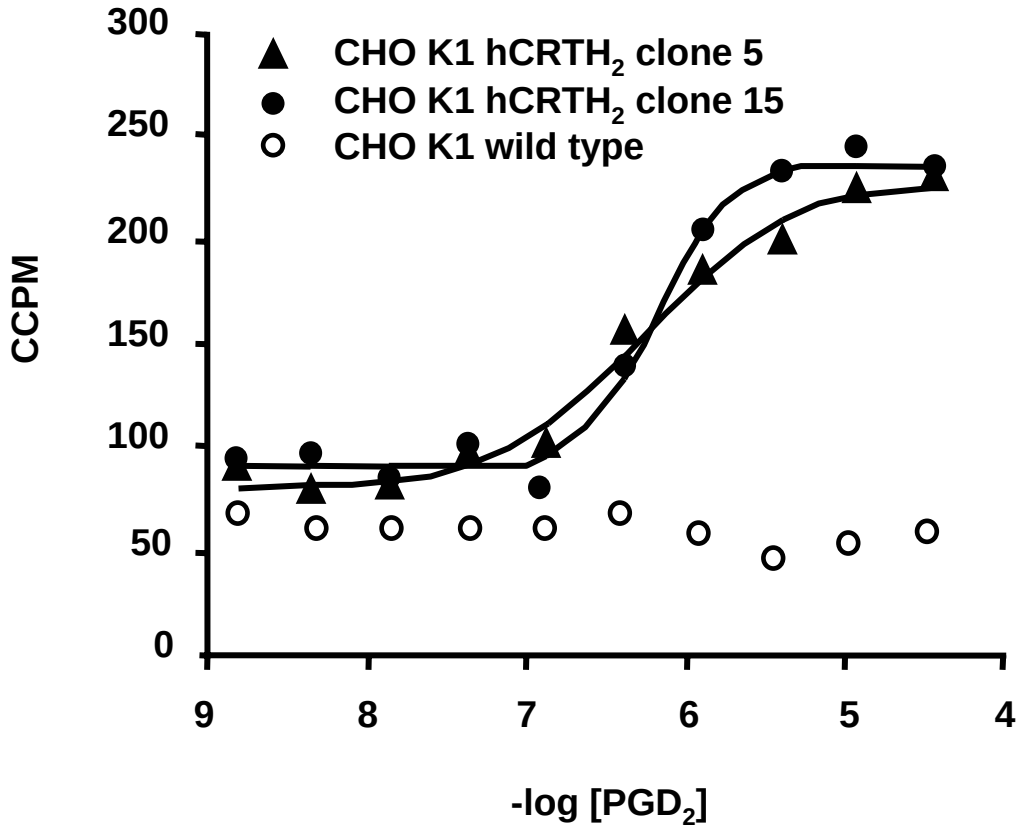
300
250
200
150
100
50
0
CCPM
CHO K1 hCRTH2 clone 5
CHO K1 hCRTH2 clone 15
CHO K1 wild type
9
8
7
6
5
4
-log [PGD2]

Figure 2

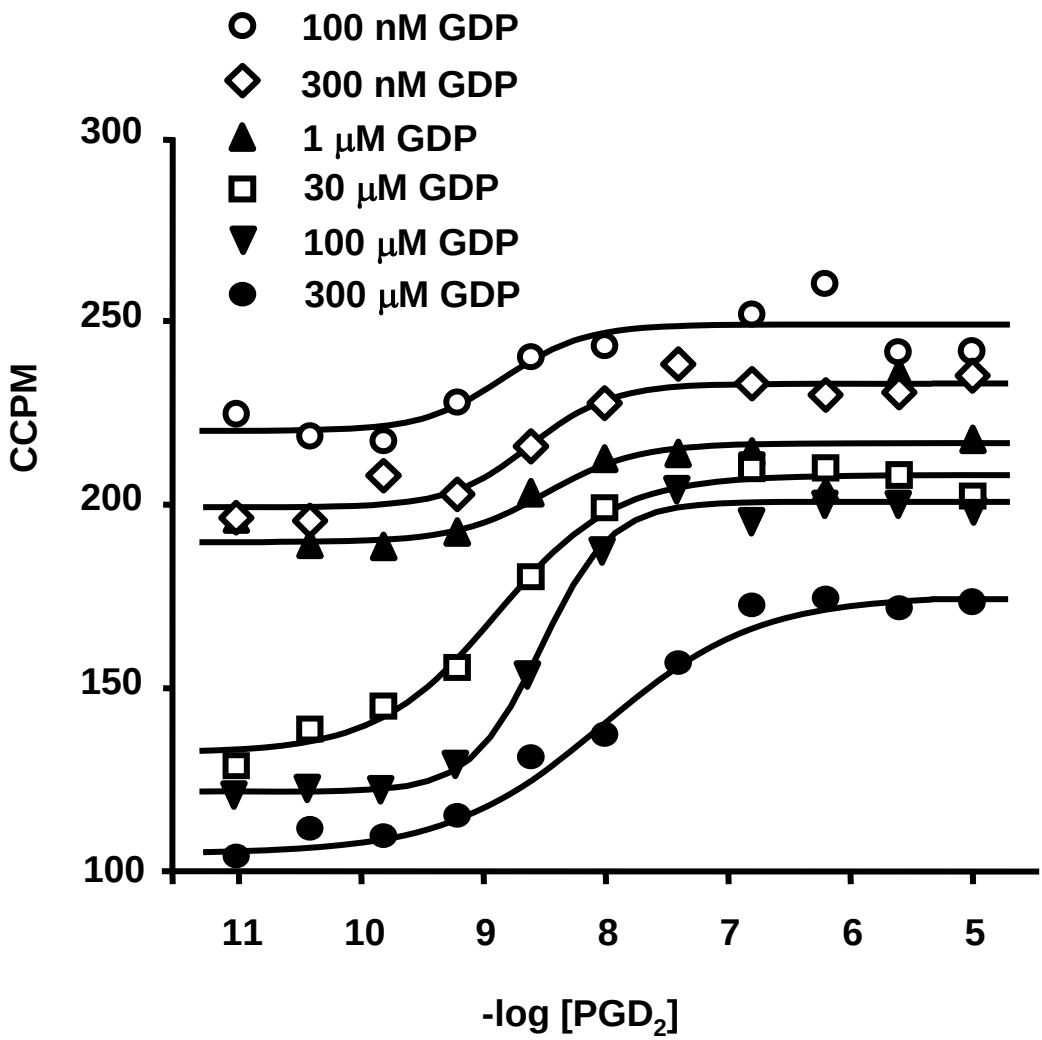
100 nM GDP
300 nM GDP
1 μM GDP
30 μM GDP
100 μM GDP
300 μM GDP
300
250
200
150
100
CCPM
11
10
9
8
7
6
5
-log [PGD2]

Figure 3

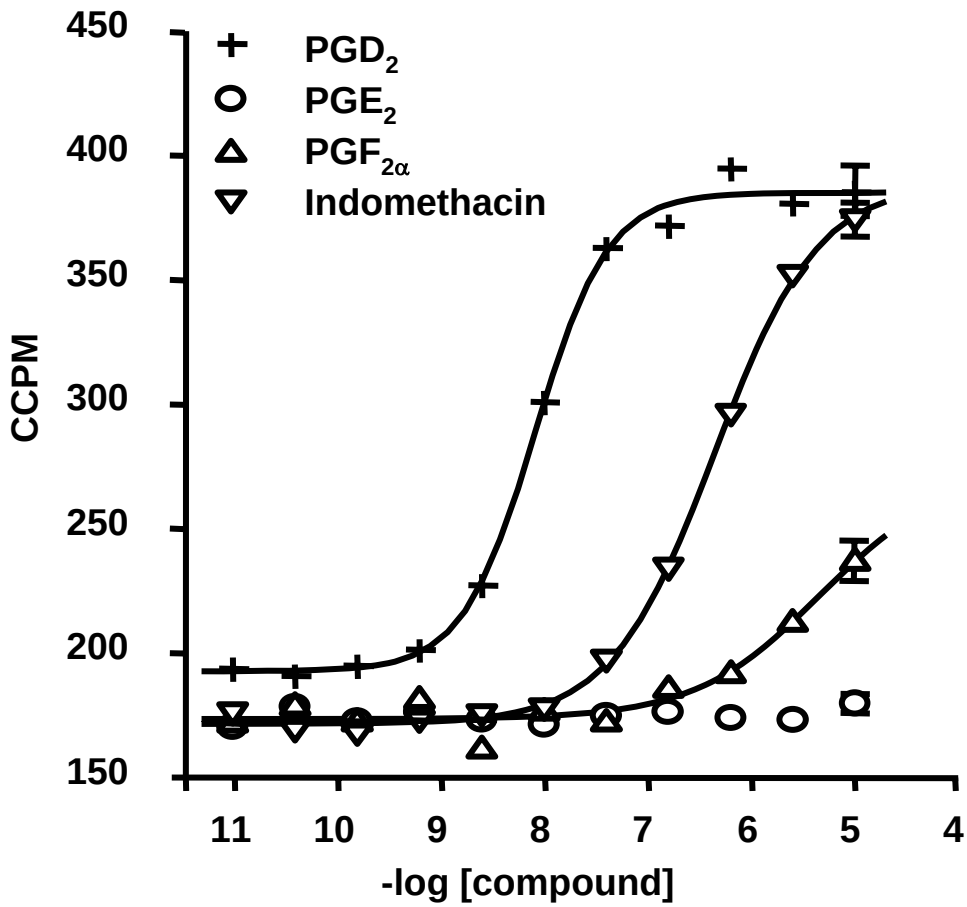
450
400
350
300
250
200
150
CCPM
PGD2
PGE2
PGF2α
Indomethacin
11
10
9
8
7
6
5
4
-log [compound]

Figure 4

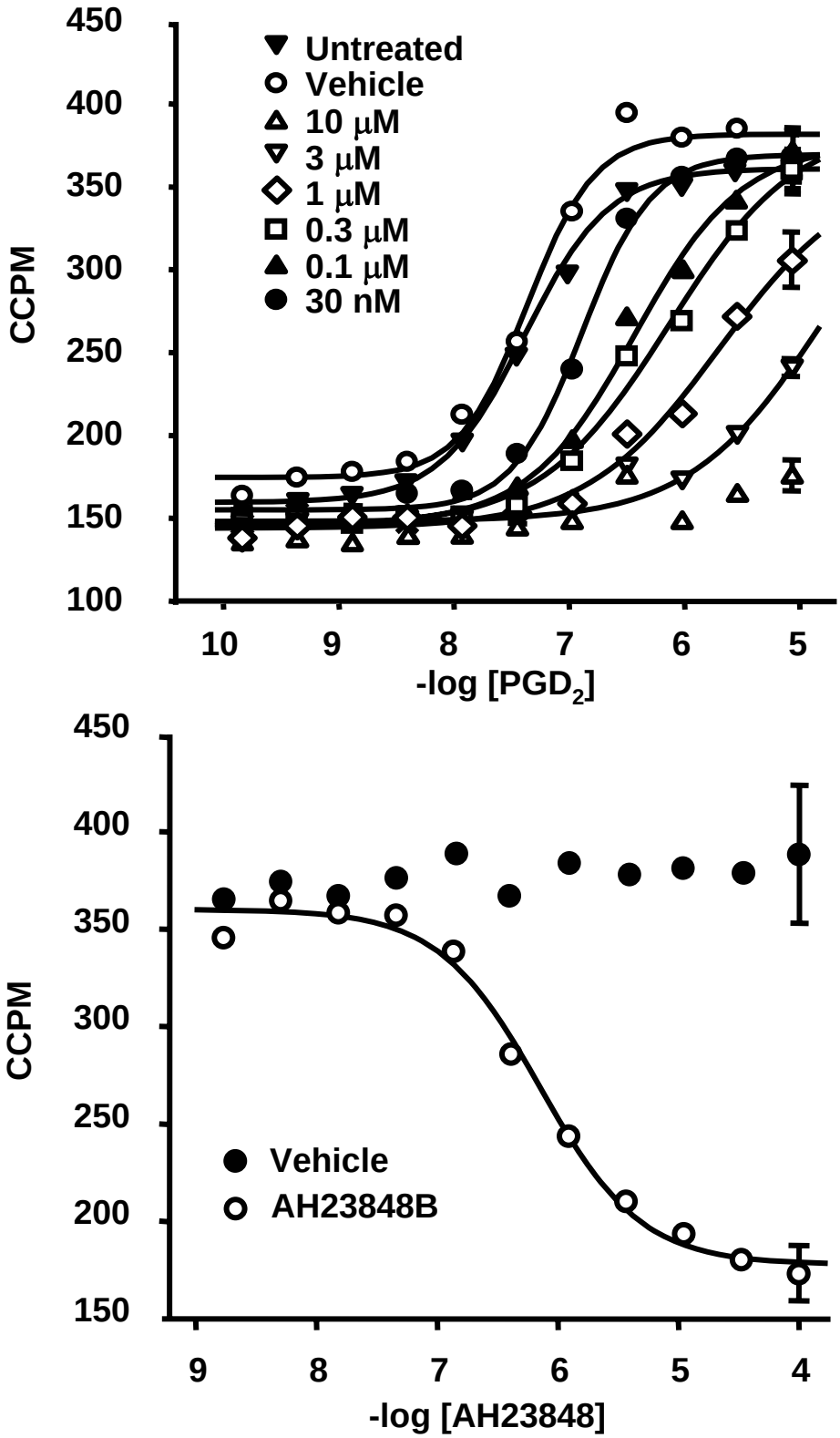
450
400
350
300
250
200
150
100
CCPM
Untreated
Vehicle
10 μM
3 μM
1 μM
0.3 μM
0.1 μM
30 nM
10
9
8
7
6
5
-log [PGD2]
450
400
350
300
250
200
150
CCPM
Vehicle
AH23848B
9
8
7
6
5
4
-log [AH23848]

Figure 5

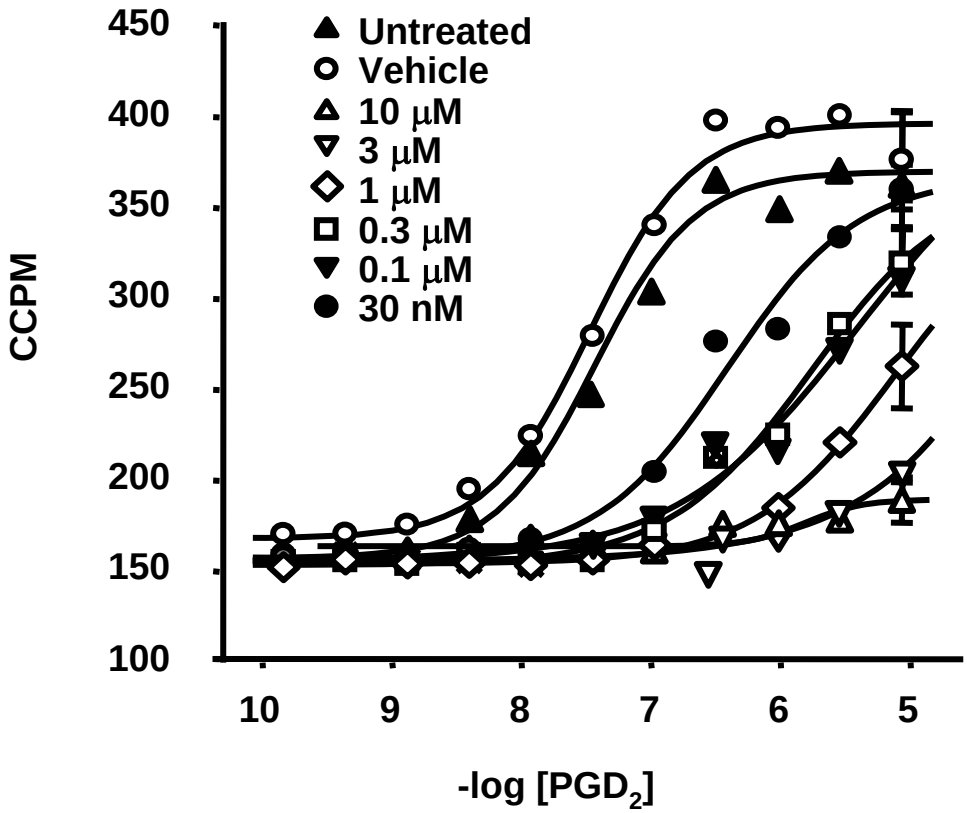
450
400
350
300
250
200
150
100
CCPM
Untreated
Vehicle
10 μM
3 μM
1 μM
0.3 μM
0.1 μM
30 nM
10
9
8
7
6
5
-log [PGD2]

Figure 6

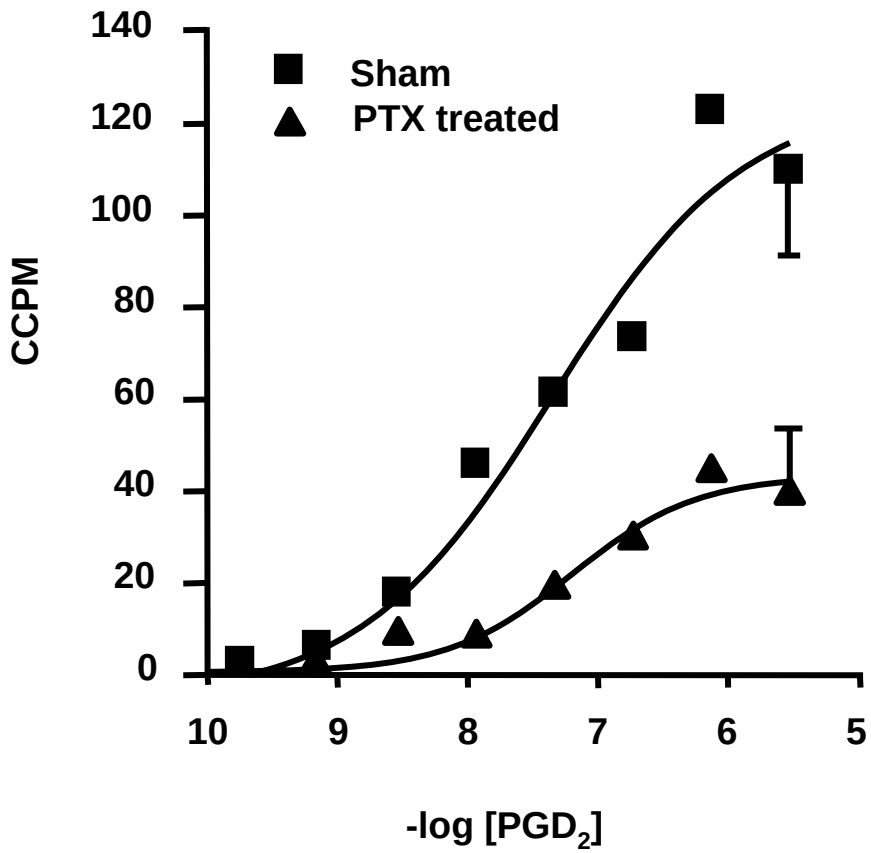
140
120
100
80
60
40
20
0
CCPM
Sham
PTX treated
10
9
8
7
6
5
-log [PGD2]

Figure 7

CHO $G\alpha_{16z49}$ $hCRTH_2$ + PTX - $[Ca^{2+}]_i$

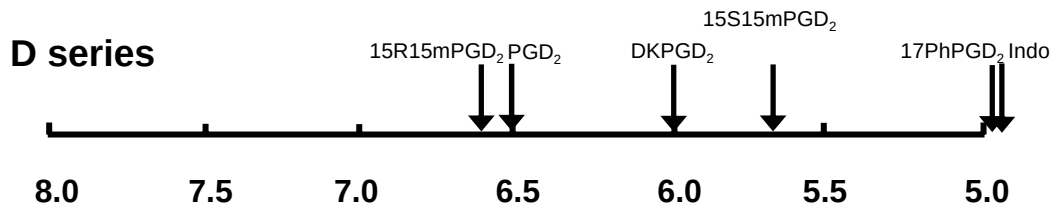

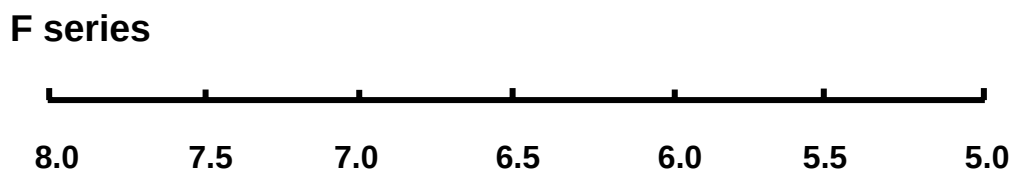

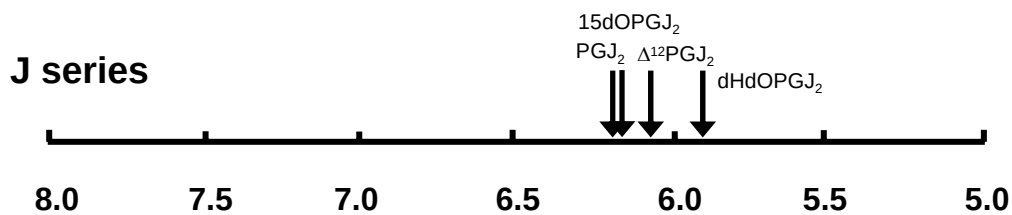

CHO K1 $hCRTH_2$ - $[^{35}S]$-GTPγS

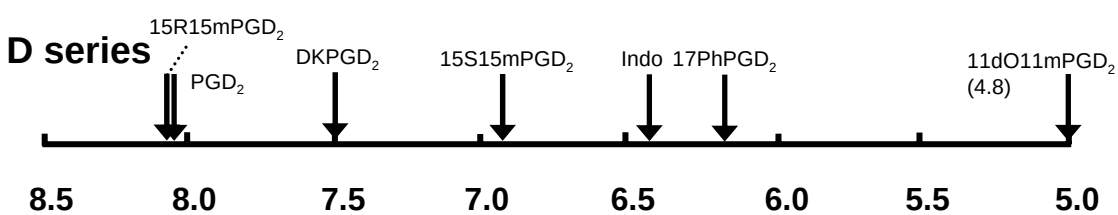

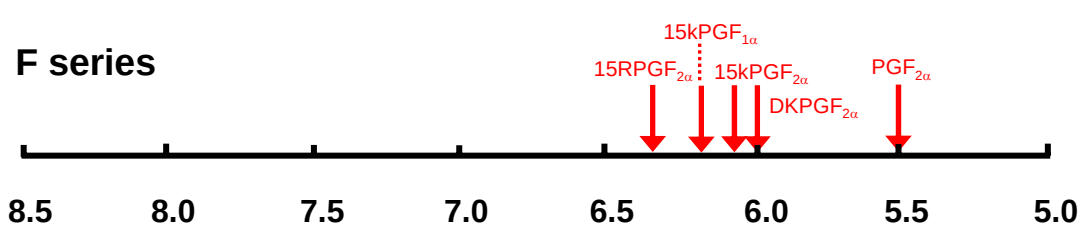

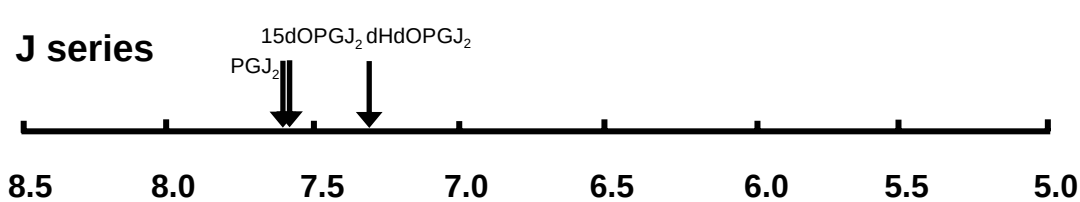

Figure 8

CHO K1 hCRTH$_2$ – [^{35}S]-GTPγS

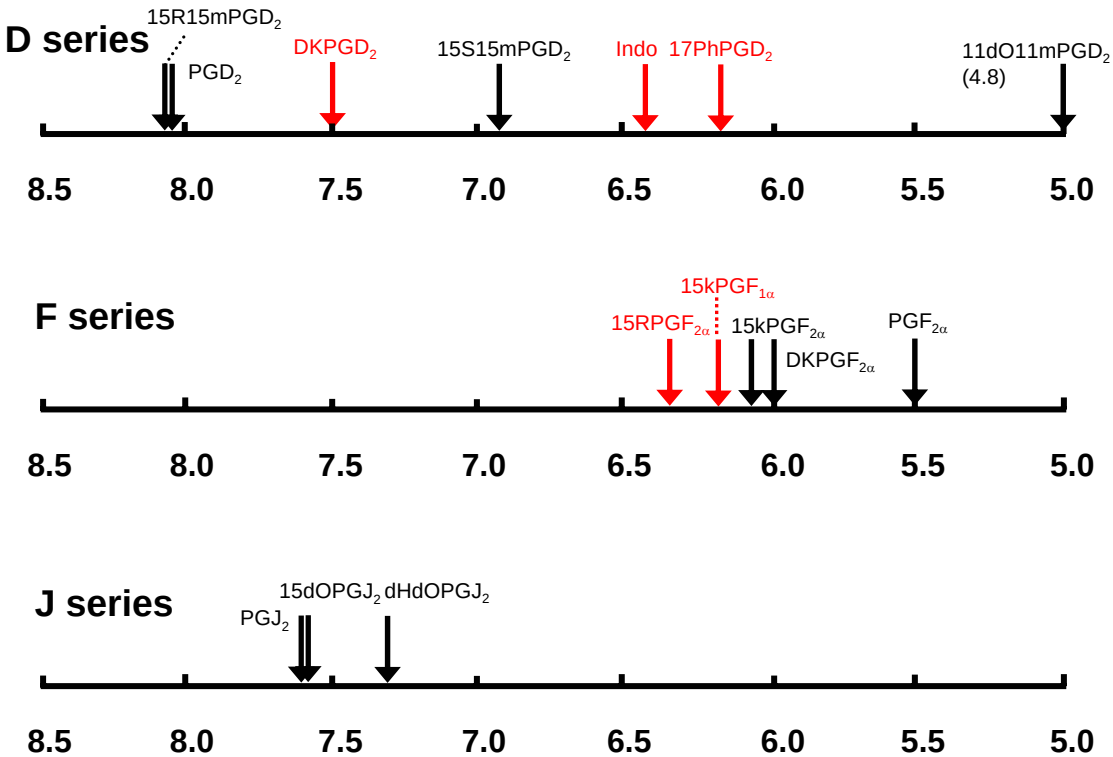

CHO K1 hCRTH$_2$ – [Ca^{2+}]$_i$

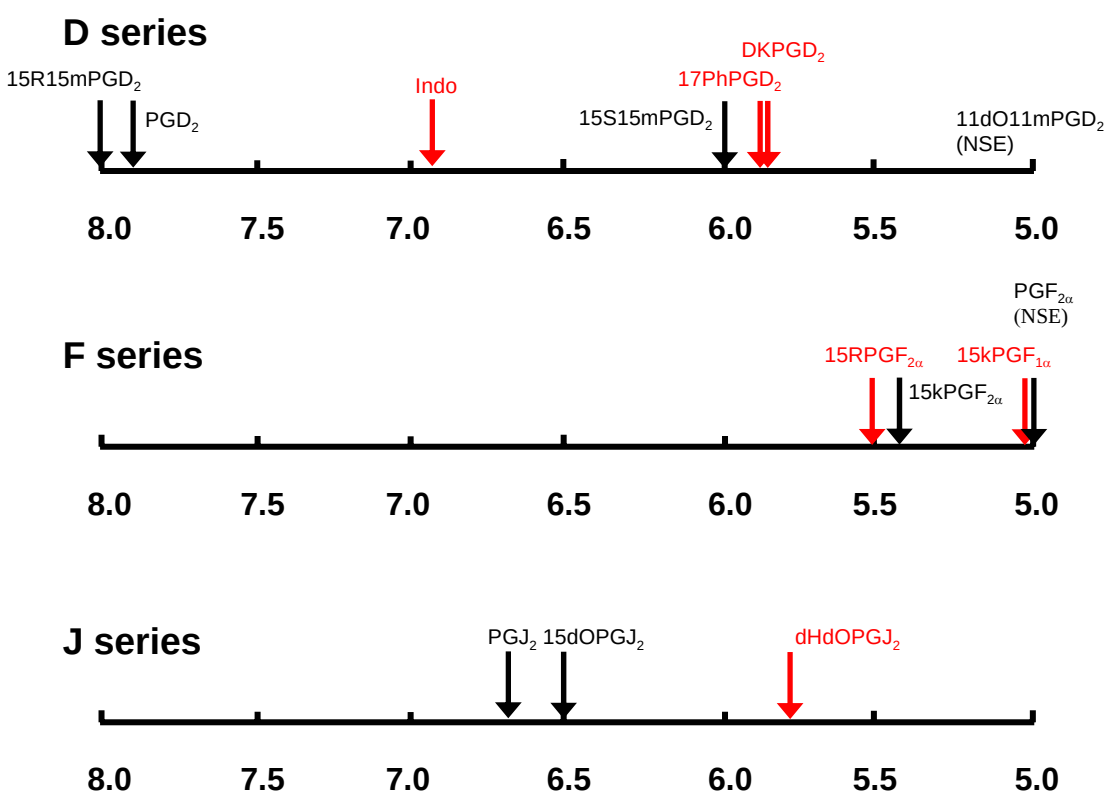

Figure 9.

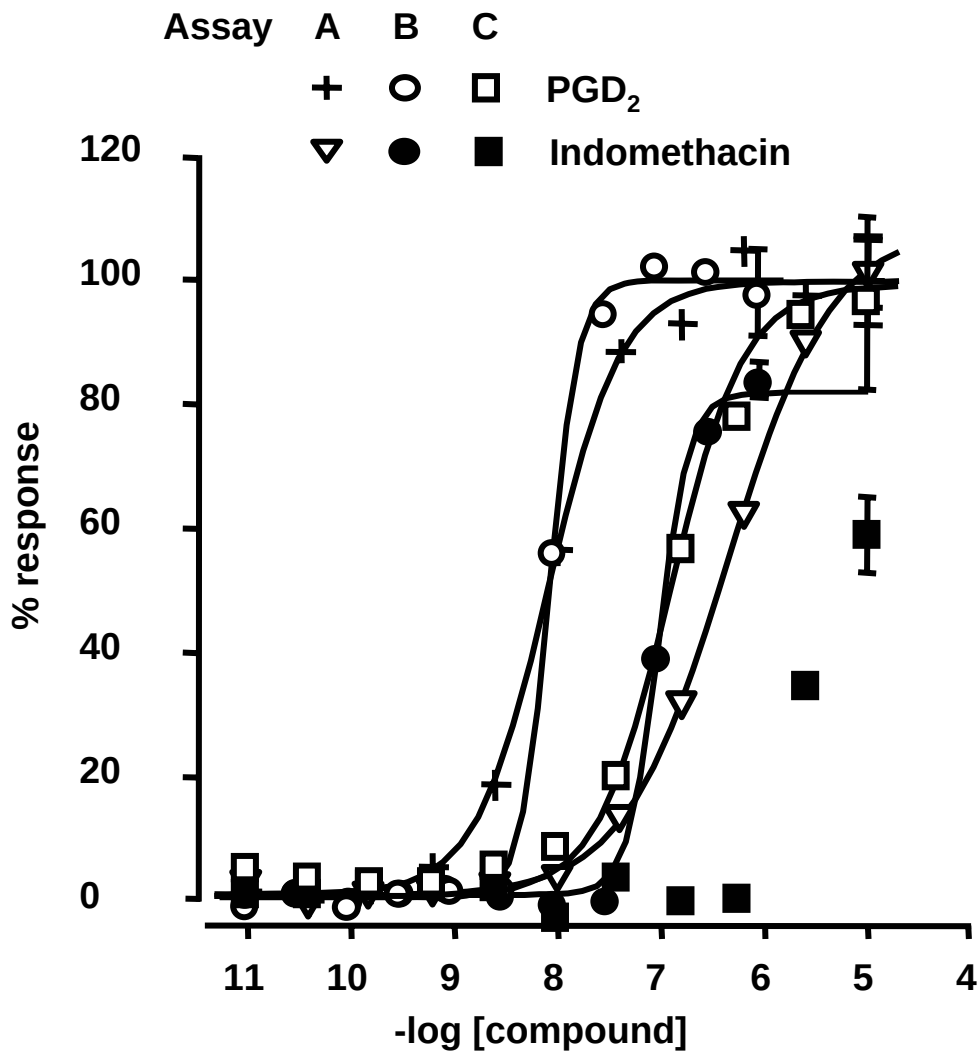
Assay A B C
PGD2
Indomethacin
120
100
80
60
40
20
0
% response
11 10 9 8 7 6 5 4
-log [compound]

Chapter 6:

Receptor desensitisation & $G_{i/o}$ / G_q synergy: impact on agonist stimulus trafficking at human prostanoid $CRTH_2$ receptors.

6.1 Summary:

Agonist stimulus trafficking by calcium-coupled human prostanoid $CRTH_2$ receptors has been described in chapters 3 to 5. During these studies it was noted that exposure of receptor-expressing cells to prostaglandin D_2 (PGD_2) desensitised the cells to subsequent exposure to prostanoid agonists. In this chapter, the desensitisation phenomena have been investigated using a range of pharmacological techniques. Uridine 5′ triphosphate (UTP) has been used as a non-prostanoid agonist with which to investigate cross-desensitisation events.

PGD_2 & UTP stimulated calcium mobilisation in cells expressing recombinant prostanoid $hCRTH_2$ & endogenous purinergic $P2_{Y2}$ receptors with and without co-expression of chimeric $G\alpha_{16z49}$ G-proteins. Calcium fluxes were transient: maximum fluorescence (representing $[Ca^{2+}]_i$) occurred at 3 s (UTP) to 12 s (PGD_2) post agonist addition; recovery to baseline was achieved by 10 mins post-addition. UTP responses were partially pertussis toxin (PTX) sensitive indicating coupling to $G_{i/o}$ but also to another calcium coupled G-protein (presumably $G\alpha_q$).

PGD_2 responses in chimera-expressing cells were insensitive to the absence of calcium in the assay buffer but were reduced in non chimera-expressing cells (67 % E_{max} reduction; 0.7 log unit pEC_{50} reduction). Paradoxically, the maximum effect elicited by UTP increased by 21 - 29 % in the absence of calcium while potency decreased by 0.6 log units. Responses to both agonists were sensitive to the phospholipase Cβ inhibitor U71322 and the calcium-store depleting agent thapsigargin. Taken together, these results suggest a combination of internal store release and plasma membrane calcium entry for both agonists.

PGD_2 produced rapid & long-lasting (> 120 min) desensitisation of $hCRTH_2$ receptors. The desensitisation was biphasic manner: phase 1. inhibition of E_{max} and pEC_{50} within 1min; phase 2. further inhibition of E_{max}. Maximal desensitisation occurred 30 min post-challenge. Concentrations of PGD_2 sub-threshold with respect to calcium mobilisation produced non-significant desensitisation at 30 min post exposure. Application of PGD_2 at concentrations either below EC_{15} or above EC_{100} resulted in total inhibition of responses to re-application of the same concentration of agonist. In the range EC_{16}-EC_{99} inhibition followed a bell-shaped relationship suggesting the presence of two inhibition mechanisms. Inhibition at low concentrations of PGD_2 was unaffected by PTX suggesting a non $G_{i/o}$ G-protein

mediated mechanism. Desensitisation was unaffected by treatment with the PKA inhibitor H89, the PKA activator dibutyryl cyclic adenosine 5′ monophosphate, or the PKC inhibitor GF109203X, suggesting that these kinases have little role in response uncoupling.

Synergising interactions between UTP and PGD_2 were revealed in experiments where cells were exposed to both agonists. Following UTP pre-treatment, PGD_2 curves became biphasic in both cell types, with the emergence of a response phase shifted to the left of the control curve location. However, E_{max} only increased in non chimera-expressing cells suggesting that the response-increasing properties of $G\alpha_q$ stimulation can only be observed in this cell line. This may indicate that synergy between $G\alpha_{16z49}$ & $G\beta\gamma_{i/o}$ subunits could occur under normal conditions in chimera-expressing cells. Finally, following UTP pre-treatment, PGD_2 elicited small response curves in PTX-treated non chimera-expressing cells indicating that 50ng ml^{-1} PTX for 18 hr does not abolish all $G_{i/o}$ mediated coupling to $CRTH_2$ receptors.

Taken together then, these data suggest that the signalling cascade associated with $hCRTH_2$ receptor activation to be rewritten as shown. The potential for synergising interactions to occur exists in both $hCRTH_2$-expressing cell lines but appears to be present without the need for additional non-prostanoid agonists in chimera expressing cells. Thus, the stimulus trafficking observed may therefore reflect the interruption or lack of synergising interactions under PTX-treated or non-chimera-expressing conditions.

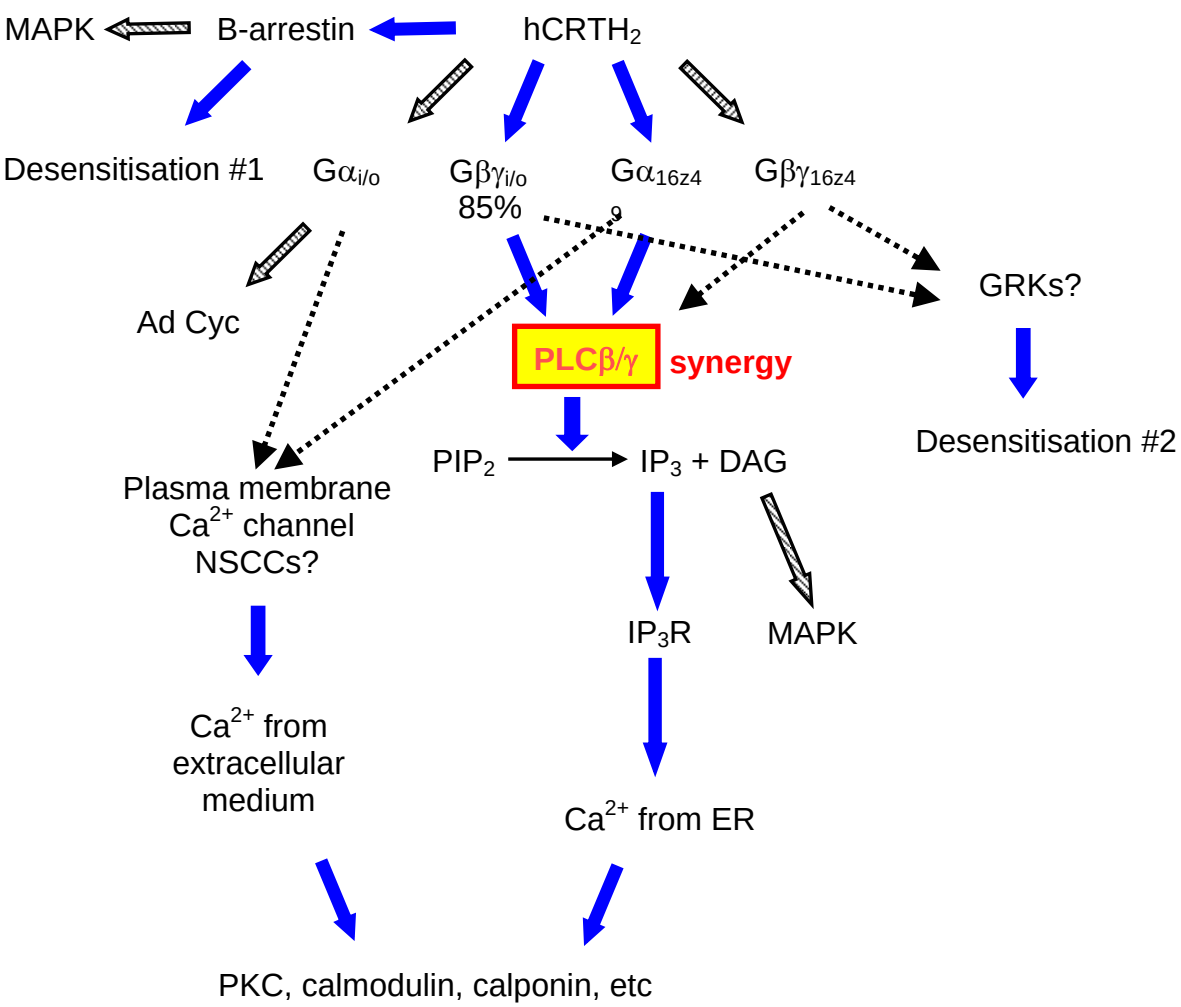
MAPK
B-arrestin
hCRTH2
Desensitisation #1
Gαi/o
Gβγi/o
85%
Gα16z4
Gβγ16z4
GRKs?
Ad Cyc
PLCβ/γ
synergy
Desensitisation #2
PIP2
IP3 + DAG
Plasma membrane
Ca2+ channel
NSCCs?
IP3R
MAPK
Ca2+ from
extracellular
medium
Ca2+ from ER
PKC, calmodulin, calponin, etc

6.2 Introduction:

The scientific literature contains many examples of studies describing the coupling of prostanoid chemoattractant receptor homologous molecule of TH_2 cell ($CRTH_2$) receptors to cellular effector mechanisms via pertussis toxin sensitive $G_{i/o}$ (refs. cited below) or, in the case of Sawyer, *et al.* (2002), promiscuous $G\alpha_{15}$ G-proteins. Biochemical readouts measured have included inhibition of cAMP accumulation and mobilisation of intracellular calcium ($[Ca^{2+}]_i$). However, despite many of these papers demonstrating biphasic or complex concentration-effect (E/[A]) curves and / or transient alterations in the concentration of $[Ca^{2+}]_i$ (Hirai, *et al.*, 2001, 2002; Monneret, *et al.*, 2002, 2003; Sawyer, *et al.*, 2002; Powell, 2003; Mimura, *et al.*, 2005; Mathiesen, *et al.*, 2005) indicative of regulatory mechanism activation, the literature contains surprisingly little comment concerning such processes. Indeed, Hirai, *et al.* (2001), report the earliest homologous desensitisation data providing the first indication that prostanoid $CRTH_2$ receptors are acutely regulated but fail to make any reference to this aspect of their data.

Acute regulation of prostanoid $CRTH_2$ receptor mediated signalling can therefore take place at the receptor or second messenger level, and of relevance to this thesis is the regulation of $[Ca^{2+}]$. G-protein coupled receptor (GPCR) desensitisation mechanisms (Chuang, *et al.*, 1996; Claing, *et al.*, 2002; Pierce, *et al.*, 2002; Reiter & Lefkowitz, 2006) and mechanisms of $[Ca^{2+}]_i$ regulation (Caride, *et al.*, 2001; Papp, *et al.*, 2003; Saris & Carafoli, 2005) have been extensively reviewed and the reader is directed to these papers for a more comprehensive treatment of the area.

Rapid desensitisation of receptor function is often a result of kinase-mediated receptor phosphorylation at specific serine or threonine residues by cAMP-dependent protein kinase A (PKA), calcium and / or diacyl glycerol (DAG) dependent PKC, and G-protein receptor kinases (GRKs; Chuang, *et al.*, 1996; Claing, *et al.*, 2002; Pierce, *et al.*, 2002; Maudsley, *et al.*, 2005). Activation of PKA and PKC occurs as a consequence of G-protein mediated second messenger production and result in phosphorylation of multiple proteins including receptor molecules of classes unrelated to the activated receptor (heterologous desensitisation; Chuang, *et al.*, 1996). GRKs are a family of seven proteins which interact with activated receptors via membrane-associated and activated G-protein $\beta\gamma$ subunits (GRKs 2 & 3). This results in co-localisation of the kinase *only* with the activated and agonist-occupied receptor (homologous

desensitisation) by which it is allosterically activated. GRKs 4, 5 & 6 make lesser contributions to desensitisation and are constitutively associated with the plasma membrane (Pitcher, *et al*., 1998; Reiter & Lefkowitz, 2006). It is unclear whether GRKs activated by one receptor type can desensitise simultaneously activated receptor molecules of another type since this would have the potential to weaken the specificity of GRK mediated desensitisation. PKA / C mediated phosphorylation of receptors results in immediate uncoupling of receptors from G-proteins though in certain cases can result in a switch in coupling preference between G-protein types, for example PKA induced switching of β_2-adrenoceptors away from G_s to G_i mediated MAPK activation (Pierce, *et al*, 2002; Maudsley, *et al*., 2005; but see commentary by Hill & Baker, 2003: it is unclear whether this represents true switching from G_s to G_i, the unmasking of ongoing promiscuous coupling to G_i, or of coupling via G_s activation of the small G-protein Rap1). On the other hand, GRK mediated phosphorylation results in recruitment of β-arrestins which sterically block G-protein interactions with the receptor and in turn recruit a complex of proteins associated with arrestin and GPCR ubiquitination and subsequent clathrin-dependent endocytosis, at least for the majority of receptors (Reiter & Lefkowitz, 2006). Almost all GPCR's are internalised in some way following phosphorylation and are either 1. dephosphorylated and recycled to the cell surface; or 2. degraded in lysosomes. While residing in endosomes, β-arrestin linked GPCRs may take part in activation of further signalling cascades through the arrestin and GRK molecules themselves (Hall, *et al*., 1999; Lefkowitz, *et al*., 2006). Thus, β-arrestin can provide a scaffold for construction of several mitogen-activated protein kinase (MAPK) signalling complexes involving extracellular signal regulated kinase (ERK), c-Jun amino terminal kinase (JNK) and other c-Src related kinases, can stabilise inhibitor of nuclear factor kappa-B (IκB), and activate PKB (aka AKT). Meanwhile, GRKs 5 & 6 promote, while GRKs 2 & 3 attenuate, β-arrestin activation of ERK, and GRK 2 inhibits AKT and may also inhibit MEK1. Furthermore, additional regulatory complexity is produced by differential β-arrestin 1 / 2 affinity for receptors (Oakley, *et al*, 2000), regulation based on β-arrestin homo- and hetero-dimerisation (Milano, *et al.*, 2006) and patterns of receptor phosphorylation dependent upon the expression and sub-cellular organisation of GRK proteins (Scott, *et al.*, 2002). Further control is achieved through cross-talk between the two kinase regulatory systems (Chuang, *et al.*, 1996). For example, PKC can associate with GRK2 resulting in

phosphorylation of the latter and an increase in affinity and V_{max} towards the activated receptor substrate (Chuang, *et al*., 1995). PKC activation can also stimulate transcription of GRK2, at least in T-lymphocytes (De Blasi, *et al.*, 1995), while PKA may produce similar changes in GRK2 activity while also promoting β-arrestin mRNA transcription and protein synthesis (Parruti, *et al*., 1993). Thus, this system has the potential to exert exquisite control of GPCR mediated signalling and co-ordination of cellular responses through non G-protein mediated mechanisms.

GRKs and protein kinases are not the only mediators of acute receptor regulation. Other more poorly characterised systems involve receptor relocation to caveolae with subsequent internalisation (Smart, *et al*., 1999), and association of regulator of G-protein signalling (RGS) proteins with receptors (Ross & Wilkie, 2000). Caveolae are small invaginations of the plasma membrane which seem to serve as foci for co-location of several signalling molecules but the processes governing receptor recruitment are not understood. RGS proteins are a diverse group whose members all contain a 130 - residue long RGS sequence and act as GTPase activating proteins (GAPs) for GPCRs. By accelerating GTPase activity, RGSs increase the speed with which signals are turned off, either when the stimulus is removed or during stimulation if the receptor is internalised or phosphorylated (Pierce, *et al*., 2002). Finally, receptor expression may also be regulated though this is over a chronic time-frame.

Regulation of $[Ca^{2+}]_i$ is achieved via calcium-regulated sequestration into the endoplasmic reticulum (ER) and mitochondria, but also by extraction into the extracellular milieu across the plasma membrane (Saris & Carafoli, 2005, for review). The endoplasmic reticulum of non muscle cells contains a high concentration of calcium bound to its carrier proteins calreticulin, calsequestrin (in sarcoplasmic reticulum), endoplasmin and several other proteins, some of which function as protein-folding chaperone proteins (Papp, *et al*., 2003). Calcium is pumped into the ER via the sarcoplasmic / endoplasmic reticulum Ca^{2+} ATPase (SERCA) protein (also known as a Type II Ca-ATPase in non muscle cells) which is regulated by Ca-calmodulin / PKA dependent phosphorylation of phospholambdan with which the pump associates (Wuytack, *et al*., 2002). The pump has the capacity to reduce the cytoplasmic $[Ca^{2+}]$ to below 1 μM. Spanning the dual membranes of mitochondria, another Ca-ATPase operates under conditions of high $[Ca^{2+}]_i$ to exchange Ca^{2+} for $2H^+$ (Saris & Carafoli, 2005). Data has also emerged suggesting the co-location of mitochondrial Ca-ATPase

molecules near to ER IP_3 receptors creating the possibility that high local concentrations of $[Ca^{2+}]_i$ sufficient to activate the pump may be produced (Rizzuto, *et al*., 1993). Plasma membranes express two calcium pumps: the Na^+/Ca^{2+} exchanger and the plasma membrane Ca-ATPase (PMCA; Caride, *et al*., 2001). The latter protein is homologous to SERCA proteins, contains 10 transmembrane spanning regions and is also regulated by Ca-calmodulin. PMCAs are encoded by four genes (termed PMCA1-4) each of which has two splice sites, A and C. Splices at the C-site result in the production of proteins with differing Ca-calmodulin regulation properties and are termed a, b and c. The Na^+/Ca^{2+} exchanger is not driven by ATP hydrolysis but instead relies upon the energy of the gradient produced by the Na^+ pump (Philipson & Nicoll, 2000). Whether this protein mediates calcium efflux or uptake therefore depends upon the polarisation state of the cell. The exchanger is a 9 transmembrane spanning molecule, also containing splice sites which allow for differential regulation by ions, phosphatidyl inositol (4,5) diphosphate (PIP_2) and protein kinase A. It is unclear whether only some or all of these mechanisms operate in CHO cells.

As stated above, published data concerning the desensitisation of prostanoid $hCRTH_2$ receptors is lacking. Mathiesen, *et al*. (2005), have demonstrated by means of a green fluorescent protein / recombinant luciferase (GFP-RLuc) bioluminescent resonance energy transfer (BRET) assay that $hCRTH_2$ receptors can activate β-arrestin through a non-PTX sensitive pathway. Mathiesen, *et al*., interpret this result as indicating direct β-arrestin activation which would mark a divergence from the general schemes outlined above. More probable is a GRK-mediated β-arrestin recruitment with subsequent activation of intracellular effectors (Smith & Luttrell, 2006; Lefkowitz, *et al*., 2006). The amino acid sequences of human and murine $CRTH_2$ receptors contain clusters of serine and threonine residues at the C-terminal end of the receptor (Abe, *et al*., 1999) consistent with the suggested requirements for long-lasting GRK/β-arrestin association with the receptor (Reiter & Lefkowitz, 2006) which is likely to prolong the persistence of this receptor in endosomes.

The flip-side of stimulus down-regulation is, of course, stimulus activation and synergism. Studies conducted in the present work examining the ability of UTP and PGD_2 to cross desensitise (heterologous desensitisation) unexpectedly revealed synergistic interactions between $G_{i/o}$ coupled prostanoid $hCRTH_2$ receptors and G_q coupled purinergic $P2_{Y2}$ receptors. Synergism or cross-talk has been reviewed in

general terms by Selbie & Hill (1998) and Cordeaux & Hill (2002), and also in terms specifically relating to calcium signalling by Werry, *et al*. (2003); the examples cited below are taken from these references. Synergistic interactions can take place at a wide range of transduction levels and can arise from combination or sharing of receptors (e.g. $GABA_{B1/2}$), receptor domains (e.g. κ and δ opioid receptors) or G-proteins (e.g. angiotensin AT_1 and bradykinin B_2 receptors), simple addition of the effects of two agonists activating the same second messengers (e.g. prostanoid $CRTH_2$ and chemokine CCR3, 4, 5 or 7 receptors), the resultant of activation of two (or more) dissimilar pathways (e.g. activation of PLCβ → Ca^{2+} → PYK2 → cSrc and PI3K → PIP_3 → cSrc), or from the conditional amplification of agonist effects usually below detection limits were it not accompanied by a co-stimulatory agonist (numerous examples, e.g. purinergic $P2_{Y2}$ and neuropeptide Y NPY_{Y1} receptors). A number of transduction events mediated by $G_{i/o}$ G-proteins cannot be observed unless accompanied by G_q-coupled receptor agonists. These interactions frequently involve the convergence of $G\alpha_q$ and $G\beta\gamma_{i/o}$ at specific transduction proteins such as PKC and PLCβ, or of $G\alpha_s$ and $G\beta\gamma_{i/o}$, for example at adenylate cyclases II & IV. However, other molecules may also be targets for the sensitising effects of one agonist on the effects of another: phosphatidyl inositol 4 kinase (PI4K) and PI(4)P 5 kinase to increase the substrate supply to PLC; $I(1,3,4,5)P_4$ production to remodel the ER and increase sensitivity to IP_3; calpain to cleave the C-terminal of PLCβ and increase its activity; $I(1,4,5)P_3$ receptor sensitisation; priming and / or triggering of Ca^{2+} release from distinct sub-compartments of the ER calcium store or from mitochondria; regulation of Ca^{2+}-ATPase or exchange proteins (see above). The significance of these phenomena to the studies presented in this thesis is two-fold: firstly, any constitutive activation of a pathway with the potential to cross-talk with the coupling of prostanoid $hCRTH_2$ receptors could lead to the generation of pharmacology based on synergistic interactions (both stimulatory and regulatory) rather than on a direct linear link to G-protein activation; and secondly, if synergism can occur, then the coupling partners expressed in CHO $G\alpha_{16z49}$ $hCRTH_2$ cells, which represent both $G_{i/o}$ and a chimera based on a $G\alpha_q$ class G-protein may synergise on a routine basis.

The studies described in this chapter were conceived in order to shed light on mechanisms of recombinant prostanoid $hCRTH_2$ receptor desensitisation by pharmacological means. In the course of their execution evidence relating to synergistic

interactions between $hCRTH_2$ receptors and endogenously expressed purinergic $P2_{Y2}$ receptors was gathered. The two data sets provide insights into the behaviour of this intriguing prostanoid receptor and provide more context to assist with interpretation of stimulus trafficking data.

6.3 Results:

6.3.1 Experiments with CHO K1 & CHO Ga_{16z49} cells.

Uridine triphosphate (UTP; 1.7 nM – 100 μM) produced concentration-related increases in fluorescence in CHO K1 and CHO $G\alpha_{16z49}$ cells (pEC_{50}, E_{max} [normalised FLIPR intensity units (NFIU)]; 6.3 ± 0.2, 235 ± 50, and 6.1 ± 0.1, 156 ± 2, respectively). Prostaglandin D_2 (PGD_2; (0.17 nM – 10 μM)) was without effect in either cell line.

6.3.2 UTP signal transduction in CHO K1 $hCRTH_2$ & CHO Ga_{16z49} $hCRTH_2$ cells.

6.3.2.1 **Effect of extracellular calcium & of pertussis toxin on UTP & PGD_2 responses.**

UTP was an agonist in both $hCRTH_2$-expressing cell lines (CHO K1 $hCRTH_2$ cells pEC_{50} 6.4 ± 0.1; CHO $G\alpha_{16z49}$ $hCRTH_2$ cells pEC_{50} UTP 6.2 ± 0.1). Overnight culture with pertussis toxin (PTX; 50 ng ml^{-1}) diminished UTP E_{max} in both cell lines (CHO K1 $hCRTH_2$ cells 17 ± 3 % inhibition ($P < 0.05$); CHO $G\alpha_{16z49}$ $hCRTH_2$ cells 23 ± 3 % inhibition ($P < 0.05$); Figure 1.) with no alteration of pEC_{50}. Removal of extracellular calcium (Ca^{2+}_x) from the assay system produced an 11 – 16 % decrease in basal fluorescence counts for which all data were corrected. In CHO $G\alpha_{16z49}$ $hCRTH_2$ cells removal of Ca^{2+}_x did not affect PGD_2 E_{max} or pEC_{50} (Table 1; Figure 1). However, in CHO K1 $hCRTH_2$ cells removal of Ca^{2+}_x resulted in a 67 ± 6 % reduction in PGD_2 E_{max} ($P < 0.01$), with a concomitant rightward pEC_{50} shift of 0.7 ± 0.3 log units ($P = 0.05$). In both $hCRTH_2$ expressing cell lines the removal of Ca^{2+}_x resulted in an unexpected increase in UTP E_{max} (CHO K1 $hCRTH_2$ cells 21 ± 4 % ($P < 0.05$); CHO $G\alpha_{16z49}$ $hCRTH_2$ cells 29 ± 14 % (NS)) with a decrease in potency of c. 0.6 log units (NS).

Following PTX treatment, removal of Ca^{2+}_x resulted in similar increases in UTP E_{max} (CHO K1 $hCRTH_2$ cells 19 ± 4 % ($P < 0.05$); CHO $G\alpha_{16z49}$ $hCRTH_2$ cells 25 ± 17 % (NS)) and pEC_{50}. However, PGD_2 responses in CHO $G\alpha_{16z49}$ $hCRTH_2$ cells were no longer insensitive to Ca^{2+}_x: E_{max} was reduced by 35 ± 18 % ($P < 0.05$) with a non-significant 0.2 log unit decrease in pEC_{50}.

6.3.2.2 **Experiments with inhibitors of the calcium mobilisation pathway**

Data describing the effect of calcium mobilisation pathway inhibitors on basal and PGD_2-stimulated fluorescence has been presented previously in chapter 4.

UTP (1.7 nM – 100 μM) E/[A] curves were unaffected by pre-treatment with either vehicle, H-89 or ryanodine (Figures 2, 3 & 4). U71322 treatment totally abolished agonist responses in CHO $G\alpha_{16z49}$ $hCRTH_2$ cells ± PTX and reduced the E_{max} in CHO K1 $hCRTH_2$ cells (41 % inhibition [control 214 ± 34; U71322 treated 118 ± 28 NFIU; $P < 0.01$]). Thapsigargin totally abolished fluorescence increases in response to UTP in both cell lines ± PTX (where applicable). However, in the presence of thapsigargin, UTP produced small but reproducible concentration-related reductions in fluorescence in both cell types. These were not abolished by PTX treatment. Experiments using heparin and β-ARK 495-689 were not performed using UTP as agonist.

6.3.3 Time course of UTP & PGD_2 calcium response generation & recovery in $hCRTH_2$ expressing cells.

Exposure of $hCRTH_2$ expressing cells to PGD_2 and UTP resulted in transient increases in fluorescence representing increased $[Ca^{2+}]_i$ (Figure 5). The time required to reach maximum fluorescence varied in the order PGD_2 in CHO K1 $hCRTH_2$ (c. 12 s) > PGD_2 in CHO $G\alpha_{16z49}$ $hCRTH_2$ (c. 10 s) > UTP (both cell types equivalent; c. 3 s). Fluorescence decayed rapidly for both agonists in all settings and had declined by approximately 90 – 110 % of the peak level at 5 min post challenge depending upon the concentration of agonist applied (Figures 6 & 7). Fluorescence decayed further and reached a new steady state level at 10 min post challenge. Where $G\beta\gamma_{i/o}$ coupling was intact, the new steady state level was above the original baseline level (NS); following PTX treatment the new steady state was not significantly different to the starting baseline. Fluorescence was observed to fall below the starting baseline level at 5 min post challenge for both agonists in all settings and for vehicle in CHO K1 $CRTH_2$ cells (Figure 8; vehicle was not tested in CHO $G\alpha_{16z49}$ $hCRTH_2$ cells). In all subsequent studies 2nd treatments were applied 11 min post 1st treatment.

6.3.4 Characteristics of UTP & PGD_2 response desensitisation in $hCRTH_2$ expressing cells.

6.3.4.1. **Effect of a single PGD_2 concentration on subsequent PGD_2 dilution series challenge.**

In experiments where PGD_2 E/[A] curves (2nd treatment) were applied to $CRTH_2$ expressing cells pre-treated with a single concentration of PGD_2 (1st treatment), PGD_2

produced a profound and long-lasting desensitisation of the cells to subsequent PGD_2 challenge (Figure 9). In CHO $G\alpha_{16z49}$ $hCRTH_2$ cells the desensitisation consisted of two phases: an acute phase between t = 0 and t = 60 s characterised by a reduction in both E_{max} and rightward shift of the PGD_2 pEC_{50} (Figure 10; E_{max} sd 0 – 18 %); a slower phase between t = 60 s and t = 10 min characterised by a further inhibition of E_{max} but with no further change in pEC_{50}. The time to peak inhibition decreased with increasing first treatment PGD_2 concentration; inhibition of E_{max} but not of pEC_{50} began to reverse between t = 60 min and t = 120 min. Concentrations of PGD_2 below the threshold for stimulation of $[Ca^{2+}]_i$ (5 nM PGD_2) also produced non-significant reductions in E_{max} at t = 30min. In the continued presence of first treatment PGD_2, second treatment PGD_2 E/[A] curves were shifted to the right of the calculated PGD_2 occupancy curve (calculations based on K_d estimated in chapter 4; Figure 11) with concomitant curve depression in a manner reminiscent of non-competitive antagonism. Pre-treatment of cells with PGD_2 (0.17 nM – 10 μM) produced concentration-related inhibition of PGD_2 EC_{70} (at t = 11 min pIC_{50} 7.1 ± 0.2, n_H 1.5 ± 0.3, max effect 98 ± 3 % inhibition; cf. time matched agonist control pEC_{50} 7.4 ± 0.1, n_H 1.2 ± 0.2; Figure 12). Pre-treatment of cells with the partial agonist 15 keto $PGF_{2\alpha}$ also elicited concentration dependent inhibition of PGD_2 (at t = 11 min pIC_{50} 5.5 ± 0.1, n_H 2.0 ± 1.3, max effect 85 ± 2 % inhibition; time matched agonist control pEC_{50} 5.9 ± 0.2, n_H 2.9 ± 1.9, E_{max} 75 ± 10 %).

6.3.4.2. **Effect of protein kinase inhibitors & activators on PGD_2 induced desensitisation.**

Application of the protein kinase C inhibitor GF109203X (1 μM), the protein kinase A inhibitor H89 (1 μM), the protein kinase A activator dibutyryl cyclic adenosine monophosphate (dbcAMP, 1 μM), or combinations of GF109203X with either H89 or dbcAMP to $hCRTH_2$ expressing cells produced effects on intracellular calcium indistinguishable from that of vehicle (0.25 % DMSO; Figure 13). First treatment PGD_2 E/[A] curve pEC_{50} was lower than previously observed (CHO K1 $hCRTH_2$ 6.9 ± 0.03; CHO $G\alpha_{16z49}$ $hCRTH_2$ 7.1 ± 0.05; $P < 0.05$) and was unaffected by incubation with any of these agents (Figure 14). The subsequent application of PGD_2 EC_x (nominal values of x = 0 – 100 in increments of 10, then five subsequent two-fold increases in concentration) to wells previously exposed to first treatment agonist

resulted in the generation of inhibition curves. In vehicle-incubated cells to which PGD_2 EC_{80} was applied on second treatment pIC_{50} was lower than the pEC_{50} values described above (CHO K1 $hCRTH_2$ pIC_{50} 6.8 ± 0.3; CHO $G\alpha_{16z49}$ $hCRTH_2$ pIC_{50} 6.7 ± 0.3). Second treatment inhibition curve pIC_{50} decreased with increasing EC_x concentration (Figure 15). In CHO $G\alpha_{16z49}$ $hCRTH_2$ cells, pIC_{50} declined with increasing EC_x to a limit at 2 x EC_{100} following which no further decrease was observed; pIC_{50} decreased at all EC_x tested in CHO $G\alpha_{16z49}$ $hCRTH_2$ cells however, the highest EC used was subsequently found to be EC_{100}. E_{max} was unaffected by the EC_x applied (Figure 16). Neither pIC_{50} nor E_{max} were sensitive to incubation with protein kinase inhibitors / activators.

6.3.4.3. **Effect of agonist dilution series application on subsequent challenge with dilution series of the same agonist.**

Experiments were conducted in which PGD_2 or UTP E/[A] dilution series (2nd treatment) were applied to $hCRTH_2$ expressing cells pre-treated with dilution series of the same agonist, such that the same amount of agonist was added twice to each well. In such experiments reapplication of agonist was found to elicit a bell-shaped E/[A] curve for both PGD_2 and UTP, in both cell lines, with and without PTX treatment (Figure 17 & Table 2). The exception to this was PGD_2 in CHO K1 $hCRTH_2$ cells + PTX where responses were abolished by the toxin. PGD_2 2nd treatment curves were observed to have an ascending phase right-shifted with respect to the control curve, while those to UTP were observed to be superimposable with the control curve to the point of inflection of the bell shaped curve. Apart from the changes in maximum effect described above, removal of Ca^{2+}_x did not otherwise alter the relationship between 1st and 2nd treatment agonist curves.

6.3.4.4. **Effect of agonist dilution series application on subsequent challenge with dilution series of a different agonist**

In similar experiments in which PGD_2 and UTP E/[A] curves were generated in cells pre-treated with dilution series of the other agonist (i.e., PGD_2 following UTP, and *vice versa*), a range of effects were observed (Figure 18 & Table 2). Pre-treatment of CHO $G\alpha_{16z49}$ $hCRTH_2$ cells with PGD_2 produced an inhibition of UTP responses ($P < 0.05$) which was not observed in PTX treated cells. However, in CHO K1 $hCRTH_2$ cells, the

same treatment with PGD_2 resulted in a small left-shift and increase in UTP E_{max}, irrespective of PTX treatment (NS). Where the pre-treatment involved application of a UTP dilution series, PGD_2 E/[A] curves became biphasic with a similar E_{max} in CHO Ga_{16z49} $hCRTH_2$ cells but became biphasic with a markedly enhanced E_{max} in CHO K1 $hCRTH_2$ cells ($P < 0.01$). In the absence of extracellular calcium, PGD_2 curves following UTP 1st treatment were monophasic with similar E_{max} values to those obtained with calcium present; EC_{50} values were the same as the EC_{50} of the first phase in the biphasic curves. Furthermore, PGD_2 2nd treatment resulted in the production of concentration-related increases in $[Ca^{2+}]_i$ in PTX treated CHO K1 $hCRTH_2$ cells previously exposed to a UTP dilution series.

6.3.5 Data Tables

Follow on next page.

Table 1. PGD_2 and UTP E/[A] curve parameters with and without pertussis toxin (PTX) treatment, and with and without calcium added to assay buffer. Buffer did not contain EGTA. Slope parameters were in the ranges: CHO $G\alpha_{16z49}$ $hCRTH_2$: PGD_2 0.9 - 1.4, UTP 1.2 - 1.8; CHO K1 $hCRTH_2$: PGD_2 1.5 - 1.9, UTP 1.3 - 1.6. NSE denotes no significant effect. Data are mean ± sem; n=6 from three independent experiments except * n=5.

		CHO $G\alpha_{16z49}$ $hCRTH_2$		**CHO K1 $hCRTH_2$**	
		E_{max}	pEC_{50}	E_{max}	pEC_{50}
PTX treatment	Calcium in buffer	**PGD_2**			
	✓	197 ± 2	7.5 ± 0.09	99 ± 3	7.5 ± 0.08
		194 ± 5	7.5 ± 0.06	41 ± 2	6.9 ± 0.18
✓	✓	43 ± 1	6.5 ± 0.06	NSE	-
✓		30 ± 2	6.1 ± 0.1*	NSE	-
		UTP			
	✓	235 ± 2	6.2 ± 0.04	226 ± 1	6.4 ± 0.05
		296 ± 12	5.8 ± 0.02	268 ± 4	5.8 ± 0.02
✓	✓	180 ± 4	6.1 ± 0.03	187 ± 2	6.3 ± 0.02
✓		225 ± 8	5.5 ± 0.02	218 ± 4	5.7 ± 0.01

Table 2. PGD_2 & UTP E/[A] curve data (2nd treatment) from application to $hCRTH_2$ expressing cells pre-treated (1st treatment) with dilution series of either the same agonist (same amount of agonist added twice to each well) or with the other agonist (an amount of both agonists added to each well). Key: 1st T – 1st treatment; 2nd T – 2nd treatment; X – either E or I as defined in the column 'X='; NSE – no significant effect; NC – no calcium in buffer. Where no data in column 'Phase 2'curves were monophasic. Where X = I, curves were bell-shaped; where X = E curves consisted of two sigmoidal E/[A] curves, both with positive slope. Data are mean ± sem; n=3 from three independent experiments.

			CHO $G\alpha_{16z49}$ $hCRTH_2$					**CHO K1 $hCRTH_2$**				
			Phase 1		Phase 2			Phase 1		Phase 2		
1st T	2nd T	PTX	E_{max}	pEC_{50}	X_{max}	pXC_{50}	X=	E_{max}	pEC_{50}	X_{max}	pXC_{50}	X=
PGD_2	PGD_2	×	57 ± 1	7.6 ± 0.18	18 ± 2	5.8 ± 0.09	I	NSE	-	-	-	-
"	"	✓	NSE	-	-	-	-	NSE	-	-	-	-
UTP	UTP	×	107 ± 4	6.6 ± 0.1	22 ± 3	4.9 ± 0.04	I	110 ± 4	6.6 ± 0.1	13 ± 4	4.9 ± 0.03	I
"	"	✓	83 ± 7	6.5 ± 0.02	15 ± 2	4.7 ± 0.07	I	73 ± 3	6.4 ± 0.03	7 ± 1	4.9 ± 0.06	I
PGD_2	UTP	×	162 ± 6	6.7 ± 0.08	-	-	-	241 ± 5	6.5 ± 0.06	-	-	-
"	"	✓	183 ± 1	6.3 ± 0.03	-	-	-	211 ± 7	6.3 ± 0.07	-	-	-
UTP	PGD_2	×	98 ± 13	7.7 ± 0.08	161 ± 3	6.1 ± 0.03	E	92 ± 12	7.7 ± 0.05	148 ± 1	6.4 ± 0.05	E
"	"	✓	28 ± 1	5.8 ± 0.08	-	-	-	14 ± 3	7.5 ± 0.15	-	-	-
PGD_2	PGD_2	× (NC)	187 ± 5	7.8 ± 0.05	158 ± 5	6.1 ± 0.01	I	169 ± 4	8.3 ± 0.04	-	-	-

6.4 Discussion:

In this chapter, I have employed a number of pharmacological techniques to shed light on the mechanisms of prostanoid $hCRTH_2$ receptor mediated response normalisation and desensitisation in CHO cells. UTP was selected as a comparative agonist because of the well-established and consistent expression of mainly $G\alpha_q$-coupled purinergic $P2_{Y2}$ receptors on CHO cells (e.g. Dickenson *et al*., 1998), and because other agonists tested (acetyl choline, adrenergic receptor agonists noradrenaline & phenylephrine, and sphingosine 1 phosphate) failed to produce robust calcium signals in my hands.

Earlier results I obtained (chapter 4) suggested that PGD_2-stimulated elevations of intracellular calcium were independent of the presence of extracellular calcium. In those studies (and the present ones) calcium sequestration with EGTA was not included so a lack of effect could have indicated the presence of sufficient residual calcium to allow normal transduction to proceed. The observation made in this chapter of PGD_2 & UTP response calcium-dependence was therefore unexpected. Because of the manner of data normalisation, the 10 % decrease in basal fluorescence associated with calcium removal from the assay buffer could have led to an approximately 25 % increase in the apparent agonist E_{max}. For this reason, data was corrected for the change in baseline. The conversion of PGD_2 response calcium-insensitivity in CHO $G\alpha_{16z49}$ $hCRTH_2$ cells to a state of calcium-sensitivity by incubation with PTX suggests that $G\beta\gamma_{i/o}$ coupling is insensitive to $Ca^{2+}{}_x$. However, this is at odds with the observation of calcium sensitivity in CHO K1 $hCRTH_2$ cells without PTX treatment. Assuming that this result is not an artefact of double-expression or antibiotic selection, these findings can only be reconciled by postulating some form of amplification associated with co-recruitment of $G\beta\gamma_{i/o}$ and $G\alpha_{16z49}$ to response generation and further data in support of this notion is discussed below. Thus, it now appears that PGD_2 elicits both mobilisation of intracellular calcium and simultaneous calcium influx through membrane located calcium channels. $G\beta\gamma$ subunits are known to activate L-type calcium channels (Viard, *et al.*, 2001) but these are not expressed on CHO cells (Yoshida, *et al*., 1992). A number of other voltage-independent calcium channels are expressed on CHO cells including TRP1 (store-operated) calcium channels (Vaca & Sampieri, 2002) and non-selective cation channels 1 & 2 (NSCC1 & 2; Kawanabe, *et al*., 2001). A simple linear scheme linking receptor activation, store depletion and channel opening cannot adequately accommodate all of these data whereas NSCCs are known to be activated by

GPCRs via $G\alpha_q$ and $G\alpha_{12/13}$ (Kawanabe, *et al*., 2003, 2004). If NSCC's are involved in the calcium dependence of PGD_2 responses in CHO K1 $hCRTH_2$ cells and in chimera-expressing cells following PTX treatment then their activation by $G_{i/o}$ and G_{16z49} subunits (or directly via β-arrestin) is implied and suggests that NSCC's are more promiscuous with respect to G-proteins than previously recognised. Furthermore, in almost perfect juxtaposition with the PGD_2 data is the UTP E/[A] curve right-shift with E_{max} *elevation* in the absence of calcium. This implies that $P2_{Y2}$ activation results in both calcium entry and ER release with the former occurring with higher agonist potency. The influx of extracellular calcium appears to *dampen* ER calcium release via an unknown negative feedback mechanism. Whilst UTP E/[A] curves were partially sensitive to PTX indicating mixed $G\alpha_{i/o}$ and $G\alpha_q$ coupling, the effect of calcium removal was unaltered by toxin treatment and therefore seems related to $G\alpha_q$ coupling for this agonist. Clearly, the net result of calcium influx across the plasma membrane (amplification or down-regulation of endoplasmic reticulum (ER) calcium release) depends on the panoply of molecular events accompanying receptor activation. Interestingly, these results are not consistent with the investigations made using various inhibitors of the transduction pathway. For both $hCRTH_2$ (chapter 4) and $P2_{Y2}$ calcium mobilisation was found to be wholly inhibited by U71322 (PLCβ inhibitor), thapsigargin (calcium store depleting agent) and, for $hCRTH_2$ only, by heparin (IP_3R inhibitor) suggesting that calcium was totally derived from the intracellular stores. However, in the presence of thapsigargin, both UTP and PGD_2 elicited inhibitory E/[A] curves which may relate to stimulation of the postulated $Ca^{2+}{}_x$-activated negative feedback mechanism – possibly involving a calcium-pump. To summarise: $hCRTH_2$ & $P2_{Y2}$ receptor activation both result in calcium entry across the plasma membrane in addition to release from the ER; calcium entry may involve NSCC's which may therefore display greater G-protein promiscuity than previously recognised; removal of extracellular calcium removes the postulated negative-feedback mechanism in ER calcium release for $G\alpha_q$ coupled $P2_{Y2}$ receptors, but decreases total calcium mobilisation for $G\beta\gamma_{i/o}$ or $G\alpha_{16z49}$ coupled $CRTH_2$ receptors, with no change in settings where $CRTH_2$ is coupled through both $G\beta\gamma_{i/o}$ and $G\alpha_{16z49}$ suggesting synergy between the latter two mechanisms.

Before examining the ability of PGD_2 and UTP to desensitise receptors to further agonist challenge, it was necessary to establish the time-course of agonist responses and

whether calcium fluxes returned to resting levels following agonist exposure. UTP generated fluorescence changes reached a maximum much more rapidly than PGD_2, presumably as a result of being both $G\alpha_q$ and $G\beta\gamma_{i/o}$ coupled with associated co-operative activation of PLCβ. Indeed, PGD_2 response maxima were also achieved in chimera-expressing cells more rapidly than in non chimera-expressing cells. Calcium levels rapidly returned to near-resting levels indicating activation of calcium sequestration / removal mechanisms: new steady-state levels were attained by 10 mins post-agonist exposure. The observation that the profile of calcium mobilisation and recovery was similar for both agonists in both cell types implies that the calcium pumps responsible for $[Ca^{2+}]_i$ normalisation were similarly expressed and activated under the diverse conditions employed. Fluorescence level recovery was more complete where $G_{i/o}$ signalling was inhibited by PTX but the difference was minor. Therefore, in subsequent experiments the 11min incubation used as standard post 1st addition was sufficient for $[Ca^{2+}]_i$ recovery before addition of the 2nd intervention.

PGD_2 produced potent, long-lasting desensitisation of $hCRTH_2$ receptors to subsequent PGD_2 challenge in both $hCRTH_2$ expressing cell lines (homologous desensitisation). In CHO $G\alpha_{16z49}$ $hCRTH_2$ cells this was characterised by two phases. The first (rapid) phase produced inhibition of both E_{max} and agonist pEC_{50}. The second (slow) phase resulted in further E_{max} inhibition but with no further change in agonist potency. By analogy with the behaviour of antagonists at receptors, changes such as these are consistent with a combination of receptor removal (cf. receptor alkylation experiments) and response uncoupling (cf. non competitive antagonists). The analogy cannot explain how the agonist response curves come to lie so far to the right of the occupancy curve (even allowing for the use of an agonist radioligand to determine binding) since a competitive antagonist has not been employed. The notion that PGD_2 itself, once it has elicited an agonist response, continues to occupy the receptors in the guise of a non-activating compound (antagonist) seems unsatisfactory since at first glance a molecule cannot change its intrinsic efficacy. However, if a temporally separated coupling of the receptor to another transduction pathway occurred then it is conceivable that the presence of the second coupling partner might confer an altered conformation on the receptor's ligand binding site and therefore alter affinity and / or efficacy through time. Furthermore, if the ligand were to combine with more than one site of interaction and was agonist at only one of these sites which had lower affinity for the agonist and which

desensitised on activation, then the response curve might lie to the right of the observed occupancy curve and the apparent agonist intrinsic efficacy might alter. Some support for this notion comes from the fact that if one calculates an apparent pA_2 based on control curve EC_{15} responses, the value obtained (7.8 ± 0.2) is similar to the K_d (8.6 ± 0.04) for this agonist and remains constant irrespective of the treated curve used. Indeed, other puzzling aspects of the pharmacology of this receptor might also be explained: the discrepant B_{max} values obtained either by saturation binding or by extrapolation from radioligand / protein linearity data (chapters 4 and 7); discrepant antagonist affinity values (chapter 3); putative agonist activity at high concentrations in the antagonist molecule GW853481X (chapter 7); multiphasic [^{3}H]-PGD_2 displacement curves (chapter 7). An alternative mechanism might involve allosteric modulation of the receptor by intracellular proteins recruited to it during the desensitisation process such as β-arrestin and G-protein coupled receptor kinases (GRKs; Reiter & Lefkowitz, 2006, for review) however, such modulation has not been previously reported. In the present studies, where inhibition curves were produced against varying PGD_2 EC_x concentrations, behaviour consistent with competitive interaction was not observed: IC_{50}'s tended toward a limiting value (CHO $G\alpha_{16z49}$ $hCRTH_2$ 6.2 ± 0.03; CHO K1 $hCRTH_2$ 6.6 ± 0.1) at [PGD_2] above EC_{100} in a manner reminiscent of an allosteric interaction.

Where PGD_2 EC_{70} was applied to cells 11min after E/[A] curve construction, the resulting IC_{50} lay 0.3 log units to the right of the EC_{50} for both the full agonist PGD_2 and the partial agonist 15 keto $PGF_{2\alpha}$. This implies a causal relationship between calcium mobilisation and desensitisation. However, concentrations of PGD_2 sub-threshold with respect to calcium mobilisation still produced noticeable (though non-significant) desensitisation at 30 min post-challenge. Although it is possible that low PGD_2 concentrations resulted in the mobilisation of calcium below the detection limit of the assay, this result seems to imply that desensitisation does not have an obligate requirement for calcium. In other words, desensitisation appears not to be a consequence of IP_3 generation, or of NSCC activation but could be related to cAMP inhibition or to β-arrestin recruitment (Mathiesen, *et al.*, 2005; see below). Because cAMP inhibition would be expected to reduce PKA activation, and therefore to reduce receptor phosphorylation, this mechanism seems an unlikely explanation. Indeed, involvement of PKA and PKC have both been excluded by the failure of the compounds

H89, dibutyryl cAMP and GF109203X to affect PGD_2-induced desensitisation. Thus the most probable mechanisms for PGD_2 stimulated $hCRTH_2$ receptor desensitisation are β-arrestin and GRK recruitment. Indeed, Gallant, *et al*. (2007) have now shown that when co-expressed in HEK293(T) cells along with various signalling molecules, CRTH2 recruits GRKs 2, 3 & 4 and is internalised via an arrestin 3 – dynamin dependent pathway. The data presented here suggests the presence of two desensitisation mechanisms which could relate to differential GRK recruitment, GRK-mediated vs. direct arrestin recruitment, ortho- and allo- steric agonist site occupation, activation of an alternative G-protein mediated desensitisation pathway, or perhaps temporal and spatial segregation of coupling partners such as that described by Shenoy and Lefkowitz (2005) for the angiotensin ATII receptor mediated activation of ERK1/2. Interestingly, Gallant, *et al*., produced approximate EC_{50} values for receptor internalisation of 70 – 180 nM, shifted to the right of agonist mediated cAMP accumulation EC_{50} values. However, the data I present here for functional desensitisation demonstrates approximately equivalent EC_{50} and IC_{50} values suggesting a difference between the coupling of desensitisation and internalisation. As demonstrated by Mathiesen, *et al.* (2005), β-arrestin recruitment by $hCRTH_2$ may display its own antagonist pharmacology and an examination of the desensitisation characteristics of the panel of agonists used in these studies will be presented in chapter 7. The lack of PKA / C involvement in desensitisation should have excluded the possibility of heterologous receptor desensitisation and this was generally observed to be the case (see below). These findings are contrary to those of Gallant, *et al*., (2007) who observed that both PKA- and PKC-dependent phosphorylation of the receptor were required for internalisation. Nonetheless, assuming that GRK activation is taking place, and that PKA / C activation is not occurring, even to a small extent, this result would imply that GRKs activated by one receptor molecule do not have the capacity to inhibit simultaneously-activated receptor molecules of another type lending further support to the specific relationship between GRK activation and receptor desensitisation propounded by Lefkowitz and others (Pierce, *et al*., 2002; Reiter & Lefkowitz, 2006).

A further aspect of homologous $hCRTH_2$ receptor desensitisation was revealed by experiments in which a PGD_2 dilution series was applied to cells previously exposed to the same dilution series. In these assays, it was observed that the magnitude of the inhibition was greater than the magnitude of the stimulation at low concentrations of

PGD_2 such that responses were completely ablated. This again implies a non-causal link between G-protein mediated sequelae of receptor activation and desensitisation. However, re-plotting the data as shown in Figure 20 suggests that two mechanisms may be in operation: a non PTX-sensitive desensitisation capable of completely inhibiting the response to low concentrations of PGD_2, and a second mechanism which appears to become more efficacious as [PGD_2] increases and which may be causally linked. Following PTX treatment, total inhibition was observed at all [PGD_2] tested in chimera-expressing cells suggesting that the mechanism in operation at low [PGD_2] is non $G\alpha_{i/o}$-protein dependent. Since the effect of PTX is to reduce overall response magnitude, the failure to observe the second mechanism coming into play may simply reflect insufficient calcium mobilisation to trigger it. One scenario might involve initial desensitisation through non G-protein activated GRKs 5 & 6 and possibly β-arrestin recruitment, while the second phase results from G-protein activated GRK recruitment.

Homologous desensitisation was also observed with UTP at $P2_{Y2}$ receptors but the process differed from $hCRTH_2$ receptor desensitisation in several respects: 1. No inhibition was observed until UTP EC_{30} was achieved. 2. Above UTP EC_{30} inhibition proceeded in a monophasic sigmoidal fashion, reaching maximum inhibition only at EC_{100}. 3. PTX treatment did not alter $P2_{Y2}$ desensitisation. No information regarding the molecular identity of the desensitisation partners has been generated here but the similarity between the monophasic inhibition of UTP responses and the second phase of the biphasic PGD_2 mediated desensitisation makes it tempting to speculate that these processes are similar. Furthermore, the first phase of $hCRTH_2$ receptor desensitisation is specific to this receptor and may be another indicator of non-G-protein mediated β-arrestin recruitment. Lastly, because the potency of the UTP desensitisation curve is right-shifted compared with the calcium mobilisation curve, a lack of signal amplification with respect to desensitisation is implied which is not typical of sequential activation of several steps in a cascade, each with a hyperbolic stimulus-effect relationship. Therefore, desensitisation may occur proximal to receptor stimulation (for example, Gβγ mediated GRK activation).

Similar experiments designed to detect heterologous desensitisation between $hCRTH_2$ and $P2_{Y2}$ receptors provided results critical to the interpretation of stimulus trafficking data presented in earlier chapters. Firstly, activation of each receptor type resulted in increased potency of responses through the other receptor in both $hCRTH_2$ receptor

expressing cell types *irrespective of PTX treatment* (with the sole exception of PGD_2 responses following UTP treatment in PTX-exposed CHO $G\alpha_{16z49}$ cells). In CHO K1 $hCRTH_2$ cells, but not chimera-expressing cells, this was accompanied by elevations in agonist maximal effects and is a critical finding: PTX has been assumed to produce 100 % $G_{i/o}$ inhibition but the ability of PGD_2 to elicit responses following UTP exposure in PTX treated cells clearly indicates that some calcium mobilisation activity remains which could be mediated by $G_{i/o}$ and since no evidence in support of an alternative coupling pathway has been obtained, this seems the most likely scenario. Secondly, the effect of $P2_{Y2}$ activation on PGD_2 E/[A] curves resulted in the latter becoming clearly biphasic (Figure 18). In both $hCRTH_2$ expressing cell lines, phase 1 of PGD_2 responses had higher potency than PGD_2 in non-UTP exposed cells; phase 2 was of lower potency and in CHO $G\alpha_{16z49}$ cells resulted in the production of a similar E_{max} to that obtained in non-UTP treated cells. However, in CHO K1 $hCRTH_2$ cells, E_{max} was enhanced by c. 50 % representing the amplifying effect of simultaneous $G\alpha_{q/11}$ and $G\beta\gamma_{i/o}$ activation. In chimera-expressing cells the chimera and $G\beta\gamma_{i/o}$ may therefore synergise to produce the overall response observed. Since the $G\alpha_{16}$ backbone of the chimera belongs to the $G_{q/11}$ family of G-proteins this seems probable and presumably takes place at the level of PLCβ (Cordeaux & Hill, 2002; Werry, *et al*., 2003), though this is not proven and other mechanisms may be involved. Taken together, then, these two pieces of data suggest that under the conditions employed in earlier chapters under which trafficked agonist responses were observed, synergising interactions could have been taking place, at least in chimera-expressing cells. Interestingly, in the absence of extracellular calcium, PGD_2 responses were still potentiated but in a monophasic fashion leading to considerably higher agonist potency. This suggests that the synergising interaction leads to greater release of intracellular calcium and reveals again the presence of a calcium reducing mechanism triggered in the presence of extracellular calcium. Finally, it is possible to extract some comparisons from figures 2, 3 and 4 in which a fixed concentration of indomethacin (3μM) has been used to pre-treat cells in which UTP E/[A] curves were subsequently produced. Despite the methodological differences, similar effects on UTP potency & maximum effect have been produced suggesting that the effects seen are related to the receptor rather than specifically to the agonist used.

Trafficked responses could therefore be reflections of altered synergy, which in itself is a form of stimulus trafficking, but may not have the simple relationship to G-protein

activation first assumed. Indeed, in both $hCRTH_2$ expressing cell lines, differences in relative activity could represent differing abilities to trigger synergising interactions. Two possibilities arise from this: 1. F series prostanoids are largely partial because as a class they cannot trigger synergism; and opposed to this 2. F series molecules are inactive in CHO K1 $hCRTH_2$ cells precisely because they *do* rely on a synergistic interaction which is not available to them in these cells. In chimera-expressing cells under normal conditions it seems very likely that synergism is occurring but what about in CHO K1 $hCRTH_2$ cells and chimera-expressing cells following PTX treatment? Whilst the data do show that PTX inhibition of $G_{i/o}$ is not total, the residual PGD_2 mediated calcium mobilisation in PTX treated CHO K1 $hCRTH_2$ cells under synergising conditions is barely detectable. Furthermore, in experiments where twice the density (4×10^5 well^{-1}) of CHO $G\alpha_{16z49}$ $hCRTH_2$ cells were plated out and treated with the same PTX concentration PGD_2 E/[A] curves were identical to those produced under standard conditions suggesting that 50 ng ml^{-1} PTX for 18 hr produces a very high degree of blockade. In chimera-expressing cells PTX treatment produces a profound reduction in E_{max} and rightward shift in potency indicative of interruption of the synergising interaction. Synergistic interactions would require simultaneous $G_{i/o}$ and $G\alpha_q$ activation. The data presented here suggest that this does not occur except in non-PTX treated chimera-expressing cells. Finally, while there is no evidence of an unobserved $G\alpha_q$ activation through an undetected or unknown transduction pathway, for example through endogenous release of arachidonic acid for which flurbiprofen has been included in the cell culture medium, or constitutive receptor activation in a G_q coupled pathway, no experiments specifically designed to look for it have been conducted. Taken together, then, while synergising interactions have not been ruled out requiring their consideration as a possible contaminant of stimulus trafficking data, the likely impact is small and could possibly be related to certain specific molecules.

In addition to altering the emphasis placed on stimulus trafficking data these data cast new light on other aspects of the data gathered during this project. If $G\alpha_{16z49}$ and $G\beta\gamma_{i/o}$ synergise under 'normal' conditions in CHO $G\alpha_{16z49}$ $hCRTH_2$ cells then this may explain the lack of sensitivity to extracellular calcium until PTX treatment effectively disrupts the synergising interaction. The transduction cascade resulting from prostanoid $hCRTH_2$ receptor activation presented in chapter 4 therefore needs some revision (Figure 21). The larger number of [^{3}H]-PGD_2 binding sites detected in CHO $G\alpha_{16z49}$

$hCRTH_2$ cell membranes may not reflect altered receptor or G-protein expression but rather may indicate altered G-protein or β-arrestin recruitment. Therefore the R:G stoichiometry relevant to response generation in PTX treated chimera-expressing cells is unknown. Similarly, responses to E-series prostaglandins observed in chimera-expressing host cells may have arisen through a synergising interaction between a poorly expressed population of $G_{i/o}$ coupled EP receptors (EP_3?) and the chimera. Finally, the method of GTPγS assay employed in chapter 5 did not utilise antibody capture techniques but it is now clearly vital to establish which G-proteins accumulated [^{35}S]-GTPγS in response to PGD_2.

Synergistic interactions involving $CRTH_2$ receptors have been postulated to account for the supramaximal effects of 15 deoxy $\Delta^{12,14}$ PGJ_2 at the receptor in transfected L1.2 cell migration and calcium mobilisation assays (Sugimoto, *et al*., 2005) but to date no direct evidence has been gathered. Indeed, biphasic E/[A] curves with amplified maximum effects have been observed for PGD_2 in an eosinophil shape change assay (Böhm, *et al*., 2004). These authors also attributed PTX-insensitive calcium mobilisation to $G\alpha_{q/11}$ activation though this may instead reflect $G\alpha_z$ mediation (but see Chapter 4: $G\alpha_z$ coupling in CHO cells is unlikely). Mast cells, the likely physiological source of inflammatory-cell recruiting PGD_2, also produce other agents which have the potential to synergise with $CRTH_2$ receptor activation such as histamine, platelet activating factor (PAF), thromboxane A_2, leukotrienes B4, C4 & D4 and eotaxin, while T-cells (which also secrete PGD_2 (Tanaka, *et a*l., 2000)) produce cytokines such as IL-4 and IFNγ. Such interactions are likely to have physiological relevance in inflammatory cells expressing the receptor. For example, in addition to expressing PLCγ-activating T-cell receptor (TCR)/CD_3 complexes (Chan, *et al*., 1992; Pezzicoli & Baldari, 2005), T-cells also express PLCβ-activating $G_{i/o}$ coupled CCR3, 4, 5 and 7 chemokine receptors (Alexander *et al*., 2006; Abbas & Lichtman, 2003). Co-activation of the latter receptors might reasonably be expected to contribute to whole cell IP_3 and DAG levels in an additive fashion (ignoring the impact of factors such as compartmentalisation and signalling complex association). However, as Werry, *et al*. (2003) point out, synergising interactions could theoretically arise at multiple points in the transduction cascades dependent upon the precise molecular species activated in each pathway. Of greater potential interest, though, is the observation that TCR activates PLCγ1 through activation of an intermediary protein tyrosine kinase, Zap70, which phosphorylates

PLCγ1 at Y319 (Pezzicoli & Baldari, 2005). PLCβ also contains multiple targets for serine, threonine and tyrosine protein kinases and it has been noted previously that PKA or PKC mediated phosphorylation of PLC isoforms can variously lead to stimulation or inhibition depending upon the context (Werry, *et al*., 2003, for review). Although the potential for this interaction has long been recognised (e.g. Selbie & Hill, 1998) there is a huge gap in the scientific literature concerning this point: can immune cell receptors trigger synergising interactions with chemokine / chemoattractant receptors through phosphorylation of key molecules at convergent points in their signalling cascades? Another aspect of cascade convergence also deserves mention: Phospholipases Cβ & Cγ1 use the same substrate, phosphoinositide 4,5 biphosphate as well as the pro-inflammatory phosphoinositide 3 kinase (PI3K) group of enzymes. One can reasonably expect these enzymes to compete with each other for substrate, particularly under conditions where substrate is limiting. The interaction at this level is likely to be complex: PI3Kγ can be activated by Gβγ subunits with apparently no preference for particular βγ complex combinations (Vanhaesenbroeck, *et al.*, 2001) while PI3Kδ in T-cells is activated downstream of TCR activation. Indeed, Stubbs, *et al*. (2002), have noted that indomethacin & PGD_2 can elicit activation of LY-294002-sensitive PI3K in [human?] eosinophils & basophils although this was in an apparently PTX-insensitive system. Both PI3K activation, and Pyk2 activation arising from Ca^{2+} mobilisation can converge upon c-Src activation resulting in another level of cross-talk (reviewed in Selbie & Hill, 1998). Once activated, these pathways are likely to compete for phosphoinositide lipids resulting in fine-tuning of the overall response (Figure 21). Recently, activation of PI3K enzymes (presumed to be PI3Kδ and therefore Gβγ mediated) by $CRTH_2$ has been demonstrated confirming the value of studying this area of transduction (Xue, *et al*., 2006).

In the next chapter I will examine the desensitisation pharmacology of a series of prostanoid molecules, and expand on the characteristics of selected 'atypical' compounds, before drawing my conclusions from this thesis.

6.5 Figure caption list:

Figure 1. UTP and PGD_2 E/[A] curves in CHO $G\alpha_{16z49}$ $hCRTH_2$ and CHO K1 $hCRTH_2$ cells with and without calcium in the assay buffer following PTX treatment (where applicable). Buffer did not contain EGTA. Data are mean ± sem of three independent experiments.

Figure 2. Effect of inhibitors of cell signalling molecules on UTP E/[A] curves in CHO K1 $hCRTH_2$ cells. All inhibitors were added at 3μM final assay concentration in 0.25 % DMSO vehicle. Data are mean ± sd of three independent experiments.

Figure 3. Effect of inhibitors of cell signalling molecules on UTP E/[A] curves in CHO $G\alpha_{16z49}$ $hCRTH_2$ cells. All inhibitors were added at 3 μM final assay concentration in 0.25 % DMSO vehicle. Data are mean ± sd of three independent experiments.

Figure 4. Effect of inhibitors of cell signalling molecules on UTP E/[A] curves in CHO $G\alpha_{16z49}$ $hCRTH_2$ cells treated with PTX. All inhibitors were added at 3 μM final assay concentration in 0.25 % DMSO vehicle. Data are mean ± sd of three independent experiments.

Figure 5. Representative calcium flux time courses in response to exposure of cells to 10 μM PGD_2 or 30 μM UTP (representing EC_{100} for each agonist) in CHO $G\alpha_{16z49}$ $hCRTH_2$ (blue lines) and CHO K1 $hCRTH_2$ (black lines) cells.

Figure 6. Time course of PGD_2 and UTP stimulated calcium transients in CHO $G\alpha_{16z49}$ $hCRTH_2$ cells with and without PTX treatment. Agonist concentrations were as

indicated in figure legends. Basal fluorescence at the start of the experiment was subtracted from all data. Data are mean ± sem of six determinations from three independent experiments.

Figure 7. Time course of PGD_2 and UTP stimulated calcium transients in CHO K1 $hCRTH_2$ cells with and without PTX treatment. Agonist concentrations were as indicated in figure legends. Basal fluorescence at the start of the experiment was subtracted from all data. Data are mean ± sem of six determinations from three independent experiments.

Figure 8. Representative data showing effect of vehicle addition on fluorescence in CHO K1 $hCRTH_2$ cells without PTX treatment. Basal fluorescence at the start of the experiment was subtracted from all data.

Figure 9. Desensitising effect of fixed PGD_2 EC_x concentrations on subsequent PGD_2 E/[A] curve generation in CHO $G\alpha_{16z49}$ $hCRTH_2$ cells without PTX treatment at 5 mins post exposure to 1st treatment (see *Methods* for details). Data are mean ± sem of three independent experiments.

Figure 10. Desensitising effect of fixed PGD_2 EC_x concentrations on subsequent response to 10 μM PGD_2 (top panel) and PGD_2 E/[A] curve pEC_{50} (bottom panel) in CHO $G\alpha_{16z49}$ $hCRTH_2$ cells without PTX treatment at varying times post exposure to 1st treatment (see *Methods* for details). Data points absent from pEC_{50} data plot following 10 μM PGD_2 first treatment represent points where curve fitting could not be achieved

due to the small response sizes obtained. Data are mean ± sem of three independent experiments.

Figure 11. Concentration / fractional occupancy curve calculated from saturation binding data presented in chapter 4 (using an average K_d for the two $hCRTH_2$ expressing cell lines of 2.5 nM) plotted with a concentration / fractional response curve for PGD_2 based on control curve data in $CHOG\alpha_{16z49}$ $hCRTH_2$ cells.

Figure 12. Activation and inhibition PGD_2 E/[A] curves in CHO $G\alpha_{16z49}$ $hCRTH_2$ cells. Activation curve (positive-going, resulting in an EC_{50}) was prepared as normal. Inhibition curve (negative going resulting in an IC_{50}) was prepared by adding PGD_2 EC_{70} to cells 11 min after PGD_2 'activation curve' was added. Data are mean ± sem of three independent experiments.

Figure 13. Effect of adding the PKA inhibitor H89, the PKA activator dibutyryl cyclic adenosine monophosphate (dbcAMP), the PKC inhibitor GF109203X (GF), vehicle (veh; 0.25 % DMSO) or combinations as indicated on basal fluorescence in CHO $G\alpha_{16z49}$ $hCRTH_2$ and CHO K1 $hCRTH_2$ cells. Data are mean ± sem of three independent experiments.

Figure 14. Effect of adding the PKA inhibitor H89, the PKA activator dibutyryl cyclic adenosine monophosphate (dbcAMP), the PKC inhibitor GF109203X (GF), vehicle (veh; 0.25 % DMSO) or combinations as indicated on 1st treatment PGD_2 E/[A] curves in CHO $G\alpha_{16z49}$ $hCRTH_2$ and CHO K1 $hCRTH_2$ cells. Data are mean ± sem of three independent experiments.

Figure 15. Effect of adding the PKA inhibitor H89, the PKA activator dibutyryl cyclic adenosine monophosphate (dbcAMP), the PKC inhibitor GF109203X (GF), vehicle (veh; 0.25 % DMSO) or combinations as indicated on 2nd treatment PGD_2 inhibition curve pIC_{50} in CHO $G\alpha_{16z49}$ $hCRTH_2$ and CHO K1 $hCRTH_2$ cells. Data are mean ± sem of three independent experiments.

Figure 16. Effect of adding the PKA inhibitor H89, the PKA activator dibutyryl cyclic adenosine monophosphate (dbcAMP), the PKC inhibitor GF109203X (GF), vehicle (veh; 0.25 % DMSO) or combinations as indicated on 2nd treatment PGD_2 inhibition curve I_{max} in CHO $G\alpha_{16z49}$ $hCRTH_2$ and CHO K1 $hCRTH_2$ cells. Data are mean ± sem of three independent experiments.

Figure 17. Desensitisation of PGD_2 and UTP stimulated calcium mobilisation in CHO $G\alpha_{16z49}$ $hCRTH_2$ and CHO K1 $hCRTH_2$ cells with and without PTX treatment. Agonist dilution series (2nd treatment) were added to cells previously exposed to a dilution series of the same agonist (1st treatment) such that each well received the same concentration of agonist twice. Data are mean ± sem of three independent experiments.

Figure 18. Synergy between PGD_2 and UTP stimulated calcium mobilisation in CHO $G\alpha_{16z49}$ $hCRTH_2$ and CHO K1 $hCRTH_2$ cells with and without PTX treatment. Agonist dilution series (2nd treatment) were added to cells previously exposed to a dilution series of the other agonist (1st treatment) such that wells received concentrations of PGD_2 followed by UTP or *vice versa*. Data are mean ± sem of three independent experiments.

Figure 19. PGD_2 E/[A] curves (2nd treatment) in CHO $G\alpha_{16z49}$ $hCRTH_2$ and CHO K1 $hCRTH_2$ cells following UTP exposure (1st treatment) in the absence of calcium in the assay buffer. EGTA was not added. Data are mean ± sem of three independent experiments.

Figure 20. Data presented in Figure 17. replotted as % inhibition (wrt. control curve calcium mobilisation) vs. PGD_2 concentration for agonists undergoing homologous desensitisation in CHO $G\alpha_{16z49}$ $hCRTH_2$ cells. Data are mean ± sem of three independent experiments.

Figure 21. Schematic representation of signal transduction pathways in CHO $G\alpha_{16z49}$ $hCRTH_2$ cells based on data described here and in chapter 4. Abbreviations: $hCRTH_2$ – human chemoattractant receptor homologous molecule of Th2 cells; Gα & Gβγ – alpha subunit and beta/gamma subunit complex of GTP-binding protein; PLCβ/γ – phospholipase C β or γ; PIP_2 – phosphatidyl inositol diphosphate; DAG – diacyl glycerol; IP_3 – inositol (1,4,5) triphosphate; IP_3R – inositol (1,4,5) triphosphate receptor; ER – endoplasmic reticulum; MAPK – mitogen activated protein kinase; GRK – G-protein coupled receptor kinase; NSCC – non-specific cation channel; PKC – protein kinase C; Ad cyc – adenylate cyclase. Blue arrows indicate steps supported by evidence generated in this thesis; shaded arrows indicate steps supported by evidence presented in the literature; dashed arrows indicate postulated links. Red and yellow highlighting indicates possible points of synergy in cascade.

6.6 Figures

Follow on next page.

Figure 1.

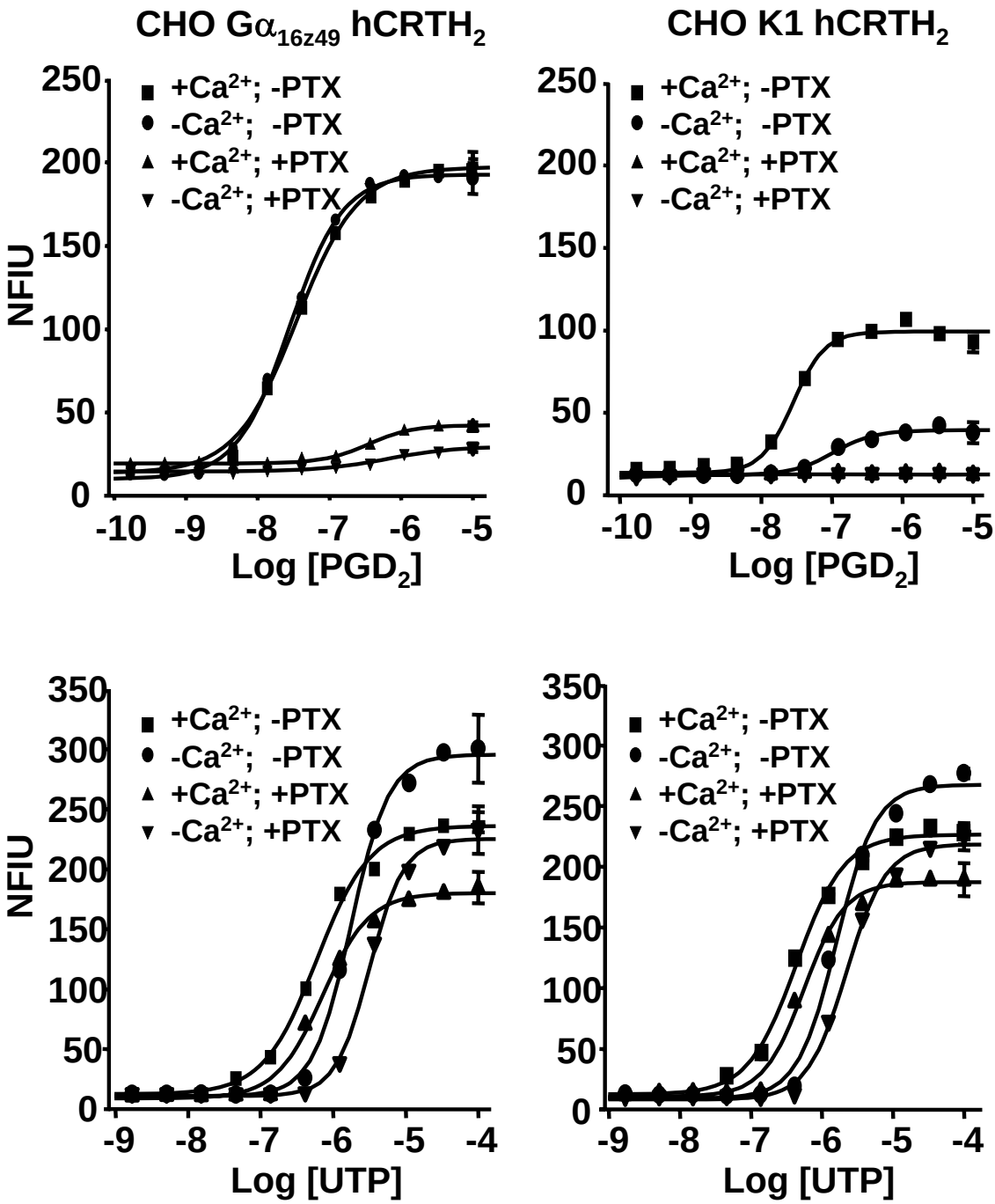
CHO Gα16z49 hCRTH2
CHO K1 hCRTH2
+Ca2+; -PTX
-Ca2+; -PTX
+Ca2+; +PTX
-Ca2+; +PTX
NFIU
Log [PGD2]
Log [UTP]
250
200
150
100
50
0
350
300
-10
-9
-8
-7
-6
-5
-4

Figure 2.

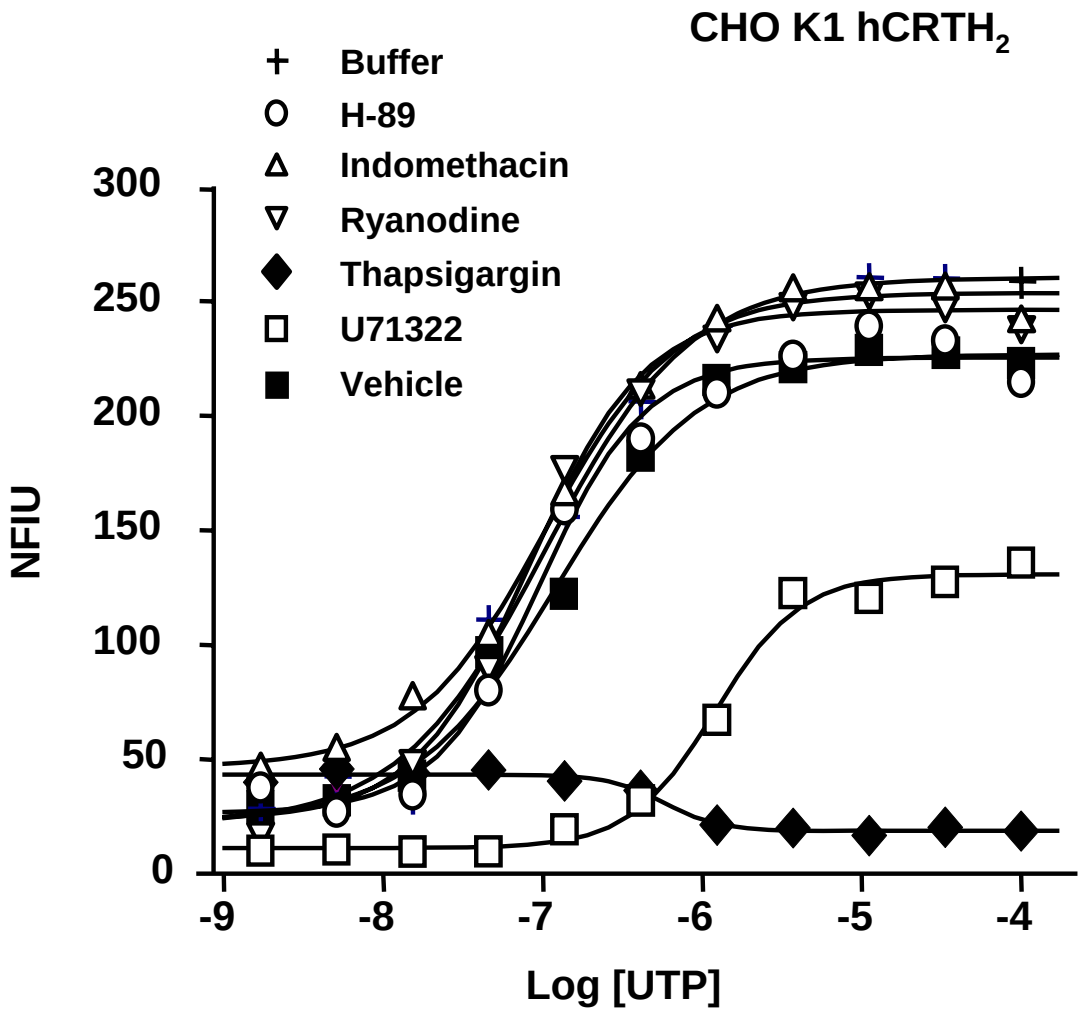
CHO K1 hCRTH2
Buffer
H-89
Indomethacin
Ryanodine
Thapsigargin
U71322
Vehicle
NFIU
300
250
200
150
100
50
0
-9
-8
-7
-6
-5
-4
Log [UTP]

Figure 3.

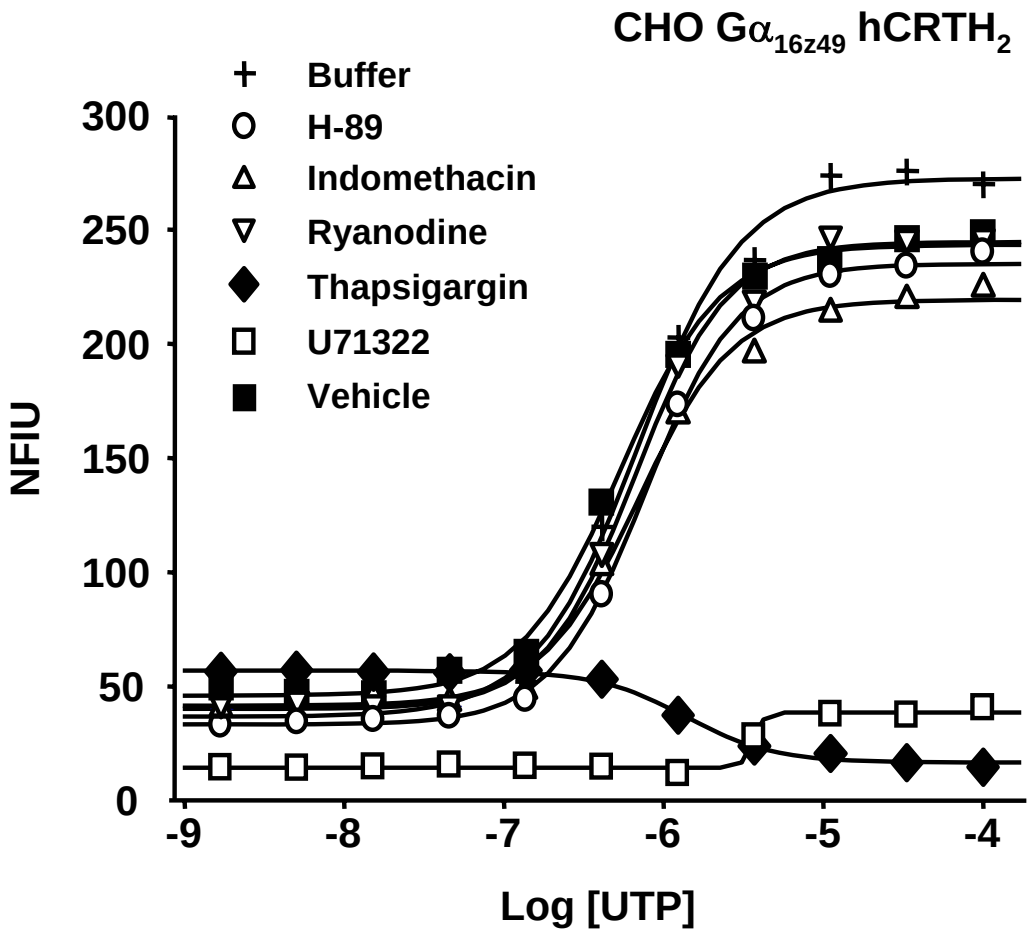
CHO Gα16z49 hCRTH2
Buffer
H-89
Indomethacin
Ryanodine
Thapsigargin
U71322
Vehicle
NFIU
300
250
200
150
100
50
0
-9
-8
-7
-6
-5
-4
Log [UTP]

Figure 4.

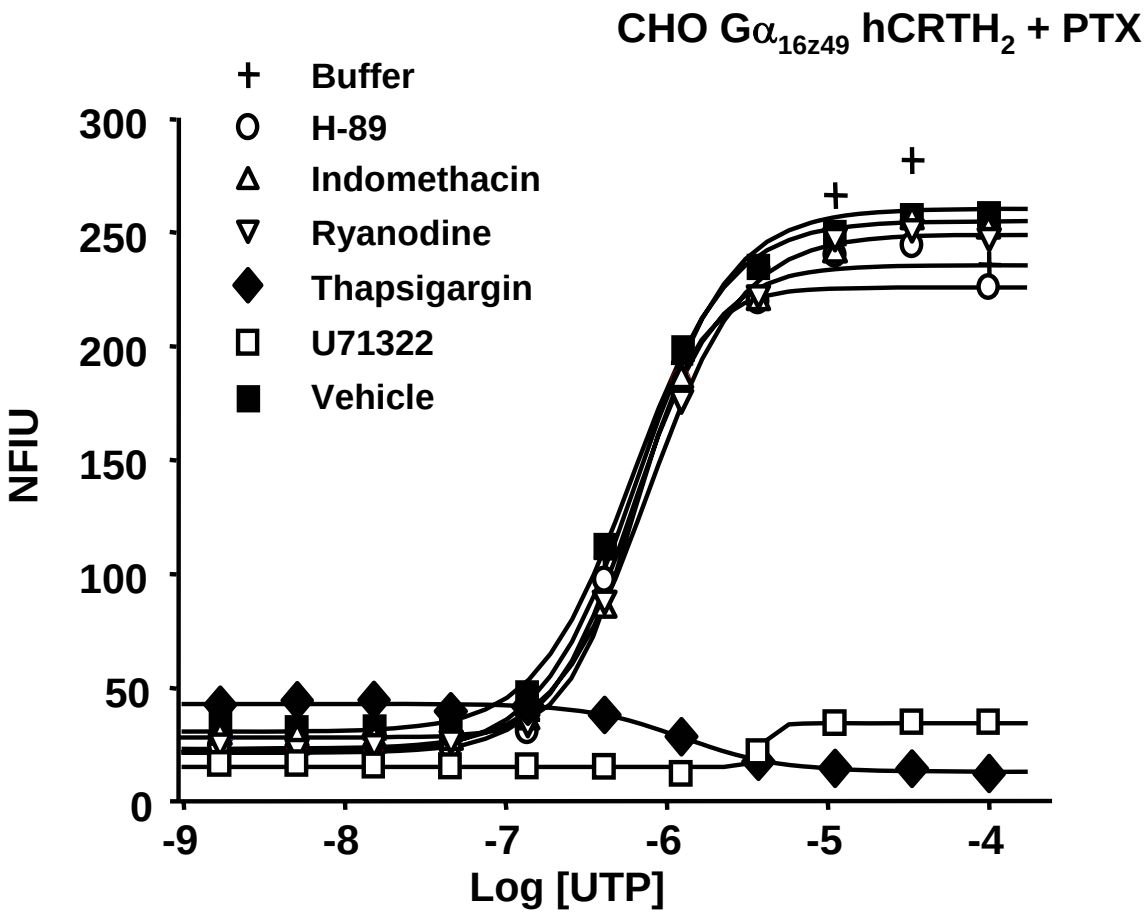
CHO Gα16z49 hCRTH2 + PTX
Buffer
H-89
Indomethacin
Ryanodine
Thapsigargin
U71322
Vehicle
NFIU
300
250
200
150
100
50
0
-9
-8
-7
-6
-5
-4
Log [UTP]

Figure 5.

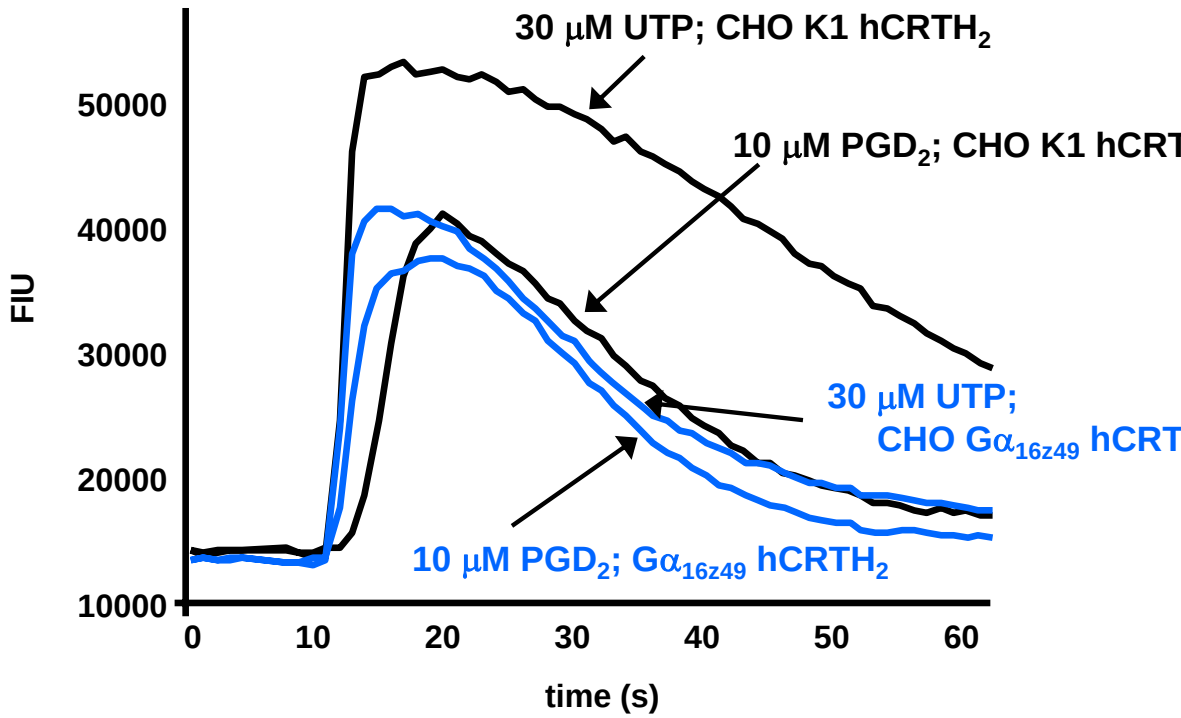
30 μM UTP; CHO K1 hCRTH2
10 μM PGD2; CHO K1 hCRT
30 μM UTP;
CHO Gα16z49 hCRT
10 μM PGD2; Gα16z49 hCRTH2
FIU
50000
40000
30000
20000
10000
0
10
20
30
40
50
60
time (s)

Figure 6.

CHO K1 hCRTH$_2$

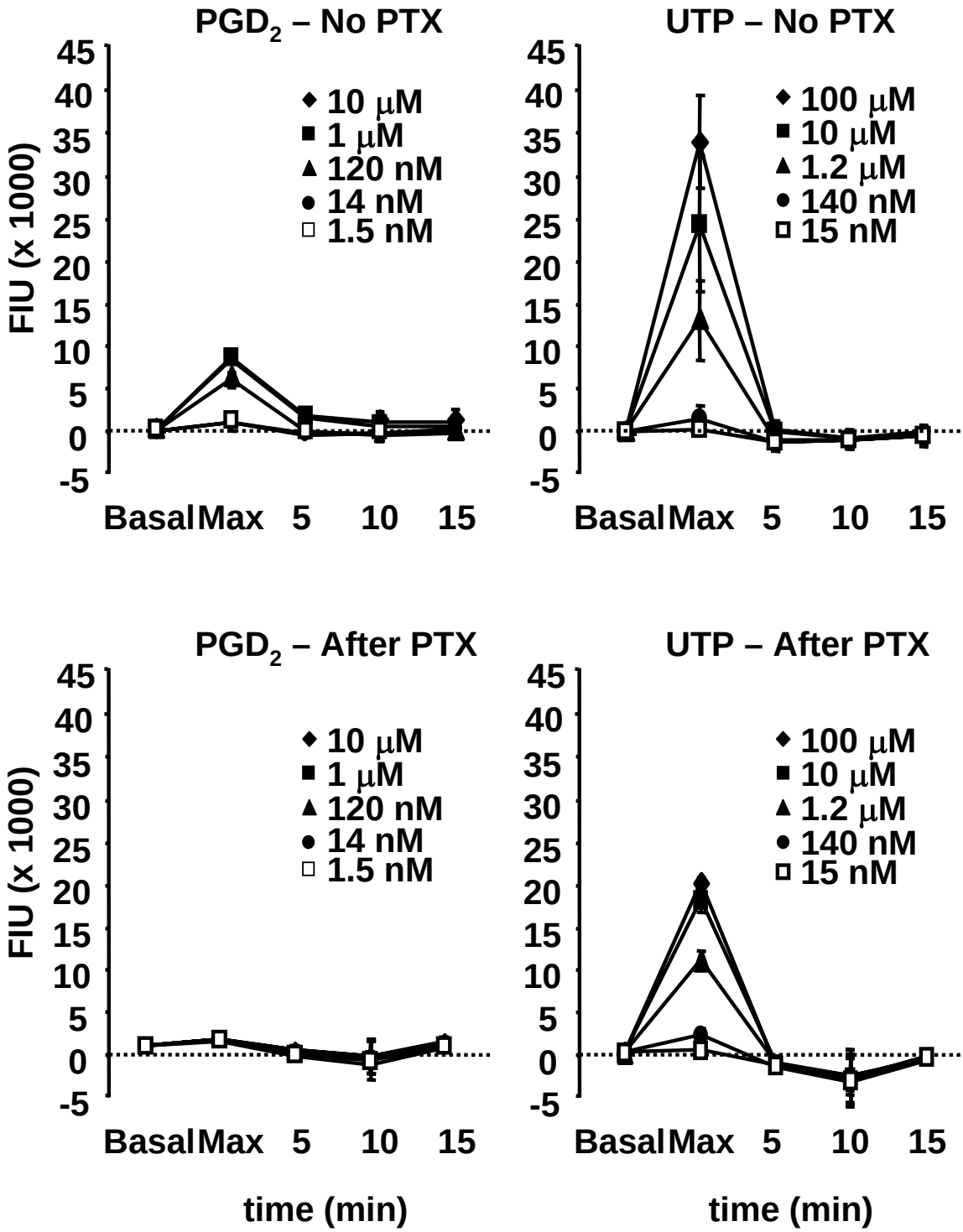

Figure 7.

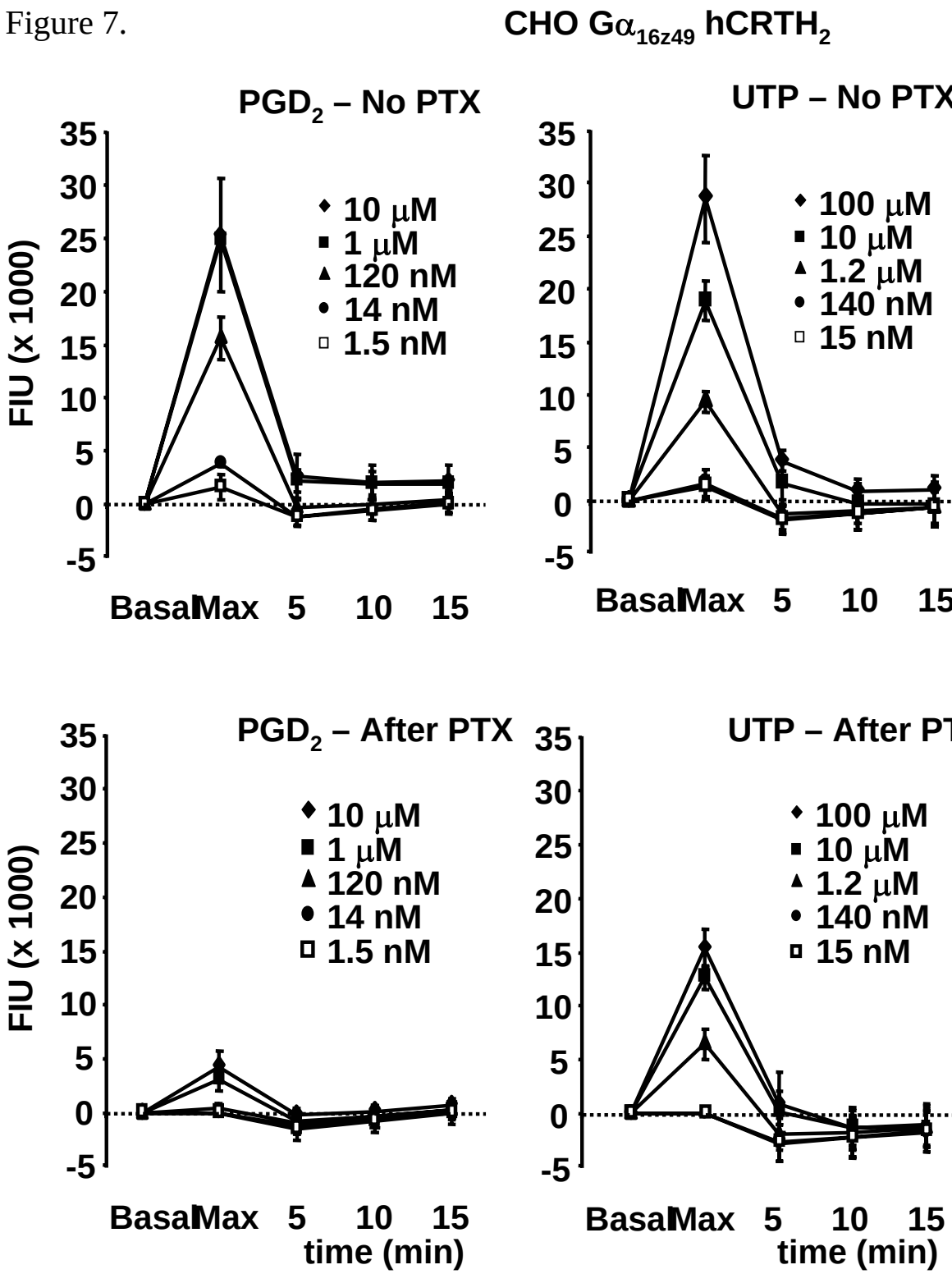
CHO Gα16z49 hCRTH2
PGD2 – No PTX
10 μM
1 μM
120 nM
14 nM
1.5 nM
UTP – No PTX
100 μM
10 μM
1.2 μM
140 nM
15 nM
PGD2 – After PTX
10 μM
1 μM
120 nM
14 nM
1.5 nM
UTP – After PT
100 μM
10 μM
1.2 μM
140 nM
15 nM
FIU (x 1000)
35
30
25
20
15
10
5
0
-5
Basal
Max
5
10
15
time (min)

Figure 8.

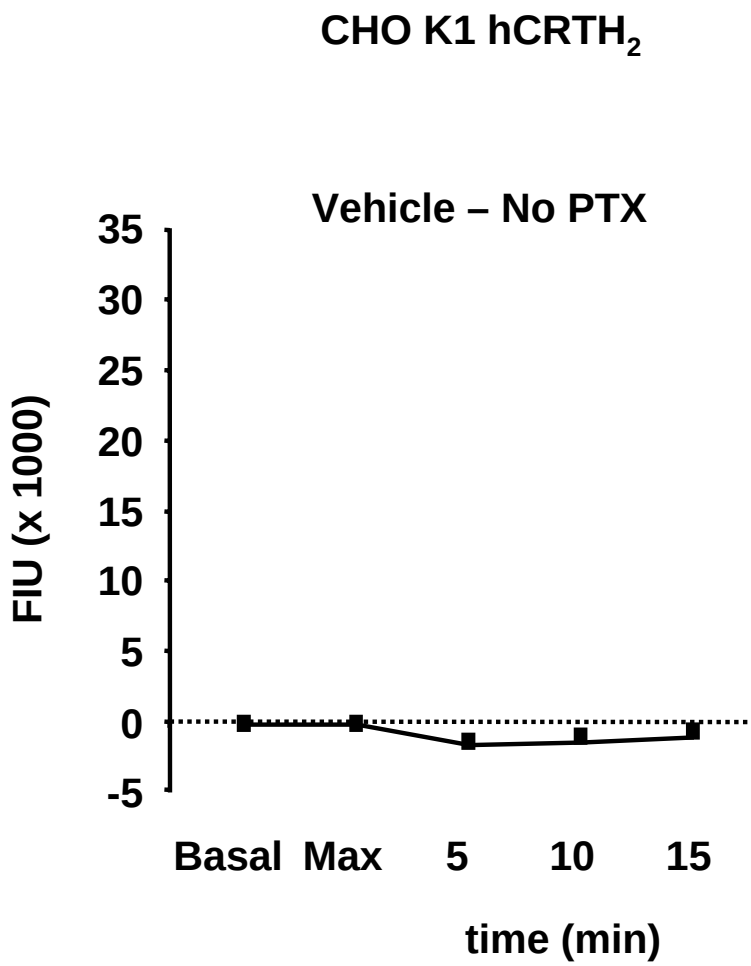
CHO K1 hCRTH2
Vehicle – No PTX
FIU (x 1000)
35
30
25
20
15
10
5
0
-5
Basal
Max
5
10
15
time (min)

Figure 9.

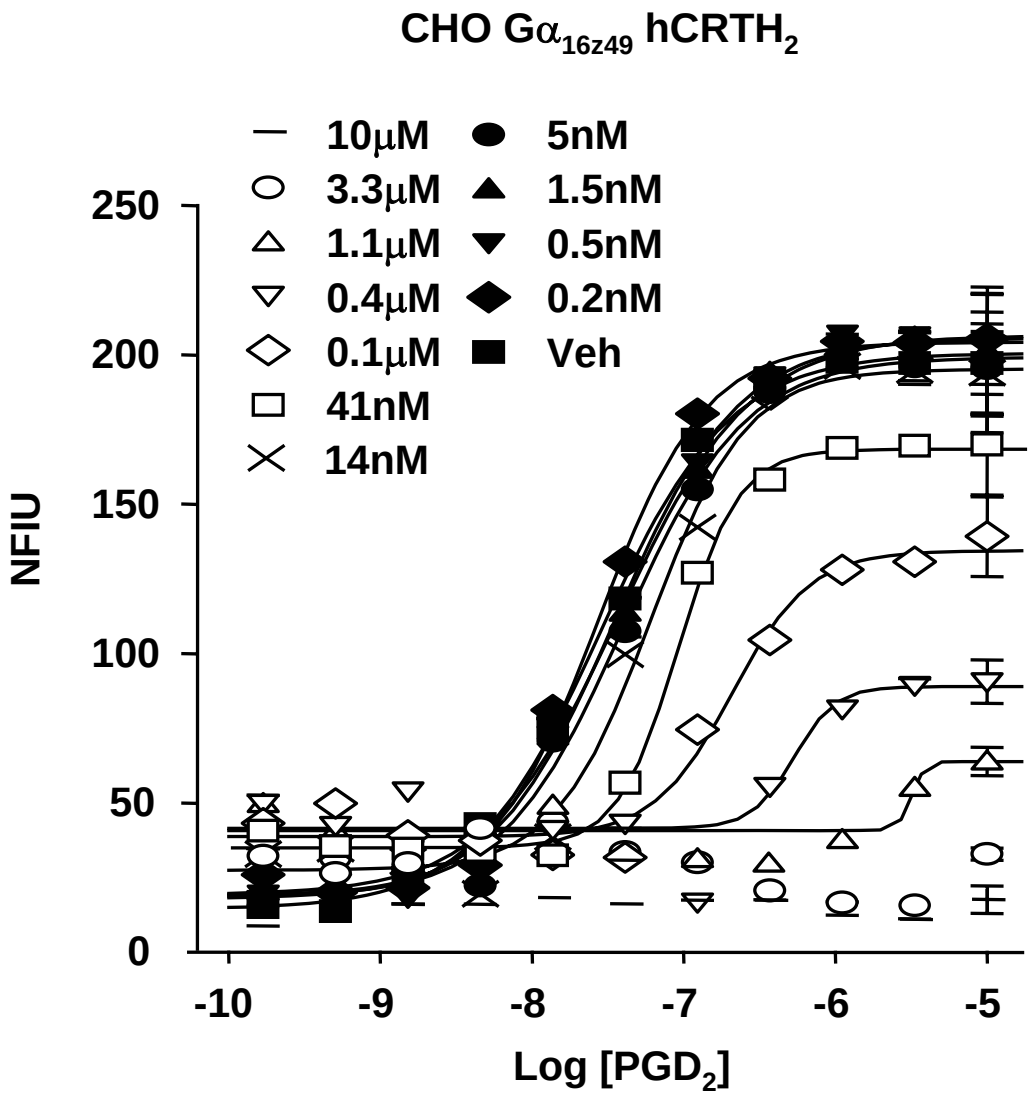
CHO Gα16z49 hCRTH2
10μM
3.3μM
1.1μM
0.4μM
0.1μM
41nM
14nM
5nM
1.5nM
0.5nM
0.2nM
Veh
NFIU
250
200
150
100
50
0
-10
-9
-8
-7
-6
-5
Log [PGD2]

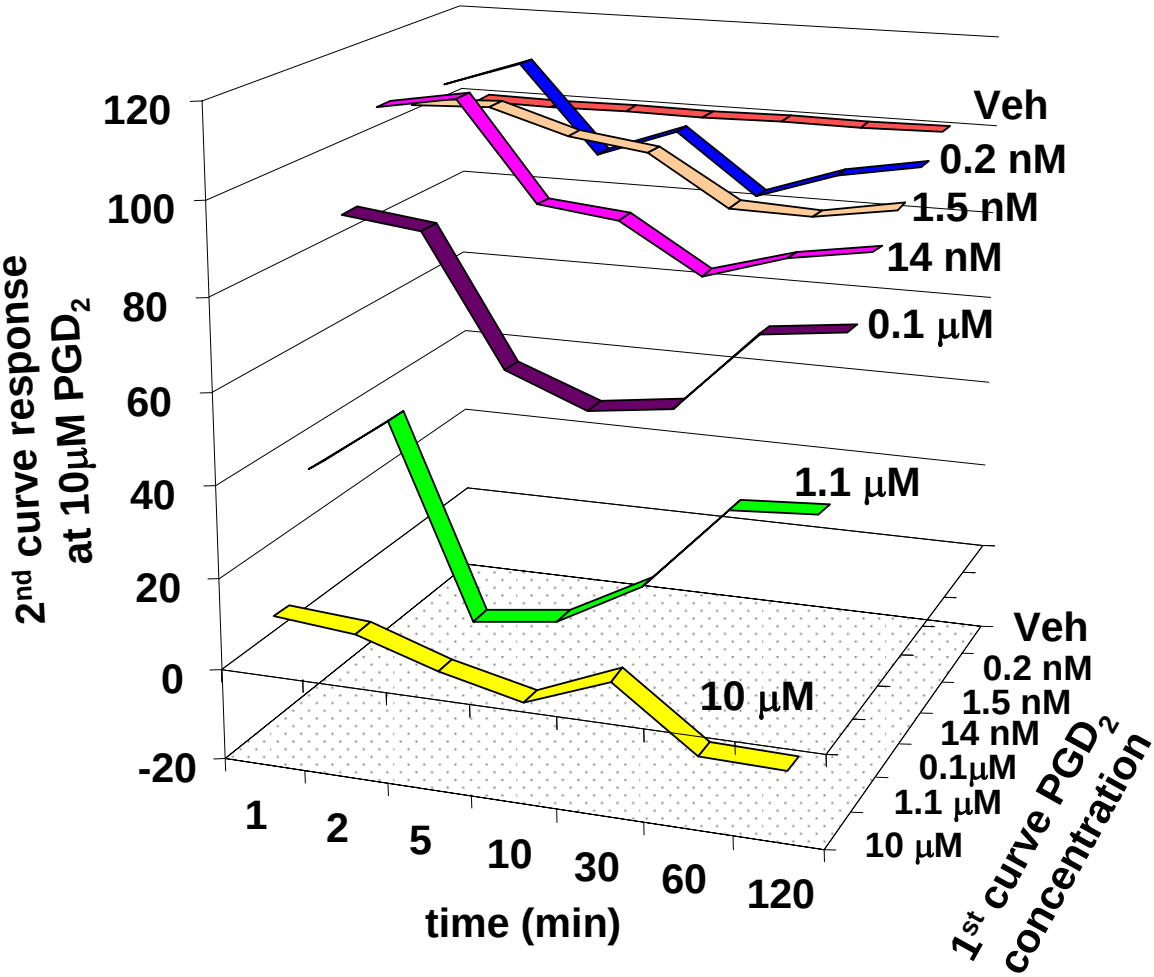
2nd curve response at 10μM PGD2
120
100
80
60
40
20
0
-20
Veh
0.2 nM
1.5 nM
14 nM
0.1 μM
1.1 μM
10 μM
1
2
5
10
30
60
120
time (min)
Veh
0.2 nM
1.5 nM
14 nM
0.1μM
1.1 μM
10 μM
1st curve PGD2 concentration

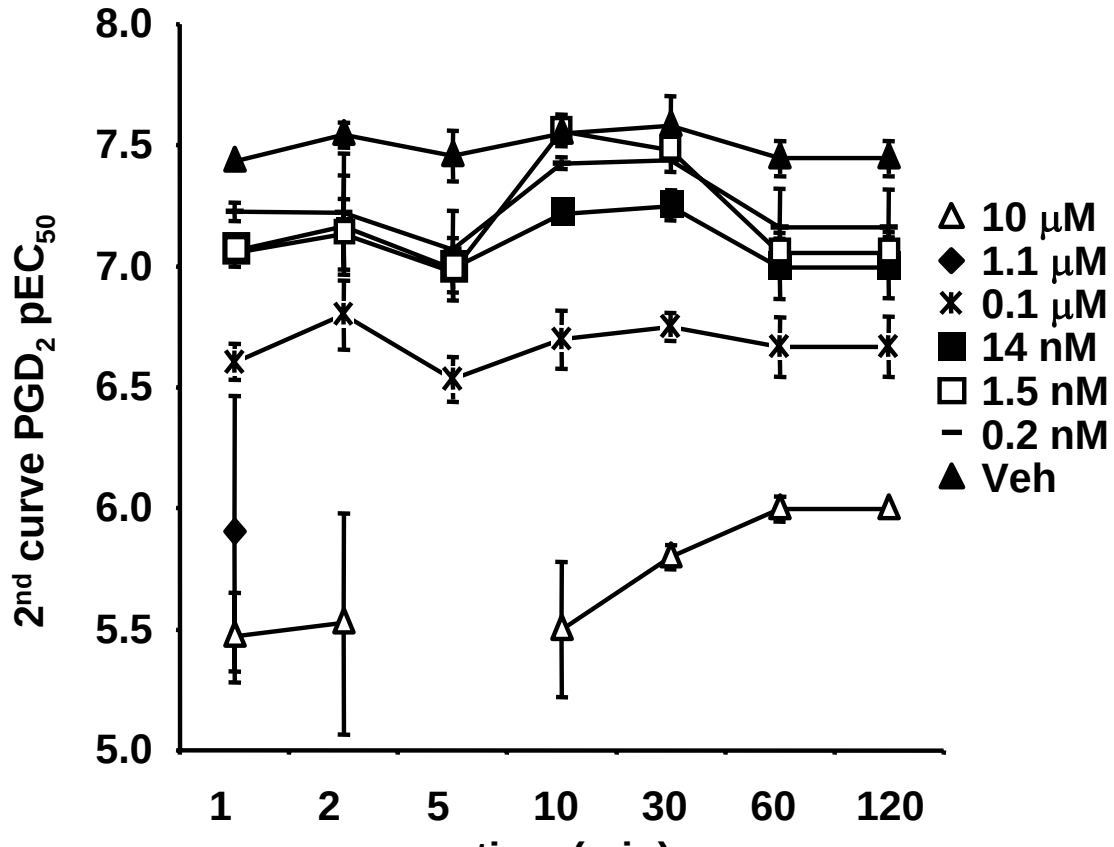
2nd curve PGD2 pEC50
8.0
7.5
7.0
6.5
6.0
5.5
5.0
1
2
5
10
30
60
120
10 μM
1.1 μM
0.1 μM
14 nM
1.5 nM
0.2 nM
Veh

Figure 11.

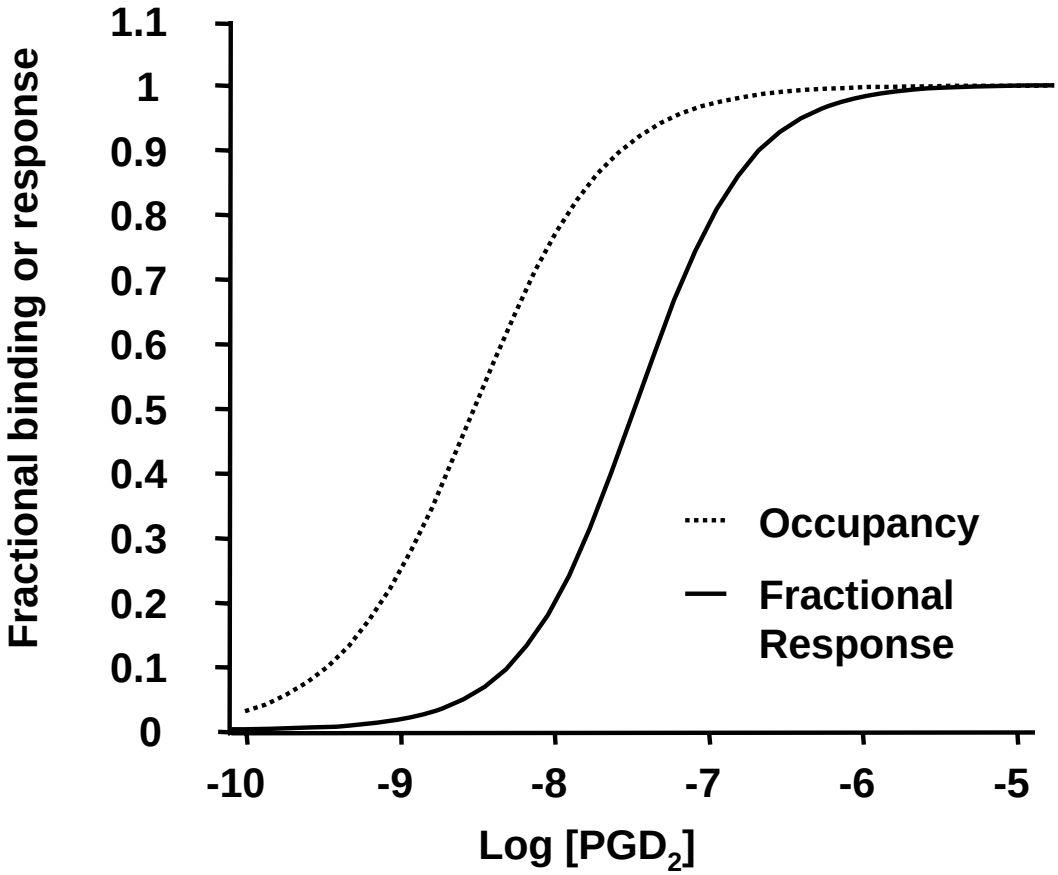
Fractional binding or response
1.1
1
0.9
0.8
0.7
0.6
0.5
0.4
0.3
0.2
0.1
0
-10
-9
-8
-7
-6
-5
Log [PGD2]
Occupancy
Fractional Response

Figure 12.

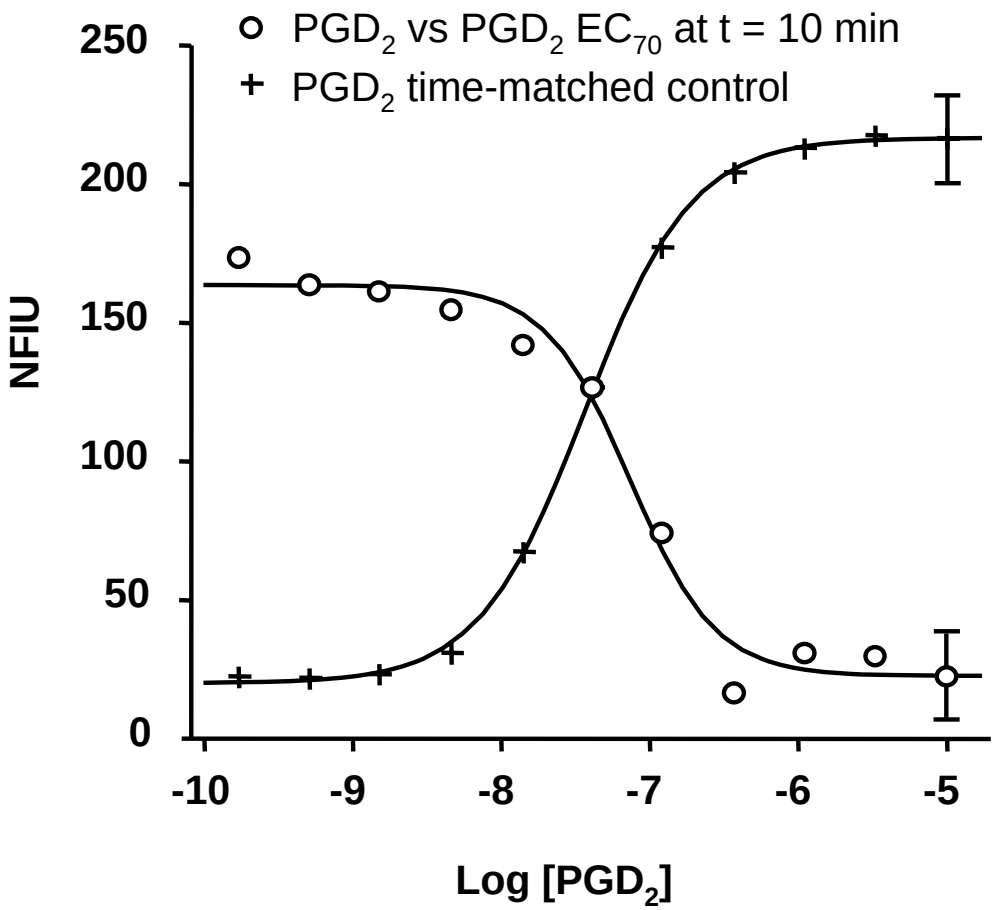
PGD2 vs PGD2 EC70 at t = 10 min
PGD2 time-matched control
250
200
150
100
50
0
NFIU
-10
-9
-8
-7
-6
-5
Log [PGD2]

Figure 13.

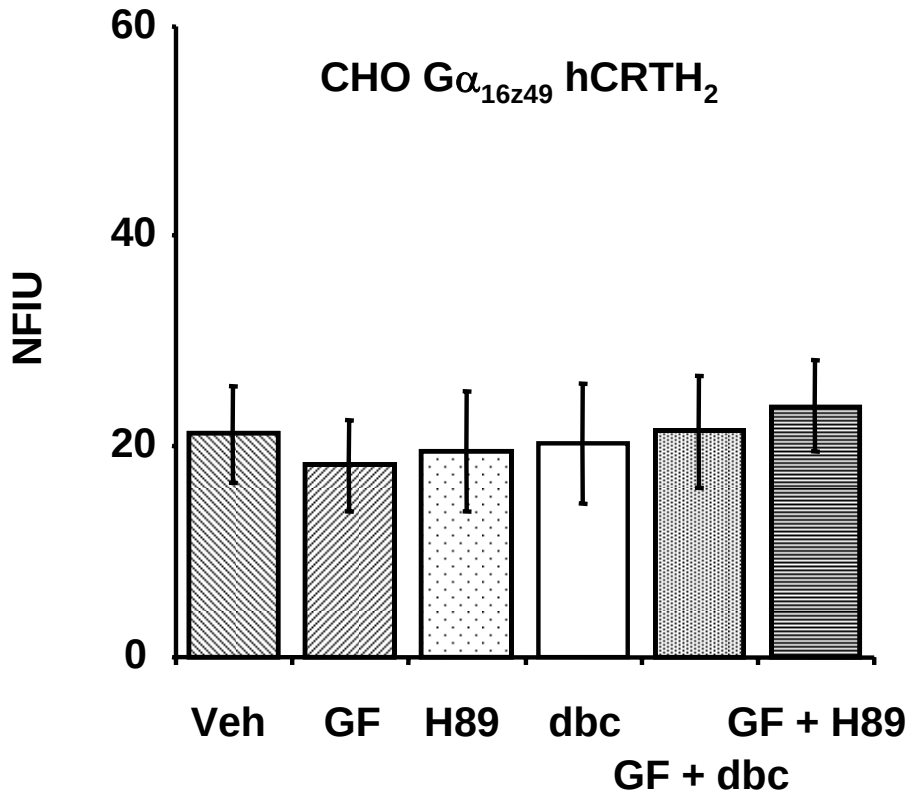
CHO Gα16z49 hCRTH2
NFIU
60
40
20
0
Veh
GF
H89
dbc
GF + H89
GF + dbc

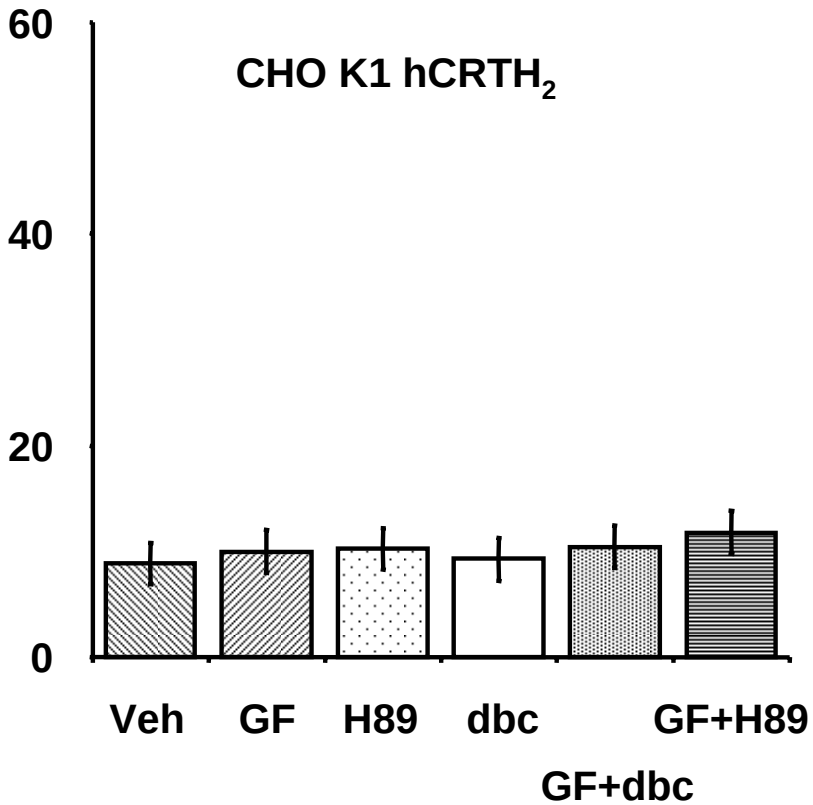
CHO K1 hCRTH2
60
40
20
0
Veh
GF
H89
dbc
GF+H89
GF+dbc

Figure 14.

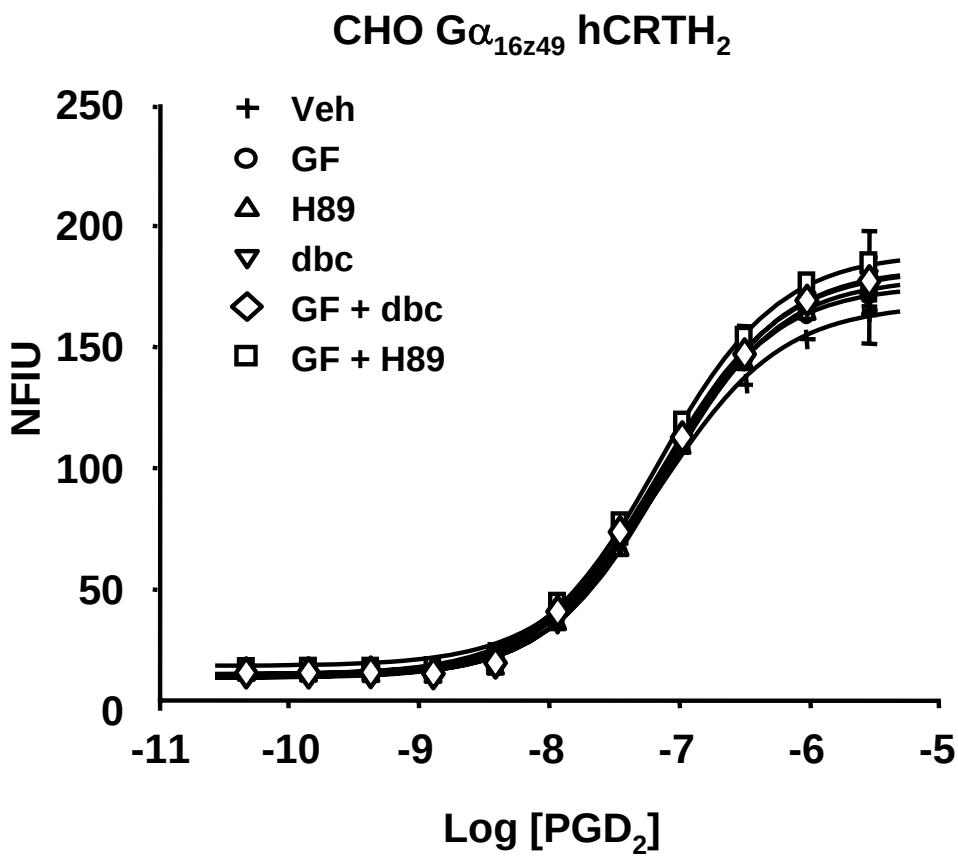
CHO Gα16z49 hCRTH2
Veh
GF
H89
dbc
GF + dbc
GF + H89
NFIU
250
200
150
100
50
0
-11
-10
-9
-8
-7
-6
-5
Log [PGD2]

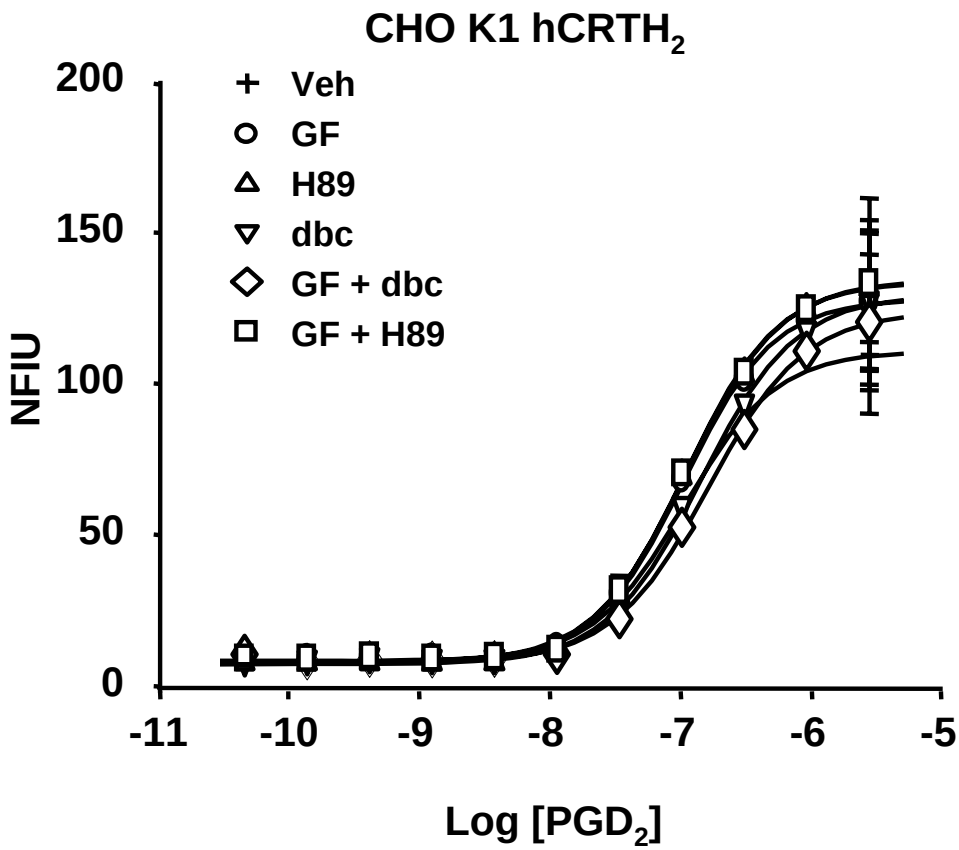
CHO K1 hCRTH2
Veh
GF
H89
dbc
GF + dbc
GF + H89
NFIU
200
150
100
50
0
-11
-10
-9
-8
-7
-6
-5
Log [PGD2]

Figure 15.

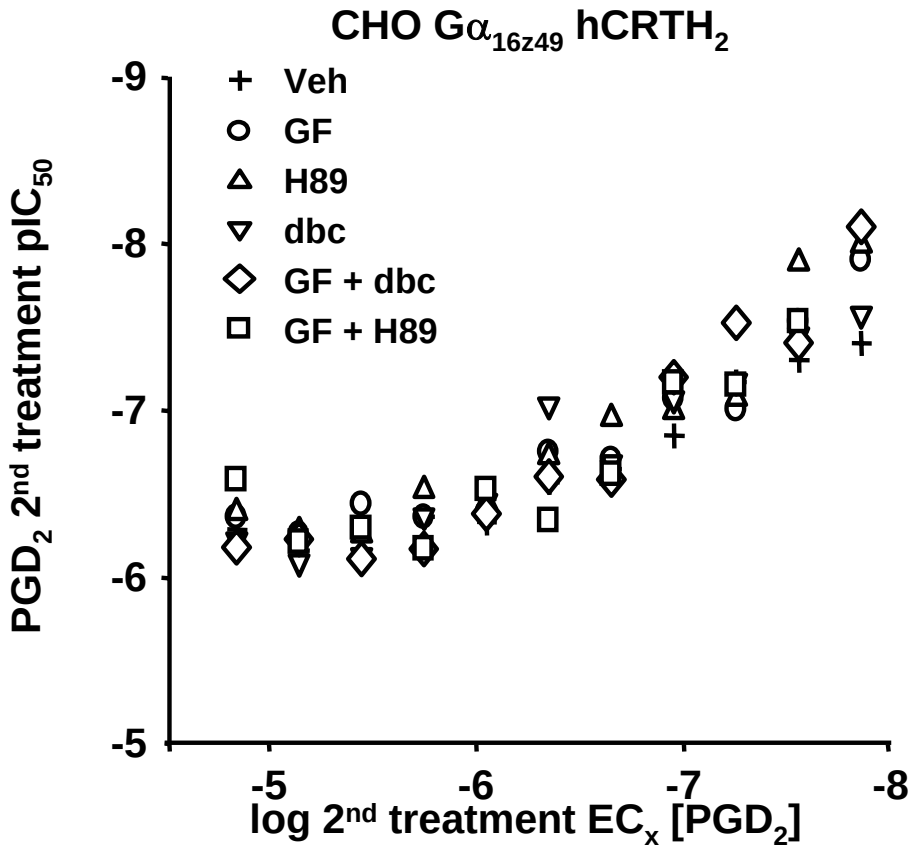
CHO Gα16z49 hCRTH2
Veh
GF
H89
dbc
GF + dbc
GF + H89
PGD2 2nd treatment pIC50
-9
-8
-7
-6
-5
-5
-6
-7
-8
log 2nd treatment ECx [PGD2]

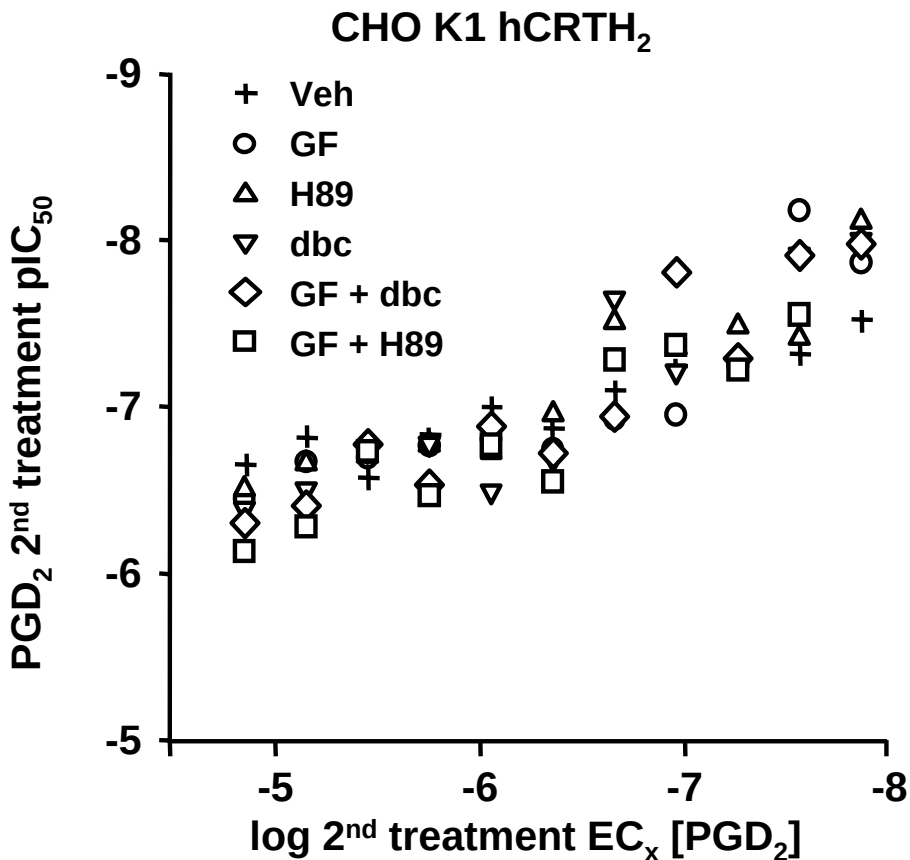
CHO K1 hCRTH2
Veh
GF
H89
dbc
GF + dbc
GF + H89
PGD2 2nd treatment pIC50
-9
-8
-7
-6
-5
-5
-6
-7
-8
log 2nd treatment ECx [PGD2]

Figure 16.

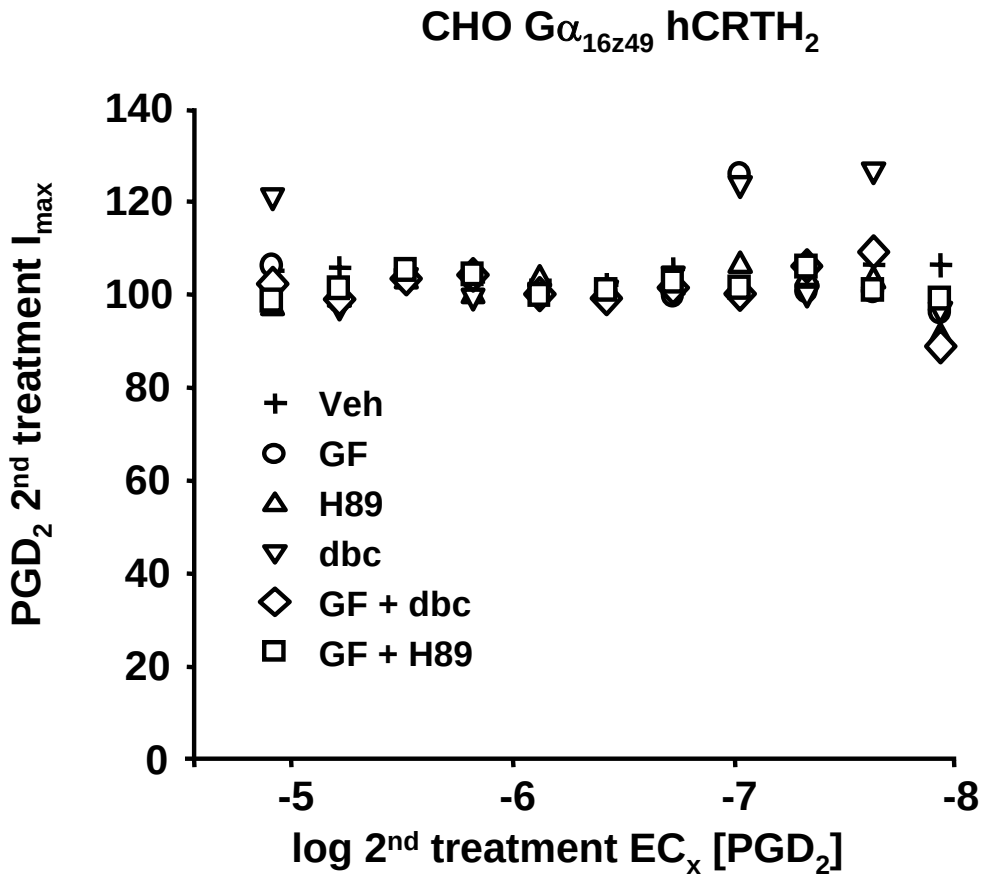
CHO Gα16z49 hCRTH2
PGD2 2nd treatment Imax
140
120
100
80
60
40
20
0
-5
-6
-7
-8
log 2nd treatment ECx [PGD2]
Veh
GF
H89
dbc
GF + dbc
GF + H89

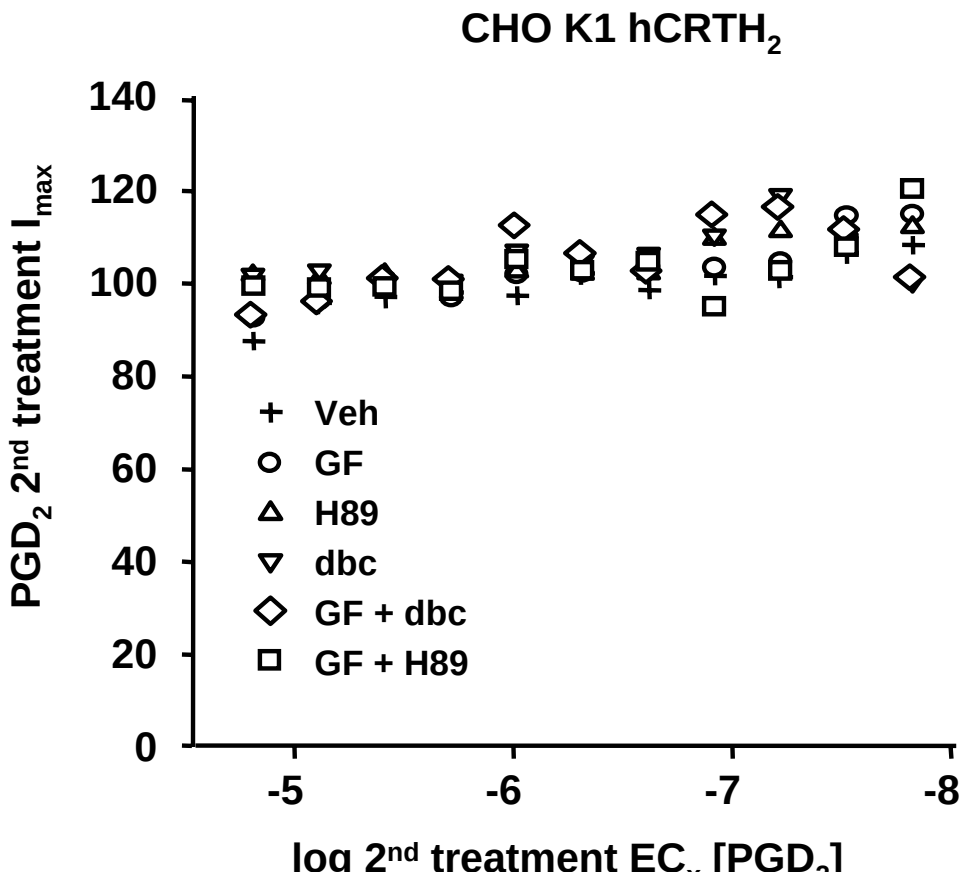
CHO K1 hCRTH2
PGD2 2nd treatment Imax
140
120
100
80
60
40
20
0
-5
-6
-7
-8
log 2nd treatment ECx [PGD2]
Veh
GF
H89
dbc
GF + dbc
GF + H89

Figure 17.

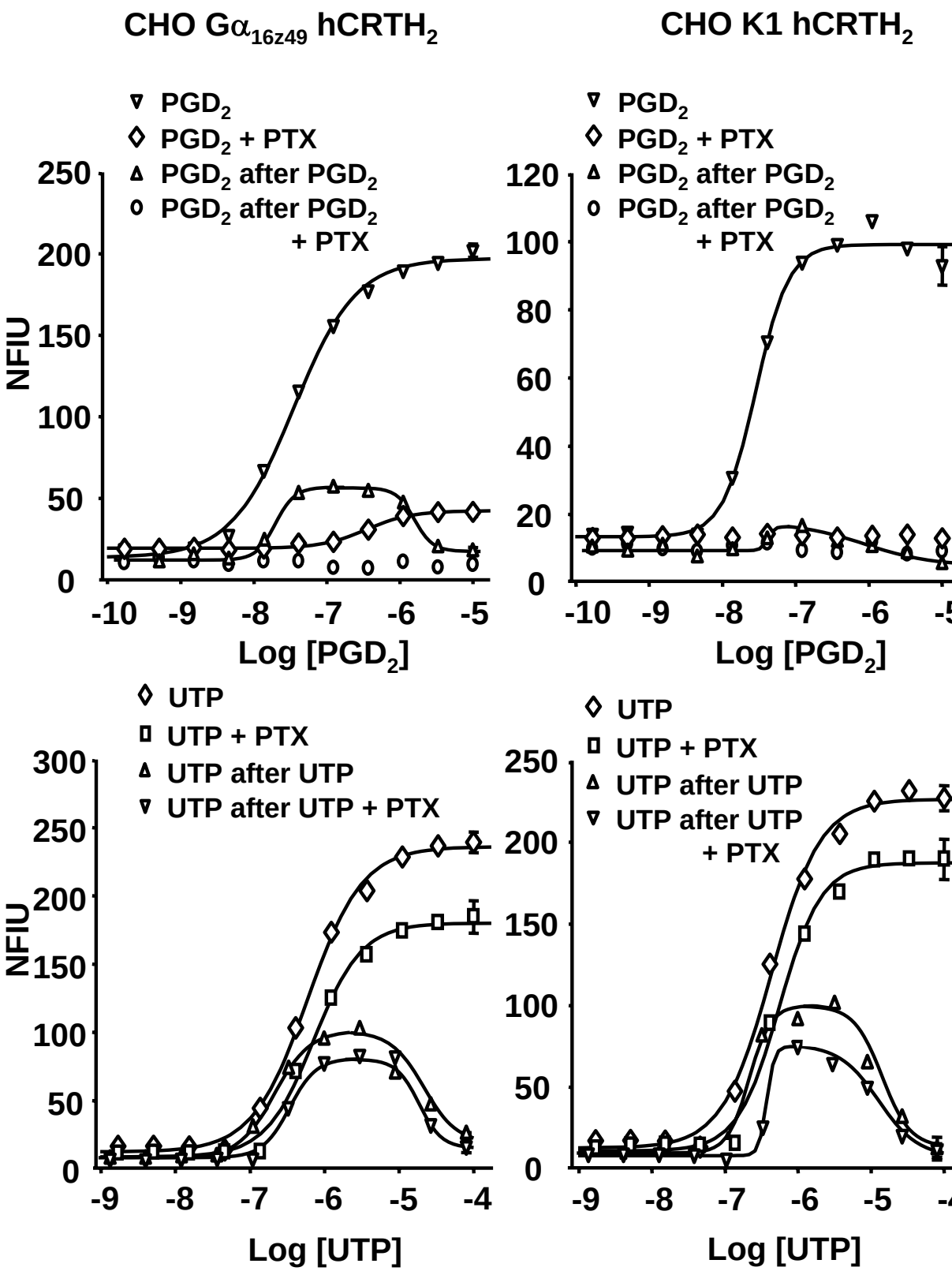
CHO Gα16z49 hCRTH2
CHO K1 hCRTH2
PGD2
PGD2 + PTX
PGD2 after PGD2
PGD2 after PGD2 + PTX
NFIU
Log [PGD2]
UTP
UTP + PTX
UTP after UTP
UTP after UTP + PTX
Log [UTP]

Figure 18.

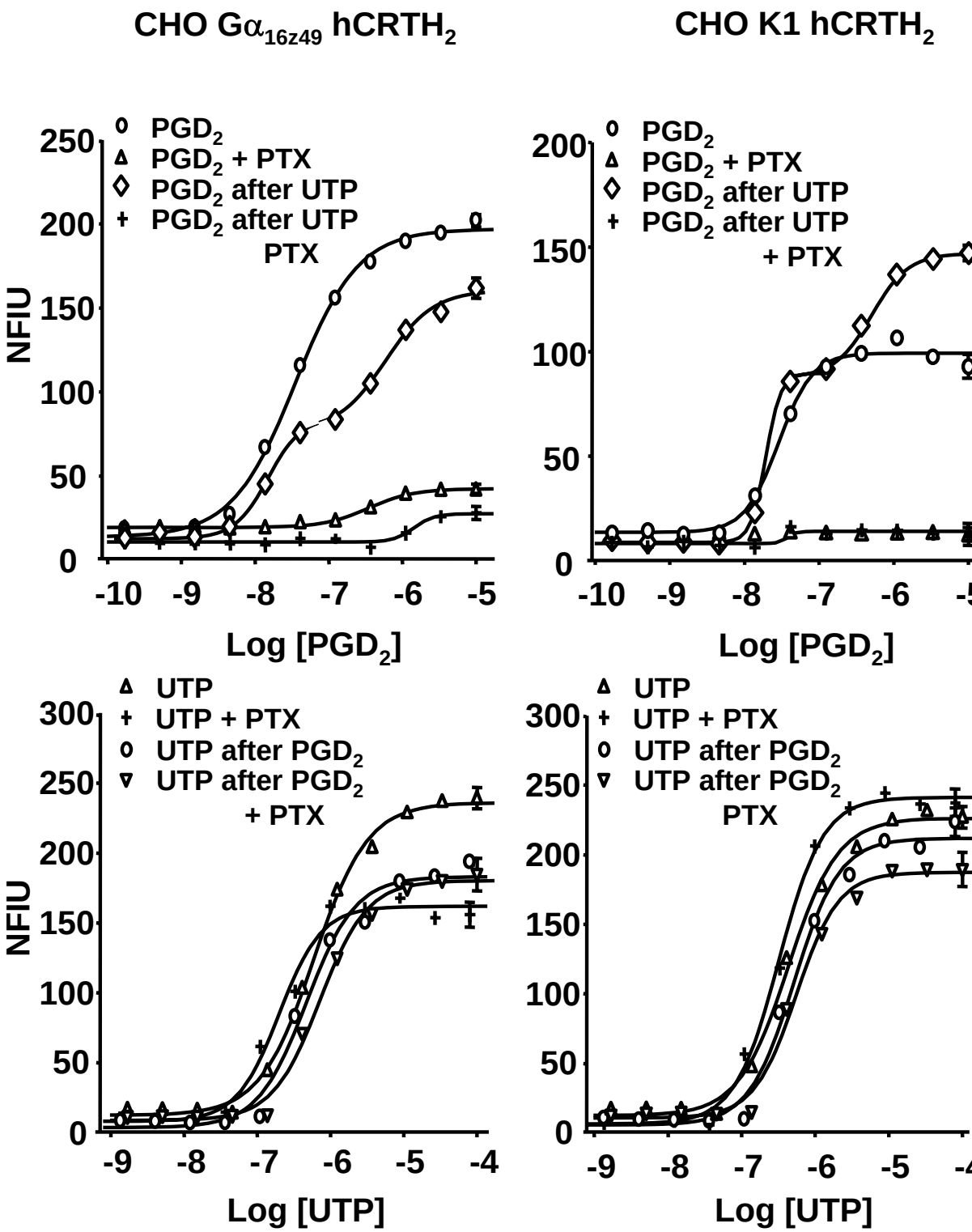
CHO Gα16z49 hCRTH2
CHO K1 hCRTH2
PGD2
PGD2 + PTX
PGD2 after UTP
PGD2 after UTP PTX
PGD2 after UTP + PTX
NFIU
Log [PGD2]
UTP
UTP + PTX
UTP after PGD2
UTP after PGD2 + PTX
UTP after PGD2 PTX
Log [UTP]

Figure 19.

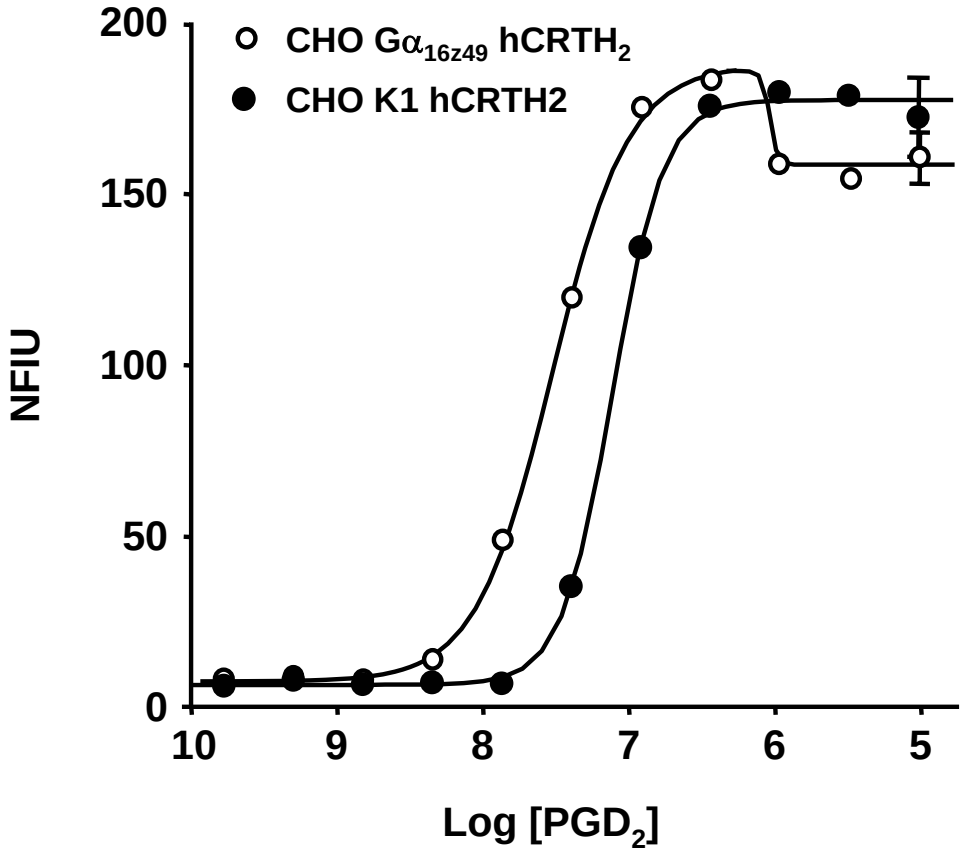
CHO Gα16z49 hCRTH2
CHO K1 hCRTH2
200
150
100
50
0
NFIU
10
9
8
7
6
5
Log [PGD2]

Figure 20.

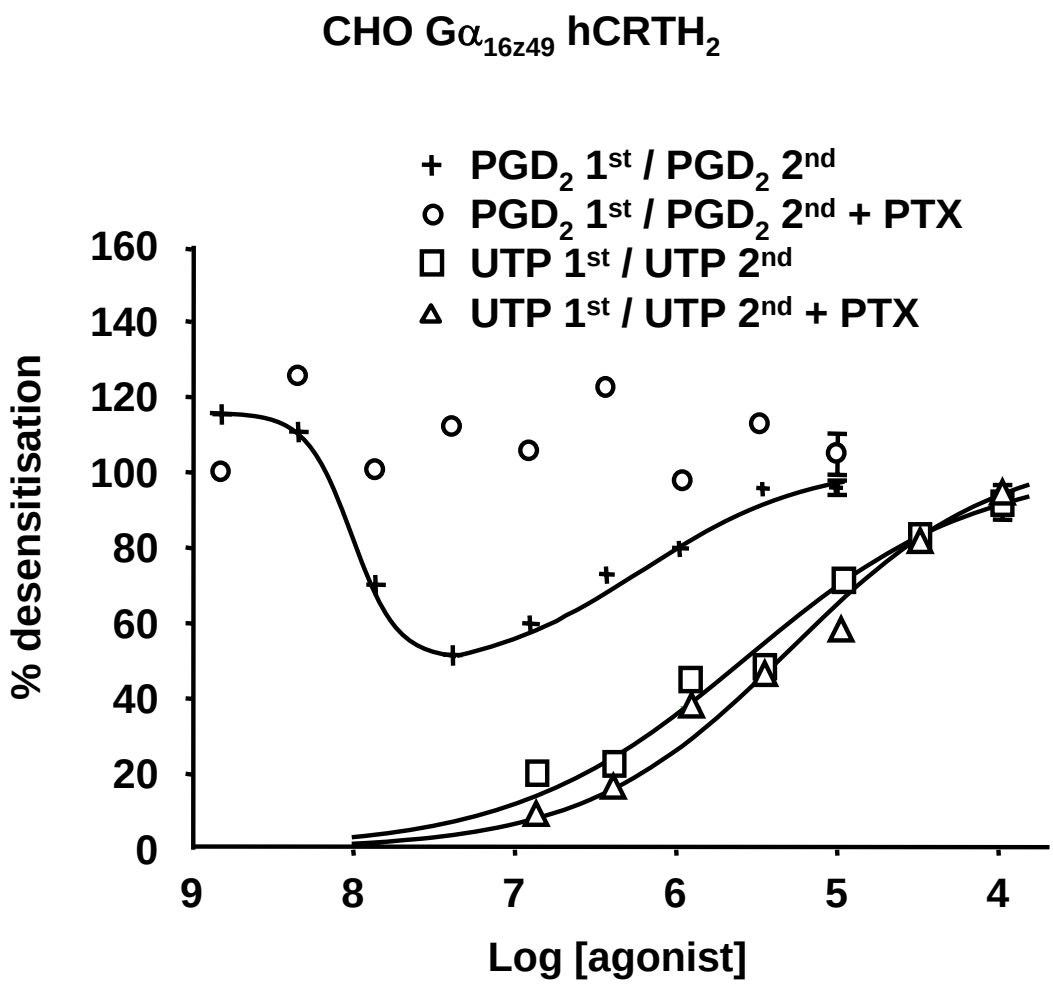
CHO Gα16z49 hCRTH2
PGD2 1st / PGD2 2nd
PGD2 1st / PGD2 2nd + PTX
UTP 1st / UTP 2nd
UTP 1st / UTP 2nd + PTX
% desensitisation
160
140
120
100
80
60
40
20
0
9
8
7
6
5
4
Log [agonist]

Figure 21.

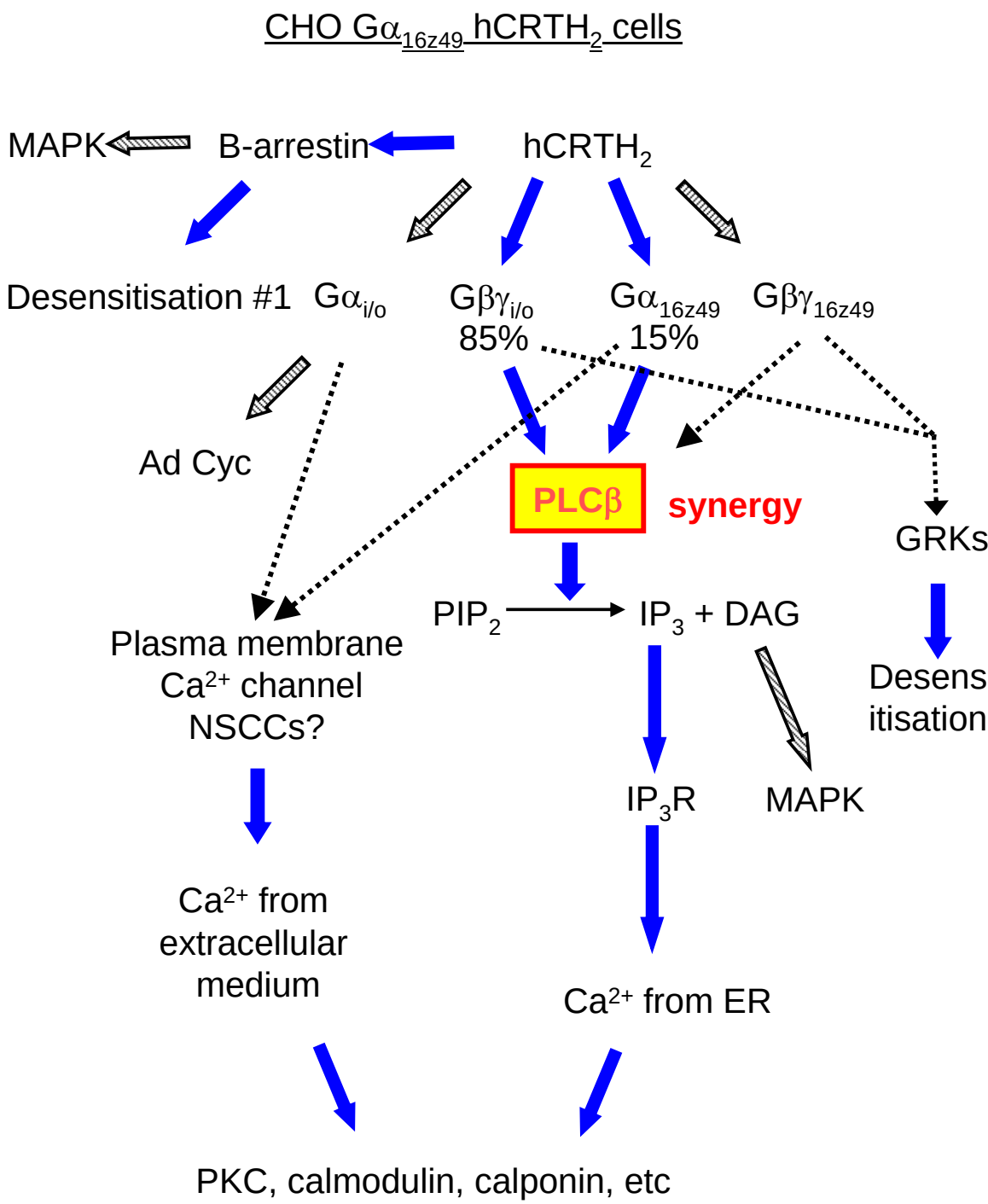
CHO Gα16z49 hCRTH2 cells
MAPK
B-arrestin
hCRTH2
Desensitisation #1
Gαi/o
Gβγi/o
85%
Gα16z49
15%
Gβγ16z49
Ad Cyc
PLCβ
synergy
GRKs
PIP2
IP3 + DAG
Plasma membrane
Ca2+ channel
NSCCs?
Desens
itisation
IP3R
MAPK
Ca2+ from
extracellular
medium
Ca2+ from ER
PKC, calmodulin, calponin, etc

Chapter 7:

Prostanoid receptor agonists of human $CRTH_2$ receptors: pharmacology of receptor desensitisation reveals atypical behaviour. Can ligands induce receptor desensitisation without activation?

7.1 Summary:

In chapter 6, the ability of agonists of $hCRTH_2$ receptors to desensitise the receptor to subsequent agonist challenge was investigated. In this chapter, these studies have been extended to examine the ability of a panel of diverse prostanoid molecules to elicit desensitisation.

Molecules previously shown to be agonists at $hCRTH_2$ receptors desensitised them against subsequent exposure to PGD_2 EC_{80} resulting in pIC_{50} values that either correlated with their calcium-mobilisation pEC_{50} values (CHO $G\alpha_{16z49}$ $hCRTH_2$ r^2 = 0.83) or were in loose agreement with them (CHO K1 $hCRTH_2$ r^2 = 0.35). Unexpectedly, a large group of molecules devoid of agonist activity in either the calcium mobilisation or [^{35}S]-GTPγS accumulation assays also partially inhibited PGD_2 EC_{80} responses in a concentration-related manner. Typically maximum inhibition values for these latter molecules were in the range 20 – 50 % in chimera-expressing cells and 40 – 70 % in non-chimeric cells. The lower maximum inhibition values observed in chimeric cells may reflect lower functional inhibition of synergy-amplified PGD_2 responses in this cell line.

A group of partial agonists, antagonists, and 'non-agonist inhibitors' were profiled further using Schild analyses in calcium mobilisation, [^{35}S]-GTPγS accumulation and [^{3}H]-PGD_2 radioligand displacement assays. GTPγS assay agonist pEC_{50} and antagonist pA_2 values were consistently higher than the corresponding values in calcium assays. The results for each class of compounds are summarised as follows:

<u>Antagonists:</u> In addition to the previously identified $hCRTH_2$ antagonists AH23848B and GW853481X, the compound 13,14 dihydro 15 keto PGE_2 was also found to be an antagonist of $CRTH_2$ receptors (No agonism; pIC_{50} (Ca^{2+}) 5.6, pA_2 (Ca^{2+}) 5.2 & (GTPγS) 5.7; pIC_{50} (binding) 6.1). The GTPγS assay antagonist profile was complex and indicated an interaction with two sites.

<u>Partial agonists:</u> The compounds $PGF_{2\alpha}$, 15 R $PGF_{2\alpha}$ and 13,14 dihydro 15 keto $PGF_{2\alpha}$ were partial agonists at $hCRTH_2$ receptors in both assay formats: agonist pEC_{50} and antagonist pA_2 values were in agreement. Binding pIC_{50} values also correlated except for 15 R $PGF_{2\alpha}$.

<u>Non-agonist inhibitors:</u> 19 hydroxy prostaglandins A_2, E_2 & $F_{2\alpha}$ were non-agonist inhibitors of PGD_2 responses in calcium assays (CHO $G\alpha_{16z49}$ pIC_{50}, I_{max}: 7.5, 21 %;

7.1, 35 %; 5.8, 32 %, respectively) but were devoid of effect in GTPγS assays. Calcium assay Schild analysis demonstrated c. 20 % depression of PGD_2 E/[A] curve maxima at all concentrations with no dextral curve shift while binding assays also indicated an interaction with the receptor. PGE_2 was also a non-agonist inhibitor of PGD_2 responses (pIC_{50} 7.4-7.7) but with additional antagonist affinity for the receptor (Ca^{2+} pA_2 4.9-5.2; GTPγS pK_b 5.6).

Non-agonist inhibitors may trigger receptor desensitisation via activation of a pathway independent of G-protein mediated agonism. This may involve non-G-protein dependent recruitment of GRKs 5 & 6, or β-arrestin activation. These data may also point to possible heterologous desensitisation of $CRTH_2$-mediated responses in chimera-expressing cells by activation of the postulated EP_3 receptor in these cells. Clearly, further investigation is needed to elucidate the precise pharmacological events underpinning these observations.

7.2 Introduction:

Whilst the journal-based scientific literature contains relatively few papers describing antagonists of prostanoid $CRTH_2$ receptors (Birkinshaw, *et al*., 2006; Armer, *et al*., 2005; Sugimoto, *et al*., 2005), the patent literature contains many examples of such compounds (see Wei & Bacon, 2005, for review). In at least one case, these molecules have demonstrated an ability to selectively antagonise one $CRTH_2$ mediated response while leaving others unaffected (Mathiesen, *et al*., 2005) which may involve so-called permissive antagonism (Kenakin, 2005). Similarly, as described in earlier chapters of this thesis, agonists possessing the ability to direct stimuli towards particular response pathways have also been observed at this receptor. In the cases of PGD_2 and 15 keto $PGF_{2\alpha}$, at least, this agonism was accompanied by receptor desensitisation, resulting in an inability of agonist-exposed receptors to respond to subsequent agonist challenge. It therefore seemed reasonable to assay the panel of prostanoid molecules used in earlier chapters for desensitisation and / or antagonist activity in a calcium mobilisation assay measured against an EC_{80} response to PGD_2 at $hCRTH_2$ receptors expressed in CHO cells either with or without the chimeric $G\alpha_{16z49}$ G-protein.

As expected, pre-treatment with agonist molecules resulted in concentration-related inhibition of PGD_2 EC_{80} responses. However, a range of non-agonist molecules also possessed inhibitory activity and in this chapter the behaviour of these molecules has been investigated using pharmacological methods. Finally, a radioligand binding assay has been developed in order to shed light on the nature of the interaction of these molecules with the receptor.

7.3 Results:

7.3.1 Calcium flux assay

7.3.1.1 **Inhibition of PGD_2 EC_{80} by prostanoid molecules**

7.3.1.1.1 CHO $G\alpha_{16z49}$ cells without PTX treatment.

The panel of prostanoid molecules screened for agonism in CHO $G\alpha_{16z49}$ $hCRTH_2$ cells without PTX pre-treatment was also screened for their ability to inhibit responses to an EC_{80} of PGD_2 (D_2EC_{80}; Table 1; Figure 1). PGD_2 inhibited D_2EC_{80} with a maximum inhibition (I_{max}) of 102 ± 0.3 %, pIC_{50} 8.5 ± 0.07. In contrast to the lack of *agonism* previously observed in 65 % of compounds, no inhibitory effect was only shown by 6 % of compounds. Potent inhibitory effects were observed for prostanoid molecules of the A, E and Tx series (e.g. 11 dehydro TxB_2, 19 (R) hydroxy PGA_2, 19 (R) hydroxy PGE_2 & PGE_2). Inhibitory potency (pIC_{50}) data correlated poorly with agonist potency (pEC_{50}) data (Figure 2; correlation coefficient (r^2) = 0.01). For regression analysis, where compounds were inactive in the agonism (pEC_{50}) data set, a value of 4.5 was assigned. Therefore, the true r^2 value is lower than 0.01. However, when compounds devoid of *agonism* were removed from the data set, the correlation was greatly improved (r^2 = 0.83). Therefore compounds could be grouped into two sets: 1. Compounds whose pEC_{50} and pIC_{50} values correlated reasonably well, and 2. Compounds with divergent pEC_{50} and pIC_{50} values (highlighted in Table 1). The rank order of inhibitory potency for the most active compounds (inhibitory potency, pIC_{50}, relative inhibitory activity [RI_{max} cf. PGD_2 = 100]) was: PGD_2 (8.5) = 11 dehydro TxB_2 (8.3, 44) > Δ^{17} 6 keto $PGF_{1\alpha}$ (7.7, 14) > 19 R hydroxy PGA_2 (7.5, 21) = PGE_1 (7.4, 44) = PGE_2 (7.4, 38) = PGE_3 (7.3, 34) > 19 R hydroxy PGE_2 (7.1, 35) > 19 R hydroxy $PGF_{1\alpha}$ (6.9, 27) = 20 hydroxy PGE_2 (6.8, 4) = 2,3 dinor 11β $PGF_{2\alpha}$ (6.8, 18) = 15 R 19 R hydroxy $PGF_{2\alpha}$ (6.7, 23) = 13,14 dihydro PGE_1 (6.7, 48) > 20 hydroxy $PGF_{2\alpha}$ (6.6, 14) = PGD_3 (6.6, 73) = 13,14 dihydro 15 keto $PGF_{2\alpha}$ (6.6, 27) = 15 deoxy PGD_2 (6.5, 94). All non-agonist inhibitory compounds produced RI_{max} values below 53 % cf. PGD_2 except for 11 dehydro 2,3 dinor TxB_2 (5.4, 86) and 15 R 19 R hydroxy PGE_2 (5.4, 93). Conversely, all agonist inhibitory compounds produced RI_{max} values above 70 % cf. PGD_2 except for $PGF_{2\alpha}$ (5.6, 27).

7.3.1.1.2 CHO $G\alpha_{16z49}$ cells + PTX treatment.

The same panel of molecules was screened for D_2EC_{80} inhibition in CHO $G\alpha_{16z49}$ $hCRTH_2$ cells with PTX pre-treatment (Table 1; Figure 3). Under these conditions, PGD_2 inhibited D_2EC_{80} with a maximum inhibition (I_{max}) of 91 ± 2 % and pIC_{50} 7.9 ± 0.3. No inhibitory effect was shown by 26 % of compounds. Inhibitory potency (pIC_{50}) data correlated poorly with pEC_{50} data in the same cells (Figure 4; correlation coefficient (r^2; excluding iloprost) = 0.19). (As before, pXC_{50} = 4.5 was assigned to compounds devoid of agonism or inhibition so the true r^2 is lower than 0.19). Almost all of the compounds displaying potent inhibitory effects in the absence of PTX treatment only achieved a modest percentage inhibition of D_2EC_{80} at the highest concentration tested (e.g. 11 dehydro TxB_2, Δ^{17} 6 keto $PGF_{1\alpha}$, 19 R hydroxy PGA_2, PGE_1, PGE_2, PGE_3 & 19 R hydroxy PGE_2 and so on). When the regression was repeated but only with compounds producing both pEC_{50} and pIC_{50} values, r^2 = 0.58. Therefore compounds could be grouped into three sets:

1. Compounds whose pEC_{50} and pIC_{50} values correlated reasonably well;
2. Compounds with agonist activity but no inhibitory activity (i.e. possessing pEC_{50} but not pIC_{50} values);
3. Compounds with inhibitory activity but no agonist activity (i.e. possessing pIC_{50} but not pEC_{50} values; highlighted in Table 1).

A number of compounds appeared to enhance D_2EC_{80} activity, however because the signal remaining after PTX treatment is so small, minor changes in response translate into large changes in percentage response; therefore, these small changes are unlikely to be biologically significant. The rank order of inhibitory potency for the most active compounds (pIC_{50}, RI_{max} cf. PGD_2 = 100) was: 15 R 15 methyl PGD_2 (8.4, 76) > PGD_2 (7.9) > 13,14 dihydro 15 keto PGD_2 (7.2, 46) > PGD_3 (6.9, 105) = 15 deoxy PGD_2 (6.8, 115) = PGJ_2 (6.7, 157) = 15 deoxy $\Delta^{12,14}$ PGJ_2 (6.6, 69) > 9,10 dihydro 15 deoxy $\Delta^{12,14}$ PGJ_2 (6.2, 96) = 15 S 15 methyl PGD_2 (6.0, 24) > Δ^{12} PGJ_2 (5.9, 120) = 17 phenyl PGD_2 (5.9, 120) = 15 keto $PGF_{1\alpha}$ (5.9, 98) > 15 R $PGF_{2\alpha}$ (5.6, 108).

7.3.1.1.3 CHO K1 cells without PTX treatment.

Finally, the panel of prostanoids was screened for D_2EC_{80} inhibition in CHO K1 $hCRTH_2$ cells without PTX treatment (Table 1; Figure 5). 17 % of compounds were without inhibitory effect: these were often (but not always) the same molecules that

were without effect in CHO $G\alpha_{16z49}$ $hCRTH_2$ cells without PTX treatment. These data also did not correlate well with agonist pEC_{50} data generated in the same cell line (r^2 = 0.002; Figure 6). Removal of non-agonist compounds from the data set resulted in an improved correlation but r^2 was still low (0.35). However, as with data generated in chimera-expressing cells without PTX treatment, compounds could be grouped into agonists with inhibitory activity and non-agonists with inhibitory activity (highlighted in Table 1). The rank order of inhibitory potency for the most active compounds (pIC_{50}, RI_{max} cf. PGD_2 = 100) was: 19 R hydroxy PGA_2 (8.9, 52) > 11 dehydro TxB_2 (8.7, 56) > 15 R 15 methyl PGD_2 (8.4, 74) > PGD_2 (8.0) > Iloprost (7.8, 79) = PGE_2 (7.7, 51) > PGA_2 (7.2, 51) = 6 keto $PGF_{1\alpha}$ (7.2, 53) = 20 hydroxy PGE_2 (7.1, 89) = 13,14 dihydro $PGF_{1\alpha}$ (7.0, 53) > 16,16 dimethyl PGD_2 (6.8, 76) = 15 R 19 R hydroxy $PGF_{1\alpha}$ (6.6, 48). Only 41 % of non-agonist inhibitory compounds produced RI_{max} values below 55 % cf. PGD_2; 36 % produced values above 70 %. The greatest RI_{max} value was observed for 20 hydroxy PGE_2 (89 ± 3). However, as with chimera-expressing cells without PTX treatment, 70 % of agonist inhibitory compounds produced RI_{max} values above 70 % cf. PGD_2; 15 deoxy PGD_2 produced an RI_{max} value of 18 ± 3 %.

Overall, twelve compounds were non-agonist inhibitors at $hCRTH_2$ receptors in both CHO K1 and CHO $G\alpha_{16z49}$ cells (e.g. 11 dehydro TxB_2, 13,14 dihydro 15 keto PGE_1, 19(R) hydroxy PGA_2, PGA_2 & PGE_2). However, a further group of twenty-seven diverse molecules were inhibitors only in the chimera-expressing cell line. These molecules are listed in Figure 7.

7.3.1.2 **Analysis of competition**

Analysis of competition (Schild analysis) was performed on a group of thirteen molecules representing a spectrum of full and partial agonist, antagonist, and inhibitor activities (Table 2; Figures 8 & 9). When added to cells, test compounds produced calcium mobilisation data in agreement with data reported in earlier chapters. The exceptions to this were GW853481X, which when tested to 100 μM revealed weak partial agonist activity (vehicle was constant at 1 % DMSO), and PGD_3, which was significantly more potent as an agonist than previously noted. Because agonist exposure could produce an inhibition of subsequent agonist responses, it was possible to estimate an antagonist potency for agonist molecules. Agonist and partial agonist pEC_{50} values agreed well with pA_2 estimates for most molecules; the values for GW853481X

did not agree: pEC_{50} was 1.4 (CHO K1) – 1.8 (CHO $G\alpha_{16z49}$) log units lower than pK_b. The analyses revealed previously unrecognised antagonist activity in PGE_2 and 13,14 dihydro 15 keto PGE_2, and inhibitor activity in 19 R hydroxy PGE_2 and 19 R hydroxy PGA_2. The full agonists PGD_3 and 17 phenyl PGD_2 were not investigated any further.

7.3.2 [^{35}S]-guanosine triphosphate binding assay

7.3.2.1 **Single antagonist concentration pA_2 determination**

The antagonist properties of a single concentration of the same set of molecules was profiled at $hCRTH_2$ receptors in CHO K1 cells using [^{35}S]-GTPγS binding (Table 3; Figure 10). Indomethacin was a full agonist and could not be tested further. GW853481X was devoid of agonist effects to 10 μM and shifted the PGD_2 E/[A] curve beyond the detectable range resulting in an affinity estimate of > 1 μM. The affinity estimates and baseline elevations for 13,14 dihydro 15 keto $PGF_{2\alpha}$ (pA_2, baseline cf. PGD_2 E_{max}: 5.6 ± 0.1; 49 ± 3 %), 15 R $PGF_{2\alpha}$ (6.4 ± 0.1; 68 ± 4 %), $PGF_{2\alpha}$ (5.8 ± 0.2; 33 ± 0.7 %), 15 keto $PGF_{2\alpha}$ (pA_2 5.8 ± 0.2, 44 ± 2 %) and 15 keto $PGF_{2\alpha}$ (pA_2 6.1 ± 0.1, 70 ± 2 %) were in agreement with their partial agonist activity previously observed in this system (Chapter 5). The compounds PGE_2 and 13,14 dihydro 15 keto PGE_2 were devoid of agonist effects, as previously observed, but yielded pA_2 estimates of 5.8 ± 0.2 and 5.7 ± 0.06, respectively. Finally, 19 R hydroxy prostaglandins A_2, E_2 & $F_{2\alpha}$ were without effect.

7.3.2.2 **Analysis of competition**

Generally, the agonist potency of partial agonists (15 keto $PGF_{2\alpha}$, 15 keto $PGF_{1\alpha}$, 15 R $PGF_{2\alpha}$ and 13,14 dihydro 15 keto $PGF_{2\alpha}$) was 0.5 log units lower in this assay than previously observed in this system (Table 3; Figure 11); $PGF_{2\alpha}$ was inactive as an agonist; PGE_2 demonstrated previously unobserved agonist properties (pEC_{50} 5.1 ± 0.2, E_{max} 21 ± 3 %. However, with the exception of 13,14 dihydro 15 keto $PGF_{2\alpha}$, when agonist molecules were tested for antagonist activity, antagonist potencies were commensurate with previously obtained agonist data (Table 3) and also agreed well with pA_2 estimates generated from a single agonist concentration. Where antagonist potencies were estimated, the values were 0.4-1.6 log units higher than the corresponding values generated in calcium mobilisation assays. Complex antagonist

behaviour was shown by 13,14 dihydro 15 keto PGE_2: no effect was observed up to 3 μM; at 10 μM, responses to low concentrations of PGD_2 were observed to shift right while high concentrations were unaffected, resulting in curve steepening; at 30 μM, curves were seen to be biphasic while at 100 μM curves were once again monophasic, right-shifted, and corresponded only to the first phase of the biphasic curve. The affinity of 13,14 dihydro 15 keto PGE_2 was therefore in the range: phase 1 - 5.5 to 5.0, phase 2 – 4.5 to 4.0. Finally, 19 R hydroxy prostaglandins A_2, E_2 & $F_{2\alpha}$ were without effect.

7.3.3 [^{3}H]-PGD$_2$ filtration binding assay

7.3.3.1 **Method development**

In the following text, the data presented are in the order CHO K1 $hCRTH_2$ membranes followed by CHO $G\alpha_{16z49}$ $hCRTH_2$ membranes. The relationship between membrane protein concentration and ligand binding (protein linearity) at 2.2 nM radioligand was found to be linear to 12.8 & 1.2 μg well^{-1} membrane protein (Figure 12). Estimates of B_{max} derived from the protein linearity assay were 52 & 139 pmol mg^{-1}. Radioligand vehicle (15 % acetonitrile + 29 % methanol v v^{-1} in distilled water) inhibited 3.5 nM [^{3}H]-PGD_2 binding in a concentration-dependent manner resulting in an IC_{50} of 3.3 % v v^{-1} (final assay volumes of vehicle mixture per volume of assay buffer; Figure 13). Assays were therefore designed to avoid vehicle effects but where this was not possible, i.e. saturation binding assays, data were corrected for vehicle effects. Saturation binding data analysed by non-linear regression and linear Scatchard transformation are reported in Chapter 4. Estimates of K_d & B_{max} were: 2.7 ± 2 nM, 3.6 ± 1.1 pmol mg^{-1}; 2.3 ± 0.5 nM, 9.9 ± 2.9 pmol mg^{-1}. Association of radioligand with membranes was found to be essentially complete by 20 mins with some diminution of counts by 60 min (Figure 14); subsequent assays were performed using a 30 min equilibration time. Total binding in wells at plate edges was c. 20 % lower than in other wells of the plate and were therefore not used.

7.3.3.2 **Prostanoid molecule competition binding**

Competition binding assays were performed using 2 nM radioligand concentration, and 17 & 6 μg well^{-1} membrane protein. The amount of membrane used was based on the

B_{max} estimates obtained by non-linear regression of saturation binding and was predicted to result in 17 & 15 % binding of radioligand to receptor in a 200 µl reaction volume. Recalculation based on the higher B_{max} estimates indicates that 100 % ligand binding may occur at both membranes.

Prostanoid molecules displaced [^{3}H]-PGD_2 from CHO K1 h$CRTH_2$ membranes but the results were variable (Figure 15). Total binding at low concentrations of displacing agent (max binding) varied from row-to-row of the plate. Data was therefore normalised to max binding in each row. Within individual E/[A] curves, data was also variable creating the impression that curves were biphasic. This was generally not a consistent finding for any given molecule and the relative contributions of the two phases varied from curve-to-curve. Data was therefore analysed according to a single-site model (Table 4).

A comparison of the key data generated for the most extensively profiled compounds is shown in Table 4.

7.3.4 Data Tables

Follow on next page.

Table 1. Inhibition of Prostaglandin D_2 (PGD_2) EC_{80} by prostanoid molecules in CHO K1 $hCRTH_2$ cells and CHO $G\alpha_{16z49}$ $hCRTH_2$ cells with and without pertussis toxin (PTX) treatment. Data for compounds which did not elicit agonist calcium mobilisation responses are underlined; an asterisk denotes compounds that produced agonist effects but no inhibition. Data are mean ± sem of four independent assay occasions.

	CHO $G\alpha_{16z49}$ $hCRTH_2$				**CHO K1 $hCRTH_2$**	
	-PTX		**+PTX**			
Compound	**pIC_{50}**	**RI_{max}**	**pIC_{50}**	**RI_{max}**	**pIC_{50}**	**RI_{max}**
15 (R) 15 methyl PGD_2	-	-	8.4 ± 0.2	76 ± 20	8.4 ± 0.1	74 ± 0.4
PGD_2	8.5 ± 0.07	100	7.9 ± 0.3	100	8.0 ± 0.04	100
15 (R) 15 methyl $PGF_{2\alpha}$	-	-	-	NSE	-	44 ± 6
15 deoxy PGD_2	6.5 ± 0.06	94 ± 3	6.8 ± 0.06	115 ± 20	5.6 ± 0.04	18 ± 3
PGJ_2	6.2 ± 0.05	90 ± 5	6.7 ± 0.12	157 ± 2	6.3 ± 0.04	71 ± 6
15 deoxy $\Delta^{12,14}$ PGJ_2	6.0 ± 0.06	79 ± 6	6.6 ± 0.3	69 ± 9	6.3 ± 0.1	78 ± 3
15 (S) 15 methyl PGD_2	-	-	6.0 ± 0.1	24 ± 11	5.9 ± 0.03	75 ± 1
13,14 dihydro 15 keto PGD_2	6.0 ± 0.05	101 ± 4	7.2 ± 0.4	46 ± 20	6.3 ± 0.1	73 ± 3
Δ^{12} PGJ_2	5.7 ± 0.06	86 ± 3	5.9 ± 0.1	120 ± 10	5.5 ± 0.3	68 ± 12
9,10 dihydro 15 deoxy $\Delta^{12,14}$ PGJ_2	5.8 ± 0.09	79 ± 5	6.2 ± 0.06	96 ± 20	5.9 ± 0.02	72 ± 1
17 phenyl PGD_2	5.7 ± 0.06	89 ± 8	5.9 ± 0.3	120 ± 15	5.6 ± 0.03	82 ± 3
PGD_3	6.6 ± 0.17	73 ± 15	6.9 ± 0.2	105 ± 13	-	16 ± 11
15 keto $PGF_{2\alpha}$	5.6 ± 0.06	92 ± 8	-	94 ± 28	5.4 ± 0.1	65 ± 4
PGD_1	5.5 ± 0.06	89 ± 4	7.2 ± 1.5	106 ± 21	5.8 ± 0.1	64 ± 1
15 (R) $PGF_{2\alpha}$	5.1 ± 0.03	91 ± 2	5.6 ± 0.01	108 ± 8	5.4 ± 0.1	64 ± 6

16,16 dimethyl PGD_2	5.2 ± 0.04	84 ± 5	-	44 ± 21	6.8 ± 0.03	76 ± 3
15 keto $PGF_{1\alpha}$	-	47 ± 9	5.9 ± 0.1	98 ± 22	5.3 ± 0.02	64 ± 3
$PGF_{2\alpha}$	5.6 ± 0.1	27 ± 1	-	-39 ± 11	-	48 ± 3
Butaprost methyl ester	-	-	-	-18 ± 8	5.0 ± 0.04	82 ± 2
Latanoprost	-	-	-	80 ± 2	-	36 ± 6
Cloprostenol	-	-	-	-45 ± 3	5.2 ± 0.2	72 ± 7
Misoprostol	-	-	-	-59 ± 50	-	-16 ± 8
15 (S) 15 methyl $PGF_{2\alpha}$	-	-	-	45 ± 7	4.9 ± 0.1	59 ± 2
13,14 dihydro 15 keto $PGF_{2\alpha}$	6.6 ± 0.5	27 ± 6	-	44 ± 12	-	48 ± 10
11 deoxy 11 methylene PGD_2	5.6 ± 0.1	32 ± 9	-	15 ± 6	-	33 ± 8
$PGF_{3\alpha}$	5.5 ± 0.2	34 ± 5	-	67 ± 10	5.5 ± 0.1	65 ± 3
11 dehydro TxB_2	8.3 ± 0.5	29 ± 3	-	-24 ± 6	8.7 ± 0.1	56 ± 3
15 (R) 19 (R) hydroxy $PGF_{2\alpha}$	6.7 ± 0.2	23 ± 1	-	NSE	-	NSE
13,14 dihydro PGE_1	6.7 ± 0.2	48 ± 5	-	30 ± 10	-	27 ± 4
PGE_3	7.3 ± 0.3	34 ± 4	-	NSE	-	20 ± 4
20 hydroxy $PGF_{2\alpha}$	6.6 ± 0.2	14 ± 3	-	45 ± 14	-	19 ± 3
13,14 dihydroxy 15 keto PGA_2	5.7 ± 0.3	25 ± 4	-	NSE	-	20 ± 3
6 keto $PGF_{1\alpha}$	5.6 ± 0.2	19 ± 1	-	35 ± 13	7.2 ± 0.03	53 ± 5
6 keto PGE_1	6.2 ± 0.1	51 ± 9	-	-28 ± 5	5.4 ± 0.04	68 ± 2
Δ^{17} 6 keto $PGF_{1\alpha}$	7.7 ± 0.4	14 ± 3	-	-33 ± 13	-	12 ± 2
PGA_2	6.3 ± 0.5	27 ± 6	-	NSE	7.2 ± 0.1	51 ± 7

15 (R) PGE_2	5.8 ± 0.4	24 ± 6	-	NSE	-	28 ± 2
$PGF_{1\alpha}$	5.5 ± 0.06	53 ± 15	-	-27 ± 5	-	10 ± 2
PGA_1	5.9 ± 0.06	25 ± 3	-	NSE	6.4 ± 0.1	45 ± 0.4
13,14 dihydro $PGF_{1\alpha}$	-	21 ± 1	-	19 ± 2*	7.0 ± 0.03	53 ± 5
13,14 dihydro 15 keto PGE_2	5.6 ± 0.1	21 ± 9	-	23 ± 6	5.6 ± 0.1	61 ± 0.4
13,14 dihydro 15 keto $PGF_{1\alpha}$	5.8 ± 0.4	26 ± 18	-	46 ± 12	-	29 ± 6
PGE_1	7.4 ± 0.2	44 ± 4	-	-33 ± 4*	-	NSE
15 keto PGE_1	5.8 ± 0.4	28 ± 4	-	34 ± 9	-	17 ± 6
19 (R) hydroxy $PGF_{1\alpha}$	6.9 ± 0.7	27 ± 9	-	NSE	-	NSE
PGD_1 alcohol	-	NSE	-	NSE*	-	19 ± 4
15 (R) 15 methyl PGE_2	5.3 ± 0.2	37 ± 6	-	NSE	-	NSE
PGI_2	5.3 ± 0.3	15 ± 5	-	-	-	-
15 (R) 19 (R) hydroxy $PGF_{1\alpha}$	-	NSE	-	NSE	6.6 ± 0.7	48 ± 29
13,14 dihydro 15 keto PGE_1	5.7 ± 0.2	23 ± 6	-	NSE	6.2 ± 0.3	51 ± 3
13,14 dihydro 15 (R) PGE_1	5.6 ± 0.1	32 ± 3	-	35 ± 12	-	17 ± 5
11 dehydro 2,3 dinor TxB_2	5.4 ± 0.3	86 ± 2	-	18 ± 4	-	25 ± 6
19 (R) hydroxy PGA_2	7.5 ± 0.5	21 ± 6	-	NSE	8.9 ± 0.1	52 ± 6
TxB_2	-	NSE	-	29 ± 8	-	NSE
15 (R) 19 (R) hydroxy PGE_2	5.4 ± 0.3	93 ± 6	-	-51 ± 18	-	NSE
PGK_1	5.9 ± 0.4	26 ± 2	-	NSE	-	17 ± 8
15 keto PGE_2	5.4 ± 0.3	24 ± 3	-	NSE	-	NSE

20 hydroxy PGE_2	6.8 ± 0.4	40 ± 7	-	-27 ± 6	7.1 ± 0.03	89 ± 3
15 (R) PGE_1	5.6 ± 0.3	33 ± 8	-	36 ± 8	-	57 ± 4
11β 13,14 dihydro 15 keto $PGF_{2\alpha}$	-	15 ± 6	-	38 ± 4	-	NSE
19 (R) hydroxy $PGF_{2\alpha}$	5.8 ± 0.4	32 ± 8	-	14 ± 7	-	46 ± 5
19 (R) hydroxy PGE_2	7.1 ± 0.7	35 ± 8	-	29 ± 20	6.2 ± 0.03	85 ± 5
2,3 dinor 11β $PGF_{2\alpha}$	6.8 ± 0.3	18 ± 2	-	NSE*	-	15 ± 3
PGK_2	-	NSE	-	28 ± 6	-	NSE
PGI_3	5.6 ± 0.2	22 ± 4	-	-41 ± 2	6.2 ± 0.04	77 ± 5
PGE_2	7.4 ± 0.3	38 ± 3	-	55 ± 23	7.7 ± 0.1	51 ± 6
19 (R) hydroxy PGE_1	5.6 ± 0.1	30 ± 7	-	NSE	-	NSE
PGB_2	-	34 ± 10	-	33 ± 7	-	48 ± 6
11deoxyPGE_1	-	-	-	-61 ± 17*	-	NSE
Cicaprost	-	-	-	NSE	-	NSE
Sulprostone	-	-	-	33 ± 16	-	25 ± 10
BW245C	-	-	-	NSE	-	17 ± 5
Butaprost free acid	-	-	-	-28 ± 10	-	NSE
17 phenyl PGE_2	-	-	-	NSE	4.9 ± 0.04	71 ± 1
16,16 dimethyl PGE_2	-	-	-	-24 ± 2	5.0 ± 0.1	71 ± 7
Iloprost	-	-	10.2 ± 0.1	-30 ± 12	7.8 ± 0.02	79 ± 4
Indomethacin	5.6 ± 0.06	98 ± 6	5.6 ± 0.3	107 ± 18	5.7 ± 0.03	83 ± 2
GW853481X	6.1 ± 0.2	72 ± 7	6.4 ± 0.3	106 ± 8	5.5 ± 0.04	77 ± 3

Table 2. Summary of calcium mobilisation competition analysis (Schild analysis) data in CHO $G\alpha_{16z49}$ $hCRTH_2$ and CHO K1 $hCRTH_2$ cells. Data are presented describing the effect of test compound (antagonist) on the cells (1st addition) and the subsequent effect of the test compounds on PGD_2 E/[A] curves (2nd addition). Data are mean ± sem of 3 independent experiments. GW853481X was included as a positive control. Terms in table are: pEC_{50} – negative log concentration producing 50 % of a maximal effect determined by curve fitting; E_{max} – curve asymptote at maximal effect; $E_{max}\downarrow$ - depression of agonist E/[A] curve maximum effect; pK_b – antagonist affinity determined by non-linear regression of Schild analysis data; pA_2 - antagonist affinity estimate from effect of a single antagonist concentration.* - no antagonist affinity estimate generated. E.g, addition of GW853481X to CHO $G\alpha_{16z49}$ $hCRTH_2$ cells produced low potency agonism (pEC_{50} 4.5 ± 0.1, E_{max} 5 ± 3 %); following incubation (11 min 37 ºC) the same cells were challenged with PGD_2 E/[A] curves, each curve being generated in the presence of a fixed concentration of test compound; under these conditions, GW853481X antagonised PGD_2 E/[A] curves resulting in a pK_b estimate of 6.3 ± 0.16.

Compound	**Addition**	**CHO $G\alpha_{16z49}$ $hCRTH_2$**	**CHO K1 $hCRTH_2$**
GW853481X	1st	pEC_{50} 4.5 ± 0.1; E_{max} 5 ± 3 %	pEC_{50} 4.6 ± 0.15; E_{max} 11 ± 4 %
	2nd	No inhibition of PGD_2 E_{max} ; pK_b 6.3 ± 0.16	No inhibition of PGD_2 E_{max} ; pK_b 6.0 ± 0.17 Non-receptor mediated agonism?
Indomethacin	1st	-	pEC_{50} 6.4 ± 0.2; E_{max} 83 ± 12 %
	2nd	-	PGD_2 E_{max} depressed; pA_2 6.1 ± 0.1 Partial agonist
PGD_3	1st	-	pEC_{50} 6.3 ± 0.2; E_{max} 117 ± 9 %
	2nd	-	PGD_2 E_{max} depressed; pA_2 6.7 ± 0.1 Full agonist

17 phenyl PGD_2	1st	-	pEC_{50} 6.2 ± 0.2; E_{max} 101 ± 6 %
	2nd	-	PGD_2 E_{max} depressed; pA_2 6.0 ± 0.1 Full agonist
15 R 15 methyl $PGF_{2\alpha}$	1st	-	pEC_{50} 5.7 ± 0.1; E_{max} 64 ± 9 %
	2nd	-	PGD_2 E_{max} depressed; pA_2 5.7 ± 0.1 Partial agonist
15 R $PGF_{2\alpha}$	1st	-	pEC_{50} 5.0 ± 0.2; E_{max} 66 ± 12 %
	2nd	-	PGD_2 E_{max} depressed; pA_2 5.2 ± 0.1 Partial agonist
13,14 dihydro 15 keto $PGF_{2\alpha}$	1st	pEC_{50} 5.1 ± 0.2; E_{max} 40 ± 8 %	pEC_{50} 4.8 ± 0.2; E_{max} 40 ± 11 %
	2nd	PGD_2 E_{max} depressed; pA_2 5.0 ± 0.1 Partial agonist	PGD_2 E_{max} depressed; pA_2 5.2 ± 0.1 Partial agonist
$PGF_{2\alpha}$	1st	pEC_{50} 5.1 ± 0.1; E_{max} 40 ± 6 %	pEC_{50} 4.7 ± 0.2; E_{max} 51 ± 8 %
	2nd	PGD_2 E_{max} depressed; pA_2 5.0 ± 0.03 Partial agonist	PGD_2 E_{max} depressed *. Partial agonist
13,14 dihydro 15 keto PGE_2	1st	NSE	NSE
	2nd	pA_2 5.2 ± 0.2 Antagonist	pA_2 5.2 ± 0.1 Antagonist
PGE_2	1st	NSE	NSE

PGE_2 (contd.)	2nd	pA_2 5.2 ± 0.2 Antagonist	pA_2 4.9 ± 0.2 Antagonist
19 R hydroxy PGE_2	1st	NSE	NSE
	2nd	PGD_2 E_{max} 20 ± 5 % ↓ @ 30 μM; no pEC_{50} shift Inhibitor	PGD_2 E_{max} 22 ± 7 % ↓ @ 30 μM; no pEC_{50} shift Inhibitor
19 R hydroxy PGA_2	1st	NSE	NSE
	2nd	PGD_2 E_{max} 20 ± 8 % ↓ all curves cf. control; no pEC_{50} shift. Inhibitor	PGD_2 E_{max} 26 ± 9 % ↓ all curves cf. control; no pEC_{50} shift. Inhibitor
19 R hydroxy $PGF_{2\alpha}$	1st	NSE	NSE
	2nd	NSE Inactive	NSE Inactive

Table 3. Summary of [^{35}S]-GTPγS competition analysis (Schild analysis) data and single antagonist concentration shift (Single Conc) data in CHO $G\alpha_{16z49}$ $hCRTH_2$ and CHO K1 $hCRTH_2$ cells. Data are presented for effect of test compound on basal activity (agonism) and the subsequent effect of the test compounds on PGD_2 E/[A] curves (antagonism). Data are mean ± sem of 3 independent experiments. Terms in table are: pEC_{50} – negative log concentration producing 50 % of a maximal effect determined by curve fitting; E_{max} – curve asymptote at maximal effect; $E_{max}\downarrow$ - depression of agonist E/[A] curve maximum effect; pK_b – antagonist affinity determined by non-linear regression of Schild analysis data; pA_2 - antagonist affinity estimate derived from effect of a single antagonist concentration.

Compound	Property	Single Conc.	Schild analysis
GW853481X	Agonism	NSE	NSE
	Antagonism	$pA_2 > 6.0$	pA_2 7.6 ± 0.1; curve shift too great at concentrations used to test effects on PGD_2 E_{max}
AH23848B	Agonism	-	NSE
	Antagonism	-	pK_b 6.9 ± 0.2; PGD_2 E_{max} no effect
15 keto $PGF_{1\alpha}$	Agonism	Basal 44 ± 2 %	pEC_{50} 5.7 ± 0.1; E_{max} 35 ± 4 %
	Antagonism	pA_2 5.8 ± 0.2	pA_2 5.9 ± 0.1; PGD_2 $E_{max}\downarrow$
15 keto $PGF_{2\alpha}$	Agonism	Basal 70 ± 2 %	pEC_{50} 5.7 ± 0.1; E_{max} 57 ± 3 %
	Antagonism	pA_2 6.1 ± 0.1	pA_2 6.3 ± 0.1; PGD_2 $E_{max}\downarrow$
15 R $PGF_{2\alpha}$	Agonism	Basal 68 ± 4 %	pEC_{50} 6.0 ± 0.1; E_{max} 37 ± 5 %
	Antagonism	pA_2 6.4 ± 0.1	pA_2 6.2 ± 0.1; PGD_2 $E_{max}\downarrow$

13,14 dihydro 15 keto $PGF_{2\alpha}$	Agonism	Basal 49 ± 3 %	pEC_{50} 5.4 ± 0.2; E_{max} 47 ± 4 %
	Antagonism	pA_2 5.6 ± 0.1	pA_2 5.2 ± 0.1; PGD_2 E_{max} no effect
$PGF_{2\alpha}$	Agonism	Basal 33 ± 0.7 %	pEC_{50} 5.1 ± 0.2; E_{max} 21 ± 3 %
	Antagonism	pA_2 5.8 ± 0.2	pA_2 5.6 ± 0.1; PGD_2 E_{max} non sig. ↓
13,14 dihydro 15 keto PGE_2	Agonism	NSE	NSE
	Antagonism	pA_2 5.7 ± 0.08	Complex, biphasic; phase 1 5.5-5.0; phase 2 4.5-4.0
PGE_2	Agonism	NSE	NSE
	Antagonism	pA_2 5.8 ± 0.2	pK_b 5.6 ± 0.3; PGD_2 E_{max} no effect
19 R hydroxy PGE_2	Agonism	NSE	NSE
	Antagonism	NSE	NSE
19 R hydroxy PGA_2	Agonism	NSE	NSE
	Antagonism	NSE	NSE
19 R hydroxy $PGF_{2\alpha}$	Agonism	NSE	NSE
	Antagonism	NSE	NSE

Table 4. Key data for selected prostanoid molecules generated in calcium mobilisation & [^{35}S]-GTPγS accumulation (functional) assays, and in [^{3}H]-PGD_2 competition binding assays. Terms are: pEC_{50} / pIC_{50} – negative log concentration producing 50 % of a maximal effect determined by curve fitting; E_{max} / I_{max} – curve asymptote at maximal effect, or if curve-fitting not possible, the maximum effect at the highest concentration tested; both cases E - agonism, I - inhibition, R - relative to PGD_2 max effect; AOC – analysis of competition by the method of Schild (C – competitive, NC – non-competitive, PA – partial agonist, E_{max}↓ or ↑ - depression or elevation of agonist maximum effect; NSt – no curve shift); pK_b – antagonist affinity determined by non-linear regression of Schild analysis data; pA_2 - antagonist affinity estimate derived from effect of a single antagonist concentration;* - no estimation of antagonist affinity generated.

Assay type	**Calcium mobilisation**						**[^{35}S]-GTPγS accumulation**			**[^{3}H]-PGD_2 competition binding**
Biological system	CHO $G\alpha_{16z49}$ $hCRTH_2$ cells			CHO K1 $hCRTH_2$ cells			CHO K1 $hCRTH_2$ membranes			
	pEC_{50}, RE_{max}	pIC_{50}, RI_{max}	AOC	pEC_{50}, E_{max}	pIC_{50}, RI_{max}	AOC	pEC_{50}, E_{max}	pA_2	AOC	pIC_{50}, I_{max}
Agonists										
PGD_2	7.8, 1.0	8.5, 1.0	-	7.9, 1.0	8.0, 1.0	-	8.1, 1.0	-	-	7.4, 0.92
Indomethacin	-, 0.58	5.6, 0.98	-	6.9, 0.84	5.7, 0.83	pA_2 6.1, PA	6.4, 1.13	-	-	7.5, 0.65
Partial Agonists										
17 phenyl PGD_2	6.2, 1.22	5.7, 0.89	-	5.9, 0.86	5.6, 082	pA_2 6.0, PA	6.2, 1.11	-	-	6.7, 0.87
15 keto $PGF_{2\alpha}$	6.0, 0.73	5.6, 0.98	-	5.4, 0.58	5.4, 0.65	-	6.1, 0.62	6.1	pA_2 6.3; PA	7.1, 0.92
15 keto $PGF_{1\alpha}$	5.6, 0.28	-, 0.47	-	-, 0.16	5.3, 0.63	-	6.2, 0.37	5.8	pA_2 5.9, PA	6.7, 0.90

15 R $PGF_{2\alpha}$	5.5, 0.55	5.1, 0.92	-	5.5, 0.73	5.4, 0.64	pA_2 5.2, PA	6.3, 0.54	6.4	pA_2 6.2, PA	7.9, 0.89
$PGF_{2\alpha}$	-, 0.17	5.6, 0.27	pA_2 5.0; PA	-, 0.54	-, 0.48	pEC_{50} 4.7, PA*	5.5, 0.48	5.8	pA_2 5.6, PA	6.7, 0.88
13,14 dihydro 15 keto $PGF_{2\alpha}$	-, 0.12	6.6, 0.27	pA_2 5.0; PA	NSE	-, 0.48	pA_2 5.2; PA	6.0, 0.39	5.6	pA_2 5.2, PA	6.1, 0.96
Antagonists										
AH23848B	NSE	-, 0.24	pK_b 5.6, C	NSE	6.2, 1.0	pA_2 5.5, C	-	-	pK_b 6.9, C	6.7, 0.79
GW853481X	NSE	6.1, 0.72	pK_b 6.3, C	NSE	5.5, 0.77	pK_b 6.0, C	-	>6	pK_b 7.6, NC	7.4, 0.90
13,14 dihydro 15 keto PGE_2	NSE	5.6, 0.21	pA_2 5.2	NSE	5.6, 0.61	pA_2 5.2	NSE	5.7	Complex	6.1, 0.78
Calcium mobilisation inhibitors										
19 R hydroxy PGA_2	NSE	7.5, 0.21	NSt; 20% E_{max} ↓	NSE	8.9, 0.52	NSt; 26% E_{max} ↓	NSE	NSE	NSE	7.1, 0.71
19 R hydroxy PGE_2	NSE	7.1, 0.35	NSt; 20% E_{max} ↓	NSE	6.2, 0.85	NSt; 22% E_{max} ↓	NSE	NSE	NSE	6.0, 0.78
19 R hydroxy $PGF_{2\alpha}$	NSE	5.8, 0.32	NSE	NSE	-, 0.46	NSE	NSE	NSE	NSE	No fit
11 dehydro TxB_2	NSE	8.3, 0.29	-	NSE	8.7, 0.56	-	NSE	-	-	-
PGE_2	NSE	7.4, 0.38	pA_2 4.9	NSE	7.7, 0.51	pA_2 5.2	NSE	5.8	pK_b 5.6, C	6.5, 0.88

7.4 Discussion:

Agonist activation of $hCRTH_2$ receptors results in desensitisation of the receptor, as described in Chapter 6. Under these circumstances, the pIC_{50} of PGD_2 EC_{80} inhibition approximates the agonist pEC_{50} for both full (PGD_2) and partial (15 keto $PGF_{2\alpha}$) agonists. Profiling of a range of prostanoid agonists confirmed that this was so for all molecules possessing agonist activity but also revealed inhibitory activity in non-agonist molecules. This was presumed to herald antagonist affinity for the receptor but analyses of antagonist competition (Schild analyses) demonstrated that non-agonist inhibitors did not shift PGD_2 E/[A] curves. Indeed, some compounds were inhibitors only in $hCRTH_2$-expressing CHO $G\alpha_{16z49}$ cells or CHO K1 cells (but not both) suggesting that they were not simple competitive antagonists at the receptor and that the observed inhibition was related to a cellular process. Furthermore, whereas agonists typically elicited greater than 70 % maximum inhibition of PGD_2 EC_{80} responses, non-agonist molecules typically only produced less than 50 % inhibition, suggesting differences in the mechanism of inhibition. Non-agonist compounds inhibiting PGD_2-stimulated calcium mobilisation in *both* cell types were devoid of antagonist activity in GTPγS assays ruling out other solely receptor-based modes of antagonism such as allosteric inhibition and underlining the need for a whole-cell system in order to observe these phenomena. It seems unlikely that the highly polar prostanoid molecules would be able to cross the plasma membrane but even if they did, non-specific modes of inhibition such as Fluo-3 quenching & calcium inhibition, and non-receptor based modes of action such as PLCβ inhibition, would lead to the same degree of inhibition in both cell types since calcium coupling has been shown to be the same in both cell types (but could easily be ruled out by testing for activity against a non-prostanoid receptor in the same cells such as purinergic $P2_{Y2}$ receptors).

A possible explanation for these observations is receptor-mediated stimulation of a process independent of the G-protein mediated agonist effects I have studied. As suggested in Chapter 6, this may involve activation of GRK's 5 & 6 or β-arrestin recruitment. Data generated in chimera-expressing cells following PTX treatment were variable as a result of the small signal size and so it is not possible to discuss the relative contributions of $G\alpha_{i/o}$ and $G\alpha_{16z49}$ systems to the observed phenomena. However, the data do suggest that molecules have differential ability to inhibit $hCRTH_2$ receptor mediated agonism in chimera- and non-chimera- expressing cells which may relate to

differential GRK expression or activation. Indeed, as noted in Chapter 6, receptor desensitisation appears to involve a non-G-protein mediated process at low agonist concentrations and a G-protein-mediated process at higher concentrations related to the magnitude of calcium mobilisation responses; the partial inhibition by non-agonist molecules may relate to the first phase of inhibition. Because the potential exists for at least three molecules to be involved in non-G-protein mediated inhibition (GRKs 5, 6 & β-arrestin) the differing degrees of inhibition observed may represent differential recruitment of these molecules or of G-protein recruited molecules.

A much wider range of prostanoid molecule structures were capable of eliciting response inhibition than were capable of eliciting G-protein mediated agonism. Whilst this clearly indicates that the structural requirements for triggering the inhibitory response are less stringent than those for stimulating 'agonism', the relationship of the pharmacophoric contact points for each response in 3-D space is unknown and cannot be deduced from these data. The binding pocket could be identical with differing degrees of conformational change underlying the differential responses observed. Alternatively, different amino acid residues could be contacted by different molecules. Indeed, non G-protein responses could be mediated by binding to a completely distinct site either with or without allosteric interaction with the G-protein activating binding site. Whilst saturation binding detected a single population of binding sites, competition binding curves were frequently bi- or multi- phasic but deficiencies in the binding method used casts doubt on the validity of this observation (see below). Nonetheless, the ability of other prostanoid molecules such as PGE_2 and the stable thromboxane metabolite 11 dehydro TxB_2 to inhibit PGD_2-mediated receptor activation adds another level of complexity to the regulation of this receptor pathway *in vivo* and provides a means by which endogenous synthesis of the non-agonist PGE_2 by CHO cells can lead to the observed inhibition of $CRTH_2$ mediated responses in these cells (see Chapter 3). Interestingly, 11 dehydro TxB_2 has been the subject of an earlier paper describing full agonist properties of the molecule in human eosinophils and basophils (Böhm, *et al*., 2004), whereas in the present studies it was devoid of agonist effect but possessed inhibitory properties. The system studied by Böhm involved non PTX-sensitive calcium mobilisation by $hCRTH_2$ receptors endogenously expressed in these granulocytes which the authors attribute to $G\alpha_{q/11}$ activation but which could conceivably involve $G\alpha_z$ activation (but see Chapter 4: $G\alpha_z$ coupling is unlikely in

CHO cells). Therefore, this molecule may possess a dramatic ability to create trafficked agonist stimuli and should be investigated further.

A larger number of molecules were able to inhibit PGD_2 EC_{80} responses in chimera-expressing cells than in CHO K1 cells. This may relate to disruption of synergistic interactions between $G\alpha_{16z49}$ and $G\beta\gamma_{i/o}$ mediated response pathways in these cells, as discussed in Chapter 6, though the mechanism by which this might take place is unclear. Indeed, the non PTX-sensitive calcium mobilisation observed by Böhm, *et al.* (2004), may suggest that this receptor can couple to, and therefore synergise with, $G\alpha_{q/11}$ under normal physiological conditions. It was also noted in Chapter 3 that a calcium-coupled EP prostanoid receptor may be expressed in these cells raising the possibility that agonism of this receptor might lead to inhibition of the $hCRTH_2$ response pathway (heterologous desensitisation). Simple intervention with receptor antagonists for prostanoid EP_1 (e.g. AstraZeneca's ZD6416; Sarkar, *et al.*, 2003) and EP_3 (e.g. Merck's L-798,106; Juteau, *et al.*, 1999) receptors would shed light on this question. However, it does seem likely that the lower maximal inhibitions observed in the chimera-expressing cell line are due to weaker functional inhibition of the $G\alpha_{16z49}$ / $G\beta\gamma_{i/o}$ synergy-amplified agonist responses in this cell line.

Agonist potencies and antagonist affinities were consistently higher in [^{35}S]-GTPγS assays compared to the corresponding calcium mobilisation assays. This had previously been noted for GW853481X and AH23848B in Chapter 4 and an attribution to pathway-dependent affinity was postulated. In the light of the present data, however, it seems more probable that compound affinity has been influenced by assay methodology, perhaps because of the inclusion of saponin to facilitate passage of compounds into membrane vesicles. However, 13,14 dihydro 15 keto PGE_2, which has been characterised as an antagonist of $hCRTH_2$ receptors, displayed complex behaviour in Schild analysis commensurate with an interaction at two sites. Further experimentation is required to determine if this is a real effect, and if so, what it signifies. One possibility is that because the assay methodology was optimised for the detection of agonism, inverse agonist properties have been missed and this should also be investigated.

The binding assay data generated here is a useful indicator of an interaction with the receptor but cannot be relied upon to provide quantitative information because of deficiencies in the method employed. Following the detection of a profound vehicle

effect, [^{3}H]-PGD$_2$ saturation binding assays had to be restricted to a low concentration range. This failed to achieve full saturation of the receptor and may have missed the lower agonist affinity receptor population observed by Sawyer, *et al* (2002), and predicted here by back-calculation from protein linearity data. Accurate estimation of B_{max} is therefore impossible under the conditions employed but is likely to be substantially larger than the values calculated from saturation data. Allowing for a 50 % error on the estimates calculated from the protein linearity data, there could be more than enough protein to completely bind all of the available radioligand, leading to 100 % depletion and marked under-estimation of competing ligand affinity. As suggested above, and also by Mathiesen, *et al*. (2005), multiple binding sites may exist on this receptor which would further obscure estimation of receptor expression and could complicate displacement curve generation through allosteric interaction. Another possible explanation involves the impact of receptor occupation by two agonists with differing efficacy for the reciprocal interaction between receptor and G-protein (Costa, *et al*., 1992). As noted in chapter 6, there are several aspects of the pharmacology of this receptor that would be consistent with the presence of two (or more) binding sites. One puzzling aspect of the binding data is the observation of high affinity for almost all compounds tested irrespective of their functional potencies. While there is no *a priori* reason to expect a correlation, a trend often emerges, but that was not the case here. Initially taken to represent a methodological deficiency, this phenomenon may also be evident in the data presented by Sawyer *et al.*, (2002) in which 13,14 dihydro 15 keto PGF$_{2\alpha}$ is a high affinity displacer of [^{3}H]-PGD$_2$ (pK$_i$ 8.5) but a low potency agonist in a cAMP inhibition assay (pEC$_{50}$ 6.2). Therefore the present data may indicate a true phenomenon but for the reasons given above, and the observed high variability of binding assay data, definitive data from a re-developed assay using either [^{125}I]-PGD$_2$ or, preferably, an iodinated antagonist radioligand, should be generated. Other improvements could include performing the reaction at 4 ºC, increasing the ligand concentration (cut with cold ligand if iodinated versions are employed), reducing the membrane concentration, increasing the reaction volume, re-dissolving the radioligand in a more benign vehicle, and reformatting the assay to use scintillation proximity assay (SPA) technology. However, these considerations aside, it does appear that PGD$_2$ is displaced from the receptor by non-agonist inhibitors (i.e. molecules devoid of agonist activity but which inhibit D$_2$EC$_{80}$ responses), that displacement curves may be bi- or

multi-phasic, and that the maximum displacement achieved may be partial in some cases. The exact nature of the affinity, phases and kinetics of ligand interaction is one of the key questions remaining and is vital to a full understanding of the behaviour of this receptor.

Overall, while non G-protein mediated, receptor-stimulated receptor desensitisation has not been proven, it remains an attractive explanation for the ability of non-'agonist' molecules to inhibit PGD_2 EC_{80} responses in cell-based, but not membrane-based, systems. Alternatively, these data may point to binding site or coupling pathway dependent signalling and molecules such as these provide another means by which this intriguing chemoattractant receptor can be regulated in physiological and pathological situations. Finally, an exciting avenue of research has been opened and further experimentation is clearly warranted: greater definition of the nature of the interaction these molecules have with the receptor, and measurement or visualisation of changes in cell-surface receptor behaviour are obvious targets. Whilst an antagonist of this receptor is unlikely to provide a 'wonder-drug', the arrival of $CRTH_2$ in the family of GPCRs and an understanding of the pleiotropic response pathways this receptor stimulates may herald a re-definition of the term 'polypharmacology' and ultimately lead to the search for agents with selectivity at the stimulus trafficking level.

7.5 Figure caption list:

Figure 1. Inhibition of PGD_2 EC_{80} by prostanoid molecules in calcium mobilisation assay using CHO $G\alpha_{16z49}$ $hCRTH_2$ cells. Data are mean ± sem of three independent experiments.

Figure 2. Correlation plot of agonist and inhibitor potencies for prostanoid molecules in calcium mobilisation assays using CHO $G\alpha_{16z49}$ $hCRTH_2$ cells. Data are mean ± sem of three independent experiments. Terms are: pEC_{50} – negative log of the agonist concentration required to elicit 50 % of the maximum effect to that agonist; pIC_{50} - negative log of the inhibitor concentration required to elicit 50 % of the maximum inhibition by that agonist; in both cases parameters determined by curve fitting. Dashed line indicates perfect 1:1 correlation.

Figure 3. Inhibition of PGD_2 EC_{80} by prostanoid molecules in calcium mobilisation assay using CHO $G\alpha_{16z49}$ $hCRTH_2$ cells following pertussis toxin (50 ng ml^{-1}) treatment. Data are mean ± sem of three independent experiments.

Figure 4. Correlation plot of agonist and inhibitor potencies for prostanoid molecules in calcium mobilisation assays using CHO $G\alpha_{16z49}$ $hCRTH_2$ cells following pertussis toxin (50ng ml^{-1}) treatment. Data are mean ± sem of three independent experiments. Terms are: pEC_{50} – negative log of the agonist concentration required to elicit 50 % of the maximum effect to that agonist; pIC_{50} - negative log of the inhibitor concentration required to elicit 50 % of the maximum inhibition by that compound; in both cases parameters determined by curve fitting. Dashed line indicates perfect 1:1 correlation.

Figure 5. Inhibition of PGD_2 EC_{80} by prostanoid molecules in calcium mobilisation assay using CHO K1 $hCRTH_2$ cells following pertussis toxin (50 ng ml^{-1}) treatment. Data are mean ± sem of three independent experiments.

Figure 6. Correlation plot of agonist and inhibitor potencies for prostanoid molecules in calcium mobilisation assays using CHO K1 $hCRTH_2$ cells following pertussis toxin (50 ng ml^{-1}) treatment. Data are mean ± sem of three independent experiments. Terms are: pEC_{50} – negative log of the agonist concentration required to elicit 50 % of the

maximum effect to that agonist; pIC_{50} - negative log of the inhibitor concentration required to elicit 50 % of the maximum inhibition by that compound; in both cases parameters determined by curve fitting. Dashed line indicates perfect 1:1 correlation.

Figure 7. Venn diagram depicting the incidence of non-agonist inhibitory prostanoid molecules (i.e. Molecules possessing inhibitory activity but not possessing agonist activity) in CHO $G\alpha_{16z49}$ - (lower region) and CHO K1 - (upper region) $hCRTH_2$ cells. Overlapping area shows molecules displaying this behaviour in both cell types.

Figure 8. Analysis of competition (Schild analysis) of representative compounds at $hCRTH_2$ receptors expressed in CHO $G\alpha_{16z49}$ cells, and (inset) agonist activity of test compounds determined in the same assay, using a calcium mobilisation assay. Upper two panels ($PGF_{2\alpha}$ and 13,14 dihydro 15 keto $PGF_{2\alpha}$) are partial agonists; middle two panels (GW853481X and 13,14 dihydro 15 keto PGE_2) are antagonists; lower two panels (19 R hydroxy PGA_2 and PGE_2) are inhibitors which do not possess agonist activity. Data are mean ± sem of three independent experiments. Key to symbols in all panels: + vehicle, ● 41 nM, ○ 100 nM, × 400 nM, □ 1.1 μM, ◇ 3.3 μM, △ 10 μM & ▽ 30 μM compound.

Figure 9. Analysis of competition (Schild analysis) of representative compounds at $hCRTH_2$ receptors expressed in CHO K1 cells, and (inset) agonist activity of test compounds determined in the same assay, using a calcium mobilisation assay. Upper two panels ($PGF_{2\alpha}$ and 13,14 dihydro 15 keto $PGF_{2\alpha}$) are partial agonists; middle two panels (GW853481X and 13,14 dihydro 15 keto PGE_2) are antagonists; lower two panels (19 R hydroxy PGA_2 and PGE_2) are inhibitors which do not possess agonist activity. Data are mean ± sem of three independent experiments. Key to symbols in all panels: + vehicle, ● 41 nM, ○ 100 nM, × 400 nM, □ 1.1 μM, ◇ 3.3 μM, △ 10 μM & ▽ 30 μM compound.

Figure 10. Effect of single concentration (10μM, except 19 R hydroxy PGA_2 = 1 μM) of representative compounds on PGD_2 E/[A] curves at $hCRTH_2$ receptors expressed on CHO K1 cell membranes using a [^{35}S]-GTPγS accumulation assay. Upper two panels ($PGF_{2\alpha}$ and 13,14 dihydro 15 keto $PGF_{2\alpha}$) are partial agonists; middle two panels

(GW853481X and 13,14 dihydro 15 keto PGE_2) are antagonists; lower two panels (19 R hydroxy PGA_2 and PGE_2) are inhibitors which do not possess agonist activity. Data are mean ± sem of four independent experiments; abscissa: -log [compound], ordinate: cpm. Key to symbols in all panels: ○ vehicle, + test molecule treated.

Figure 11. Analysis of competition (Schild analysis) of representative compounds at $hCRTH_2$ receptors expressed on CHO K1 cell membranes using a [^{35}S]-GTPγS accumulation assay. Upper two panels ($PGF_{2\alpha}$ and 13,14 dihydro 15 keto $PGF_{2\alpha}$) are partial agonists; middle two panels (GW853481X and 13,14 dihydro 15 keto PGE_2) are antagonists; lower two panels (19 R hydroxy PGA_2 and PGE_2) are inhibitors which do not possess agonist activity. Data are mean ± sem of four independent experiments; abscissa: -log [PGD_2], ordinate: cpm. Key to symbols in all panels: + untreated, ○ vehicle, ● 300 nM, × 1 μM, □ 3 μM, ◇ 10 μM, ▽ 30 μM & △ 100 μM compound.

Figure 12. Relationship between total binding and membrane protein (protein linearity) for membranes derived from CHO K1- (upper panel) and CHO $G\alpha_{16z49}$- (lower panel) $hCRTH_2$ cells. Membranes were incubated with 2.2 nM [^{3}H]-PGD_2 for 60 min at room temp. Data are triplicate determinations from a single experimental occaision.

Figure 13. Effect of radioligand vehicle (15 % acetonitrile + 29 % methanol v v^{-1} in distilled water) on total binding of 3.5 nM [^{3}H]-PGD_2 to membranes derived from CHO K1 $hCRTH_2$ cells. Membranes were incubated with ligand for 60 min at room temp. Data are mean ± sem of triplicate determinations from a single experimental occasion.

Figure 14. Displacement of [^{3}H]-PGD_2 (2 nM) binding by prostanoid molecules at CHO K1 $hCRTH_2$ membranes. Reaction mixtures were incubated for 30 min at room temp. prior to rapid filtration onto a glass fibre filtermat and scintillation counting. Because of the high degree of row-to-row variability, data have been normalised to total binding in that row. Data are mean ± sem of normalised data from three independent experiments.

7.6 Figures

Follow on next page.

Figure 1.

CHO $G\alpha_{16z49}$ $hCRTH_2$

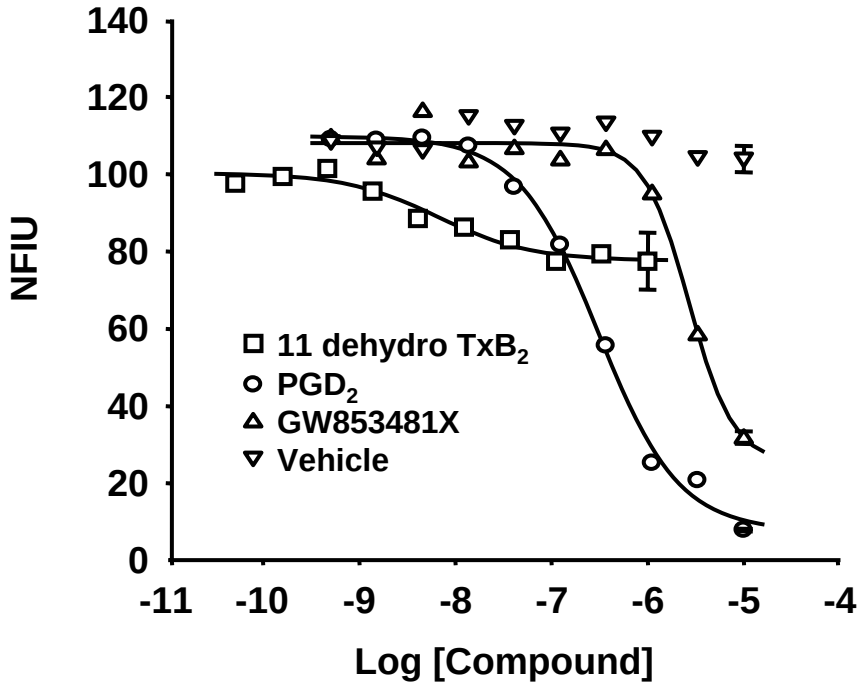

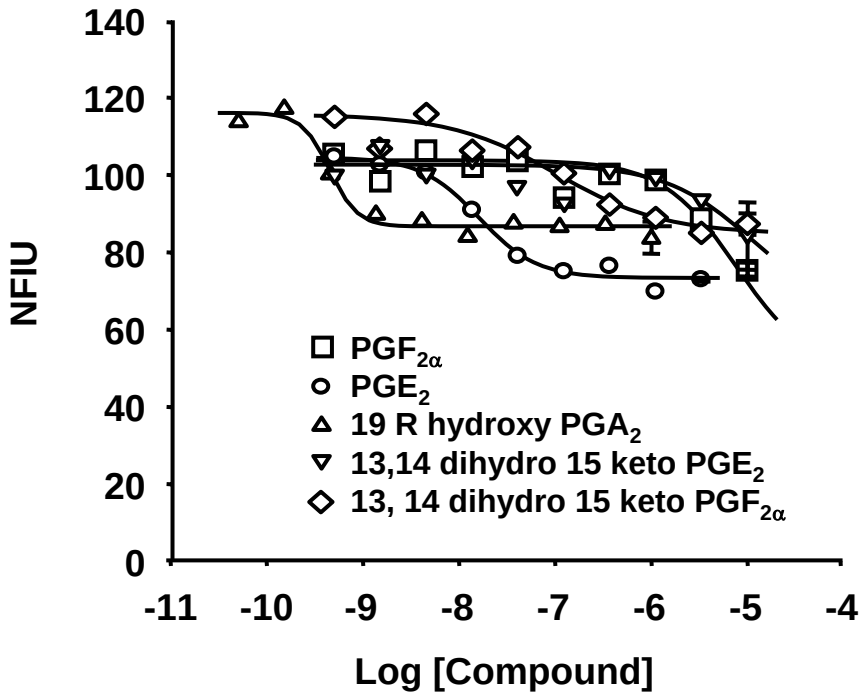

Figure 2.

CHO $G\alpha_{16z49}$ $hCRTH_2$

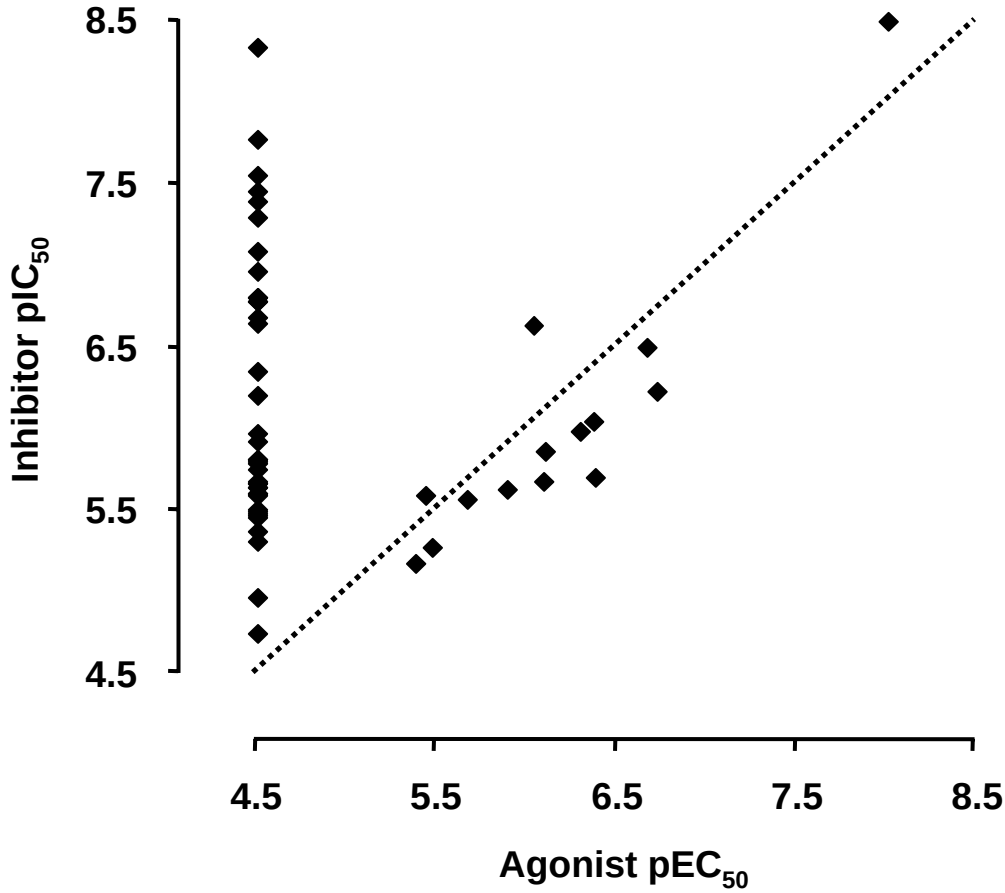

Figure 3.

CHO $G\alpha_{16z49}$ $hCRTH_2$ + PTX

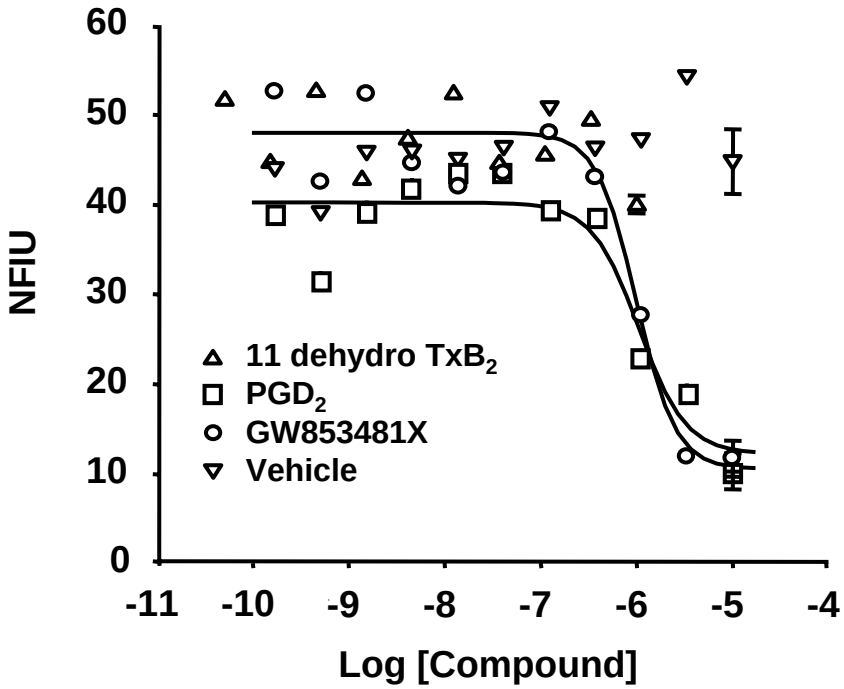

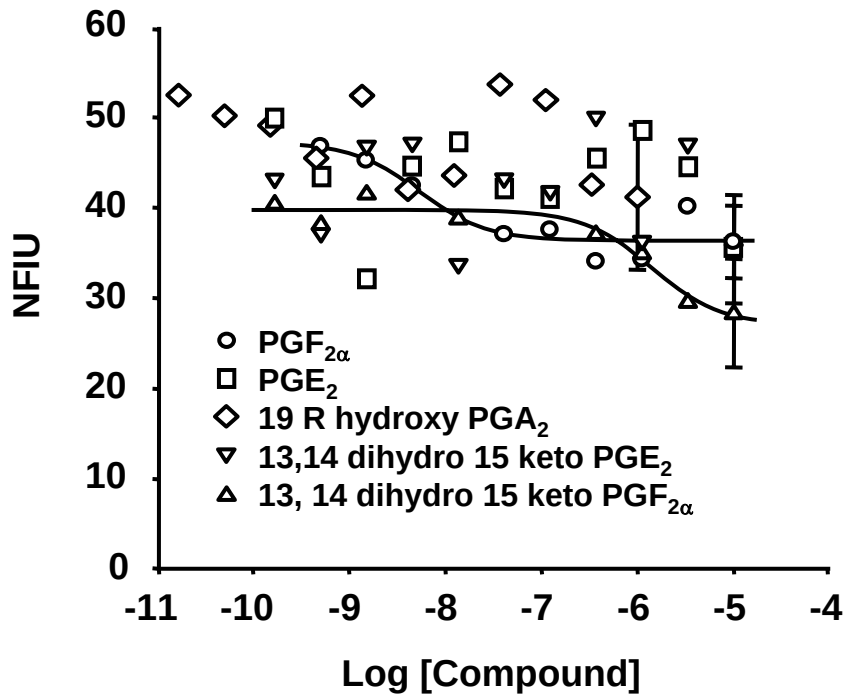

Figure 4.

CHO $G\alpha_{16z49}$ $hCRTH_2$ + PTX

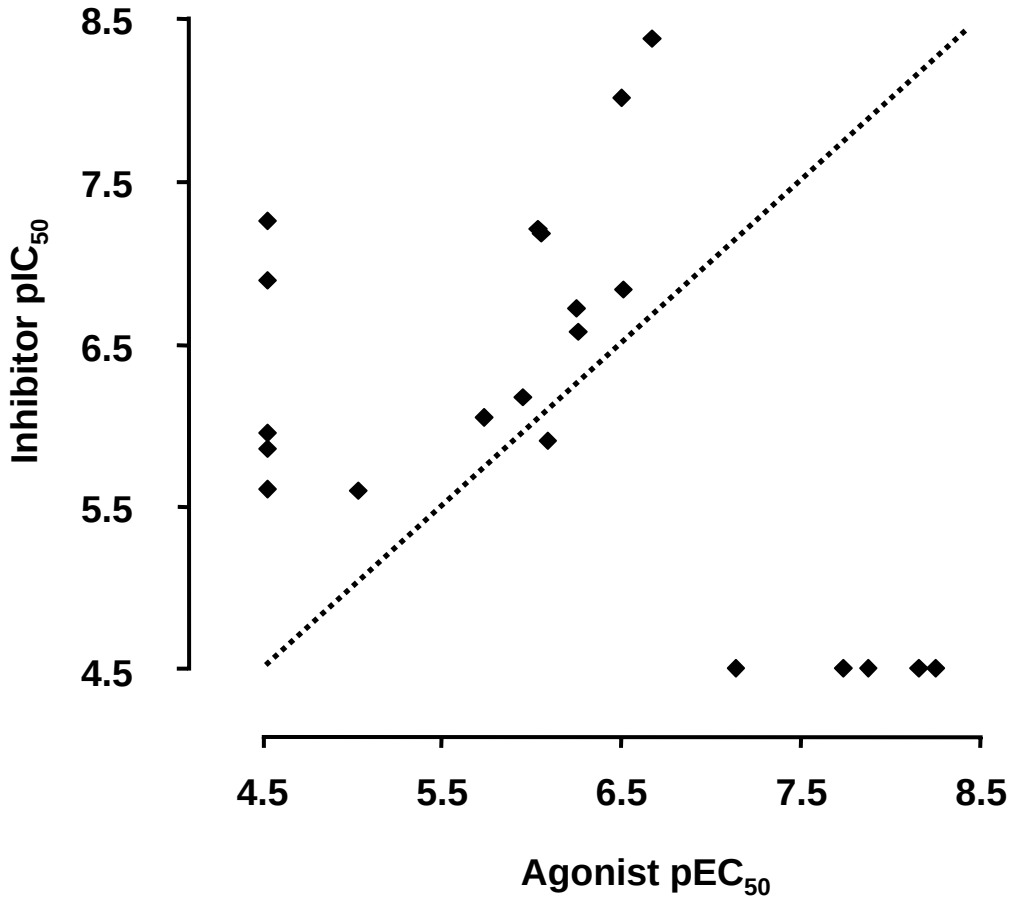

Figure 5. **CHO K1 hCRTH$_2$**

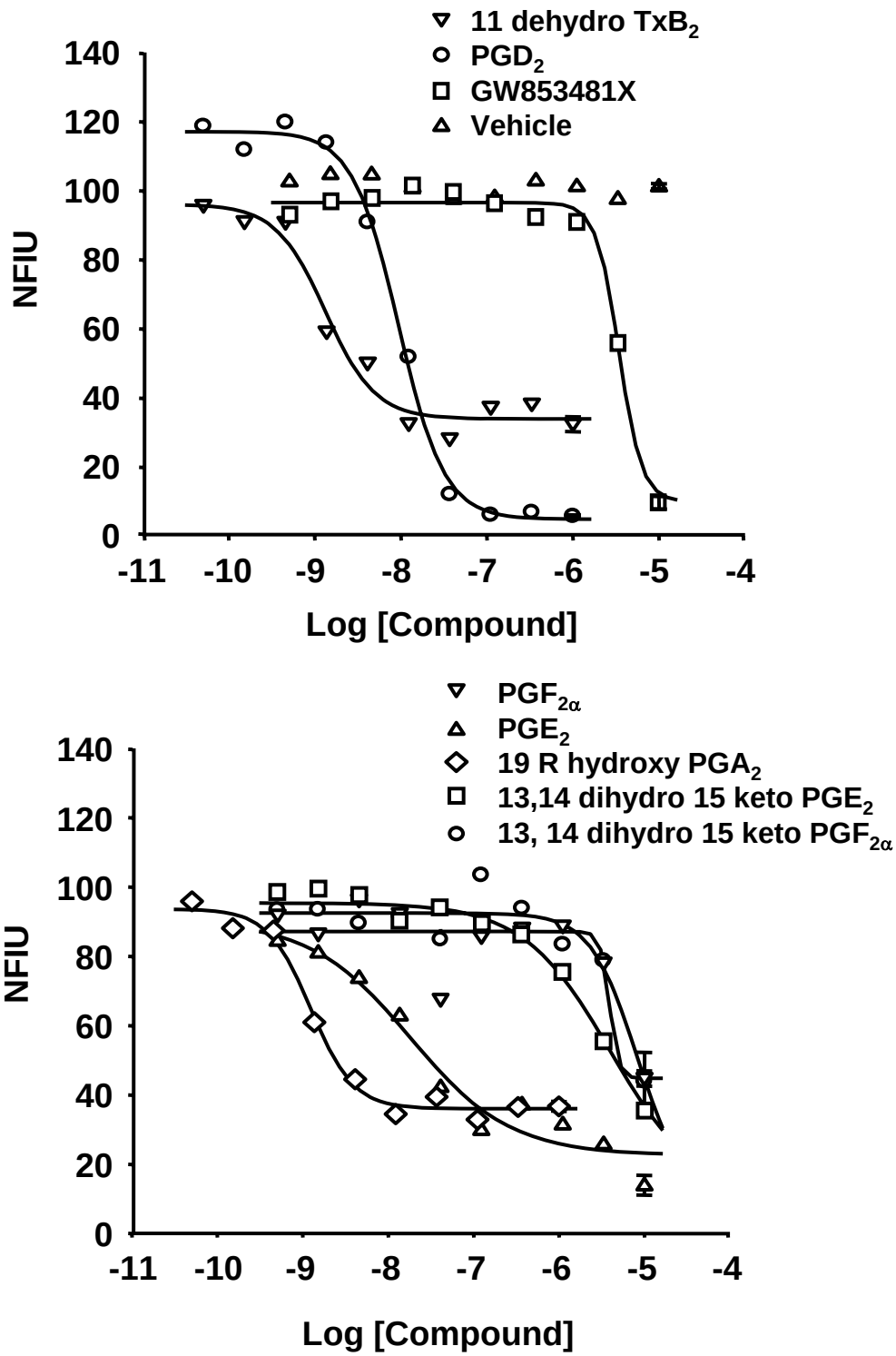

Figure 6.

CHO K1 hCRTH$_2$

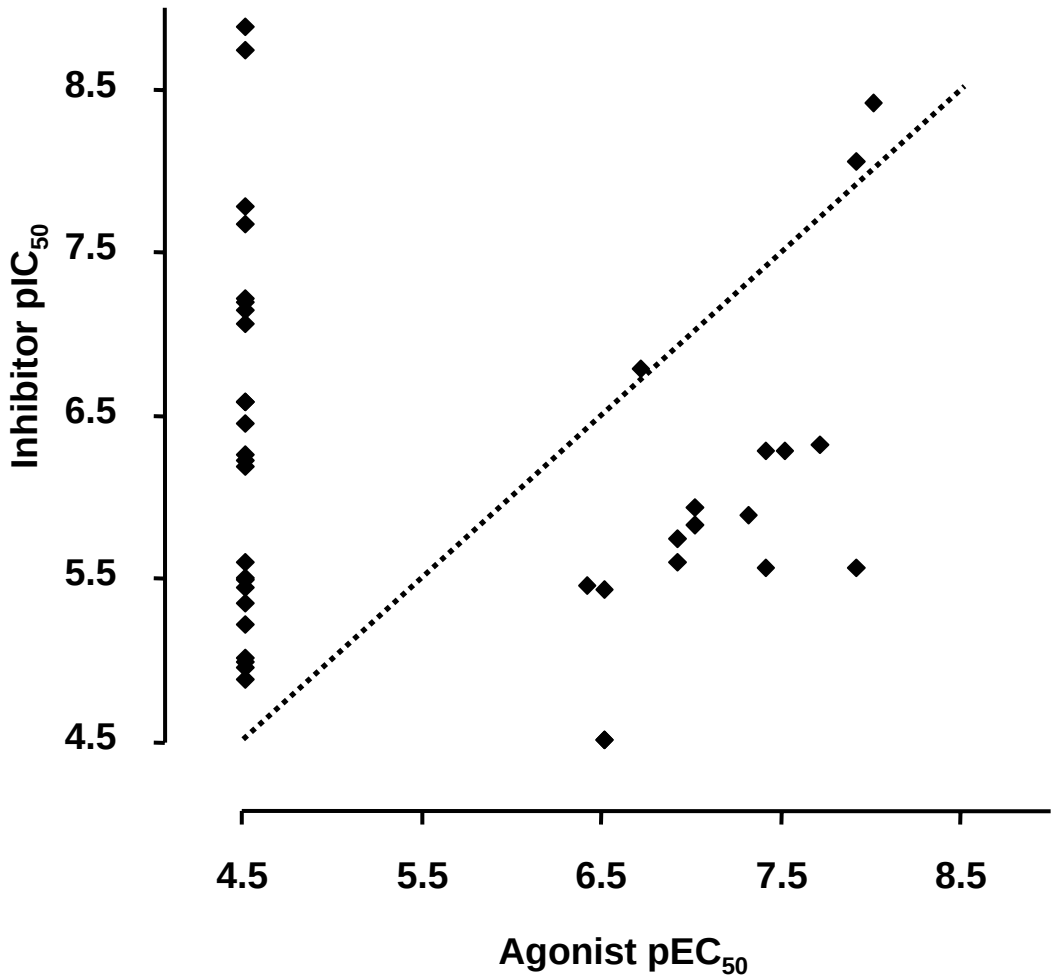

Figure 7.

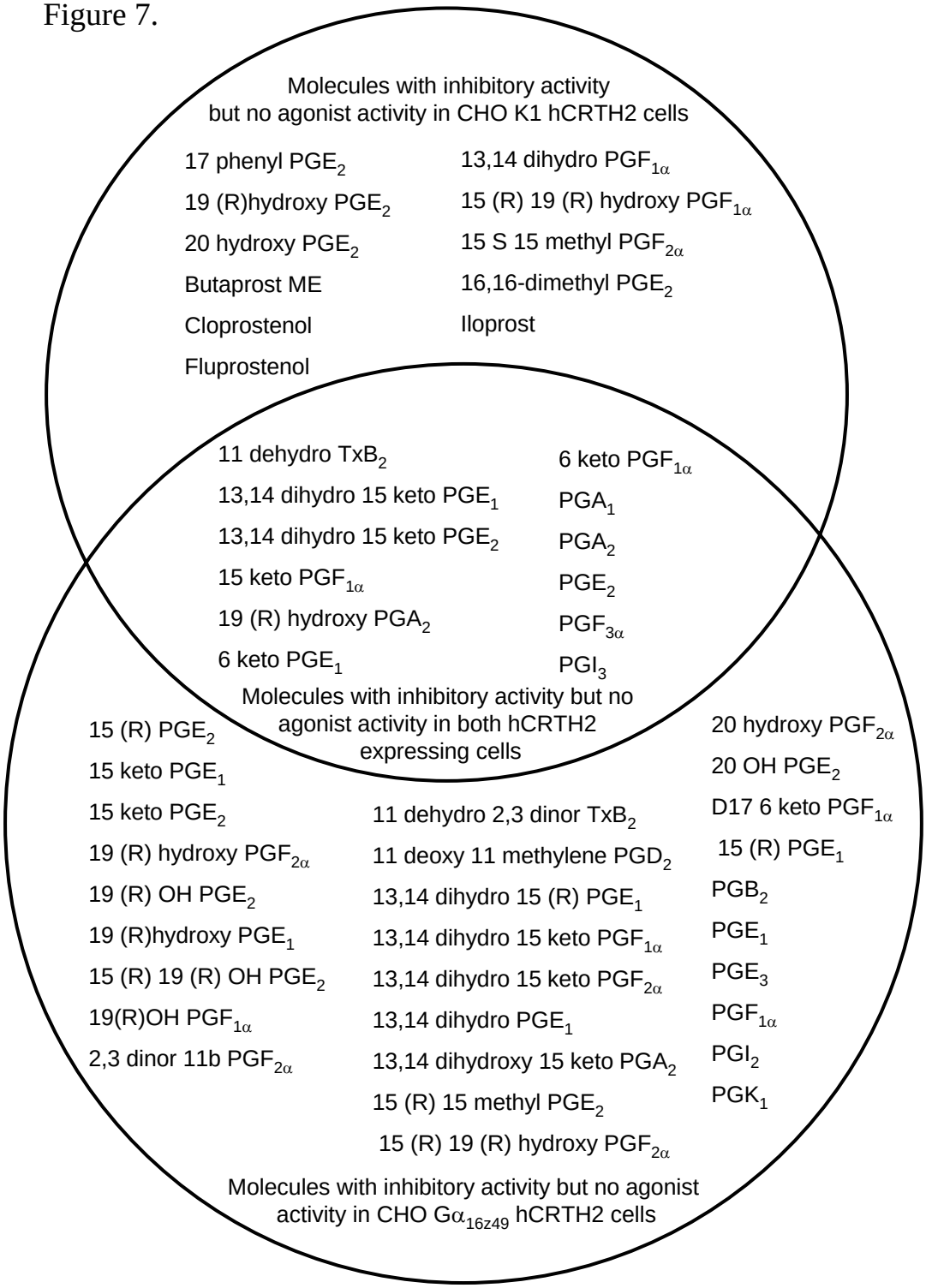

CHO $G\alpha_{16z49}$ $hCRTH_2$

Figure 8.

CHO $G\alpha_{16z49}$ $hCRTH_2$

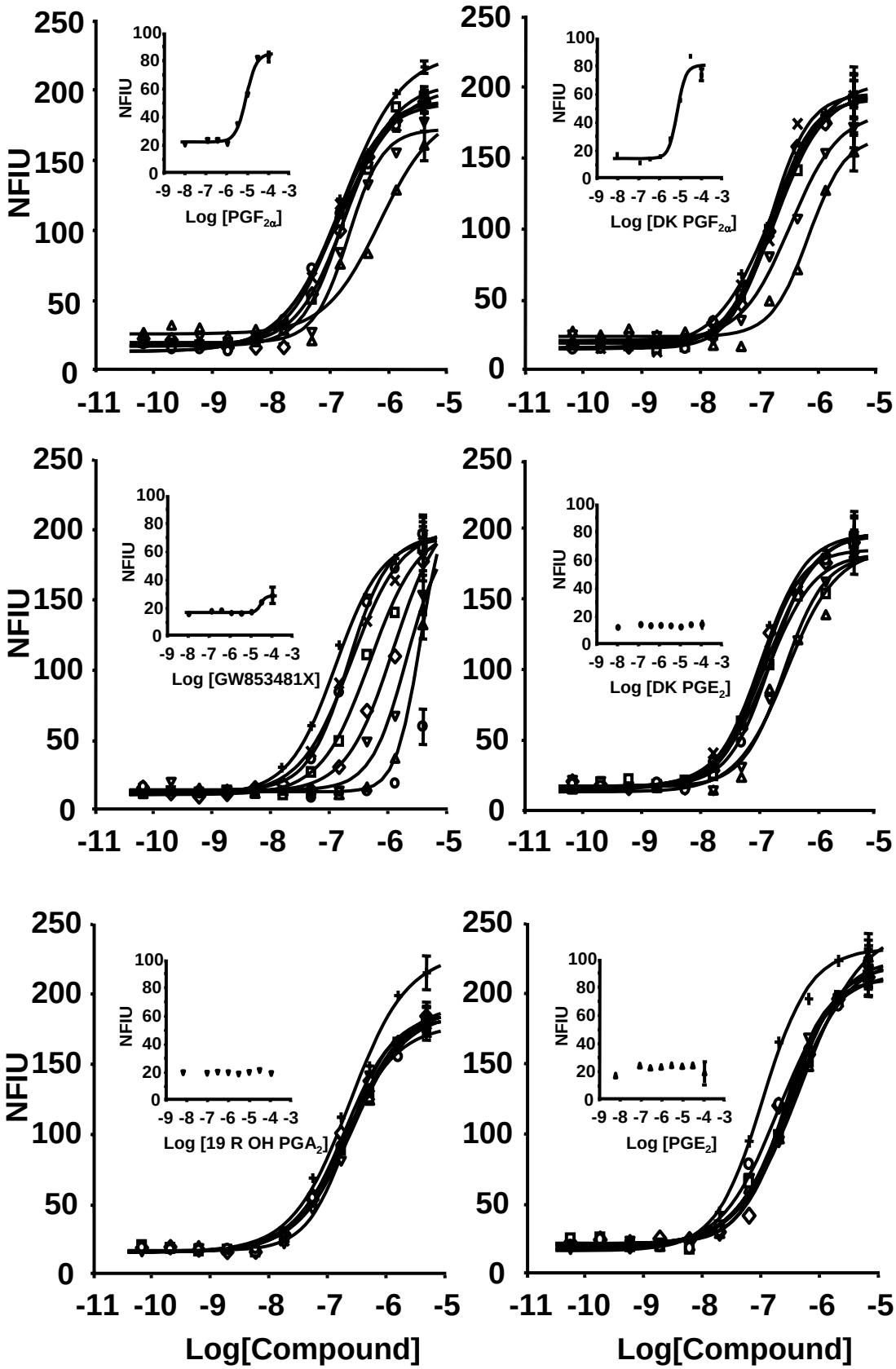

Figure 9.

CHO K1 hCRTH$_2$

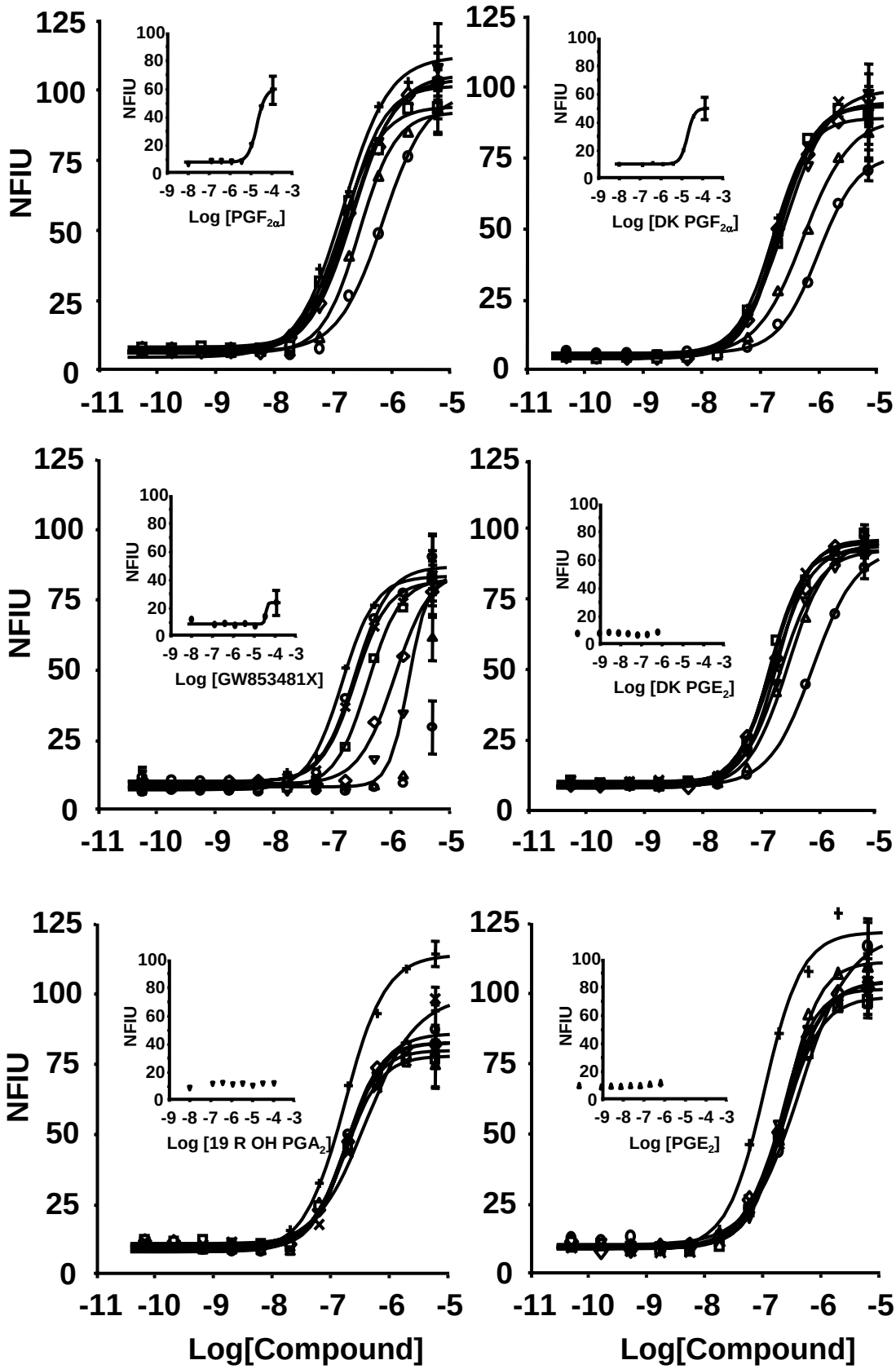

Figure 10.

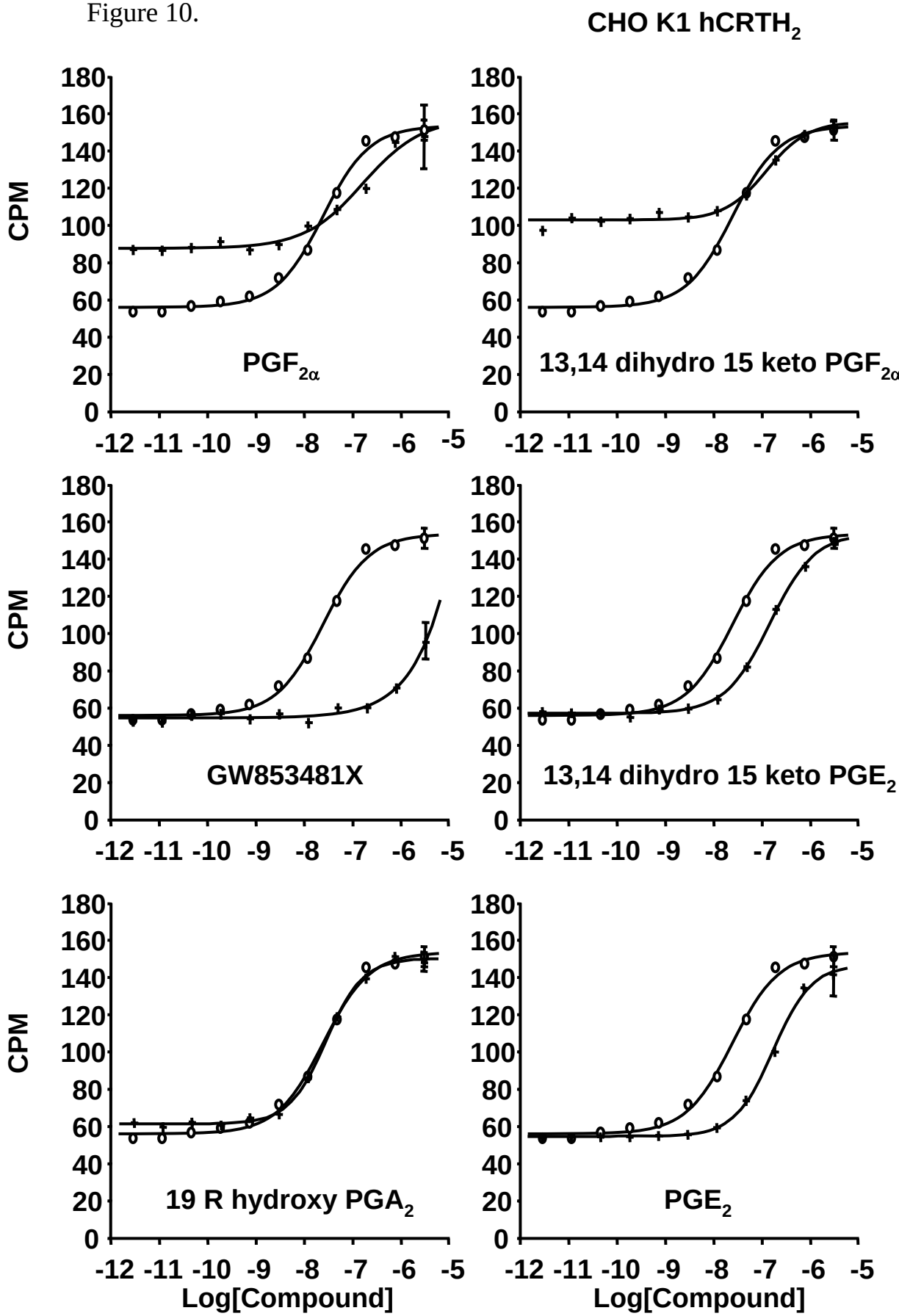
CHO K1 hCRTH2
CPM
PGF2α
13,14 dihydro 15 keto PGF2α
GW853481X
13,14 dihydro 15 keto PGE2
19 R hydroxy PGA2
PGE2
Log[Compound]
Log[Compound]

Figure 11.

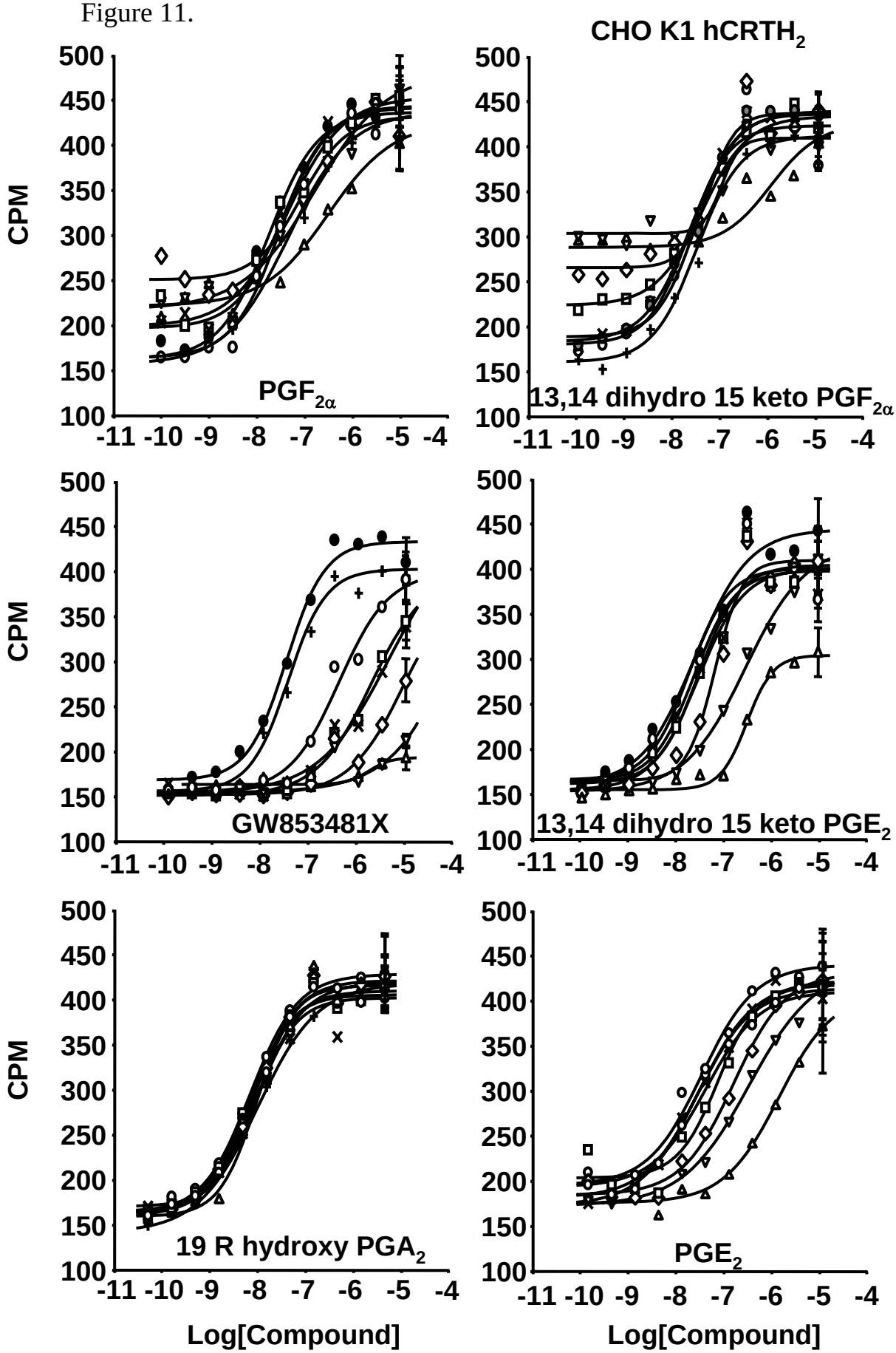
CHO K1 hCRTH2
CPM
PGF2α
13,14 dihydro 15 keto PGF2α
GW853481X
13,14 dihydro 15 keto PGE2
19 R hydroxy PGA2
PGE2
Log[Compound]
Log[Compound]

Figure 12.

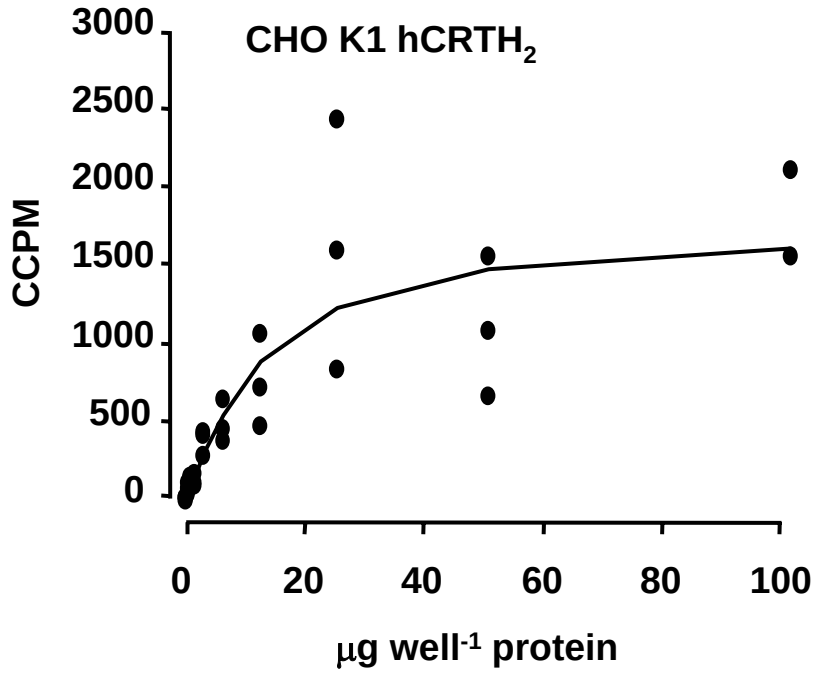
CHO K1 hCRTH2
CCPM
3000
2500
2000
1500
1000
500
0
0
20
40
60
80
100
μg well-1 protein

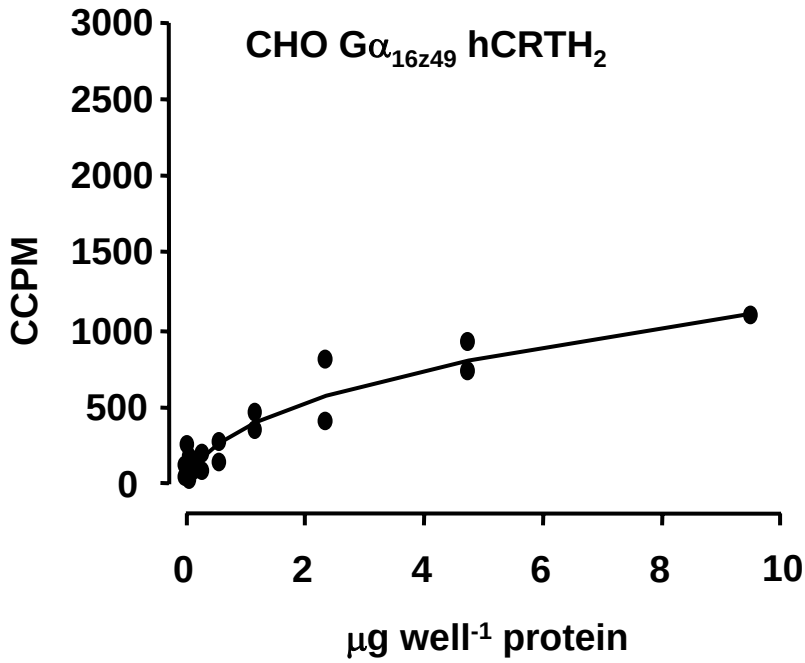
CHO Gα16z49 hCRTH2
CCPM
3000
2500
2000
1500
1000
500
0
0
2
4
6
8
10
μg well-1 protein

Figure 13.

CHO K1 hCRTH$_2$

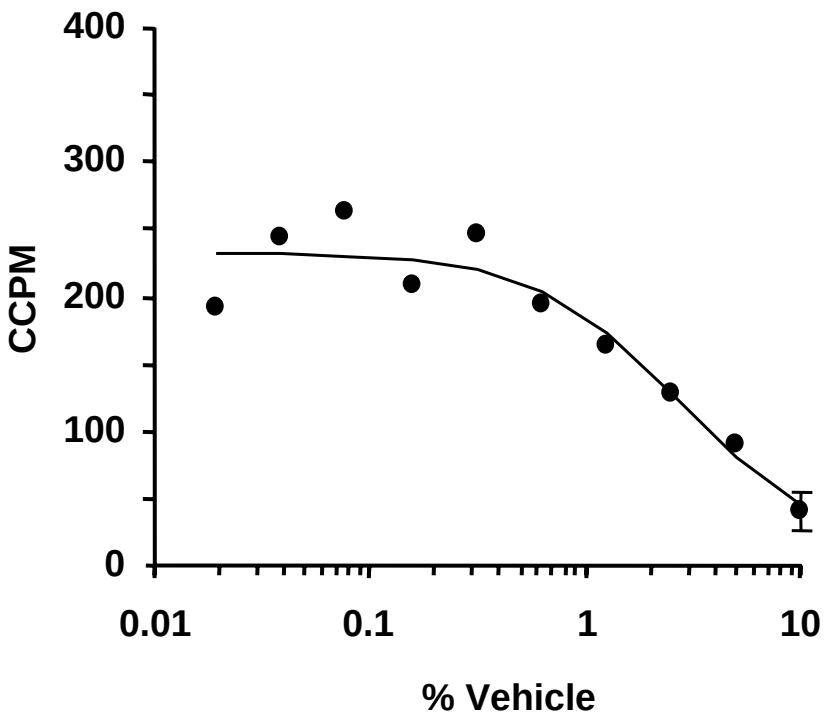

Figure 14.

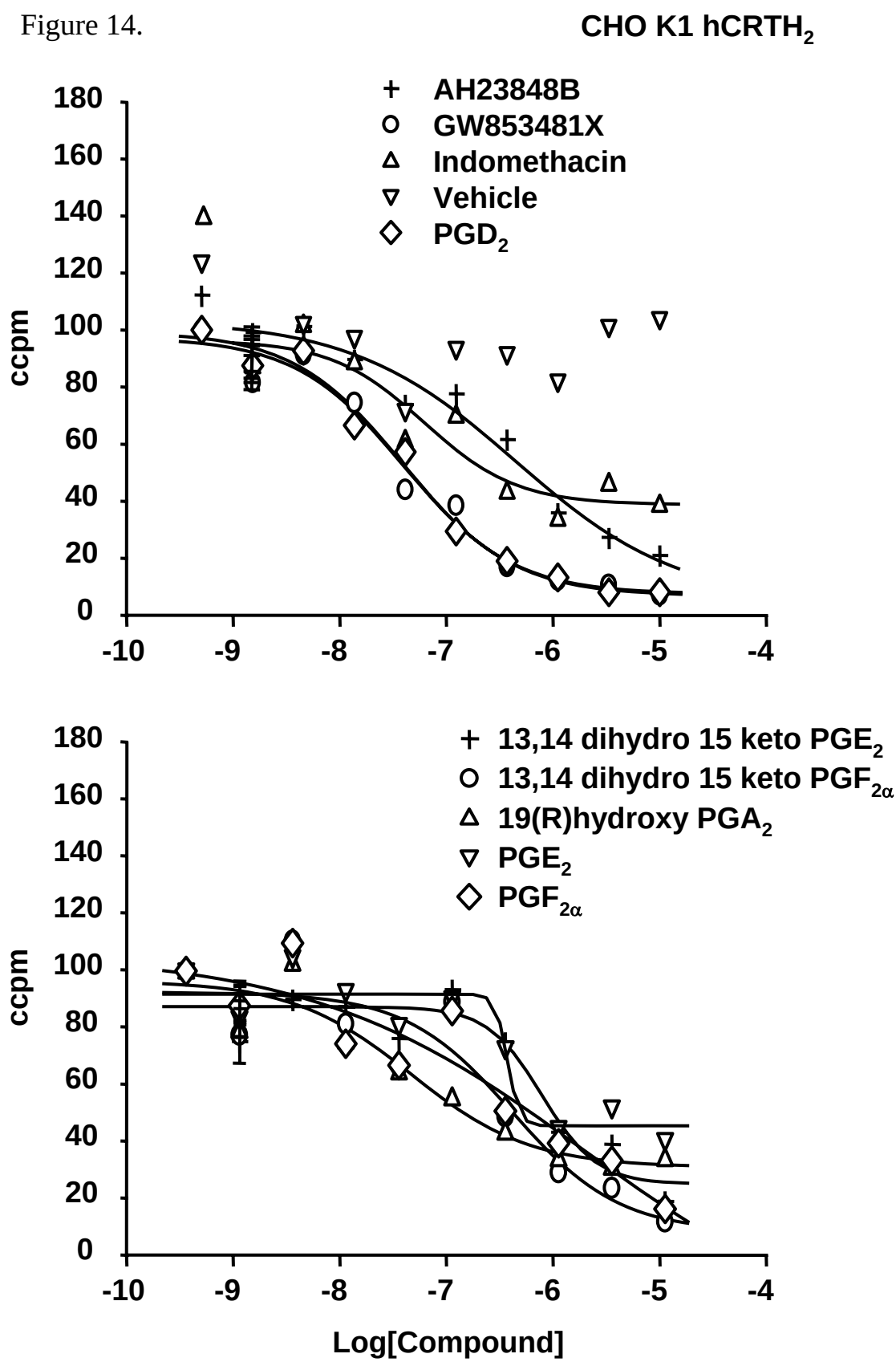
CHO K1 hCRTH2
AH23848B
GW853481X
Indomethacin
Vehicle
PGD2
ccpm
180
160
140
120
100
80
60
40
20
0
-10
-9
-8
-7
-6
-5
-4
13,14 dihydro 15 keto PGE2
13,14 dihydro 15 keto PGF2α
19(R)hydroxy PGA2
PGE2
PGF2α
Log[Compound]

Chapter8: Final Remarks

In this thesis I have examined the relationship between five alternative expressions of efficacy by recombinant prostanoid $hCRTH_2$ receptors expressed in CHO cells:

1. $G\alpha_{16z49}$ + $G\beta\gamma_{i/o}$ mediated calcium mobilisation in whole cells (dual coupling).
2. $G\alpha_{16z49}$ mediated calcium mobilisation (whole cells).
3. $G\beta\gamma_{i/o}$ mediated calcium mobilisation (whole cells).
4. $G\alpha_{i/o}$ mediated [^{35}S]-GTPγS accumulation in cell membranes.
5. Non $G_{i/o}$ mediated, non syntopic inhibition of receptor activation (whole cells).

Where relevant, the involvement of $G\beta\gamma_{i/o}$ subunits has been demonstrated, that of $G\alpha_{16z49}$ has been deduced, while that of $G\alpha_{i/o}$ has been assumed based on the deductions made in the calcium assays. $G\alpha_z$ and $G\alpha_{q/11}$ *are* expressed in these cells but their involvement in $hCRTH_2$ receptor signal transduction has been excluded. Receptor : G-protein stoichiometry has been shown to be non-equivalent in the cell lines studied but the exact extent of the disparity has been clouded by reliance on an agonist radioligand. A greater degree of equivalence was expected between $G\beta\gamma_{i/o}$ (calcium) and $G\alpha_{i/o}$ (GTPγS) assays through the use of the same cell line to provide the biological system in each case. However this was not specifically demonstrated, and true equivalence is unlikely to have been achieved because of the rigours of the membrane preparation procedure. Whilst these are important considerations of which one should be mindful in arriving at a balanced interpretation of the data, they do not invalidate the approaches taken.

Agonist pharmacology in the dual-coupled setting may have been influenced by synergistic interaction of the chimeric Gα and native Gβγ subunits, possibly at the PLCβ activation level. While synergism between two distinct receptor types would invalidate these data, because the interaction here is via a single receptor type, alterations in agonist behaviour observed in moving to single-coupling settings can still be considered an expression of agonist-directed stimulus trafficking.

Two Gα-based readouts ($G\alpha_{16z49}$ mediated calcium mobilisation and $G_{i/o}$ based GTPγS accumulation) provided similar agonist rank order data but with evidence of differences consistent with altered response coupling efficiency. However, when Gα coupling data were compared with Gβγ coupling data, marked alterations in agonist behaviour were observed including reversals of agonist potency rank orders, reversals of agonist relative

activity orders and examples of compounds reducing in potency while others increased in potency. Data such as these are not consistent with 'strength of stimulus' based changes and are considered to be evidence of agonist-directed stimulus trafficking.

Since the $G_{i/o}$ observed in the GTPγS assay is assumed to be derived from the same heterotrimers as the $G\beta\gamma_{i/o}$ observed in calcium mobilisation assay, then the occurrence of trafficked agonist stimuli might point to a novel integrated activation paradigm of Gβγ subunits in which receptor / agonist-dependent and GTP hydrolysis-dependent conformation changes in Gα subunits combine to provide a resultant activation of Gβγ subunits.

A surprising finding was that non-agonist molecules (as shown in calcium mobilisation and GTPγS accumulation assays) could partially inhibit PGD_2 responses in a manner apparently not related to competitive antagonism. Agonist molecules also inhibit responses to subsequent PGD_2 exposure but this is related to receptor desensitisation. The mechanism by which non-agonist inhibitors exert their effect has not been elucidated but may relate to non-G-protein mediated GRK activation. This phenomenon displayed its own pharmacophore suggesting an interaction at a different (but possibly overlapping) binding site. Kinetic radioligand binding assays are needed in order to test for allosteric inhibition of PGD_2 responses: the binding assay developed here is significantly flawed and an alternative assay should be developed. However, these considerations aside, competition binding data may have revealed the presence of multiple radioligand interaction sites.

Several areas present opportunities for further study:

1. Radioligand binding assay redevelopment, possibly with an antagonist radioligand.
2. Assessment of the molecular identities of the G-proteins giving rise to the [^{35}S]-GTPγS accumulation signal through antibody capture techniques.
3. Investigation into the properties of 11 dehydro thromboxane B_2 which may be a highly sensitive indicator of stimulus trafficking and which may be a highly potent non-agonist inhibitor of PGD_2; and
4. Investigation into the molecular processes underpinning agonist-induced receptor desensitisation.

The data I have presented demonstrate the critical dependence of agonist pharmacology on both G-protein coupling partner and assay methodology, and contribute to our current understanding of efficacy in relation to agonist stimulus trafficking.

Chapter 9: Acknowledgements.

I'd like to thank the following individuals for their contributions to this work:

Professor Stephen Hill (Institute of Cell Signalling, Queen's Medical Centre, Nottingham, UK.) for supervising the project and guiding my thinking.

Drs. Mike Allen & Shelagh Wilson (Screening & Compound Profiling & Centre of Excellence for External Drug Discovery, GSK R&D, Third Avenue, Harlow, Essex, CM19 5AW) who arranged for the sponsorship of this work by GSK.

Ms. Nicola Hawley (Institute of Cell Signalling, Queen's Medical Centre, Nottingham, UK.) for provision of β-ARK 495-689 pcDNA.

Tanja Alnadaf & Dr. Bob Ames (Biological Reagents & Assay Development, GSK R&D, Medicines Research Centre, Gunnels Wood Road, Stevenage, Herts., SG1 2NY, UK) for preparation of CHO $G\alpha_{16z49}$ cell line.

Dr. Ashley Barnes & Emma Koppe (GSK, as above) for preparation of CHO $hCRTH_2$ cell lines

Emma Koppe & Olutu Oganah (GSK, as above) for adaptation of adherent CHO K1 $hCRTH_2$ cell line to suspension culture

Jim Coote & the late Bob Middleton (GSK, as above) for production of CHO K1 $hCRTH_2$ cell membranes used in [^{35}S]-GTPγS accumulation assay.

Chapter 10: References.

ABBAS, A. K. & LICHTMAN, A. H. (2003). Cellular and Molecular Immunology 2nd edition. Saunders, Philadelphia.

ABE, H., TAKESHITA, T., NAGATA, K., ARITA, T., ENDO, Y., FUJITA, T., TAKAYAMA, H., KUBO, M. & SUGAMURA, K. (1999). Molecular cloning, chromosome mapping and characterization of the mouse CRTH2 gene, a putative member of the leukocyte chemoattractant receptor family. *Gene*, **227**, 71-77.

ALBRECHT, F. E., XU, J., MOE, O. W., HOPFER, U., SIMONDS, W. F., ORLOWSKI, J. & JOSE, P. A. (2000). Regulation of NHE3 activity by G protein subunits in renal brush-border membranes. *Am. J. Physiol. – Reg. Integ. Comp. Physiol.*, **278**, R1064-R1073.

ALEXANDER, S. P. H., MATHIE, A. & PETERS, J. A. (2006). Guide to receptors and channels, 2nd edition. *Br. J. Pharmacol.*, **147 (S3)**, S26-S28.

AKIN, D., ONARAN, H. O. & GURDAL, H. (2002). Agonist-directed trafficking explaining the difference between response pattern of naratriptan and sumatriptan in rabbit common carotid artery. *Br. J. Pharmacol.*, **136**, 171-176.

ARIENS, E. J. (1954). Affinity and intrinsic activity in the theory of competitive inhibition. I. Problems and theory. *Arch. Int. Pharmacodyn. Ther.*, **99**, 32-49.

ARMER, R. E., ASHTON, M. R., BOYD, E. A., BRENNAN, C. J., BROOKFIELD, F. A., GAZI, L., GYLES, S. L., HAY, P. A., HUNTER, M. G., MIDDLEMISS, D., WHITTAKER, M., XUE, L. & PETTIPHER, R. (2005). Indole-3-acetic acid antagonists of the prostaglandin D_2 receptor CRTH2. *J. Med. Chem.*, **48**, 6174-6177.

ARUNLAKSHANA., O. & SCHILD, H. O. (1959). Some quantitative uses of drug antagonists. *Br. J. Pharmacol.*, **14**, 48-58.

BAUER, P. H., CENG, J. B., GLADUE, R. P., LI, B., NEOTE, K. S. & ZHANG, J. (2002). Methods for the identification of compounds useful for the treatment of disease states mediated by prostaglandin D2. European Patent Application EP1170594 A2.

BELLEAU, B. (1964). A molecular theory of drug action based on induced conformational perturbations of receptors. *J. Med. Chem.*, **7**, 776-784.

BIRKINSHAW, T. N., TEAGUE, S. J., BEECH, C., BONNERT, R. V., HILL, S., PATEL, A., REAKES, S., SANGANEE, H., DOUGALL, I. G., PHILLIPS, T. T., SALTER, S., SCHMIDT, J., ARROWSMITH, E. C., CARRILLO, J. J., BELL, F. M.,

PAINE, S. W. & WEAVER, R. (2006). Discovery of potent CRTh2 (DP_2) receptor antagonists. *Bioorg. Med. Chem. Letts.*, **16**, 4287-4290.

BLACK, J. W. & LEFF, P. (1983). Operational models of pharmacological agonism. *Proc. Roy. Soc. Lond. B*, **220**, 141-162.

BÖHM, E., STURM, G. J. ,WEIGLHOFER, I., SANDIG, H., SHICHIJO, M., MCNAMEE, A., PEASE, J. E., KOLLROSER, M., PESKAR, B. A. & HEINEMANN, A. (2004). 11-dehydro-thromboxane B2, a stable thromboxane metabolite, is a full agonist of chemoattractant receptor-homologous molecule expressed on TH2 cells (CRTH2) in human eosinophils and basophils. *J. Biol. Chem.*, **279**, 7663-7670.

BOS, C. L., RICHEL, D. J., RITSEMA, T., PEPPELENBOSCH, M. P. & VERSTEEG, H. H. (2004). Prostanoids and prostanoid receptors in signal transduction. *Int. J. Biochem. Cell Biol.*, **36**, 1187-1205.

BRADY, A. E., WANG, Q., ALLEN, P. B., RIZZO, M., GREENGARD, P. & LIMBIRD, L. E. (2005). α2-adrenergic agonist enrichment of spinophilin at the cell surface involves βγ subunits of G_i proteins and is preferentially induced by the $\alpha 2_A$-subtype. *Mol. Pharm.*, **67**, 1690-1696.

BREYER, R. M., BAGDASSARIAN, C. K., MYERS, S. A. & BREYER, M. D. (2001). Prostanoid receptors: subtypes and signalling. *Ann. Rev. Pharmacol. Toxicol.*, **41**, 661-690.

BRITTAIN, R. T., BOUTAL, L., CARTER, M. C., COLEMAN, R. A., COLLINGTON, E. W., GEISOW, H. P., HALLETT, P., HORNBY, E. J., HUMPHREY, P. P., JACK, D., KENNEDY, I., LUMLEY, P., MCCABE, P. J., SKIDMORE, I. F., THOMAS, M. & WALLIS, C. J. (1985). AH23848: a thromboxane receptor-blocking drug that can clarify the pathophysiologic role of thromboxane A_2. *Circulation.*, **72**, 1208-1218.

BROWNE, G. S., NELSON, C., NGUYEN, T., ELLIS, B. A., DAY, R. O. & WILLIAMS, K. M. (1999). Stereoselective and substrate-dependent inhibition of hepatic mitochondria beta-oxidation and oxidative phosphorylation by the non-steroidal anti-inflammatory drugs ibuprofen, flurbiprofen, and ketorolac. *Biochem. Pharmacol.*, **57**, 837-844.

BURGEN, A. S. V. (1966). Conformational changes and drug action. *Fed. Proc.*, **40**, 2723-2728.

BUSKIEWICZ, I., PESKE, F., WIEDEN, H. J., GRYCZYNSKI, I., RODNINA, M. V. & WINTERMEYER, W. (2005). Conformations of the signal recognition particle protein Ffh from Escherichia coli as determined by FRET. *J. Molec. Biol.*, **351**, 417-430.

CABRERA-VERA, T. M., VANHAUWE, J., THOMAS, T. O., MEDKOVA, M., PREININGER, A., MAZZONI, M. R., & HAMM, H. E. (2003). Insights into G protein structure, function, and regulation. *Endoc. Revs.*, **24**, 765-781.

CARIDE, A. J., PENHEITER, A. R., FILOTEO, A. G., BAJZER, Z., ENYEDI, A. & PENNISTON, J. T. (2001). The plasma membrane calcium pump displays memory of past calcium spikes. Differences between isoforms 2b and 4b. *J. Biol. Chem.*, **276**, 39797-39804.

CASEY, P. J., FONG, H. K., SIMON, M. I. & GILMAN, A. G. (1990). G_z, a guanine nucleotide-binding protein with unique biochemical properties. *J. Biol. Chem.*, **265**, 2383-2390.

CHAN, A. C., IWASHIMA, M., TURCK, C. W. & WELLS, A. (1992). ZAP-70: a 70 kd protein-tyrosine kinase that associates with the TCR ζ chain. *Cell*, **71**, 649-662.

CHAMBERS, J., PARK, J., CRONK, D., CHAPMAN, C., KENNEDY, F. R., WILSON, S. & MILLIGAN, G. (1994). Beta 3-adrenoceptor agonist-induced down-regulation of Gs_α and functional desensitization in a Chinese hamster ovary cell line expressing a beta 3-adrenoceptor refractory to down-regulation. *Biochem. J.*, **303**, 973-978.

CHANDRASEKHARAN, N. V., DAI, H., ROOS, K. L., EVANSON, N. K., TOMSIK, J., ELTON, T. S. & SIMMONS, D. L. (2002). COX-3, a cyclooxygenase-1 variant inhibited by acetaminophen and other analgesic/antipyretic drugs: cloning, structure, and expression. *Proc Nat. Acad. Sci. USA.*, **99**, 13926-13931.

CHANDRASEKHARAN, N. V. & SIMMONS, D. L. (2004). The cyclooxygenases. *Genome Biol.*, **5**, 241.

CHOWDHURY, B., ADAK, M. & BOSE, S. K. (2003). Flurbiprofen, a unique non-steroidal anti-inflammatory drug with antimicrobial activity against Trichophyton, Microsporum and Epidermophyton species. *Letts App. Microbiol.*, **37**, 158-161.

CHOY, W.Y. & FORMAN-KAY, J. D. (2001). Calculation of ensembles of structures representing the unfolded state of an SH3 domain. *J. Mol. Biol.*, **308**, 1011-1032.

CHUANG, T. T., IACOVELLI, L., SALLESE, M. & DE BLASI, A. (1996). G protein-coupled receptors: heterologous regulation of homologous desensitization and its implications. *Trends Pharmacol Sci*., **17**, 416-421.

CHUANG, T. T., LEVINE, H., 3rd., & DE BLASI, A. (1995). Phosphorylation and activation of beta-adrenergic receptor kinase by protein kinase C. *J. Biol. Chem*., **270**, 18660-18665.

CLAING, A., LAPORTE, S. A., CARON, M. G. & LEFKOWITZ, R. J. (2002). Endocytosis of G protein-coupled receptors: role of G protein-coupled receptor kinases and β-arrestin proteins. *Prog. Neurobiol*., **66**, 61-79.

CLARK, A. J. (1926). The antagonism of acetylcholine by atropine. *J. Physiol. (Lond.)*, **61**, 547-556.

CLARK, A. J. (1937). General Pharmacology: Heffter's Handbuch der Experimental Pharmacology (Ergband 4), Springer-Verlag, Berlin.

CLARKE, W. P. & BOND, R. A. (1998). The elusive nature of efficacy. *Trends Pharmacol. Sci.*, **19**, 270-276.

COLEMAN, R. A., SMITH, W. L. & NARUMIYA, S. (1994). International Union of Pharmacology VIII. Classification of prostanoid receptors: properties, distribution and structure of the receptors and their subtypes. *Pharmacol. Rev*., **46**, 205-229.

COLQUHOUN, D. (1987). Affinity, efficacy and receptor classification: is the classical theory still useful? In: *Perspectives on Hormone Receptor Classification*. BLACK, J. W. *et al.*, (eds.), Alan R. Liss, New York.

COLQUHOUN, D. (1993). The binding issue. *Nature*, **366**, 510-511.

COLQUHOUN, D. (1998). Binding, gating, affinity and efficacy. *Br. J. Pharmacol.*, **125**, 923-947.

COLQUHOUN, D. (2006a). The quantitative analysis of drug-receptor interactions: a short history. *Trends Pharmacol. Sci.*, **27**, 149-157.

COLQUHOUN, D. (2006b). Agonist activated ion channels. *Br. J. Pharmacol.*, **147**, S17-S26.

CONKLIN, B. R., FARFEL, Z., LUSTIG, K. D., JULIUS, D. & BOURNE, H. R. (1993). Substitution of three amino acids switches receptor specificity of Gq alpha to that of Gi alpha. *Nature*, **363**, 274-276.

CORDEAUX, Y. & HILL, S.J. (2002). Mechanisms of cross-talk between G-protein-coupled receptors. *Neurosignals*, **11**, 45-57.

COSTA, T. & HERZ, A. (1989). Antagonists with negative intrinsic activity at δ-opioid receptors coupled to GTP-binding proteins. *Proc. Natl. Acad. Sci. USA*, **86**, 7321-7325.

COSTA, T., OGINO, Y., MUNSON, P. J., ONARAN, H. O. & RODBARD, D. (1992). Drug efficacy at guanine nucleotide-binding regulatory protein-linked receptors: thermodynamic interpretation of negative antagonism and of receptor activity in the absence of ligand. *Mol. Pharm.*, **41**, 549-560.

CRIDER, J. Y., GRIFFIN, B. W. & SHARIF, N. A. (2000). Endogenous EP_4 prostaglandin receptors coupled positively to adenylyl cyclase in Chinese hamster ovary cells: pharmacological characterization. *Prost. Leuk. Essent. Fatty Acids*, **62**, 21-26.

CUSSAC, D., NEWMAN-TANCREDI, A., DUQUEYROIX, D., PASTEAU, V. & MILLAN, M. J. (2002). Differential activation of Gq/11 and Gi_3 proteins at 5-hydroxytryptamine$_{2C}$ receptors revealed by antibody capture assays: influence of receptor reserve and relationship to agonist-directed trafficking. *Mol. Pharmacol.*, **62**, 578-589.

DAVIS, R. J., MURDOCH, C. E., ALI, M., PURBRICK, S., RAVID, R., BAXTER, G. S., TILFORD, N., SHELDRICK, R. L., CLARK, K. L. & COLEMAN, R. A. (2004). EP_4 prostanoid receptor-mediated vasodilatation of human middle cerebral arteries. *Br. J. Pharmacol.*, **141**, 580-585.

DE BLASI, A., PARRUTI, G. & SALLESE, M. (1995). Regulation of G protein-coupled receptor kinase subtypes in activated T lymphocytes. Selective increase of beta-adrenergic receptor kinase 1 and 2. *J. Clin. Invest.*, **95**, 203-210.

DE LAPP, N. W. MCKINZIE, J. H., SAWYER, B. D., VANDERGRIFF, A., FALCONE, J., MCCLURE, D. & FELDER, C. C. (1999). Determination of [^{35}S]guanosine-5'-O-(3-thio) triphosphate binding mediated by cholinergic muscarinic receptors in membranes from Chinese hamster ovary cells and rat striatum using an anti-G protein scintillation proximity assay. *J. Pharmacol. Exp. Ther.*, **289**, 946-955.

DEFEA, K. A., ZALEVSKY, J., THOMA, M. S., DERY, O., MULLINS, R. D. & BUNNETT, N. W. (2000). β-arrestin-dependent endocytosis of proteinase-activated receptor 2 is required for intracellular targeting of activated ERK1/2. *J. Cell Biol.*, **148**, 1267-1281.

DEL CASTILLO , J. & KATZ, B. (1957). Interaction at end-plate receptors between different choline derivatives. *Proc. R. Soc. Lond. B*, **146**, 369-381.

DELEAN, A., STADEL J. M. & LEFKOWITZ, R. J. (1980). A ternary complex model explains the agonist-specific binding properties of the adenylate cyclase-coupled β-adrenergic receptor. *J. Biol. Chem*., **255**, 7108-7117.

DICKENSON, J. M., BLANK, J. L. & HILL, S. J. (1998). Human adenosine A1 receptor and P2Y2-purinoceptor-mediated activation of the mitogen-activated protein kinase cascade in transfected CHO cells. *Br. J. Pharmacol.,* **124**, 1491-1499.

DICKENSON, J. M. & HILL, S. J. (1998). Human 5-$HT1_B$ receptor stimulated inositol phospholipid hydrolysis in CHO cells: synergy with Gq-coupled receptors. *Eur. J. Pharmacol*., **348**, 279-285.

DICKENSON, J. M. & HILL, S. J. (1998). Involvement of G-protein βγ subunits in coupling the adenosine A_1 receptor to phospholipase C in transfected CHO cells. *Eur. J. Pharmacol.*, **355**, 85-93.

DING, S., YAO, D., DEENI, Y. Y., BURCHELL, B., WOLF, C. R. & FRIEDBERG, T. (2001). Human NADPH-P450 oxidoreductase modulates the level of cytochrome P450 CYP2D6 holoprotein via haem oxygenase-dependent and -independent pathways. *Biochem. J*., **356**, 613-619.

DOWNES, G. B. & GAUTUM, N. (1999). The G-protein subunit gene families. *Genomics*, **62**, 544-552.

EHRLICH, P. (1913). Chemotherapeutics: Scientific principles, methods and results. *Lancet*, **2**, 445.

EVRARD, P. A., CUMPS, J. & VERBEECK, R. K. (1996). Concentration-dependent plasma protein binding of flurbiprofen in the rat: an in vivo microdialysis study. *Pharm. Res*., **13**, 18-22.

FITZSIMONS, C. P., GOMPELS, U. A., VERZIJL, D., VISCHER, H. F., MATTICK, C., LEURS, R. & SMIT, M. J. (2006). Chemokine-directed trafficking of receptor stimulus to different G proteins: selective inducible and constitutive signaling by human herpesvirus 6-encoded chemokine receptor U51. *Mol. Pharmacol*., **69**, 888-898.

FURCHGOTT, R. F. (1955). The pharmacology of vascular smooth muscle. *Pharmacol. Revs*., **7**, 183-265.

FURCHGOTT, R. F. (1966). The use of β-haloalkylamines in the differentiation of receptors and in the determination of dissociation constants of receptor-agonist complexes. In: *Advances in Drug Research,* **3**, 21-55. HARPER, N. & SIMMONDS, A. B., (eds.), Academic Press, London & New York.

GADDUM, J. H. (1937). The quantitative effects of antagonistic drugs. *J. Physiol.*, **89**, 7P-9P.

GALLANT, M. A., SLIPETZ, D., HAMELIN, E., ROCHDI, M. D., TALBOT, S. D. E., BRUM-FERNANDES, A. J. & PARENT, J. L. (2007). Differential regulation of the signaling and trafficking of the two prostaglandin D2 receptors, prostanoid DP receptor and CRTH2. *Eur. J. Pharmacol.*, **557**, 115-123.

GASPARINI, L., ONGINI, E., WILCOCK, D. & MORGAN, D. (2005). Activity of flurbiprofen and chemically related anti-inflammatory drugs in models of Alzheimer's disease. *Brain Res. - Brain Res. Revs.* **48**, 400-408.

GAZI, L., GYLES, S., ROSE, J., LEES, S., ALLAN, C., XUE, L., JASSAL, R., SPEIGHT, G., GAMBLE, V. & PETTIPHER, R. (2005). Δ^{12}-prostaglandin D_2 is a potent and selective CRTH2 receptor agonist and causes activation of human eosinophils and Th2 lymphocytes. *Prost. Other Lip. Meds.*, **75**, 153-167.

GERVAIS, F. G., CRUZ, R. P. G., CHATEAUNEUF, A., GALE, S., SAWYER, N., NANTEL, F., METTERS, K. M. & O'NEILL, G. P. (2001). Selective modulation of chemokinesis, degranulation, and apoptosis in eosinophils through the PGD_2 receptors CRTH2 and DP. *J. Allergy Clin. Immunol.*, **108**, 982-988.

GERVAIS, F. G., MORELLO, J-P., BEAULIEU, C., SAWYER, N., DENIS, D., GREIG, G., MALEBRANCHE, A. D. & O'NEILL, G. P. (2005). Identification of a potent and selective synthetic agonist at the CRTH2 receptor. *Mol. Pharm.*, **67**, 1834-1839.

GHANOUNI, P., GRYCZYNSKI, Z., STEENHUIS, J. J., LEE, T. W., FARRENS, D. L., LAKOWICZ, J. R. & KOBILKA, B. K. (2001). Functionally different agonists induce distinct conformations in the G protein coupling domain of the β_2 adrenergic receptor. *J. Biol. Chem.*, **276**, 24433-24436.

GILMAN, A. G. (1995). Nobel Lecture. G-proteins and regulation of adenylyl cyclase. *Biosci. Rep.*, **15**, 65-97.

GRAESER, D. & NEUBIG, R. R. (1992). Methods for the study of receptor / G-protein interactions. In: *Signal Transduction: A Practical Approach*. MILLIGAN, G. (ed), IRL Press, Oxford, New York, Tokyo.

GROSCH, S., SCHILLING, K., JANSSEN, A., MAIER, T. J., NIEDERBERGER, E. & GEISSLINGER, G. (2005). Induction of apoptosis by R-flurbiprofen in human colon carcinoma cells: involvement of p53. *Biochem. Pharmacol.*, **69**, 831-839.

GROSCH, S., TEGEDER, I., SCHILLING, K., MAIER, T. J., NIEDERBERGER, E. & GEISSLINGER, G. (2003). Activation of c-Jun-N-terminal-kinase is crucial for the induction of a cell cycle arrest in human colon carcinoma cells caused by flurbiprofen enantiomers. *FASEB J.*, **17**, 1316-1318.

HALDANE, J. B. S. (1930). Enzymes; Longmans, Green & Co.

HALL, R. A., PREMONT, R. T., CHOW, C. W., BLITZER, J. T., PITCHER, J. A., CLAING, A., STOFFEL, R. H., BARAK, L. S., SHENOLIKAR, S., WEINMAN, E. J., GRINSTEIN, S. & LEFKOWITZ, R. J. (1998). The β_2-adrenergic receptor interacts with the Na^+/H^+-exchanger regulatory factor to control Na^+/H^+ exchange. *Nature*, **392**, 626-630.

HALL, R. A., PREMONT, R. T. & LEFKOWITZ, R. J. (1999). Heptahelical receptor signalling: beyond the G protein paradigm. *J. Cell Biol.*, **145**, 927-932.

HATA, A. N. & BREYER, R. M. (2004). Pharmacology and signaling of prostaglandin receptors: multiple roles in inflammation and immune modulation. *Pharmacol. Ther.*, **103**, 147-166.

HATA, A. N., LYBRAND, T. P. & BREYER, R. M. (2005a). Identification of determinants of ligand binding affinity and selectivity in the prostaglandin D_2 receptor CRTH2. *J. Biol. Chem.*, **280**, 32442-32451.

HATA, A. N., LYBRAND, T. P., MARNETT, L. J. & BREYER, R. M. (2005b). Structural determinants of arylacetic acid nonsteroidal anti-inflammatory drugs necessary for binding and activation of the prostaglandin D_2 receptor CRTH2. *Mol. Pharmacol.*, **67**, 640-647.

HEUSLER, P., PAUWELS, P. J., WURCH, T, NEWMAN-TANCREDI, A., TYTGAT, J., COLPAERT, F. C. & CUSSAC, D. (2005). Differential ion current activation by human 5-HT_{1A} receptors in Xenopus oocytes: Evidence for agonist-directed trafficking of receptor signaling. *Neuropharmacol.*, **49**, 963-976.

HILL, A. V. (1909). The mode of action of nicotine and curare determined by the form of the contraction curve and the method of temperature coefficients. *J. Physiol.*, **39**, 361-373.

HILL, S. J. (2006). G-protein-coupled receptors: past, present and future. *Br. J. Pharmacol.*, **147**, S27-S37.

HILL, S. J. & BAKER, J. G. (2003). The ups and downs of Gs- to Gi-protein switching. *Br. J. Pharmacol.*, **138**, 1188-1189.

HIRAI, H., TANAKA, K., TAKANO, S., ICHIMASA, M., NAKAMURA, M., & NAGATA, K. (2002). Agonistic effect of indomethacin on a prostaglandin D_2 receptor, CRTH2. *J. Immunol.*, **168**, 981-985.

HIRAI, H., TANAKA, K., YOSHIE, O., OGAWA, K., KENMOTSU, K., TAKAMORI, Y., ICHIMASA, M., SUGAMURA, K., NAKAMURA, M., TAKANO, S., & NAGATA, K. (2001). Prostaglandin D_2 selectively induces chemotaxis in T-helper type 2 cells, eosinophils, and basophils via seven-transmembrane receptor CRTH2. *J. Exp. Med.* **193**, 255-261.

HO, M. K. C., CHAN, J. H. P., WONG, C. S. S. & WONG, Y. H. (2004). Identification of a stretch of six divergent amino acids on the $\alpha5$ helix of $G\alpha_{16}$ as a major determinant of the promiscuity and efficiency of receptor coupling. *Biochem. J.*, **380**, 361-369.

HO, M. K., YUNG, L. Y., CHAN, J. S., CHAN, J. H., WONG, C. S. & WONG, Y. H. (2001). $G\alpha_{14}$ links a variety of Gi- and Gs- coupled receptors to the stimulation of phospholipase C. *Br. J. Pharmacol.*, **132**, 1431-1440.

INAZU, N. & FUJII, T. (1996). Ovarian carbonyl reductase activity in rats at persistent oestrus. *J. Reprod. Fert.*, **108**, 123-130.

ISHIZUKA, T., MATSUI, T., OKAMOTO, Y., OHTA, A. & SHICHIJO, M. (2004). Ramatroban (BAY u 3405): a novel dual antagonist of TXA_2 receptor and $CRTh_2$, a newly identified prostaglandin D_2 receptor. *Cardiovasc. Drug Revs.*, **22**, 71-90.

ISMAILOV, I. I., MCDUFFIE, J. H. & BENOS, D. J. (1994). Protein kinase A phosphorylation and G protein regulation of purified renal Na^+ channels in planar bilayer membranes. *J. Biol. Chem.*, **269**, 10235-10241.

JACOBS, S. & CAUTRECASES, P. (1976). The mobile receptor hypothesis and 'cooperativity' of hormone binding application to insulin. *Biochem. Biophys. Acta.*, **433**, 482-495.

JUTEAU, H., GAREAU, Y., LABELLE, M., STURINO, C. F., SAWYER, N., TREMBLAY, N., LAMONTAGNE, S., CARRIERE, M. C., DENIS, D. & METTERS, K. M. (2001). Structure-activity relationship of cinnamic acylsulfonamide analogues on the human EP_3 prostanoid receptor. *Bioorg. Med. Chem.*, **9**, 1977-1984.

KARGMAN, S., WONG, E., GREIG, G. M., FALGUEYRET. J. P., CROMLISH, W., ETHIER, D., YERGEY, J. A., RIENDEAU, D., EVANS, J. F., KENNEDY, B., TAGARI, P., FRANCIS, D. A. & O'NEILL, G. P. (1996). Mechanism of selective

inhibition of human prostaglandin G/H synthase-1 and -2 in intact cells. *Biochem. Pharmacol.*, **52**, 1113-1125.

KASLOW, H. R. & BURNS, D. L. (1992). Pertussis toxin and target eukaryotic cells: binding, entry, and activation. *FASEB J.*, **6**, 2684-2690.

KAWANABE, Y., HASHIMOTO, N. & MASAKI, T. (2003). Molecular mechanisms for the activation of Ca^{2+}-permeable nonselective cation channels by endothelin-1 in C6 glioma cells. *Biochem. Pharmacol.*, **65**, 1435-1439.

KAWANABE, Y., HASHIMOTO, N. & MASAKI, T. (2004). Characterization of G proteins involved in activation of nonselective cation channels and arachidonic acid release by norepinephrine/alpha1A-adrenergic receptors. *Am. J. Physiol. - Cell Physiol.*, **286**, C596-600.

KAWANABE, Y., OKAMOTO, Y., ENOKI, T., HASHIMOTO, N. & MASAKI, T. (2001). Ca^{2+} channels activated by endothelin-1 in CHO cells expressing endothelin-A or endothelin-B receptors. *Am. J. Physiol. - Cell Physiol.*, **281**, C1676-C1685.

KENAKIN, T. (1995). Agonist-receptor efficacy I: mechanisms of efficacy and receptor promiscuity. *Trends Pharmacol. Sci.*, **16**, 188-192.

KENAKIN, T. (1995b). Agonist-receptor efficacy II: agonist trafficking of receptor signals. *Trends Pharmacol. Sci.*, **16**, 232-238.

KENAKIN, T. (1996). The classification of seven transmembrane receptors in recombinant expression systems. *Pharmacol. Revs.*, **48**, 413-463.

KENAKIN, T. (1997). Protean agonists. Keys to receptor active states?. *Annals N. Y. Acad. Sci.*, **812**, 116-125.

KENAKIN, T. (1999). The measurement of efficacy in the drug discovery agonist selection process. *J. Pharmacol. Toxicol. Methods.*, **42**, 177-187.

KENAKIN, T. (2001). Inverse, protean, and ligand-selective agonism: matters of receptor conformation. *FASEB J.*, **15**, 598-611.

KENAKIN, T. (2002a). Drug efficacy at G protein-coupled receptors. *Ann. Rev. Pharmacol. Toxicol.*, **42**, 349-379.

KENAKIN, T. (2002b). The ligand paradox between affinity and efficacy: can you be there and not make a difference? *Trends Pharmacol. Sci*, **23**, 275-280.

KENAKIN, T. (2002c). Efficacy at G-protein-coupled receptors. *Nature Revs. Drug Disc.*, **1**, 103-110.

KENAKIN, T. (2002d). Recombinant roulette versus the apparent virtues of 'natural' cell receptor systems: receptor genotypes versus phenotypes. *Trends Pharmacol. Sci*., **23**, 403-404.

KENAKIN, T. (2003). Ligand-selective receptor conformations revisited: the promise and the problem. *Trends Pharmacol. Sci*, **24**, 346-354.

KENAKIN, T. (2004). a) Drug Receptor Theory, b) Drug Antagonism, & c) Pharmacological Assay Formats: Binding. In: *A Pharmacology Primer: Theory, Application and Methods.* Elsevier Academic Press, San Diego & London.

KENAKIN, T. (2004d). Principles: Receptor theory in pharmacology. *Trends Pharmacol. Sci*, **25**, 186-192.

KENAKIN, T. (2004e). Efficacy as a vector: the relative prevalence and paucity of inverse agonism. *Mol. Pharm*., **65**, 2-11.

KENAKIN, T. (2005). New concepts in drug discovery: collateral efficacy and permissive antagonism. *Nature Revs.: Drug Disc.*, **4**, 919-927.

KILTS, J. D., GERHARDT, M. A., RICHARDSON, M. D., SREERAM, G., MACKENSEN, G. B., GROCOTT, H. P., WHITE, W. D., DAVIS, R. D., NEWMAN, M. F., REVES, J. G., SCHWINN, D. A. & KWATRA, M. M. (2000). Beta$_2$-adrenergic and several other G protein-coupled receptors in human atrial membranes activate both G_s and G_i. *Circ. Res*., **87**, 705-709.

KNADLER, M. P., BRATER, D. C. & HALL, S. D. (1989). Plasma protein binding of flurbiprofen: enantioselectivity and influence of pathophysiological status. *J. Pharmacol. Exp. Therap.*, **249**, 378-384.

KOSTENIS, E., WAELBROECK, M. & MILLIGAN, G. (2005). Promiscuous Gα proteins in basic research and drug discovery. *Trends Pharmacol. Sci*., **26**, 595-602.

KUNG, M., STADELMANN, B., BRODBECK, U. & BUTIKOFER, P. (1997). Addition of G418 and other aminoglycoside antibiotics to mammalian cells results in the release of GPI-anchored proteins. *FEBS Letts.*, **409**, 333-338.

LANGLEY, J. N. (1905). On the reaction of cells and of nerve endings to certain poisons, chiefly as regards the reaction of striated muscle of nicotine and curari. *J. Physiol. (Lond.)*, **33**, 374-413.

LEFKOWITZ, R. J., RAJAGOPAL, K. & WHALEN, E. J. (2006). New roles for β-arrestins in cell signalling: not just for seven-transmembrane receptors. *Molec. Cell*., **24**, 643-652.

LEW, M. J. & ANGUS, J. A. (1995). Analysis of competitive agonist-antagonist interactions by nonlinear regression. *Trends Pharmacol. Sci.*, **16**, 328-337.

LIU, A. M. F., HO, M. K. C., WONG, C. S. S., CHAN, J. H. P., PAU, A. H. M. & WONG, Y. H. (2003). $G\alpha_{16/z}$ chimeras efficiently link a wide range of G protein-coupled receptors to calcium mobilisation. *J. Biomol. Screen.*, **8**, 39-49.

LOCHT, C. & ANTOINE, R. (1995). A proposed mechanism of ADP-ribosylation catalyzed by the pertussis toxin S1 subunit. *Biochimie*, **77**, 333-340.

LOCKHART, L. K. & McNICOL, A. (1999). The phospholipase C inhibitor U73122 inhibits phorbol ester-induced platelet activation. *J. Pharmac. Exp. Ther.*, **289**, 721-728.

LOVERING, A. L., RIDE, J. P., BUNCE, C. M., DESMOND, J. C., CUMMINGS, S. M. & WHITE, S. A. (2004). Crystal structures of prostaglandin D_2 11-ketoreductase (AKR1C3) in complex with the nonsteroidal anti-inflammatory drugs flufenamic acidand indomethacin. *Cancer Res.*, **64**, 1802-1810.

LUCH, A., COFFING, S. L., TANG, Y. M., SCHNEIDER, A., SOBALLA, V., GREIM, H., JEFCOATE, C. R., SEIDEL, A., GREENLEE, W. F., BAIRD, W. M., & DOEHMER, J. (1998). Stable Expression of Human Cytochrome P450 1B1 in V79 Chinese Hamster Cells and Metabolically Catalyzed DNA Adduct Formation of Dibenzo[a,l]pyrene. *Chem. Res. Toxicol.*, **11**, 686 – 695.

LUTTRELL, L. M., FERGUSON, S. S., DAAKA, Y., MILLER, W. E., MAUDSLEY, S., DELLA ROCCA, G. J., LIN, F., KAWAKATSU, H., OWADA, K., LUTTRELL, D. K., CARON, M. G. & LEFKOWITZ, R. J. (1999). β-arrestin-dependent formation of β_2 adrenergic receptor-Src protein kinase complexes. *Science*, **283**, 655-661.

MATHIESEN, J. M., ULVEN, T., MARTINI, L., GERLACH, L. O., HEINEMANN, A. & KOSTENIS, E. (2005). Identification of indole derivatives exclusively interfering with a G protein-independent signalling pathway of the prostaglandin D_2 receptor CRTH2. *Mol. Pharm.*, **68**, 393-402.

MAUDSLEY, S., MARTIN, B. & LUTTRELL, L. M. (2005). The origins of diversity and specificity in G protein-coupled receptor signalling. *J. Pharmacol. Exp. Ther.*, **314**, 485-494.

McKENZIE, F. R. (1992). Basic techniques to study G-protein function. In: *Signal Transduction: A Practical Approach*. MILLIGAN, G. (ed.), IRL Press, Oxford, New York & Tokyo.

MCKENZIE, F. R. & MILLIGAN, G. (1990). Prostaglandin E1-mediated, cyclic AMP-independent, down-regulation of Gsα in neuroblastoma x glioma hybrid cells. *J. Biol. Chem.*, **265**, 17084-17093.

METHNER, A., HERMEY, G., SCHINKE, B. & HERMANS-BORGMEYER, I. (1997). A novel G protein-coupled receptor with homology to neuropeptide and chemoattractant receptors expressed during bone development. *Biochem. Biophys. Res. Comms.*, **233**, 336-342.

MICHAELIS, U. R., FALCK, J. R., SCHMIDT. R., BUSSE, R. & FLEMING, I. (2005). Cytochrome P4502C9-derived epoxyeicosatrienoic acids induce the expression of cyclooxygenase-2 in endothelial cells. *Art. Thromb. Vasc. Biol.*, **25**, 321-326.

MICHAELIS, M. & MENTEN, M. L. (1913). Kinetik der Invertinwirkung. *Biochem. Z.*, **49**, 333-369.

MILANO, S. K., KIM, Y. M., STEFANO, F. P., BENOVIC, J. L. & BRENNER, C. (2006). Nonvisual arrestin oligomerization and cellular localization are regulated by inositol hexakisphosphate binding. [erratum appears in *J. Biol. Chem.*, (2006), **281**, 21576]. *J. Biol. Chem.*, **281**, 9812-9823.

MILLIGAN, G. & KOSTENIS, E. (2006). Heterotrimeric G-proteins: a short history. *Br. J. Pharmacol.*, **147**, S46-55.

MILLIGAN, G. & REES, S. (1999). Chimaeric Gα proteins: their potential use in drug discovery. *Trends. Pharmacol. Sci.*, **20**, 118-124.

MIMURA, H., IKEMURA, T., KOTERA, O., SAWADA, M., TASHIRO, S., FUSI, E., UENO, K., MANABE, H., OHSHIMA, E., KARASAWA, A. & MIYAJI, H. (2005). Inhibitory effect of the 4-aminotetrahydroquinoline derivatives, selective Chemoattractant Receptor-homologous molecule expressed on T Helper 2 cell antagonists, on eosinophil migration induced by prostaglandin D_2. *J. Pharmacol. Exp. Ther.*, **314**, 244-251.

MIRSHAHI, T., LOGOTHETIS, D. E. & ROSENHOUSE-DANTSKER, A. (2006). Hydrogen-bonding dynamics between adjacent blades in G-protein β-subunit regulates GIRK channel activation. *Biophys. J.*, **90**, 2776-2785.

MODY, S. J., HO, M. K. C., JOSHI, S. A. & WONG, Y. H. (2000). Incorporation of $G\alpha_z$-specific sequence at the carboxyl terminus increases the promiscuity of $G\alpha_{16}$ toward $G\alpha_i$-coupled receptors. *Mol. Pharm.*, **57**, 13-23.

MONNERET, G., COSSETTE, C., GRAVEL, S., ROKACH, J. & POWELL, W. S. (2003). 15R-methyl-prostaglandin D_2 is a potent and selective CRTH2/DP_2 receptor agonist in human eosinophils. *J. Pharmacol. Exp. Ther.*, **304**, 349-355.

MONNERET, G., GRAVEL, S., DIAMOND, M.., ROKACH, J. & POWELL, W. S. (2001). Prostaglandin D_2 is a potent chemoattractant for human eosinophils that acts via a novel DP receptor. *Blood*, **98**, 1942-1948.

MONNERET, G., LI, H., ROKACH, J. & POWELL, W. S. (2003). 15-deoxy-$\Delta^{12,14}$-prostaglandins D_2 and J_2 are potent activators of human eosinophils. *J. Immunol.*, **168**, 3563-3569.

MONOD, J., WYMAN, J. & CHANGEUX, J. P. (1965). On the nature of allosteric transition. *J. Molec. Biol.*, **12**, 306-329.

MURAKAMI, M., NAKATANI, Y. & KUDO, I. (1996). Type II secretory phospholipase A2 associated with cell surfaces via C-terminal heparin-binding lysine residues augments stimulus-initiated delayed prostaglandin generation. *J. Biol. Chem.*, **271**, 30041-30051.

NAGATA, K. & HIRAI, H. (2003). The second PGD_2 receptor CRTH2: structure, properties, and functions in leukocytes. *Prost. Leuk. Essent. Fatty Acids*, **69**, 169-177.

NAGATA, K., TANAKA, K., OGAWA, K., KEMMOTSU, K., IMAI, T., YOSHIE, O., ABE, H., TADA, K., NAKAMURA, M., SUGAMURA, K., & TAKANO, S. (1999). Selective expression of a novel surface molecule by human Th2 cells *in vivo*. *J. Immunol.*, **162**, 1278-1286.

NAMBA, T., SUGIMOTO, Y., NEGISHI, M., IRIE, A., USHIKUBI, F., KAKIZUKA, A., ITO, S., ICHIKAWA, A., NARUMIYA, S. (1993). Alternative splicing of C-terminal tail of prostaglandin E receptor subtype EP_3 determines G-protein specificity. *Nature*, **365**, 166-170.

NARUMIYA, S., SUGIMOTO, Y. & USHIKUBI, F. (1999). Prostanoid receptors: structures, properties and functions. *Phys. Rev.*, **79**, 1193-1226.

NEUBIG, R. R., SPEDDING, M., KENAKIN, T. & CHRISTOPOULOS, A. (2003). International Union of Pharmacology Committee on Receptor Nomenclature and Drug Classification. XXXVIII. Update on terms and symbols in quantitative pharmacology. *Pharmacol. Revs.*, **55**, 597-606.

NEWMAN-TANCREDI, A. (2003a). Differential ligand efficacy at h5-HT_{1A} receptor-coupled G-protein subtypes: a commentary. *Int. Cong. Ser.*, **1249**, 101-117.

NEWMAN-TANCREDI, A., CUSSAC, D., AUDINOT, V., PASTEAU, V., GAVAUDAN, S. & MILLAN, M. J. (1999). G protein activation by human dopamine D3 receptors in high-expressing Chinese hamster ovary cells: A guanosine-5'-O-(3-[35S]thio)- triphosphate binding and antibody study. *Mol. Pharmacol.*, **55**, 564-574.

NEWMAN-TANCREDI, A., CUSSAC, D., MARINI, L. & MILLAN, M. J. (2002). Antibody capture assay reveals bell-shaped concentration-response isotherms for h5-HT_{1A} receptor-mediated $G\alpha_{i3}$ activation: conformational selection by high-efficacy agonists, and relationship to trafficking of receptor signaling. *Mol. Pharmacol.*, **62**, 590-601.

NEWMAN-TANCREDI, A., CUSSAC, D., MARINI, L., TOUZARD, M. & MILLAN, M. J. (2003b). h5-HT_{1B} receptor-mediated constitutive $G\alpha_{i3}$-protein activation in stably transfected Chinese hamster ovary cells: an antibody capture assay reveals protean efficacy of 5-HT. *Br. J. Pharmacol.*, **138**, 1077-1084.

NICKERSON, M. (1956). Receptor occupancy and tissue response. *Nature*, **178**, 697-698.

OFFERMANNS, S. & SCHULTZ, G. (1994). What are the functions of the pertussis toxin-insensitive G proteins G_{12}, G_{13} and G_z? *Molec. Cell. Endocrinol.*, **100**, 71-74.

OFFERMANNS, S. & SIMON, M. I. (1995). $G\alpha_{15}$ and $G\alpha_{16}$ couple a wide variety of receptors to phospholipase C. *J. Biol. Chem.*, **270**, 15175-15180.

ONARAN, H. O., SCHEER, A., COTECCHIA, S. & COSTA, T. (2000). A look at receptor efficacy. From the signalling network of the cell to the intramolecular motion of the receptor. In: *The Pharmacology of Functional, Biochemical, and Recombinant Systems; Handbook of Experimental Pharmacology* (Vol. 148). KENAKIN, T. P. & ANGUS, J. A. (eds.), 217–280. Springer.

PAK, Y., PHAM, N. & ROTIN, D. (2002). Direct binding of the beta1 adrenergic receptor to the cyclic AMP-dependent guanine nucleotide exchange factor CNrasGEF leads to Ras activation. *Molec. Cell. Biol.*, **22**, 7942-7952.

PAPP, S., DZIAK, E., MICHALAK, M. & OPAS, M. (2003). Is all of the endoplasmic reticulum created equal? The effects of the heterogeneous distribution of endoplasmic reticulum Ca^{2+}-handling proteins. *J. Cell Biol.*, **160**, 475-479.

PARRUTI, G., PERACCHIA, F., SALLESE, M., AMBROSINI, G., MASINI, M., ROTILIO, D. & DE BLASI, A. (1993). Molecular analysis of human beta-arrestin-1:

cloning, tissue distribution, and regulation of expression. Identification of two isoforms generated by alternative splicing. *J. Biol. Chem.*, **268**, 9753-9761.

PATON, W. D. M. (1961). A theory of drug action based on the rate of drug-receptor combination. *Proc. Roy. Acad. Sci. (Series B).*, **154**, 21-69.

PAUWELS, P. J. & COLPAERT, F. C. (2000). Heterogenous ligand-mediated Ca^{++} responses at wt and mutant α_{2A}-adrenoceptors suggest multiple ligand activation binding sites at the α_{2A}-adrenoceptor. *Neuropharmacol.*, **39**, 2101-2111.

PAUWELS, P. J. & COLPAERT, F. C. (2000b). Disperate ligand-mediated Ca^{2+} responses by wild type, mutant Ser^{200}Ala and Ser^{204}Ala α_{2A}-adrenoceptors: $G\alpha_{15}$ fusion proteins: evidence for multiple ligand activation binding sites. *Br. J. Pharmacol.*, **130**, 1505-1512.

PAUWELS, P. J. & COLPAERT, F. C. (2003). Ca^{2+} responses in Chinese Hamster Ovary-K1 cells demonstrate an atypical pattern of ligand-induced 5-HT_{1A} receptor activation. *J. Pharmacol. Exp. Ther.*, **307**, 608-614.

PAUWELS, P. J., RAULLY, I. & WURCH, T. (2003b). Dissimilar pharmacological responses by a new series of imidazoline derivatives at precoupled and ligand-activated α_{2A}-adrenoceptor states: evidence for effector pathway-dependent differential antagonism. *J. Pharmacol. Exp. Ther.*, **305**, 1015-1023.

PAUWELS, P. J., TARDIF, S., WURCH, T. & COLPAERT, F. C. (1997). Stimulated [^{35}S]GTPγS binding by 5-HT_{1A} receptor agonists in recombinant cell lines: Modulation of apparent efficacy by G-protein activation state. *Naunyn-Schmiedeberg's Arch. Pharmacol.*, **356**, 551-561.

PAUWELS, P. J., TARDIF, S. & COLPAERT, F. C. (2001). Differential signalling of both wild-type and Thr^{343}Arg dopamine D_{2short} receptor by partial agonists in a G-protein-dependent manner. *Biochem. Pharmacol.*, **62**, 723-732.

PELEG, G., GHANOUNI, P., KOBILKA, B. K. & ZARE, R. N. (2001). Single-molecule spectroscopy of the β_2 adrenergic receptor: observation of conformational substates in a membrane protein. *Proc. Nat. Acad. Sci. U. S. A.*, **98**, 8469-8474.

PERETTO, I., RADAELLI, S., PARINI, C., ZANDI, M., RAVEGLIA, L. F., DONDIO, G., FONTANELLA, L., MISIANO, P., BIGOGNO, C., RIZZI, A., RICCARDI, B., BISCAIOLI, M., MARCHETTI, S., PUCCINI, P., CATINELLA, S., RONDELLI, I., CENACCHI, V., BOLZONI, P. T., CARUSO, P., VILLETTI, G., FACCHINETTI, F., DEL GIUDICE, E., MORETTO, N. & IMBIMBO, B. P. (2005).

Synthesis and biological activity of flurbiprofen analogues as selective inhibitors of beta-amyloid$_{1-42}$ secretion. *J. Med. Chem*. **48**, 5705-5720.

PERRY, S. J., BAILLIE, G. S., KOHOUT, T. A., MCPHEE, I., MAGIERA, M. M., ANG, K. L., MILLER, W. E., MCLEAN, A. J., CONTI, M., HOUSLAY, M. D. & LEFKOWITZ, R. J. (2002). Targeting of cyclic AMP degradation to β2-adrenergic receptors by β-arrestins. *Science*, **298**, 834-836.

PEZZICOLI, A. & BALDARI, C. T. (2005). ZAP70. AfCS-Nature, doi: 10.1038/mp.a002396.01.

PFISTER, P., RISCH, M., BRODERSEN, D. E. & BOTTGER, E. C. (2003). Role of 16S rRNA Helix 44 in Ribosomal Resistance to Hygromycin B. *Antimicrob. Agents Chemother*., **47**, 1496-1502.

PHILIPSON, K. D. & NICOLL, D. A. (2000). Sodium-calcium exchange: a molecular perspective. *Ann. Rev. Physiol*., **62**, 111-133.

PIERCE, K. L., PREMONT, R. T. & LEFKOWITZ, R. J. (2002). Seven-transmembrane receptors. *Nature Revs Mol. Cell Biol*., **3**, 639-650.

PIERCE, K. L. & REGAN, J. W. (1998). Prostanoid receptor heterogeneity through alternative mRNA splicing. *Life Sci.*, **62**, 1479-1483.

PITCHER, J. A., FREEDMAN, N. J. & LEFKOWITZ, R. J. (1998). G protein-coupled receptor kinases. *Ann. Rev. Biochem*., **67**, 653-692.

POWELL, W. S. (2003). A novel PGD_2 receptor expressed in eosinophils. *Prost. Leuk. Essent. Fatty Acids*, **69**, 179-185.

RANG, H. P. (2006). The receptor concept: pharmacology's big idea. *Br. J. Pharmacol*., **147**, S9-S16.

REVERSI, A., RIMOLDI, V., MARROCCO, T., CASSONI, P., BUSSOLATI, G., PARENTI, M. & CHINI, B. (2005). The oxytocin receptor antagonist atosiban inhibits cell growth via a "biased agonist" mechanism. *J. Biol. Chem*., **280**, 16311-16318.

RIBEIRO-NETO, F. A. P. & RODBELL, M. (1989). Pertussis toxin induces structural changes in G alpha proteins independently of ADP-ribosylation. *Proc. Nat. Acad. Sci. U.S.A*., **86**, 2577-2581.

REITER, E. & LEFKOWITZ, R. J. (2006). GRKs and β-arrestins: roles in receptor silencing, trafficking and signalling. *Trends Pharmacol. Sci*., **17**, 159-165.

RIZZUTO, R., BRINI, M., MURGIA, M. & POZZAN, T. (1993). Microdomains with high Ca^{2+} close to IP_3-sensitive channels that are sensed by neighboring mitochondria. *Science,* **262**, 744-747.

RODBELL, M. (1995). Nobel Lecture. Signal transduction: evolution of an idea. *Biosci. Rep.*, **15**, 117-133.

ROSS, E. M. & WILKIE, T. M. (2000). GTPase-activating proteins for heterotrimeric G proteins: regulators of G protein signalling (RGS) and RGS-like proteins. *Ann. Rev. Biochem.*, **69**, 795-827.

SAMAMA, P., COTECCHIA, S., COSTA, T. & LEFKOWITZ, R. J. (1993). A mutation-induced activated state of the β2-adrenergic receptor: Extending the ternary complex model. *J. Biol. Chem.*, **268**, 4625-4636.

SARIS, N. E. & CARAFOLI, E. (2005). A historical review of cellular calcium handling, with emphasis on mitochondria. *Biochem.-Russia*, **70**, 187-194.

SARKAR, S., HOBSON, A. R., HUGHES, A., GROWCOTT, J., WOOLF, C. J., THOMPSON, D. G. & AZIZ, Q. (2003). The prostaglandin E_2 receptor-1 (EP-1) mediates acid-induced visceral pain hypersensitivity in humans. *Gastroenterology*, **124**, 18-25.

SAWYER, N., CAUCHON, E., CHATEAUNEUF, A., CRUZ, R. P. G., NICHOLSON, D. W., METTERS, K. M., O'NEILL, G. P. & GERVAIS, F. G. (2002). Molecular pharmacology of the human prostaglandin D_2 receptor, CRTH2. *Br. J. Pharmacol.*, **137**, 1163-1172.

SCARAMELLINI, C. & LEFF, P. (1998). A three-state receptor model: predictions of multiple agonist pharmacology for the same receptor type. *Annals N. Y. Acad. Sci.*, **861**, 97-103.

SCOTT, M. G., LE ROUZIC, E., PERIANIN, A., PIEROTTI, V., ENSLEN, H., BENICHOU, S., MARULLO, S. & BENMERAH, A. (2002). Differential nucleocytoplasmic shuttling of β.-arrestins. Characterization of a leucine-rich nuclear export signal in β-arrestin2. *J. Biol. Chem.*, **277**, 37693-37701.

SELBIE, L. A. & HILL, S. J. (1998). G protein-coupled receptor cross-talk: the fine-tuning of multiple receptor-signalling pathways. *Trends Pharmacol. Sci.*, **19**, 87-93.

SHENOY, S. K. & LEFKOWITZ, R. J. (2005). Angiotensin II-stimulated signaling through G proteins and beta-arrestin. Science's STKE: Signal Transduction Knowledge Environment, 2005(311):cm14.

SHOEMAKER, J. L., RUCKLE, M. B., MAYEUX, P. R. & PRATHER, P. L. (2005). Agonist-directed trafficking of response by endocannabinoids acting at CB2 receptors. *J. Pharmacol. Exp. Ther.*, **315**, 828-838.

SKRZYDELSKI, D., LHIAUBET, A-M., LEBEAU, A., FORGEZ, P., YAMADA, M., HERMANS, E., ROSTENE, W. & PELAPRAT, D. (2003). Differential involvement of intracellular domains of the rat NTS1 neurotensin receptor in coupling to G proteins: A molecular basis for agonist-directed trafficking of receptor stimulus. *Mol. Pharm.*, **64**, 421-429.

SPIEGEL, A. M., SHENKER, A. & WEINSTEIN, L. S. (1992). Receptor-effector coupling by G proteins: implications for normal and abnormal signal transduction. *Endoc. Revs.*, **13**, 536-565.

SMART, E. J., GRAF, G. A. MCNIVEN, M. A., SESSA, W. C., ENGELMAN, J. A., SCHERER, P. E., OKAMOTO, T. & LISANTI, M. P. (1999). Caveolins, liquid-ordered domains, and signal transduction. *Molec. Cell. Biol.*, **19**, 7289-7304.

SMITH, W. L. (1992). Prostanoid biosynthesis and mechanism of action. *Am. J. Physiol. Renal Physiol.*, **263**, F181-F191.

SMITH, W. L., DEWITT, D. L. & GARAVITO, R. M. (2000). Cyclooxygenases: structural, cellular, and molecular biology. *Ann. Rev. Biochem.*, **69**, 145-182.

SMITH, N. J. & LUTTRELL, L. M. (2006). Signal switching, crosstalk, and arrestin scaffolds: novel G protein-coupled receptor signalling in cardiovascular disease. *Hypertension*, **48**, 173-179.

STEPHENSON, R. P. (1956). A modification of receptor theory. *Br. J. Pharmacol.*, **11**, 379-393.

STUBBS, V. E., SCHRATL, P., HARTNELL, A., WILLIAMS, T. J., PESKAR, B. A., HEINEMANN, A. & SABROE, I. (2002). Indomethacin causes prostaglandin D_2-like and eotaxin-likeselective responses in eosinophils and basophils. *J. Biol. Chem.*, **277**, 26012-26020.

SU, T. & WAXMAN, D. J. (2004). Impact of dimethyl sulfoxide on expression of nuclear receptors and drug-inducible cytochromes P450 in primary rat hepatocytes. *Arch. Biochem. Biophys.*, **424**, 226-234.

SUGIMOTO, H., SHICHIJO, M., OKANO, M. & BACON, K. B. (2005). CRTH2-specific binding characteristics of [^{3}H]ramatroban and its effects on PGD_2-, 15-deoxy-

$\Delta^{12,14}$-PGJ_2- and indomethacin-induced agonist responses. *Eur. J. Pharmacol.*, **524**, 30-37.

SZPUNAR, G. J., ALBERT, K. S. & WAGNER, J. G. (1989). Pharmacokinetics of flurbiprofen in man. II. Plasma protein binding. *Res. Comms. in Chem. Pathol. Pharmacol.*, **64**, 17-30.

TAKASAKI, J., SAITO, T., TANIGUCHI, M., KAWASAKI, T., MORITANI, Y., HAYASHI, K. & KOBORI, M. (2004). A novel $G\alpha_{q/11}$-selective inhibitor. *J. Biol. Chem.*, **279**, 47438-47445.

TAMRAZI, A., CARLSON, K. E., RODRIGUEZ, A. L. & KATZENELLENBOGEN, J. A. (2005). Coactivator proteins as determinants of estrogen receptor structure and function: spectroscopic evidence for a novel coactivator-stabilized receptor conformation. *Molec. Endocrinol.*, **19**, 1516-1528.

TANAKA, K., OGAWA, K., SUGAMURA, K., NAKAMURA, M., TAKANO, S. & NAGATA, K. (2000). Cutting edge: differential production of prostaglandin D_2 by human helper T cell subsets. *J. Immunol*, **164**, 2277-2280.

TERADA, T., SUGIHARA, Y., NAKAMURA, K., SATO, R., SAKUMA, S., FUJIMOTO, Y., FUJITA, T., INAZU, N. & MAEDA, M. (2001). Characterization of multiple Chinese hamster carbonyl reductases. *Chem.-Biol. Ints.*, **130**-132, 847-861.

TIAN, Y., NEW, D. C., YUNG, L. Y., ALLEN, R. A., SLOCOMBE, P. M., TWOMEY, B. M., LEE, M. M. K. & WONG, Y. H. (2004). Differential chemokine activation of CC chemokine receptor 1-regulated pathways: ligand selective activation of $G\alpha_{14}$-coupled pathways. *Eur. J. Immunol.*, **34**, 785-795.

TREIMAN, M., CASPERSEN, C. & CHRISTENSEN, S. B. (1998). A tool coming of age: thapsigargin as an inhibitor of sarco-endoplasmic reticulum Ca^{2+}-ATPases. *Trends Pharmacol. Sci.*, **19**, 131-135.

URBAN, J. D., CLARKE, W. P., VON ZASTROW, M., NICHOLS, D. E., KOBILKA, B., WEINSTEIN, H., JAVITCH, J. A., ROTH, B. L., CHRISTOPOULOS, A., SEXTON, P. M., MILLER, K. J., SPEDDING, M. & MAILMAN, R. B. (2007). Functional selectivity and classical concepts of quantitative pharmacology. *J. Pharmacol. Exp. Ther.*, **320**, 1-13.

VACA, L. & SAMPIERI, A. (2002). Calmodulin modulates the delay period between release of calcium from internal stores and activation of calcium influx via endogenous TRP1 channels. *J. Biol. Chem.*, **277**, 42178-421887.

VAN DE WESTERLO, E, YANG, J., LOGSDON, C. & WILLIAMS, J. A. (1995). Down-regulation of the G-proteins $G_q\alpha$ and $G_{11}\alpha$ by transfected human M3 muscarinic acetylcholine receptors in Chinese hamster ovary cells is independent of receptor down-regulation. *Biochem. J.*, **310**, 559-563.

VANHAESEBROECK, B., LEEVERS, S. J., AHMADI, K., TIMMS, J., KATSO, R., DRISCOLL, P. C., WOSCHOLSKI, R., PARKER, P. J. & WATERFIELD, M. D. (2001). Synthesis and function of 3-phosphorylated inositol lipids. *Ann. Rev. Biochem.*, **70**, 535-602.

VIARD, P., MACREZ, N., MIRONNEAU, C. & MIRONNEAU, J. (2001). Involvement of both G protein alphas and beta gamma subunits in beta-adrenergic stimulation of vascular L-type Ca^{2+} channels. *Br. J. Pharmacol.*, **132**, 669-676.

VUCOJEVIĆ, V., PRAMANIK, A., YAKOVLEVA, T., RIGLER, R., TERENIUS, L. & BAKALKIN, G. (2005). Study of molecular events in cells by fluorescence correlation spectroscopy. *Cell. Molec. Life Sci.*, **62**, 535-550.

WALKER, E. M., BISPHAM, J. R. & HILL, S. J. (1998). Nonselective effects of the putative phospholipase C inhibitor, U73122, on adenosine A_1 receptor-mediated signal transduction events in Chinese hamster ovary cells. *Biochem. Pharmacol.*, **56**, 1455-1462.

WEI, T. & BACON, K. H. (2005). Small-molecule CRTH2 antagonists for the treatment of allergic inflammation: an overview. *Expert Opin. Investig. Drugs*, **14**, 769-773.

WEISS, J. M., MORGAN, P. H., LUTZ, M. W. & KENAKIN, T. P. (1996a). The cubic ternary complex receptor-occupancy model. I. Model description. *J. Theor. Biol.*, **178**, 151-167.

WEISS, J. M., MORGAN, P. H., LUTZ, M. W. & KENAKIN, T. P. (1996b). The cubic ternary complex receptor-occupancy model. II. Understanding apparent affinity. *J. Theor. Biol.*, **178**, 169-182.

WEISS, J. M., MORGAN, P. H., LUTZ, M. W. & KENAKIN, T. P. (1996c). The cubic ternary complex receptor-occupancy model. III. Resurrecting efficacy. *J. Theor. Biol.*, **181**, 381-397.

WERRY, T. D., WILKINSON, G. F. & WILLARS, G. B. (2003). Mechanisms of cross-talk between G-protein-coupled receptors resulting in enhanced release of intracellular Ca^{2+}. *Biochem. J.*, **374**, 281-296.

WESTER, M. R., YANO, J. K., SCHOCH, G. A., YANG, C., GRIFFIN, K. J., STOUT C. D. & JOHNSON, E. F. (2004). The structure of human cytochrome P450 2C9 complexed with flurbiprofen at 2.0-A resolution. *J. Biol. Chem.*, **279**, 35630-35637.

WILSON, R .J. & VOLPPE, F. (2002). Agonist fingerprint of the CRTH2 prostanoid receptor. Poster at 12th International Conference on Advances in Prostaglandin, Leukotriene & other Bioactive Lipid Research (August 25-29, 2002, Istanbul) Abst 82P.

WILSON, R. J, GIBLIN, G. M .P., ROOMANS, S., RHODES, S. A., CARTWRIGHT, K. A., SHIELD, V. J., BROWN, J., WISE, A., BEGUM, J., COOTE, J., NOEL, L. S., KENAKIN, T., GRAY, D. W. & GILES, H. (2006). GW627368X ((N-{2-[4-(4,9-diethoxy - 1 - oxo - 1,3 - dihydro - 2H - benzo [f] isoindol - 2 - yl) phenyl] acetyl} benzene sulphonamide): A novel, potent and selective prostanoid EP_4 receptor antagonist. *Br. J. Pharmacol.,* **148**, 326-339.

WISE, A., JUPE, S. C. & REES, S. (2004). The identification of ligands at orphan G-protein coupled receptors. *Ann. Rev. Pharmacol. Toxicol.*, **44**, 43-66.

WOODWARD, C., SIMON, I. & TUCHSEN, E. (1982). Hydrogen exchange and the dynamic structure of proteins. *Mol. Cell. Biochem.*, **48**, 135-160.

WURCH, T., COLPAERT, F. C. & PAUWELS, P. J. (1999). G-protein activation by putative antagonists at mutant $Thr^{373}Lys$ α_{2A} adrenergic receptors. *Br. J. Pharmacol.*, **126**, 939-948.

WURCH, T., COLPAERT, F. C. & PAUWELS, P. J. (2003). Mutation in a protein kinase C phosphorylation site of the 5-HT_{1A} receptor preferentially attenuates Ca^{2+} responses to partial as opposed to higher-efficacy $5HT_{1A}$ agonists. *Neuropharmacol.*, **44**, 873-881.

WURCH, T., OKUDA, J. & PAUWELS, P. J. (2001). Reciprocal modulation of α_{2A} adrenoceptor and $G\alpha_o$ protein states as determined by carboxy-terminal mutagenesis of a $G\alpha_o$ protein. *Mol. Pharmacol.*, **60**, 666-673.

WURCH, T. & PAUWELS, P. J. (2003). Modulation of 5-HT_{1A} receptor-mediated Ca^{2+} responses by co-expression with various recombinant $G\alpha$ proteins in CHO-K1 cells. *Naunyn-Schmiedeberg's Arch. Pharmacol.*, **369**, 99-105.

WUYTACK, F., RAEYMAEKERS, L. & MISSIAEN, L. (2002). Molecular physiology of the SERCA and SPCA pumps. *Cell Calcium*, **32**, 279-305.

WYMAN, J. & ALLEN, D. W. (1951). The problem of the heme interactions in hemoglobin and the basis of the Bohr effect. *J. Polym. Sci. [B]*, **VII**, 499-518.

XU, H., WANG, X., ZIMMERMAN, D., BOJA, E. S., WANG, J., BILSKY, E. J. & ROTHMAN, R. B. (2005). Chronic morphine up-regulates $G\alpha_{12}$ and cytoskeletal proteins in Chinese hamster ovary cells expressing the cloned μ opioid receptor. *J. Pharmacol. Exp. Ther.*, **315**, 248-255.

XUE, L., GYLES, S. L., BARROW, A. & PETTIPHER, R. (2006). Inhibition of PI3K and calcineurin suppresses chemoattractant receptor-homologous molecule expressed on Th2 cells (CRTH2)-dependent responses of Th2 lymphocytes to prostaglandin D_2. Biochem. Pharmacol., doi:10.1016/j.bcp.2006.11.021

YANG, M., SANG, H., RAHMAN, A., WU, D., MALIK, A. B. & YE, R. D. (2001). $G\alpha_{16}$ couples chemoattractant receptors to NF-κB activation. *J. Immunol.*, **166**, 6885-6892.

YOSHIDA, A., TAKAHASHI, M., NISHIMURA, S., TAKESHIMA, H. & KOKUBUN, S. (1992). Cyclic AMP-dependent phosphorylation and regulation of the cardiac dihydropyridine-sensitive Ca channel. *FEBS Letts.*, **309**, 343-349.

ZHANG, J-H., CHUNG, T. D. Y. & OLDENBURG, K. R. (1999). A Simple Statistical Parameter for Use in Evaluation and Validation of High Throughput Screening Assays. *J. Biomol. Screen.*, **4**, 67-73.